amU
Aix Marseille Université

NNT : 2024AIXM0561

THÈSE DE DOCTORAT

Soutenue à AMU — Aix-Marseille Université
le 10 décembre 2024 par

Sami VIOLLET

Study of perturbative and non perturbative properties of quantum black holes

Discipline
Physique et Sciences de la Matière

Spécialité
Physque Théorique et Mathématique

École doctorale
ED 352 Physique et Sciences de la Matière

Laboratoire/Partenaires de recherche
Centre de Physique Théorique
(CNRS UMR 7332)

Composition du jury

Kristina GIESEL Professeure, Université FAU	Rapporteure
Aurélien BARRAU Professeur, LPSC	Rapporteur
Ivan AGULLO Professeur, LSU	Examinateur
Daniel SUDARSKY Professeur, UNAM	Examinateur
Etera LIVINE Directeur de recherche, ENS de Lyon	Président du jury
Alejandro PEREZ Professeur, CPT	Directeur de thèse
Simone SPEZIALE Directeur de recherche, CPT	Invité

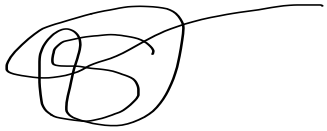
CPT

Affidavit

Je soussigné·e, Sami Viollet, déclare par la présente que le travail présenté dans ce manuscrit est mon propre travail, réalisé sous la direction scientifique de Alejandro Perez, dans le respect des principes d'honnêteté, d'intégrité et de responsabilité inhérents à la mission de recherche. Les travaux de recherche et la rédaction de ce manuscrit ont été réalisés dans le respect à la fois de la charte nationale de déontologie des métiers de la recherche et de la charte AMU relative à la lutte contre le plagiat.

Ce travail n'a pas été précédemment soumis en France ou à l'étranger dans une version identique ou similaire à un organisme examinateur.

Fait à Marseille le 15/10/2024



Cette œuvre est mise à disposition selon les termes de la Licence Creative Commons Attribution - Pas d'Utilisation Commerciale - Pas de Modification 4.0 International.

Liste de publications et participation aux conférences

Liste des publications et/ou brevets réalisées dans le cadre du projet de thèse :

1. Johannes Münch, Alejandro Perez, Simone Speziale, and Sami Viollet. Generic features of a polymer quantum black hole. Classical and Quantum Gravity, 40(13) :135003, 2023.
2. A. Perez, S. Ribisi, and S. Viollet. Modeling Quantum Particles Falling into a Black Hole : The Deep Interior Limit. Universe, 9(2) :75, 2023.
3. Alejandro Perez and Sami Viollet. Discreteness unravels the black hole information puzzle : Insights from a quantum gravity toy model. Entropy, 25(11) :1479, 2023.

Participation aux conférences et écoles d'été au cours de la période de thèse :

1. Workshop on the Black Hole Information Puzzle, Hvar, Croatia. June 20 - 24, 2022. Talk : Quantum hair in a LQG toy model : vacuum degeneracy from discreteness (contributor : Alejandro Perez and Sami Viollet).
2. LOOPS'22 summer school, Marseille, France. July 11-15, 2022.
3. LOOPS'2022 conference, Lyon, France. July 18-22, 2022. Talk : Generic features of a polymer quantum black hole (contributor : Johannes Munch, Alejandro Perez, Simone Speziale and Sami Viollet).
4. TUX Workshop 2022 (remotly), Tux, Austria. February 14-18, 2022. Talk : Modeling Quantum Particles Falling into a Black Hole : The Deep Interior Limit (contributor : Alejandro Perez, Salvatore Ribisi and Sami Viollet).
5. Quantum Gravity 2023, Nijmegen, Netherlands. July 10-14, 2023. Poster : Discreteness Unravels the Black Hole Information Puzzle : Insights from a Quantum Gravity Toy Model (contributor : Alejandro Perez, Salvatore Ribisi and Sami Viollet).
6. Quantum Effects in Gravitational Fields, Leipzig, Germany. August 28-September 1, 2023. Poster : Discreteness Unravels the Black Hole Information Puzzle : Insights from a Quantum Gravity Toy Model (contributor : Alejandro Perez and Sami Viollet).
7. TUG Workshop 2023, Paris, France. October 10-12,2023. Talk : Discreteness Unravels the Black Hole Information Puzzle : Insights from a Quantum Gravity Toy Model (contributor : Alejandro Perez and Sami Viollet).
8. Workshop : New directions on classical and quantum gravity, Grenoble, France. December 12-13,2023. Talk : Graviton corrections to Newton's potential as a test for non perturbative black hole models (contributor : Sami Viollet).
9. LOOPS'2024 conference, Fort Lauderdale, USA. May 6-10, 2024. Talk : Decoherence without dissipation in a quantum field theory model (contributor : Alejandro Perez and Sami Viollet).

Résumé

La quantification de la relativité générale représente un défi majeur, à la fois en raison de son potentiel à fournir des réponses là où la théorie classique échoue, et de la complexité technique et conceptuelle qu'elle constitue. Cette thèse se concentre particulièrement sur la physique des trous noirs, prédite par la relativité générale mais impossible à décrire entièrement par cette dernière. On s'attend à ce que ces lacunes soient comblées par une description quantique de la gravitation, ce qui fait des trous noirs des objets centraux dans le développement d'une telle théorie.

Le premier axe de cette thèse porte sur la quantification perturbative de la relativité générale. Bien que celle-ci soit non renormalisable, il est possible de la traiter comme une théorie de champs effective (EFT), permettant ainsi d'estimer des effets quantiques finis à basse énergie. La thèse compare les prédictions de cette approche, telles que les corrections quantiques au potentiel newtonien, avec celles obtenues par des modèles non perturbatifs, notamment des métriques de Schwarzschild modifiées qui évitent les singularités. Cette comparaison nécessite une gestion minutieuse de la liberté de jauge et met en évidence des failles dans certains modèles de trous noirs réguliers, menant ainsi à la proposition d'une forme générale de métrique compatible avec les calculs perturbatifs.

La thèse explore ensuite une approche non perturbative de la quantification, la Gravité Quantique à Boucles (LQG), en se concentrant sur les modèles de trous noirs dits polymères où les singularités classiques sont remplacées par des transitions vers un trou blanc. Elle discute de la signification physique des ambiguïtés présentes dans la construction de ces modèles, en déterminant quelles propriétés sont influencées par ces ambiguïtés et lesquelles en sont indépendantes. Un lien est également souligné entre ces ambiguïtés et la non-renormalisabilité de la relativité générale. Par ailleurs, la thèse propose un modèle de trou noir qui évite ces ambiguïtés et offre une description quantique complète de la géométrie du trou noir ainsi que d'un champ scalaire de matière.

Le dernier sujet abordé est celui de la perte d'information liée à l'évaporation des trous noirs. L'importance de comprendre le régime de haute courbure à proximité des singularités est particulièrement mise en avant. En s'appuyant sur des modèles jouets, cette thèse suggère que le rayonnement de Hawking pourrait rester intriqué avec des degrés de liberté géométriques présents à l'échelle de Planck. Cela permettrait que l'information, ou plus formellement l'unitarité, soit préservée même après la fin du processus d'évaporation. Ces modèles restent toutefois limités, notamment par l'hypothèse de symétrie sphérique et, plus largement, par l'absence d'une description complète de la géométrie à l'échelle de Planck. Cela souligne la nécessité de recherches plus approfondies, en particulier sur le rôle des fluctuations quantiques de la matière et de la géométrie. Dans l'ensemble, cette thèse apporte de nouvelles perspectives aux discussions actuelles sur la gravité quantique et la physique des trous noirs, tout en suggérant des pistes pour de futures explorations.

Mots clefs : Gravitation, Quantique, Trous noirs, Singularité, Information.

Abstract

The quantization of general relativity represents a major challenge, both because of its potential to provide answers where classical theory fails, and because of the technical and conceptual complexity it constitutes. This thesis focuses in particular on the physics of black holes, predicted by general relativity but impossible to describe entirely by the latter. These gaps are expected to be filled by a quantum description of gravitation, making black holes central objects in the development of such a theory.

The first focus of this thesis is the perturbative quantization of general relativity. Although the latter is non renormalizable, it is possible to treat it as an effective field theory (EFT), enabling finite quantum effects to be estimated at low energies. The thesis compares the predictions of this approach, such as quantum corrections to the Newtonian potential, with those obtained by non perturbative models, notably modified Schwarzschild metrics that avoid singularities. This comparison requires careful management of gauge freedom and highlights flaws in some regular black hole models, leading to the proposal of a general form of metric compatible with perturbative calculations.

The thesis then explores a non perturbative quantization approach, Loop Quantum Gravity (LQG), focusing on so called polymer black hole models where classical singularities are replaced by transitions to a white hole. It discusses the physical significance of ambiguities present in the construction of these models, determining which properties are influenced by these ambiguities and which are independent of them. A link is also highlighted between these ambiguities and the non-renormalizability of general relativity. Furthermore, the thesis proposes a black hole model that avoids these ambiguities and offers a complete quantum description of the black hole geometry as well as of a scalar matter field.

The final topic is the loss of information associated with black hole evaporation. The importance of understanding the high curvature regime near singularities is particularly highlighted. Based on toy models, this thesis suggests that Hawking radiation could remain entangled with geometric degrees of freedom present at the Planck scale. This would allow information, or more formally unitarity, to be preserved even after the evaporation process has ended. These models remain limited, however, notably by the assumption of spherical symmetry and, more broadly, by the absence of a complete description of Planck scale geometry. This underlines the need for further research, particularly into the role of quantum fluctuations in matter and geometry. Overall, this thesis brings new perspectives to current discussions on quantum gravity and black hole physics, while suggesting avenues for future exploration.

Key words : Gravitation, Quantum, Black holes, Singularity, Information.

Résumé étendu

Mise en contexte

Pourquoi une thérie quantique de la gravitation ?

La description la plus précise de la gravité à ce jour est fournie par la théorie de la relativité générale d'Einstein. Au cours du siècle dernier, cette théorie a bénéficié d'une validation expérimentale croissante, sans qu'aucune observation ne vienne la contredire clairement. Bien que les outils mathématiques qu'elle utilise soient complexes, la relativité générale est conceptuellement plus simple que la théorie précédente de Newton. Plutôt que de s'appuyer sur la notion de forces gravitationnelles agissant mystérieusement et instantanément entre des masses, elle explique cette interaction comme émergeant des concepts plus fondamentaux de l'espace et du temps.

Cependant, cette théorie ne donne pas une image complète de la gravitation, car elle produit des réponses non physiques et incomplètes dans certaines situations. Deux exemples clés sont le tout début de l'univers et le centre des trous noirs. Dans ces deux cas, la relativité générale prédit la présence de singularités. Selon les équations d'Einstein, les quantités physiques qui définissent la géométrie dans ces régions de l'espace-temps deviennent infinies, menant à ce que l'on appelle parfois une singularité scalaire, un point où une quantité physique scalaire diverge.

De plus, ces singularités peuvent être atteintes en un temps fini. Par exemple, un observateur peut rencontrer la singularité au centre d'un trou noir en un temps propre fini. De même, en cosmologie, la singularité marquant le début de l'univers remonte à un temps fini dans notre passé. Cela implique que les géodésiques de type temps, c'est-à-dire les trajectoires suivies par les objets à travers l'espace-temps, deviennent incomplètes dans ces scénarios et ne peuvent être étendues au-delà de la singularité. En somme, la relativité générale expose ses propres limites en prédisant des singularités au-delà desquelles elle n'offre aucune prédiction. Elle ne dit pas qu'un observateur atteignant une telle singularité sera déchiré ; au contraire, elle ne fournit aucune information.

Les équations d'Einstein, qui relient la géométrie de l'espace-temps à son contenu en matière, donnent une description classique de la gravité. Elles décrivent l'évolution de champs dynamiques, incluant les métriques et les champs de matière, de manière totalement déterministe. Cependant, nous savons que l'interaction de ces champs de matière est plus précisément décrite par le Modèle Standard (MS), qui fonctionne dans le cadre de la théorie quantique des champs (QFT). Dans ce cadre quantique, les champs de matière peuvent exister dans des superpositions d'états. Comme ces champs déterminent la forme de la géométrie sur laquelle ils évoluent, il est naturel de s'attendre à ce que la géométrie elle-même puisse aussi se trouver dans une superposition d'états. Il devient donc nécessaire de décrire la géométrie en termes quantiques, en utilisant des états dans un espace de Hilbert et des opérateurs agissant sur cet espace pour représenter les observables géométriques.

Ces effets quantiques devraient jouer un rôle crucial dans les situations où la théorie classique prédit des singularités. Dans les exemples précédemment cités de cosmologie et de trous noirs, les singularités apparaissent lorsque la matière se condense en des régions de plus en plus petites, entraînant des densités d'énergie plus élevées. Cependant, nous savons que les effets quantiques deviennent plus prononcés à des échelles de distance réduites. Par exemple, le principe d'incertitude

de Heisenberg suggère qu'il est impossible de localiser totalement la matière, comme cela serait nécessaire pour la formation d'un trou noir.

L'objectif de cette thèse est d'explorer le comportement de la matière et de l'espace temps dans de tels régimes de taille et d'énergie, en apportant des éclairages concrets sur ces conditions extrêmes. En d'autres termes, nous examinerons différentes approches de la quantification de la théorie de la relativité générale, en tentant de trouver des solutions aux problèmes posés par ces singularités.

Tentatives et obstructions

La quantification de la relativité générale est un problème réputé pour être particulièrement complexe, en partie à cause de la non renormalisabilité de cette théorie. Ce problème apparaît dans une approche spécifique de quantification appelée quantification perturbative. Il s'agit de la méthode de quantification initialement utilisée pour décrire la dynamique quantique des champs de matière constituant le Modèle Standard. Étant donné que la relativité générale est également une théorie des champs, il semble naturel d'appliquer cette méthode. Une des difficultés techniques de la quantification perturbative est de devoir traiter le problème de la renormalisation. Les calculs perturbatifs des processus quantiques (comme les phénomènes de diffusion ou de désintégration) conduisent généralement à des résultats infinis. Cependant, ces infinis peuvent être éliminés en redéfinissant les paramètres apparaissant dans le Lagrangien de la théorie utilisée. C'est ce qu'on appelle la procédure de renormalisation. Cela est possible pour toutes les théories du Modèle Standard et, plus généralement, pour toutes les théories dites renormalisables.

Cependant, il existe des cas où cette procédure n'est pas réalisable, c'est à dire que l'élimination des infinis ne peut pas se faire en redéfinissant les paramètres initiaux, mais nécessite l'ajout de termes supplémentaires dans le Lagrangien. Dans ce cas, le Lagrangien doit être complété à chaque fois que le calcul perturbatif est poussé à l'ordre suivant, puisque de nouvelles divergences apparaîtront à chaque ordre. La théorie ainsi obtenue dépendrait alors d'un nombre infini de termes et de paramètres, ces dernier ne pouvant être déterminés que de manière expérimentale. Par conséquent, la théorie serait non prédictive, nécessitant un nombre infini d'expériences avant de pouvoir être utilisée.

T'Hooft et Veltman furent les premiers à appliquer la procédure de quantification perturbative à la relativité générale, et leurs conclusions étaient les suivantes : la gravité pure est renormalisable au premier ordre (i.e. à une bpucle), mais la théorie devient non renormalisable à ce même ordre si de la matière est ajoutée. Plus tard, Goroff et Sagnotti ont montré que la gravité pure devient non renormalisable au second ordre (i.e. à deux boucles). Avec plusieurs décennie de recul , la non renormalisabilité de la relativité générale ne semble plus être un résultat très surprenant. La raison en est que l'espace temps n'est plus considéré comme une notion fondamentale, mais plutôt comme un concept devant émerger de principes plus élémentaires, encore inconnus. Aujourd'hui, il existe plusieurs approches non perturbatives de la gravité quantique (gravité quantique à boucles, théorie des cordes, théorie des ensembles causaux, triangulation causale, etc.) qui tentent de formaliser cette idée. Il semble donc bien établi que la relativité générale n'est qu'une théorie effective. Mais quel est le lien avec la non-renormalisabilité de la théorie ? En fait, il ne devrait pas être surprenant que l'étude des processus à haute énergie utilisant des degrés de liberté (d.o.f), en l'occurrence la

métrique, qui deviennent invalides à ces énergies, mène à des incohérences.

Ce n'est pas la première fois qu'une théorie non renormalisable a été reconnue comme une théorie effective, dérivant d'une théorie plus fondamentale. Ce fut le cas de la théorie non renormalisable de Fermi, qui était une théorie effective découlant de la théorie plus fondamentale de l'interaction faible. Un autre exemple est la théorie chirale perturbativee, également non renormalisable, qui n'est qu'une théorie effective émergente de la chromodynamique quantique. Bien que le traitement perturbatif des théories non renormalisables ne puisse pas être la solution ultime, car il ne peut rien nous apprendre à haute énergie, elles restent cependant prédictives à basse énergie. De même, la relativité générale peut être traitée de manière perturbative comme une théorie des champs effective (EFT), permettant de faire certaines prédictions sur le comportement quantique de la gravité à basse énergie (comparé à l'énergie de Planck).

Démarche et Résultats

Dans cette thèse, nous avons exploré l'approches perturbatives pdécrite plus haurt ainsi que des approches non perturbatives pour formuler une description quantique de la gravité. L'objectif principal était d'étudier la physique des trous noirs. Mes travaux se sont concentrés sur trois problématiques fondamentales : les premières corrections quantiques pour des grandeurs physiques comme l'énergie d'interaction autour d'un trou noir, l'étude de la singularité en son centre, et le phénomène d'évaporation des trous noirs, qui induit une perte d'information. Ce résumé revient sur les résultats obtenus et suggère des pistes de recherche futures pouvant enrichir ces travaux.

Approche inspirée par les théories effectives

Le point de départ de cette thèse a été d'adopter un traitement en termes de théorie effective des champs (Effective Field Theory, ou EFT) pour la relativité générale. Comme souligné au début de ce résumé, malgré la non renormalisabilité de la théorie, il est possible de traiter la relativité générale comme une EFT pour obtenir des prédictions finies et fiables à basse énergie, où la courbure reste faible comparée à la courbure de Planck. Cette approche permet d'obtenir des résultats indépendants de la théorie complète de la gravité quantique, encore inconnue. Toute théorie future de la gravité quantique devra reproduire ces résultats à basse énergie, tout comme la relativité générale converge vers la gravité newtonienne dans la limite appropriée. Un exemple célèbre de prédiction faite par cette approche est le calcul de la correction du potentiel de Newton à une boucle. Cependant, il existe plusieurs notions de potentiels, tant en théorie quantique des champs (QFT) qu'en relativité générale. Il n'est donc pas clair à quelles grandeurs classiques correspond ce potentiel de Newton corrigé.

Dans ce cadre, nous avons exploré comment les prédictions quantiques perturbatives peuvent être comparées aux modèles non perturbatifs de trous noirs quantiques formulés comme des métriques de Schwarzschild modifiées et dépourvues de singularité. Cette comparaison, développée en détail dans le chapitre 2, repose sur le calcul de l'énergie d'interaction entre deux sources statiques. Des prédictions sur cette énergie existent dans le cadre perturbatif, et elle peut également être estimée pour les modèles non perturbatifs de trous noirs. Comme les approches non perturbatives doivent

reproduire les prédictions perturbatives dans les régimes de faible courbure, il est essentiel que ces modèles reproduisent ces résultats dans cette limite. Nous avons porté une attention particulière à la gestion cohérente de la liberté de jauge, une source fréquente d'erreurs dans les études antérieures. Cette méthodologie rigoureuse nous a permis d'évaluer la validité de différentes métriques modifiées de Schwarzschild. Nous avons constaté que la métrique de Hayward ne reproduit pas fidèlement les corrections quantiques attendues, ce qui remet en question sa fiabilité. Nous avons proposé la forme la plus générale d'une métrique modifiée de Schwarzschild compatible avec les calculs perturbatifs.

Une perspective de recherche future serait d'étendre cette analyse à d'autres grandeurs physiques, comme les corrections quantiques à l'angle de déviation des rayons lumineux près d'un trou noir, déjà explorées dans la littérature. Comparer les métriques modifiées aux résultats perturbatifs pour ces quantités fournirait des contraintes supplémentaires sur la métrique la plus générale compatible avec les prédictions perturbatives. Si des divergences apparaissaient entre cette métrique et celle obtenue dans le chapitre 2, cela renforcerait l'idée que la description métrique de la géométrie devient inadaptée à l'échelle de Planck, illustrant ainsi l'une des principales leçons du traitement EFT de la relativité générale.

Approche inspiré de la gravité quantique à boucle

Si l'approche EFT fournit des prédictions robustes à basse énergie, elle n'apporte pas de réponses aux questions liées aux régimes de courbure planckienne. C'est pourquoi nous avons exploré une approche non perturbative de la gravité quantique, notamment la gravité quantique en boucles (Loop Quantum Gravity, ou LQG). Le chapitre 3 permet d'introduire le formalisme de la LQG. Nous avons ensuite rappelé comment des modèles de trous noirs quantiques inspirés par cette approche, appelés trous noirs polymères, peuvent être construis. Une caractéristique majeure de ces modèles est le remplacement de la singularité classique par une transition de trou noir à trou blanc (ou rebond, par analogie avec les modèles cosmologiques). Cependant, ces modèles présentent certaines limitations. Dans la suite, nous avons particulièrement insisté sur le fait que la régularisation de la dynamique classiques sur laquelle repose ces modèles n'est pas unique. Elle nécessite en particulier de procéder à des choix arbitraires de fonctions de régularisation, appelées fonctions de polymerization.

Dans le chapitre 4, nous avons étudié les effets de la modification de ces fonctions de polymérisation sur la dynamique. Nous avons constaté que les propriétés suivantes de ces modèles sont indépendantes de ce choix : la présence d'au moins une transition de trou noir à trou blanc, l'existence d'une valeur minimale pour le rayon de Schwarzschild, l'absence de singularités de courbure, la complétude des géodésiques, et la possibilité qu'une remanante subsiste à la fin du processus d'évaporation. En revanche, d'autres propriétés dépendent fortement du choix de ces fonctions : la structure asymptotique, la valeur exacte du rayon minimal de la zone, le nombre d'horizons et le nombre de rebonds.

Nous avons conclu ce chapitre en montrant que les résultats obtenus dans le chapitre 2 pouvaient imposer certaines contraintes sur cette ambiguïté. En particulier, nous avons découvert que le choix des fonctions sinusoïdales, souvent utilisé, ne permet pas de retrouver la correction quantique de l'énergie d'interaction dérivée par l'approche perturbative. Il est raisonnable de s'attendre à ce que l'obtention de corrections quantiques à des ordres plus élevés impose davantage de contraintes sur les fonctions de polymérisation. Mais comme les corrections d'ordre supérieur nécessitent de connaître les constantes de couplages irrélevantes de la gravité, cela illustre clairement que la non renormal-

isabilité de la relativité générale est liée au problème de l'ambiguïté dans le choix des fonctions de régularisation pour les modèles de trous noirs polymères.

Ces trous noirs polymères ont également l'inconvénient de ne fournir qu'une description effective de la géométrie à l'échelle de Planck (i.e. la dynamique est toujours donnée par un Hamiltonien qui est modifié par les fonctions de polymerisation), et la plupart d'entre eux ne prennent pas en compte la présence de matière. L'objectif du chapitre 5 était de s'attaquer à ces limitations tout en évitant les problèmes d'ambiguïté mis en évidence dans le chapitre précédent. Nous nous sommes concentrés sur la dynamique à l'intérieur "profond" des trous noirs, en utilisant un modèle réduit par symétrie basé sur l'équation de Klein-Gordon pour les champs scalaires. Nous avons montré que les solutions de cette équation, dans un régime où $r \ll M$ (d'où la dénomination d'intérieur profond), se comportent de manière similaire à celles du modèle à symétrie réduit de Kantowski Sachs (KS). Cette ressemblance permet d'étudier les effets de backréaction pour les champs de matière scalaire tombant dans les trous noirs, le modèle KS fournissant un cadre utile pour comprendre la dynamique près de la singularité.

Notre analyse a suggéré que l'intérieur profond d'un trou noir peut être traité comme un système quantique simplifié, où les complexités d'une théorie complète de la gravité sont évitées. En utilisant ces modèles à symétrie réduits, nous avons proposé un schéma de quantification similaire à la LQG, dans lequel l'aire des sphères de rayon r =constant acquiert un spectre discret. Ce schéma de quantification mène naturellement à un espace de Hilbert plus large que celui obtenu par la quantification habituelle de Schrödinger. Cet élargissement est paramétré par un paramètre appelé ϵ, qui caractérise la géométrie de notre modèle à l'échelle de Planck et auquel un observateur macroscopique n'est pas sensible. Remarquablement, le modèle fourni des solutions exactes, même au niveau quantique, pouvant être interprétées par des équations d'évolution effectives s'alignant avec les équations d'Einstein dans les régimes de basse énergie. Cela a établi une base solide pour explorer comment les états semi classiques pourraient se comporter près des singularités des trous noirs, suggérant que les corrections quantiques pourraient soit résoudre, soit atténuer de manière significative les divergences classiques typiquement trouvées dans ces régions.

Un aspect clé de ce modèle sur lequel nous voulons insister est que, dans le cas d'abscence de champs scalaire, nous avons traité l'opérateur de masse comme un observable de Dirac, l'avons quantifié et avons déterminé explicitement son spectre. Nous avons établi que le spectre de cet opérateur est dégénéré, avec cette dégénérescence caractérisée par le paramètre planckien ϵ, que nous avons interprété comme un "quantum hair". Une seule valeur de l'observable macroscopique M correspond à un nombre infini d'états planckiens, paramétrés par ϵ. Cela ressemble au comportement d'un système thermodynamique usuel, où un ensemble de variables d'état correspond à une multitude de configurations planckiennes.

Le modèle repose sur certaines considérations de symétrie simplificatrices, d'où le terme modèle réduit par symétrie. Mais peut-on relâcher certaines de ces contraintes de symétrie ? Dans le modèle présenté au chapitre 5, nous avons considéré uniquement des modes de champ sphériquement symétriques. Une extension intéressante serait d'introduire des modes qui brisent cette symétrie et d'examiner leur backréaction sur la géométrie. Cependant, un modèle général sans ces considérations de symétrie serait significativement plus complexe à étudier analytiquement et même numériquement. Principalement parce que la symétrie sphérique permet d'obtenir un système de dimension finie (i.e. avec un nombre fini de d.o.f), et la suppression de cette symétrie entraînerait

un modèle de dimension infinie. Malgré les complications, il pourrait être précieux de mieux comprendre comment se comportent les fluctuations du tenseur énergie impulsion dans les régions de courbure planckienne. On s'attend à ce que de fortes fluctuations de ce tenseur aient des effets significatifs sur la géométrie, suggérant que les fluctuations quantiques dans la géométrie pourraient ne pas être négligeables. Si tel est le cas, cela suporterait l'idée qu'une description effective d'une géométrie lisse et continu n'est plus acceptable dans ces régimes. Cet effet pourrait jouer un rôle particulièrement crucial dans la compréhension du processus d'évaporation des trous noirs.

Problème de la perte d'information

Le but de la dernière partie de cette thèse était d'étudier le fameux problème de la perte d'information lors du processus de formation puis d'évaporation d'un trou noir. Nous avons commencé dans le chapitre 6 par un rappel des résultats historiques de Hawking, Wald et Parker, conduisant à une perte d'information, ou plus formellement à une brisure de l'unitarité. Nous avons motivé l'idée que ce problème nécessite une compréhension approfondie du régime de gravité quantique forte près de la singularité, au-delà de l'horizon du trou noir. Cela représente un défi tant pour les perspectives holographiques que non holographiques. Dans la vision holographique, les trous noirs macroscopiques possèdent un nombre fini de d.o.f internes limités par leur surface d'horizon. Par conséquent, ils sont censés suivre une courbe de Page standard, où l'entropie de la radiation Hawking commence à diminuer à un temps où le trou noir est encore macroscopique, connue sous le nom de temps de Page. À l'inverse, dans la perspective non holographique, qui est le cadre de ce travail, le nombre de d.o.f internes à l'intérieur des trous noirs n'est pas lié par la valeur de la surface de son horizon. Dans le scénario que nous défendons, l'entropie extérieure continue de croître tant que le trou noir est macroscopique, et la purification se produit après le régime semi classique (i.e. le régime de validité du calucl de Hawking, Wald et Page). L'information est récupérée après l'évaporation complète d'un trou noir, et il est essentiel d'identifier les d.o.f de purification mis en jeu. Par la suite, comprendre comment les corrélations entre les partenaires de Hawking sont transférées dynamiquement à ces d.o.f devient crucial. Les d.o.f appropriés sont ceux qui peuvent persister après l'évaporation complète sans stocker une quantité significative d'énergie. En effet dans ce scénario il ne reste à la fin de l'évaportation au plus une énergie de masse planckienne pour la multitude de d.o.f nécessaires à la purification de la totalité du rayonnement de Hawking émis. Ces d.o.f apparaissent dans des régimes planckiens et sont ceux à partir desquels, selon le traitement EFT de la relativité générale, émerge la notion de géométrie lisse et de métriques dans lesquelles la théorie classique est formulée. Cependant, il n'existe jusqu'à présent aucune théorie non perturbative capable de les identifier clairement et de décrire complètement leur dynamique.

Dans le chapitre 7, nous montrons comment utiliser le modèle présenté dans le chapitre 5 pour illustrer le scénario que nous défendons. En effet, ce modèle a été conçu pour capturer la dynamique près de la singularité d'une excitation scalaire, visant à représenter les modes de Hawking entrants, et à inclure leur backreaction. Le modèle incorpore des d.o.f planckiens sans énergie. Plus précisément, le spectre de l'opérateur de masse montre une dégénérescence infinie due à des "quantum hair" paramétrés par la quantité ϵ. En considérant initialement une excitation scalaire corrélée à une excitation libre représentant le rayonnement de Hawking sortant, nous avons montré comment les corrélations se transfèrent dynamiquement vers le cheveu quantique ϵ à mesure que l'excitation

interne approche de la singularité. Bien que ce modèle ne suive pas l'évaporation complète d'un trou noir, il suggère qu'à la fin du processus, le rayonnement de Hawking reste intriqué avec des d.o.f géométriques planckiens, restaurant la pureté du système total.

Ce modèle est cependant trop simple pour résoudre pleinement le paradoxe de la perte d'information. En plus de ne pas décrire complètement l'évaporation d'un trou noir, ce modèle repose sur l'hypothèse de symétrie sphérique, ce qui limite le nombre de degrés de liberté à un nombre fini. Il est difficile d'aller plus loin sans une théorie complète de la gravitation quantique. Toutefois, dans le chapitre 8 nous avons présenté un modèle de théorie quantique des champs incluant un secteur caché (constitué de d.o.f locaux) permettant induire la décohérence des champs de matière sans stocker d'énergie. L'objectif était de proposer une analogie avec le processus de formation et d'évaporation d'un trou noir tel que nous l'avons imaginé jusqu'à présent. Ce modèle montre qu'un champ de matière peut développer des corrélations avec des d.o.f "cachés", représenté ici par une collection de spins, analogues aux degrés de liberté planckiens de la géométrie. Et cela uniquement dans des régimes d'énergie élevée, similaires au régime de courbure planckien pour un trou noir. De plus, cette décohérence subit par le champs se produit sans que les spins ne stockent de l'énergie. Cela est rendu possible par la dégénérescence des niveaux d'énergie du système totale, paramétrée par les différents états de spin. Cela est analogue à la dégénérescence de l'opérateur de masse paramétrée par ϵ dans le modèle réduit par symétrie du chapitre 5.

À l'avenir, nous souhaiterions explorer le rôle des fluctuations quantiques dans l'énergie du champ de matière. Nous avons déjà mentionné dans le paragraphe précédent l'intérêt de mieux comprendre le rôle des fluctuations quantiques du tenseur énergie impulsion dans des régimes de forte courbure. Cela afin de déterminer si elles induisent des fluctuations significatives de la géométrie, ce qui empêcherait une description effective de celle-ci. Il semble plus accessible, du moins dans un premier temps, de mener cette étude dans le cadre de notre modèle simplifié. Nous nous attendons à ce qu'un mode de champ voit ses fluctuations quantiques d'énergie augmenter de manière significative lorsqu'il interagit avec les spins, mais seulement pour des modes de fréquence suffisamment élevée. Cela devrait conduire à de grandes fluctuations dans l'état de spin, rendant impossible une description effective de ces derniers. Ce qui serait analogue à ce qu'on pourrait attendre pour le cas plus réaliste d'un champs de matière dans un espace temps courbe.

Mots clefs : Gravitation, Quantique, Trous noirs, SIngularité, Information

Table of Contents

Abstract 1

Abstract 2

Resume en français 3

Introduction and motivations 15

I Effective field theory treatment of general relativity 21

1 Perturbative quantization of General relativity 22

1.1 Non renormalizability of General Relativity . . . 22

1.1.1 Perturbative gravity . . . 22

1.1.2 Uniqueness of the harmonic gauge . . . 23

1.1.3 Non renormalizability of perturbative gravity . . . 26

1.2 Effective Field Theory approach . . . 27

1.2.1 The main ideas of EFT . . . 27

1.2.2 General relativity as an effective field theory . . . 30

2 Using the EFT approach to test quantum black hole models 32

2.1 Potentials in quantum field theory . . . 32

2.1.1 Scattering potential . . . 33

2.1.2 Static potential . . . 34

2.2 Perturbative quantum gravity . . . 36

2.2.1 1 loop correction to the scattering potential . . . 37

2.2.2 1 loop correction to the energy of interaction . . . 38

2.3 Comparison with modified Schwarzschild spacetime . . . 38

2.3.1 Static potential in general relativity . . . 39

2.3.2 The harmonic gauge for spherically symmetric and static spacetime . . . 40

2.3.3 The most general metric . . . 41

2.3.4 Testing modified Schwarzschild metrics with the perturbative approach 43
2.4 Conclusion 44

II Black holes in Loop Quantum Gravity **46**

3 From LQG to polymer quantum black holes **47**
3.1 General relativity as a gauge theory 48
3.1.1 Ashtekar-Barbero variables 48
3.1.2 Regularization of Ashtekar-Barbero variables : the holonomy-flux algebra 50
3.1.3 Ashtekar-Barbero variables in cosmology 53
3.2 Loop quantum cosmology 56
3.2.1 Kinematic Hilbert space of LQC 56
3.2.2 The equation of motion, a difference equation 60
3.2.3 Solvable Loop Quantum Cosmology 62
3.3 Polymerization and quantum black holes 63
3.3.1 Polymerization and effective dynamics 63
3.3.2 Polymerization applied to black holes 65
3.3.3 Interests and issues of these models 66

4 Regularization ambiguities **69**
4.1 From the classical black hole to a polymerized black hole 69
4.1.1 Minisuperspace black hole model 70
4.1.2 Ashtekar-Barbero variables 75
4.1.3 BMM polymerisation 75
4.2 Generalised polymerisation 78
4.2.1 Presentation of the setup 78
4.2.2 Dirac observables 79
4.2.3 General expression of the metric 79
4.3 Generic features of the dynamics 81
4.3.1 Evolution and fixed points 81
4.3.2 Bounces and singularity resolution 83
4.3.3 Horizons 84
4.3.4 Trapped and anti-trapped regions 87
4.4 Large distance behaviour 88

4.4.1 Asymptotic behaviour . . . 90
4.4.2 Taming quantum gravity effects outside the horizon . . . 92
4.4.3 Constraining ambiguities with the EFT approach . . . 93
4.5 Conclusion . . . 94

5 A quantum black hole model **96**
5.1 Scalar excitations falling inside a Schwarzschild black hole: the deep interior regime . . . 96
5.1.1 Solutions of the Klein-Gordon equation in the deep interior region . . . 97
5.2 The Kantowski-Sachs spacetime coupled with a massless scalar field . . . 99
5.2.1 Symmetry reduced covariant phase space . . . 99
5.2.2 The deep interior dynamics . . . 101
5.2.3 Perturbative solutions in p_ϕ/M and the dynamics in the deep interior region . . . 103
5.2.4 Validity of perturbation theory in view of applying the model to Hawking pairs . . . 104
5.3 A natural polymer quantization of the deep interior dynamics . . . 106
5.3.1 Sketch of the Schrodinger quantization . . . 107
5.3.2 The polymer quantization . . . 108
5.3.3 Quantum dynamics . . . 109
5.4 The continuum versus the polymer dynamics . . . 111
5.4.1 Quantum evolution across the classical *singularity* . . . 111
5.4.2 Dynamics of semiclassical states and tunelling across the singularity . . . 112
5.4.3 The mass operator (in the vacuum case) . . . 115
5.5 Conclusion . . . 116

III The information loss puzzle **118**

6 The essence of the puzzle and possible resolutions **119**
6.1 A brief derivation of the problem . . . 119
6.1.1 Hawking, Wald and Parker result . . . 119
6.1.2 Loss of information . . . 122
6.1.3 Assumptions and robustness of the result . . . 123
6.2 Some attempt of resolution . . . 126
6.2.1 Holographic scenarios . . . 126
6.2.2 Remnant scenarios . . . 128
6.2.3 Other scenarios . . . 129

6.2.4 A resolution based on the presence of planckian d.o.f . . . 130

7 The fate of the information in a symmetry reduced model 133

7.1 Model of a Hawking pair on our quantum geometry . . . 134

7.1.1 Construction of the initial state . . . 134

7.2 The subsystems of interest and their reduced density matrices . . . 135

7.2.1 Computation of the interference terms . . . 136

7.3 Evolution of the entanglement and correlations between the different subsystems . . . 137

7.3.1 Decoherence function . . . 138

7.3.2 Mutual information as an entanglement measure . . . 138

7.4 Conclusion . . . 143

8 Decoherence without dissipation in a QFT toy model 145

8.1 An example in quantum mechanics . . . 145

8.1.1 The Landau system . . . 146

8.1.2 Generalization of the interaction Hamiltonian . . . 148

8.2 Presentation of the $1+1$ field theory model . . . 148

8.2.1 Classical dynamics of a 1D chain of oscillators . . . 149

8.2.2 Quantization of the 1D chain . . . 150

8.2.3 Adding a local defect . . . 152

8.3 Perturbative treatment of the dynamics . . . 152

8.3.1 Perturbative resolution . . . 153

8.3.2 Choice of the interaction Hamiltonian . . . 154

8.3.3 Time evolution of the entanglement between the subsystems . . . 158

8.4 Generalization to N spins . . . 160

8.4.1 Generalization of the model . . . 161

8.4.2 Dynamics of the subsystems . . . 162

8.4.3 Degeneracy of the eigenstates . . . 165

8.5 Conclusion . . . 166

Conclusion and outlooks 168

A Background field formalism and the Heat Kernel method 172

B Boundary term 176

C Asymptotic expansion of the metric components **177**

D Completeness relations **179**

E Calculation of the Entropy using the replica trick **181**

Introduction and motivations

The most accurate description of gravity to date is provided by Einstein's theory of general relativity. Over the past century, this theory has received increasing experimental validation, with no observation to date clearly contradicting it. Although the mathematical tools it employs are complex, general relativity is conceptually simpler than Newton's earlier theory. Rather than relying on the notion of gravitational forces acting mysteriously and instantaneously between masses, it explains this interaction as emerging from the more fundamental concepts of space and time. However, this theory does not offer a complete picture of gravitation, as it produces nonphysical and incomplete answers in certain situations. Two key examples are the very beginning of the universe and the center of black holes. In both cases, general relativity predicts the presence of singularities. According to Einstein's equations, physical quantities that define the geometry in these regions of spacetime become infinite, leading to what is sometimes called a scalar singularity, a point where a scalar physical quantity diverges. Moreover, these singularities can be reached within a finite amount of time. For instance, an observer can encounter the singularity at the center of a black hole in finite proper time. Similarly, in cosmology, the singularity marking the beginning of the universe lies a finite time in our past. This implies that timelike geodesics, or the paths followed by objects through spacetime, become incomplete in these scenarios and cannot be extended beyond the singularity. Essentially, general relativity exposes its own limitations by predicting singularities beyond which it fails to provide any predictions. It does not tell that an observer reaching such a singularity will be ripped apart; instead, it offers no information at all.

Einstein's equations, which connect the geometry of spacetime to its matter content, give a classical description of gravity. They describe the evolution of dynamic fields, including metrics and matter fields, in a completely deterministic manner. However, we understand that the interaction of these matter fields is more accurately captured by the Standard Model (SM), which operates within the framework of quantum field theory (QFT). In this quantum framework, matter fields can exist in superpositions of states. Since these fields determine the shape of the geometry on which they evolve, it is natural to expect that the geometry itself could also exist in a superposition of states. Therefore, describing geometry in quantum terms, using states in a Hilbert space and operators acting on this space to represent geometric observables, becomes necessary. These quantum effects are anticipated to play a crucial role in situations where classical theory predicts singularities. In the earlier examples of cosmology and black holes, singularities form when matter condenses into increasingly smaller regions, leading to higher energy densities. However, we know that quantum effects become more pronounced at small distance scales. For instance, Heisenberg's uncertainty principle suggests that it is impossible to fully localize matter, as would be required for the formation of a black hole. The aim of this thesis is to explore the behavior of matter and spacetime in such regimes of size and energy, providing concrete insights into these extreme conditions. In other words, we will examine various approaches to quantizing the theory of general relativity, seeking solutions to the issues raised by these singularities.

The quantization of general relativity is a long standing problem with the reputation of being particularly complicated, partly because of the non-renormalizability of this theory. This problem appears in one particular quantization approach which is perturbative quantization. This is the

quantization method originally used to describe the quantum dynamics of the matter fields making up the Standard Model. Since general relativity is also a field theory, it seems natural to apply this method to it. One of the technical difficulties of perturbative quantization is that it has to deal with the problem of renormalization. In a nutshell, perturbative computation of quantum processes (such as scattering or disintegration phenomena) generally leads to infinite results. These infinities can, however, be eliminated by redefining the parameters appearing in the Lagrangian of the theory used. This is the renormalization procedure. This is possible for all Standard Model theories and, more generally, for any so-called renormalizable theories. However, there are cases where this procedure is not feasible, i.e. the elimination of infinities cannot be done by redefining the parameters initially present, but requires the addition of extra terms in the Lagrangian. In this case, the Lagrangian has to be completed each time the order of perturbations increases, since new divergences will appear at each order. The theory thus obtained would depend on an infinite number of terms and parameters that can only be fixed experimentally. The theory would therefore be non-predictive, requiring an infinite number of experiments before it could be used.

T'Hooft and Veltmann were the first to apply the perturbative quantization procedure to general relativity [1] and their conclusions were the following: pure gravity is renormalizable at first order (i.e. at one loop), but the theory becomes non renormalizable at this same order if matter is added. Later on, Goroff and Sagnotti showed that pure gravity becomes non renormalizable at second order (i.e. at two loop) [2]. In retrospect, the non-renormalizability of general relativity no longer seems a very surprising result. The reason being, spacetime is not thought as a fundamental notion, but one that emerges from more elementary concepts that are as yet unknown. Today, there exist several non-perturbative approaches to quantum gravity (loop quantum gravity, string theory, causal set theory, causal triangulation, etc.) that attempt to formalize this idea. It seems therefore well established that general relativity is only an effective theory. But what does this have to do with the non-renormalizability of the theory? Well it should not be surprising that studying high energy processes with degrees of freedom (d.o.f), in this case the metric, which no longer make sense at such energies leads to inconsistencies. This is not the first time that a non-renormalizable theory has been found to be an effective theory, emerging from a more fundamental one. This was the case with Fermi's non-renormalizable theory, which was an effective theory deriving from the more fundamental theory of the weak interaction. Another example is the Chiral perturbative theory, also non-renormalizable, being only an effective theory emerging from QCD. Although the perturbative treatment of non-renormalizable theories cannot be the end of the story, since it cannot teach us anything at high energies, they do remain predictive at low energy. Similarly, general relativity can be treated perturbatively as an effective field theory, enabling a certain number of predictions about the quantum behavior of gravity at low energy (compared with Planck energy). For a recent and pedagogical review of the subject, see [3,4]. One of the major predictions obtained by this approach was the estimation of quantum corrections to Newton's potential in the low energy regime. It took many years and the efforts of several research teams [5–7] to achieve the correct result [8]. As this result comes from the effective treatment of general relativity, it is expected to be independent of the high energy theory describing the d.o.f from which emerge the familiar notion of spacetime. Despite the fact that such a theory is still unknown, we do know that it must agree at low energies with the effective treatment of the field theory of general relativity. Just as Einstein knew that his theory of general relativity had to reproduce Newton's theory at low energy.

This quantization method will be the central subject of the first part of this thesis. In chapter

1 we will recall how, despite the non-renormalizability of general relativity, it is possible to use effective field theory techniques to extract the first quantum corrections of certain physical quantities at low energy. A famous example is the computation of the first order (or one-loop) correction of Newton's potential [9]. However, there are several notions of potentials, both in QFT and in general relativity. It is therefore not clear to which classical quantities this corrected Newton's potential corresponds. We will start chapter 2 by reviewing the different notions existing in QFT, as well as their expression at one loop for general relativity. We will show how one can choose one which has a clear classical analog. More precisely, we will consider the notion of static potential, which has been computed at one loop for general relativity [10]. This notion of potential corresponds classically to the energy of interaction of a static particle and a black hole. By computing this quantity for a Schwarzschild metric modified by quantum terms, such as the Hayward metric [11], we should recover the prediction of the one-loop computation. Indeed as motivated earlier, we expect the perturbative predictions to be recovered by other non perturbative approach to quantum gravity in the low curvature regime. This would make it possible to test quantum black hole models. We will explicitly show that the Hayward metric would not allow us to recover the perturbative prediction, and we will end by writing the more general metric able to reproduce it.

The fate of the singularities of general relativity is a central question for quantum gravity that we will address in the second part of this thesis. As explained earlier, this requires a non-perturbative quantization of Einstein's theory, in order to have a quantum theory of gravity valid in high-curvature regimes, as was the case at the first instant of the universe and at the center of black holes. One of the central features of LQG is the inherent discreteness of quantum geometry at the Planck scale. The lack of smoothness of the geometry at the fundamental level challenges the classical view of the singularities of general relativity as a frontier of spacetime geometry, and strongly suggests the possibility of a planckian dynamical description that could define dynamics beyond the limit where classical description fails. The history of the approach starts with the discovery of Ashtekar's connection variables which first suggested that the quantum dynamical evolution equations of gravity might admit a background independent finite and non perturbative formulation [12, 13]. This initial suggestion grew into the approach of LQG with the contribution of many (for reviews and text books see [14–18]). The LQG approach has produced insights about the possible nature of matter and geometry at the Planck scale and has led to new ideas about the origin of black hole thermodynamic, the generation of quantum effects in early cosmology, and stimulated hopes about the possible regularizing role of Planckian granularity (for quantum field theory and gravity).

However, a clear understanding of the question of the fate of singularities in realistic physical situations has remained a difficult one, as addressing it would actually require the (still lacking) complete dynamical control of LQG in situations involving matter and geometry d.o.f of freedom in the deep ultraviolet regime. Nevertheless, the view that the evolution across singularities should be well behaved has become consensual in the field over time thanks to the accumulated experience in simple low dimensional as well as symmetry reduced models of black holes and cosmology. The first examples of singularity avoiding models where found in the context of quantum cosmology by Martin Bojowald [19]. This seminal work grew later into a large number of contributions in the field now known as loop quantum cosmology (LQC) [20–22]. Even in these simple models the quantum dynamics can be rather involved. However, it was soon realized [23] that effective semiclassical

equations could be used to describe the dynamics across the singularity and that these equations were quite easy to describe. The domain of applicability of these techniques was extended in a variety of manners to models involving black holes [24–31] (for reviews see [32–34], for quantum modifications inspired by other approaches see [35–37]). In many of the latter cases the natural starting point has been to consider the quantum dynamics of the interior of spherically symmetric and static spacetimes of the Kantowski-Sachs type (the Schwarzschild black hole interior in the vacuum case). In all these cases the interior singularity is removed and replaced by a quantum transition across what would have been the singularity in the classical description realizing aspects of existing scenarios [38–41].

We will begin in chapter 4 by reviewing how such symmetry reduced models are constructed from the LQG formalism, and how they enable to propose an alternative scenario to the classically predicted singularities. As mentioned above, these are effective semi-classical models, although they have nothing to do with the effective treatment of gravity presented in the previous part. They are obtained by regularizing the phase-space variables and the Hamiltonian giving the classical dynamics. However, the regularization schemes commonly used are based on unjustifiable and arbitrary choices. It is not unique, and the physical significance of this scheme is not known [42]. In chapter 5, addressed this problem in the context of black holes by considering the polymer model [43] based on a specific regularization scheme. We then modified this choice in a general way while tracking the physical consequences of such changes. We were able to identify which geometric properties depend on the regularization scheme (number of black-to-white hole transitions and horizons, curvature at the transition surface, asymptotic structure, etc.) and which do not (presence of at least one black-to-white hole transition, finiteness of the Kretschmann scalar everywhere, etc.) [44]. Surprisingly, although the modifications envisaged to the regularization scheme were extremely general, the methods used enabled us to make a large number of quantitative predictions. We conclude this chapter by comparing these models with the perturbative predictions presented in chapter 2. We shall see that this makes it possible to impose constraints on the polymerization functions that reproduce the perturbative results. We will also discuss how these functions could be further constrained if the perturbative computations were performed at higher order. This will make it possible to link these ambiguities to the non renormalizability of general relativity, which has already been suggested in [42].

In chapter 5, we will then discuss the possibility of going beyond an effective description by proposing a black hole model for which the geometric d.o.f are described in a quantum manner. We started with the classical analysis of the geometry inside a black hole with a massless scalar field on top of it. We showed that when $r \ll 2M$, this massless scalar field is a good description of an ingoing particle of zero angular momentum and as well as its back reaction. We then quantized the system by assuming that the geometry inside the black hole is defined only for discrete values of r. This is a way to implement the idea of discreteness suggested in LQG. This assumption leads to a Hilbert space much bigger than in the standard continuous quantization and gives rise to a Planckian geometric parameter denoted ϵ [45]. We will motivate how this parameter can be interpreted as a quantum hair and how this model can be relevant for studying the evaporation of black holes beyond Hawking's work, as well as for addressing the so-called information loss paradox.

This phenomenon of black hole evaporation is at the root of one of the greatest conceptual problems in modern theoretical physics, most probably linked to the problem of quantum gravity.

The aim of the third part of this thesis is to address this problem in the light of what we have learned in the first chapters. In their original paper Hawking, Wald and Parker show that a black hole spontaneously emits thermal radiation towards an observer located at infinity [46–48]. We will review the main line of this computation in chapter 6. Furthermore, each of these outgoing modes forms a pair with an ingoing partner mode, and each pair is maximally entangled. The outgoing thermal radiation forms a positive energy flux escaping from the black hole. By conservation of energy, the ingoing modes induce a negative energy flux into the black hole, causing its mass to decrease. This result was revolutionary in its day, as it was the first suggestion that black holes are not inert objects and that something is capable of escaping from them. According to Hawking, Wald and Parker's computations, a black hole can radiate all its energy in a finite time. However, since the outgoing radiation is thermal, its Von Neumann entropy is not zero. If all that remains after evaporation is this radiation, this means that the state of the final system is in a mixed state. Nevertheless, it is perfectly possible for a black hole to have formed from a pure state, or more precisely from a coherent state collapsing to form a black hole. In this case, the formation of the black hole and its evaporation lead to the evolution of a pure state towards a mixed state. The entropy of the total system increases, which is in direct contradiction with the unitarity of quantum mechanics. This result has the reputation of being extremely robust. Although initially demonstrated for massless scalar fields evolving on a Schwarzschild- type metric, it was quickly generalized for other matter fields and for charged and/or rotating black holes. However, this prediction relies on a number of assumptions, such as the absence of quantum effects from the geometry or the back-reaction of matter on this geometry. Rejecting certain assumptions could open the way to solving the problem of information loss.

The first attempts to solve this problem are as old as the problem itself. We continue chapter 6 by presenting some of these attempts. One of the most popular to date proposes a mechanism whereby the thermal radiation emitted at the beginning of the evaporation is purified by the radiation emitted during the second half of the black hole's life. This requires corrections to Hawking's computation well before the black hole reaches the end of its life. This approach is sometimes referred to as non-conservative, since it asserts that the physical assumptions used by Hawking, Wald and Parker are not valid in regimes where they should be. More precisely, this purification of the radiation is achieved by quantum effects of gravity at the horizon when the black hole is still macroscopic. However, there is no evidence to suggest that such effects are important in this regime, where the curvature is very small compared to the Planck curvature. Instead, we present a more conservative approach motivated by the quantum description of gravity presented in the first chapters. In our approach, ingoing modes play a crucial role. Indeed, according to the calculations of Hawking, Wald and Parker, they completely purify the outgoing radiation. It is therefore not surprising that information is missing at the end of evaporation if we assume that only the outgoing partner modes remain, without taking into account what the ingoing modes have become. As the latter fall towards the singularity, it seems necessary to have a non-perturbative theory of quantum gravity to be able to describe their fate. As mentioned above, we currently have no such theory. Instead, we will see what certain features of the effective field theory treatment of gravity (such as the existence of d.o.f more fundamental to the Plank scale and from which emerges the notion of geometry with which we are familiar) and of LQG (such as the locality of such d.o.f) can teach us about this problem. In chapter 7, we will use the model presented in chapter 6. More precisely, the ingoing particle considered in this model will represent the ingoing Hawking particle. Since we have a good control

of the quantum dynamic, it will be possible to study how such a particle will become entangled with this ϵ d.o.f. By considering that it is initially entangled with an outgoing Hawking partner, we will deduce that the latter will also be entangled with the ϵ d.o.f. This model suggests that at the end of evaporation, the Hawking radiation, which is in a mixed state, is in fact entangled with Planckian geometric d.o.f [49]. Taking these d.o.f into account could therefore restore the purity of the total system. This model is, however, too simple in several aspects to provide a complete resolution of the information loss paradox. One problem is the assumption of spherical symmetry, which reduces the number of geometric d.o.f to a finite amount. In a more fundamental theory such as LQG, a smooth geometry should emerge from an infinite number of local and Planckian geometric d.o.f [50]. In chapter 8, we will present a QFT toy model where a quantum field evolves in an environment made of an infinite amount of local d.o.f represented by spin 1/2. We showed that the presence of such local d.o.f could impact the purity of the quantum field without changing the low energy physics. The analogy being that Planckian geometrical d.o.f inside a black hole can induce the decoherence of a matter field without this effect being significant in low energy regimes. This toy model completes the one presented in chapter 7, which illustrated this mechanism but with a finite number of d.o.f.

Part I

Effective field theory treatment of general relativity

As announced in the introduction, this part is devoted to the study of perturbative quantization of general relativity. This approach assumes that general relativity can be quantized in the same way as the field theories that make up the Standard Model. It was however observed, first by t'Hooft and Veltmann in 1974, that general relativity is not renormalizable, which destroyed people's interest in this approach; non-renormalizable theories having the reputation of not being predictive. Yet, in the modern effective field theory point of view, non-renormalizable theories can be seen as effective theories and can nevertheless provide quantitative predictions. It was only in the '90s, with the work of Donoghue and many others, that general relativity was treated as an effective field theory and a number of quantum corrections to general relativity were estimated using this approach.

We will start in chapter 1 by recalling the formalism and the procedure for concluding that general relativity is non-renormalizable. A modern and pedagogical presentation of this result can be found in [3]. As general relativity is a gauge theory, particular attention will be paid to how this gauge is treated. In particular, we will outline how this gauge is fixed at the quantum level via the Fadeev-Popov procedure. This will naturally allow us to present the historical result of t'Hooft and Veltmann showing that general relativity is non-renormalizable. This will be followed by a brief but self-consistent introduction to the construction and use of effective field theories. It will then be shown how general relativity, despite its non-renormalizability, can be treated as an effective field theory. This chapter will be closed by mentioning the typical quantum corrections to general relativity obtained by this approach, leaving a deeper analysis of these corrections for the following one.

In chapter 2, we focus on black hole physics and we will see how the quantum corrections to general relativity presented in chapter 1 can be used to constrain metric models of quantum black holes. Indeed, there is a large number of quantum black hole models formulated as modifications of the Schwarzschild metric [11,34,51,52] (and references therein). These are non-perturbative models in the sense that they are supposed to be valid in Planckian curvature regimes. As shown in [44] for the models inspired by loop quantum gravity, their construction relies partly on ambiguous choices that can have an impact on the low energy physics. But as discussed in the introduction, regardless of the foundations of such models, they must reproduce at low energy the predictions of the effective field theory treatment of general relativity. Comparing non-perturbative models with the perturbative approach can help to fix certain ambiguities or select models able to reproduce the perturbative computations. It is not clear, however, what can be compared between these two approaches. Several metrics for quantum black holes have been proposed, claiming to reproduce the same correction to Newton's potential that the perturbative approach [53–55]. However, the authors compare quantities that have no reason to be linked. The problem is that the notion of potential is no longer fundamental in QFT and that several notions of potential exist, each corresponding to different physical situations. There are therefore several ways of computing corrections to Newton's potential. Each way corresponds to a different physical situation, associated with the interaction of

different matter sources (field, static sources, etc.) [8,10,56–58]. Similarly, in general relativity, there are also several ways of deriving a notion of potential of interaction. Given a modified black hole metric, it is therefore possible to propose different ways of deriving a modified Newton's potential, each one corresponding also to different physical situations. The aim of this part is to identify a physical situation that can be described both by the perturbative treatment of general relativity and by a modified black hole metric, and then evaluate constraints that the former approach imposes on the latter. The results presented in this chapter are strongly inspired by [59]

In this chapter only, we use the signature $(1,-1,-1,-1)$, in order to align with the literature on the EFT treatment of general relativity. We take the convention $c=1$ and keep G and $\hbar$ explicit.

1 Perturbative quantization of General relativity

The main purpose of this chapter is to give a brief presentation of the reasoning that led to the status that general relativity is non-renormalizable, and then to recall how the perturbative quantization of this theory remains predictive by treating this theory as an EFT. The system considered in this section will be the spacetime coupled to a massive scalar field. We begin by writing the metric as the Minkowski metric plus a small perturbation. This construction introduces a background (described by the Minkowski metric) on which a perturbation is propagating, which will be called the graviton field. This approach is therefore referred to as background dependent, since it requires the introduction of a background, and therefore cannot be a fundamental description as explained in the introduction. Next, we shall see how the Lagrangian of the total system is written at the different perturbative order. The harmonic gauge is usually imposed as it greatly simplifies the formalism. This gauge is not unique, but we will see that it becomes so if certain boundary conditions are imposed on the graviton field. It will be particularly important that these uniqueness conditions are well understood, as they will also have to be imposed in chapter 2 when we wish to compare other approaches to this perturbative approach. This will then allow us to outline how perturbed gravity leads to a non-renormalizable quantum field theory. After a brief reminder of how effective field theories work, we will be able to justify that general relativity can be treated as such, and that its non-renormalizability does not completely ruin the predictability of this approach.

1.1 Non renormalizability of General Relativity

The non renormalizability of general relativity is a well known property of this theory. In this section, we will outline the formalism as well as the historical computations that led to this issue.

1.1.1 Perturbative gravity

The first step in the perturbative quantization of general relativity is to linearize the theory. Let us start by recalling the formulation of linearized gravity, in which a massive scalar field minimally coupled to gravity is added. The Lagrangian density of the total system is

$$\mathcal{L}=\mathcal{L}_{EH}+\mathcal{L}_{\phi}=\frac{2}{\kappa^2}\sqrt{-g}R+\sqrt{-g}\frac{1}{2}\left(g^{\mu\nu}\partial_\mu\phi\partial_\nu\phi-m^2\phi^2\right), \tag{1.1}$$

where we introduced $\kappa^2 = 32\pi G$. We then linearize the metric $g_{\mu\nu}$ by considering a small perturbation $h_{\mu\nu}$, the graviton field, on top of the Minkowski spacetime $\eta_{\mu\nu}$

$$g_{\mu\nu}(x) = \eta_{\mu\nu} + \kappa h_{\mu\nu}(x). \tag{1.2}$$

From this, it is possible to obtain the expansion in κ for the inverse metric $g^{\mu\nu}$, for the determinant g and for the Ricci scalar R. We will not explicitly write down these expansions which are extremely cumbersome and not useful for the following (but can be found in [60]). Schematically, the expansion at order κ^2 of the Lagrangian $\mathcal{L}$ can be written as follow

$$\begin{aligned}\mathcal{L} \sim & h_{\mu\nu}h_{\lambda\rho}P^{\mu\nu\lambda\rho} + \kappa\partial_\gamma h_{\mu\nu}\partial_\lambda h_{\rho\sigma}h_{\alpha\beta}V_{3G}^{\alpha\beta\rho\sigma\mu\nu} + \kappa^2\partial_\gamma h_{\mu\nu}\partial_\lambda h_{\rho\sigma}h_{\alpha\beta}h_{\delta\omega}V_{4G}^{\alpha\beta\rho\sigma\mu\nu\delta\omega} \\ & + \frac{1}{2}(\eta^{\mu\nu}\partial_\mu\phi\partial_\nu\phi - m^2\phi^2) + \kappa(\partial_\mu\phi\partial_\nu\phi h_{\rho\sigma}V_{1G2\phi}^{\mu\nu\rho\sigma} + m^2\phi^2 h_{\mu\nu}\tilde{V}_{1G2\phi}^{\mu\nu}) \\ & + \kappa^2(\partial_\mu\phi\partial_\nu\phi h_{\rho\sigma}h_{\delta\omega}V_{2G2\phi}^{\mu\nu\rho\sigma\delta\omega} + m^2\phi^2 h_{\mu\nu}h_{\delta\omega}\tilde{V}_{2G2\phi}^{\mu\nu\delta\omega}) + \mathcal{O}(\kappa^3),\end{aligned} \tag{1.3}$$

where P will be useful to determine the graviton propagator. At this stage, this operator is not invertible because of the gauge freedom of the theory. We will see in the next subsection how to treat this gauge freedom classically and in 1.1.3 how it is treated quantum mechanically in order to define properly the graviton propagator. V_{3G} will generate the 3 graviton vertex and V_{4G} the 4 graviton vertex. $V_{1G2\phi}$ and $V_{1G2\phi}$ the 1 graviton 2 ϕ vertex and $V_{2G2\phi}$ and $V_{2G2\phi}$ the 2 graviton 2 ϕ vertex. There precise expression can be found in [9], we are not going to write them since they will not be explicitly used in what follows. We will now look at how the perturbed metric is transformed by a change of coordinates, which is the gauge freedom of gravity. Let us consider an infinitesimal coordinate transformation

$$x_\mu \to x'_\mu = x_\mu + \xi_\mu(x)\ . \tag{1.4}$$

We know that the metric in the new set of coordinates is given by $g'_{\mu\nu}(x') = g_{\rho\sigma}(x)\frac{\partial x^\rho}{\partial x'^\mu}\frac{\partial x^\sigma}{\partial x'^\nu}$. It is not hard to deduce from this that the graviton field transforms as

$$h_{\mu\nu} \to h_{\mu\nu} + \partial_\mu\xi_\nu(x) + \partial_\nu\xi_\mu(x)\ . \tag{1.5}$$

It is possible to check, although it is not trivial, that the Lagrangian (1.3) is invariant under such a transformation. In the next subsection, we will see how this gauge freedom can be fixed via the harmonic condition.

1.1.2 Uniqueness of the harmonic gauge

Linearized gravity is therefore a gauge theory, and quantizing it will naturally lead us to the usual difficulties encountered in quantifying gauge theories (i.e. the non-invertibility of the propagator of the gauge field, in this case of the graviton field, noted P in the previous subsection). To avoid this problem, it is important to fix the gauge. In what follow, we will work in the so called harmonic gauge (or De Donder gauge, or Lorentz gauge) which can be written in the following ways

$$\Box x^\mu = 0 \Leftrightarrow \Gamma^\alpha_{\mu\nu}g^{\mu\nu} = 0. \tag{1.6}$$

In the context of linearized gravity, i.e. by considering (1.2), this gauge fixing condition can be written as

$$\partial^\nu h_{\mu\nu} - \frac{1}{2}\partial_\mu h = 0. \tag{1.7}$$

One can notice that this is not a complete gauge fixing since it is still possible to perform gauge transformations of the form (1.4) with $\xi_\mu(x)$ satisfying

$$\Box\xi^\mu = \partial^\nu\partial_\nu\xi^\mu = 0. \tag{1.8}$$

It is however possible to make this gauge unique by imposing appropriate boundary conditions on the metric (the situation is similar to the one in QED, where the Lorentz gauge is not a complete gauge fixing either, and one need to impose fall off conditions on the potential A^μ to completely fix the gauge [1]). This is due to a theorem that ensures the uniqueness of the solution to the harmonic equation $\Box\psi = 0$ when ψ satisfies a number of fall off conditions. In the rest of this subsection, we will review this theorem, and then see how it can be applied to our situation. The proof of this theorem will not be reviewed, but can be found in [61]. The theorem states that if a solution ψ of the harmonic equation satisfies the following conditions :

(1) ψ is bounded everywhere.
(2) In the limit $r = \sqrt{x^2+y^2+z^2} \to +\infty$ the function ψ behaves as $\psi = \mathcal{O}\left(\frac{1}{r}\right)$ and $\partial_\mu\psi = \mathcal{O}\left(\frac{1}{r}\right)$ for all time t.
(3) There is no incoming waves, i.e. in the limit $r \to +\infty$ and for all time $t_0 = t + r$ the function ψ satisfies $\frac{\partial(r\psi)}{\partial r} + \frac{\partial(r\psi)}{\partial t} = 0$.

then ψ is unique and is the null function. In order to see how one can use this theorem to establish the uniqueness of the harmonic gauge, we start by considering two sets of harmonic coordinates x^μ and x'^μ, satisfying (1.6) and related by a global diffeomorphism noted

$$x'^\mu = a^\mu + \Lambda^\mu_\nu x^\nu + \psi^\mu(x), \tag{1.10}$$

where a^μ and Λ^μ_ν parametrize respectively the global translations and the Lorentz transformations. With this notation, the metric transforms as follow

$$\begin{aligned} g'^{\alpha\beta} &= \frac{\partial x'^\alpha}{\partial x^\mu}\frac{\partial x'^\beta}{\partial x^\nu} g^{\mu\nu} \\ &= \left[\Lambda^\alpha_\mu\Lambda^\beta_\nu + \left(\Lambda^\alpha_\mu\frac{\partial\psi^\beta}{\partial x^\nu} + \Lambda^\beta_\nu\frac{\partial\psi^\alpha}{\partial x^\mu}\right) + \frac{\partial\psi^\alpha}{\partial x^\mu}\frac{\partial\psi^\beta}{\partial x^\nu}\right] g^{\mu\nu} \end{aligned} \tag{1.11}$$

[1] The infinitesimal gauge transformation of the gauge potential in QED is $A^\mu \to A^\mu + \partial^\mu c$. The equivalent of the harmonic gauge in QED is the Lorentz gauge, which is $\partial_\mu A^\mu = 0$, leaving a residual gauge transformation satisfying

$$\Box c = 0. \tag{1.9}$$

However, in addition to the Lorentz gauge, if one requires the fall conditions necessary for the applicability of the uniqueness theorem presented in subsection 1.1.2, then the only solution to (1.9) is $\partial^\mu c = 0$.

Since, by assumption, these two sets of coordinates satisfy (1.6), the functions ψ^μ also satisfy $\Box\psi^\mu = 0$. We will now assume fall off conditions on x^μ and on the metric. In the limit $r \to +\infty$:

(i) x^μ converge to a Cartesian set of coordinates as $x^\mu = \text{carthesian} + \mathcal{O}\left(\frac{1}{r}\right)$.
(ii) The metric converges to the Minkowski metric as $g_{\mu\nu} = \eta_{\mu\nu} + \mathcal{O}\left(\frac{1}{r}\right)$.
(iii) There are only outgoing gravitational waves (which is a reasonable assumption since we will be interested in isolated system) i.e. $h_{\mu\nu} = \text{Outgoing waves}$.

One can argue that if there exists another set of coordinates x'^μ, related to x^μ by (1.10) and also satisfying the properties **(i)**,**(ii)** and **(iii)** then ψ^μ must satisfy the conditions of the previous theorem and are therefore the null functions. First of all, since the coordinate transformation (1.10) is a diffeomorphism, ψ^μ is necessarily bounded everywhere, thus satisfying condition **(1)** of the uniqueness theorem. On the other hand, one can note that according to (1.10) if x^μ is a Cartesian set of coordinates at infinity, then x'^μ is also one if $\psi^\mu = \mathcal{O}\left(\frac{1}{r}\right)$ at infinity and for any time. In addition, we have assumed that the metric in the x^μ coordinates converges to the Minkowski metric at infinity in the following way

$$g^{\mu\nu} - \eta^{\mu\nu} = h^{\mu\nu} = \mathcal{O}\left(\frac{1}{r}\right) \quad \text{when} \quad r \to +\infty. \tag{1.12}$$

It follows from (1.11) that the metric in the x'^μ coordinates also converges in a similar way to the Minkowski metric if $\frac{\partial\psi^\alpha}{\partial x^\mu} = \mathcal{O}\left(\frac{1}{r}\right)$ at infinity and for all time. Hence condition **(2)** is satisfied. Finally, as in the x^μ coordinates, we want that

$$g'^{\mu\nu} - \eta^{\mu\nu} = \text{Outgoing waves} \quad \text{when} \quad r \to +\infty. \tag{1.13}$$

By using (1.11), one can see that this condition imposes at leading order in $\frac{1}{r}$

$$\left(\Lambda^\alpha_\mu \frac{\partial\psi^\beta}{\partial x^\nu} + \Lambda^\beta_\nu \frac{\partial\psi^\alpha}{\partial x^\mu}\right)\eta^{\mu\nu} = \text{Outgoing waves} \tag{1.14}$$

$$\Leftrightarrow \frac{\partial\psi^\beta}{\partial\tilde{x}^\alpha} + \frac{\partial\psi^\alpha}{\partial\tilde{x}^\beta} = \text{Outgoing waves}, \tag{1.15}$$

where we introduced $\tilde{x}^\alpha = \Lambda^\alpha_\nu x^\nu$. By using the following identity

$$\frac{\partial}{\partial x^\beta}\left(\frac{\partial\psi^\alpha}{\partial x^\nu} + \frac{\partial\psi^\nu}{\partial x^\alpha}\right) + \frac{\partial}{\partial x^\alpha}\left(\frac{\partial\psi^\nu}{\partial x^\beta} + \frac{\partial\psi^\beta}{\partial x^\nu}\right) + \frac{\partial}{\partial x^\nu}\left(\frac{\partial\psi^\beta}{\partial x^\alpha} + \frac{\partial\psi^\alpha}{\partial x^\beta}\right) = 2\frac{\partial^2\psi^\nu}{\partial x^\alpha x^\beta}. \tag{1.16}$$

One can conclude that

$$\frac{\partial^2\psi^\nu}{\partial\tilde{x}^\alpha\tilde{x}^\beta} = \text{Outgoing waves} \Leftrightarrow \psi^\nu = \text{Outgoing waves}, \tag{1.17}$$

implying that condition **(3)** is also satisfied by the ψ^μ. Therefore they satisfy all the conditions of applicability of the theorem of uniqueness and have to be the null functions. One can conclude that there is only one set of coordinates satisfying the harmonic gauge condition and the previous fall off conditions, up to global Poincaré transformations. In the next section, we will see how this gauge is fixed when perturbative gravity is treated as a quantum field theory. We will then mentioned the historical results illustrating the non renormalizability of this theory.

1.1.3 Non renormalizability of perturbative gravity

We now want to quantize the classical theory presented in section 1.1.1. To do so, it will be essential to have access to the partition function

$$Z = \int Dh_{\mu\nu} D\phi e^{\frac{i}{\hbar}\int d^4x \mathcal{L}(h_{\mu\nu},\phi)}, \tag{1.18}$$

Where $\mathcal{L}$ is given by (1.1). It is well known that for gauge theories, this integral is not well defined since it is obtained from the integration over the gauge field, here $h_{\mu\nu}$, for which there exists an infinite number of physically equivalent configurations due to the gauge freedom (1.5). This is directly related to the fact that, as discussed in the subsection 1.1.1, the operator P introduced in (1.3) is not invertible. This problem is usually solved by applying the Fadeev-Popov ghost method (see [62] for a pedagogical presentation of this procedure). The first step is to add a gauge fixing term to the Lagrangian (1.1). In the case of linearized gravity, and to impose the harmonic gauge, the following term is added

$$\mathcal{L}_{\text{gf}} = \frac{\sqrt{-g}}{\xi}\left(\partial^\nu h_{\mu\nu} - \frac{1}{2}\partial_\mu h\right)^2. \tag{1.19}$$

Schematically, this consists in adding a Gaussian to the partition function, centered on the configurations satisfying the harmonic gauge. The parameter ξ corresponds to the spread of the Gaussian, and choosing $\xi = 0$ therefore corresponds to a strong imposition of the gauge, since the Gaussian becomes a Dirac delta. In the literature the choice $\xi = 1$ is the most common one, and we shall consider this value in the following. In addition , it is important to add another term to the Lagrangian to compensate for the addition of the gauge fixing term. This is done by introducing an auxiliary field called the ghost field. In this case, the term to be added is the following one

$$\mathcal{L}_{\text{ghost}} = \sqrt{-g}\eta^{*\mu}\left(\Box\eta_\mu - \bar{R}_{\mu\nu}\eta^\nu\right) \tag{1.20}$$

with η a fermionic vector field. The total Lagrangian of the theory is thus obtained by summing (1.1), (1.19) and (1.20). From this, t'Hooft and Veltmann were able to show using the background field formalism and the Heat Kernel method (see Appendix A for a presentation of this method) that the effective one-loop action was divergent and required the addition of the following counter-term to the initial Lagrangian

$$\mathcal{L}_1 = \frac{1}{\epsilon}\left(\frac{1}{120}R^2 + \frac{7}{20}R_{\mu\nu}R^{\mu\nu}\right), \tag{1.21}$$

where ϵ is the dimensional regulator, and R and $R_{\mu\nu}$ are constructed from the background metric $g_{\mu\nu}$ [1,63]. Since the latter satisfies the classical field equations, this implies that $R = 0 = R_{\mu\nu}$ when there is no matter. Therefore, (1.21) is zero in the pure gravity case and there is no divergence in the effective action. There is no one-loop divergence in this case. On the other hand, when matter is added, the effective action diverges and the counter-term (1.21) must be added to the initial Lagrangian. We can see that the non renormalizability of gravity is beginning to be manifest: when coupled to a massless scalar field, the effective action becomes divergent at one loop and requires the addition of terms in the Lagrangian that are not initially present. Subsequently, several works showed that a similar result could be obtained when the massless field was replaced by the

electromagnetic field [64], or by a more general Yang-Mills field [64]. In addition, Goroff and Sagnotti showed that the theory became non renormalizable in the case of pure gravity at two loop order. Indeed, they computed the effective action at this order and were able to show that it diverged. In order to get rid of this divergence, they showed that it was necessary to add the following counter term

$$\mathcal{L}_2 = \frac{1}{\epsilon}\frac{209}{2880}\frac{\kappa^2}{(16\pi^2)^2}R^{\mu\nu\alpha\beta}R_{\alpha\beta\gamma\delta}R^{\gamma\delta}{}_{\mu\nu}. \tag{1.22}$$

As one can see, the divergences that appear at two loops require the addition of a new higher order curvature term. This again illustrates that the higher the order of corrections evaluated, the greater the number of terms to be added to the Lagrangian. Each term comes with a numerical factor which, after renormalization, is finite and must be determined experimentally. The usual conclusion is that an infinite number of experimental measurements must be made before the theory can be used, making it non-predictive. However, as we shall see in the next section, since these results we have gained a better understanding of how non-renormalizable theories work. In particular, we will see that it is possible to treat them as effective field theories, and that they remain predictive despite their non renormalizability.

1.2 Effective Field Theory approach

In this section, we begin by reviewing the physical principles on which EFT are based. In particular, we will explain how such theories can be constructed, before outlining how they can be used to make reliable predictions. Secondly, we shall show how gravity can be treated as an EFT. We will however keep the predictions that can be made with this approach for the section 2.2.

1.2.1 The main ideas of EFT

Let us start by presenting the ideas underlying the construction and use of effective field theories. We will only provide the minimum useful for the application of this method to gravity and to the one-loop computation. This subsection is inspired by the reviews [3, 4, 65]. A more detailed presentation of this approach can be found in the books by the same authors [66, 67]. The effective field theory approach is based on the idea that physics at different energy scales is decoupled. More precisely, it assumes that it is possible to study a physical system at a certain energy scale without taking into account the presence of any higher-energy d.o.f (we can study the ocean currents or the moon's rotation around the earth without taking into account their atomic structure). In general, they enable predictions to be made at energies lower than the energy of the d.o.f they ignore. Since we do not have a theory of everything at the moment, and in the absence of any proof that we have reached "the end of physics", it is reasonable to believe that all the theories we have at our disposal are only effective theories. And as mentioned in the introduction of this part, there is good reason to believe that this is also the case for general relativity. Intuitively, one of the reasons for thinking that such a decoupling between high-energy physics and low-energy physics occurs is that each physical effect is generally confined to a length scale inversely proportional to its energy scale. This stems directly from Heisenberg's uncertainty principle, which states that the greater the

energy of a system, the smaller its spread in space-time (this is even more directly a property of the Fourier transform). It is possible to be more precise about the effect of high energy d.o.f in the low energy limit with the following example. Let us consider a massless field interacting with a massive one of mass m. The latter is expected to have an interaction range of the order of $l \sim \frac{1}{m}$. Suppose we wish to study the system on a scale of length much longer than l, or equivalently on a scale of energy $q \ll m$, where q is the momentum transfer of the scattering process considered. This means we can proceed with the following series expansion for the massive field propagator

$$\frac{1}{m^2 - q^2} = \frac{1}{m^2} + \frac{q^2}{m^2} + \mathcal{O}\left(\frac{q^2}{m^2}\right). \tag{1.23}$$

In Fourier space, the first term of the right hand side of (1.23) corresponds to a Dirac, while subsequent terms will correspond to 2nd-order derivatives, then 4th-order derivatives, and so on. This will lead to increasingly higher order derivative terms in the Lagrangian, since the latter is constructed from field propagators. We can therefore conclude that, in the low energy limit, the effects of the most energetic d.o.f will appear in the Lagrangian as higher order derivative terms [2].

These qualitative arguments allow us to understand intuitively why a decoupling between high-energy d.o.f is decoupled from low-energy ones, and how this decoupling can lead to an effective theory. But they do not constitute proof in themselves of the validity of such effective theories. There are, however, more precise arguments in the literature [68,69] to justify this decoupling, and hence the validity of such theories. In these papers, the authors consider a general form of theory as well as the effective theories that would be obtained from them by integrating out high-energy d.o.f. They show that both theories lead to the same physical predictions when used in a common validity regime. In order to better understand how an effective theory is built from a valid high energy theory we will discuss a toy model (cf [3] for more details). Consider the following Lagrangian

$$\mathcal{L} = \frac{1}{2}(\partial_\mu \phi \partial^\mu \phi - m^2 \phi^2) + \phi F(\psi, \partial_\mu \psi) + G(\psi, \partial_\mu \psi), \tag{1.24}$$

where ϕ is a massive field of mass m and therefore represents high energy d.o.f. On the other hand, ψ represents the low energy d.o.f to which we assume experimental access. In order to have a theory describing only the d.o.f we are interested in, i.e. those carried by the ψ field, it is possible to integrate out the ϕ field. Details of the computation are presented in [3]. Considering the regime for which the energy scale of interest q is much smaller than m, we obtain the following effective Lagrangian

$$\mathcal{L}_{\text{eff}} = G(\psi) + \frac{1}{2m^2}\phi F(\psi, \partial_\mu \psi)^2 - \frac{1}{2m^4} F(\psi, \partial_\mu \psi) \Box F(\psi, \partial_\mu \psi) + ... \tag{1.25}$$

The effective Lagrangian is therefore written as an expansion of derivative (corresponding to an expansion in $\frac{q^2}{m^2}$ in the Fourier space). These terms are therefore produced by the local effect of the massive field that has been integrated out. We can see that such an effective theory is similar to gravity theory when higher order curvature terms are taken into account. As discussed in [70] (Weinberg's chapter), this suggests that general relativity is also an EFT arising from the integration

[2] This argument is not true for a massless field, which has an infinite gate and for which its propagator, of the form $\frac{1}{q}$, will lead to non-analytical contributions in Fourier space

of a massive field. Effective theories of this kind are generally non renormalizable, which is another common point with general relativity. Let us mention another toy model theory, the linear sigma model, for which it is possible to build an effective theory by integrating out high energy d.o.f. The advantage of this theory is that it is explicit enough to allow predictions (transition amplitude calculations) to be made with the full theory and compared with those made with the effective one. As shown in [3], both approaches lead to the same result. Furthermore, it is shown that the effective theory is non renormalizable. Once again, this illustrates the effectiveness of effective theories, and shows that although such theories can be non renormalizable, they are nonetheless predictive.

Let us move on to the second way of constructing effective theories. This is where the power of effective theories really appears. In the toy model (1.24), it was assumed that the fundamental theory was known, from which an effective description (1.25) could be derived by integrating over the most energetic d.o.f. If the fundamental theory is not known, this procedure is obviously not applicable, but it is nevertheless possible to construct an effective theory from scratch. Indeed, from a field that we know is not fundamental, we can write the most general Lagrangian in accordance with the assumed symmetries of the system we want to describe. From the preceding arguments, we naturally expect this Lagrangian to be written as a sum of local derivative terms of increasingly large order. As is more explicit in Fourier space, the n-order derivative terms will have a contribution of the order of $\mathcal{O}\left(\left(\frac{q}{E_{\text{eff}}}\right)^n\right)$, where q is the energy scale we are working at and E_{eff} the energy scale coming from the coupling constant of the theory, i.e. it is the cut off defining the domain of validity of the effective description.. Indeed if $q^n < E_{\text{eff}}^n$ we can decide to limit ourself to prediction of order $\mathcal{O}\left(\left(\frac{q}{E_{\text{eff}}}\right)^n\right)$ and get ride of higher order terms in the Lagrangian. However if $q^n > E_{\text{eff}}^n$, we cannot truncate the Lagrangian and no computations can be done. Once the order n at which we want to work has been chosen, we can use power counting to determine which Lagrangian terms to take into account and at which loop order. Let us write down the effective Lagrangian in the following way

$$\mathcal{L}_{\text{eff}} = E_{\text{eff}}^4 \sum_n a_n \frac{\mathcal{O}_n(\phi)}{E_{\text{eff}}^n}, \tag{1.26}$$

with c_n dimensionless numerical factors, ϕ is the dimensionless effective field, $\mathcal{O}_n$ is a differential operator acting on ϕ and containing n derivatives. Since E_{eff} has the dimension of a mass (in units $\hbar = c = 1$) and since each term in the sum is dimensionless, this ensures that $\mathcal{L}_{\text{eff}}$ has the dimension of a mass to the power of 4. . Note that, as stated earlier in this paragraph, the Lagrangian (1.26) takes the following form in Fourier space

$$\mathcal{L}_{\text{eff}} \sim E_{\text{eff}}^4 \sum_n a_n \frac{q^n}{E_{\text{eff}}^n}, \tag{1.27}$$

which allows us to confirm that indeed le term $\mathcal{O}_n$ containing n derived in (1.26) has a contribution of the order of $\mathcal{O}\left(\left(\frac{q}{E_{\text{eff}}}\right)^n\right)$. By analyzing the order of magnitude of Feynmann diagrams allowed by the Lagrangian (1.26), we can deduce Weinberg's power counting theorem [4,65] which identifies diagrams with a contribution to order n. In a few words, this theorem states that a Feynmann diagram containing N_l loops and N_i vertices originating from i derivative terms of the Lagrangian (1.26) brings a contribution of order

$$n = 2 + \sum_i N_i(i-2) + 2N_l. \tag{1.28}$$

So if we want to perform a computation to order 2, we will need to take into account only the tree diagram obtained from the $\mathcal{O}_2$ term containing 2 derivatives. If we want to go to order 4, we will have to take into account the one loop diagrams obtained from the term $\mathcal{O}_2$ and the tree diagram obtained from the term $\mathcal{O}_4$, etc. So now we understand how to use an effective theory: if we want to make predictions of order n, we need to start by measuring experimentally (or by computing from the fundamental theory if we know it) the numerical coefficients a_k for $k \leq n$. From there, it's possible to use (1.26) to make predictions up to order n. In the next subsection, we shall see how this procedure can be applied in the case of general relativity.

1.2.2 General relativity as an effective field theory

We are now going to present in a consise way how the theory of gravity, or more precisely the perturbative gravity introduced in the sousection 1.1.1, can be formulated as an EFT. We shall focus here on the case of gravity coupled to a scalar matter field, but the idea remains the same for other types of matter. The d.o.f. of interest are the metric $g_{\mu\nu}$, or more precisely the graviton field $h_{\mu\nu}$, and the scalar field ϕ. Now that we have identified the d.o.f we are interested in, we need to identify the symmetry we wish to implement. In this case, we want to build a theory invariant under diffeomorphism transformations. We therefore need to write the most general diffeomorphism invariant action. For the pure gravity part, the most general action is the following

$$L_{\text{PG}} = \sqrt{-g}\left[-\lambda - \frac{1}{16\pi G}R + c_1 R^2 + c_2 R_{\mu\nu}R^{\mu\nu} + ...\right]. \tag{1.29}$$

We anticipate the rest by considering only terms containing no more than 4 derivatives, as these will be the only terms of importance for calculations at the order we will be interested in, i.e. at order G^2. The cosmological constant $\Lambda \approx 10^{-47}\text{GeV}^4$ is small enough to be neglected in the remainder of this part (cf [57] and references therein for an analysis taking into account this constant). This approximation will be valid as long as we are interested in a regime where $\Lambda \ll \frac{2}{\kappa^2}R$, i.e. when we work at distances shorter than the cosmological one, which will be the case in the sequel. As far as the numerical coefficients c_1 and c_2 are concerned, it turns out that in the curvature regimes to which we have access experimentally, the R term in the action is so much larger than those in R^2 and $R_{\mu\nu}R^{\mu\nu}$ that the latter play no role even if the c_i coefficients were very large. The experimental constraints on them are so weak ($|c_i| < 10^{56}$ cf [71] and references therein) that they can be considered unknown. We will see later that, hopefully, they will play no role in the one loop computations. By imposing for this subsection $\hbar = 1$, one can then introduce the Planck mass $m_p = \frac{1}{\sqrt{G}}$, the Lagrangian (1.29) can be put into the form

$$L_{\text{PG}} = \frac{\sqrt{-g}m_p^4}{16\pi}\left[-\frac{R}{m_p^2} + c_1\frac{R^2}{m_p^4} + c_2\frac{R_{\mu\nu}R^{\mu\nu}}{m_p^4} + ...\right]. \tag{1.30}$$

We can see that (1.30) is of the same form as (1.26) with $\phi = g_{\mu\nu}$ and $E_{\text{eff}} = m_p$. We can now apply Weinberg's power counting theorem (1.28) to determine which terms of the Lagrangian (1.30)

should be considered and at which loop order. In the following, we will be computing at order $\left(\frac{q}{E_{\text{eff}}}\right)^4$, i.e. at order $n = 4$. And since $E_{\text{eff}} = m_p = \frac{1}{\sqrt{G}}$, we can say more directly that the computations are performed at order G^2. From (1.28), we see that $n = 4$ for $i = 4$, $N_i = 1$ and $N_l = 0$ and for $i = 2$ and $N_l = 1$. The first case corresponds to the tree diagram obtained from the terms in R^2 and $R_{\mu\nu}R^{\mu\nu}$, and the second case corresponds to the one loop diagrams from the term in R. In conclusion, Weinberg's power coutning theorem tells us that there will be at most the terms R, R^2 and $R_{\mu\nu}R^{\mu\nu}$ that are likely to bring contributions at order G^2. This theorem does not tell us anything more, and it is possible that some of these terms do not contribute at all to certain computations. To illustrate this point, we will add a scalar field ϕ via the following Lagrangian

$$L_{\text{matter}} = \sqrt{-g}\left[\frac{1}{2}\nabla_\mu\phi\nabla^\mu\phi - V(\phi) - \xi R\phi^2 + \frac{d_1}{m_p^2}R\nabla_\mu\phi\nabla^\mu\phi + \frac{d_2}{m_p^2}R^{\mu\nu}\partial_\mu\phi\partial_\mu\phi + ...\right] \tag{1.31}$$

In order to simplify the analysis, we will consider a massive scalar field minimally coupled and without self interaction. This is equivalent to imposing $V(\phi) = m\phi^2$, $\xi = 1$ and $d_1 = d_2 = 0$ (cf [57] and references therein for an analysis of more general cases). We now have everything we need to perform perturbative computations involving gravity coupled to a matter field of order G^2. The total Lagrangian of the system is obtained by summing the gravity Lagrangian (1.30), the term describing the matter field (1.31), the gauge fixing Lagrangian (1.19) and the one introducing the Fadeev-Popov ghosts (1.20). In the next section, we will present some of the quantities that can be computed with this formalism and discuss their physical meaning. But before that, let us end this section with a comment that anticipates a result to be presented in the next section. As we have seen, the terms in R^2 and $R_{\mu\nu}R^{\mu\nu}$ will play a role in computations to order G^2, and so the coefficients c_1 and c_2 will also appear in the results. According to the founding principles of effective theories discussed in the previous subsection 1.2.1, these coefficients are either measured experimentally or predicted from a more fundamental theory. In the present situation, there is neither experience nor theory to estimate them. It would therefore seem that results to order G^2 are not very informative. However, as we shall see for the scattering amplitude of two excitations of a field described by (1.31), these coefficients play no role in the low energy limit. As shown in [3], the scattering amplitude of two scalar field excitations takes the following expression

$$\mathcal{M}(q) = \frac{Gm^2}{q^2}\left(1 + 6Gm\sqrt{-q} + \frac{43}{10\pi}Gq^2\log(-q^2) + c_1Gq^2\right), \tag{1.32}$$

Only the last term contains the coefficient c_1, and this is the subdominant term in the low energy limit $q \to 0$. It is therefore natural to ignore this term, which in the end allows us to obtain a result independent of the unknown coefficients c_1 and c_2. The term proportional to c_1 is a Dirac delta in real space and therefore corresponds to an ultra local interaction. In the low energy limit, where we are concerned with the interaction of distant sources, such ultra local terms will have no effect. In the following section, we will present different notions of potential that can be computed in QFT, as well as their physical meaning. In particular, we will see that one of these notions is related to the quantity (1.32).

2 Using the EFT approach to test quantum black hole models

The aim of this chapter is to present a method for comparing the results obtained by treating gravity as an EFT with other non perturbative approaches to quantum gravity. Indeed, as we motivated in the introduction to this part and then in the subsection 1.2.1. All we know about the fundamental theory of gravity, which is still unknown, is that it reduces to the EFT formulation of gravity presented in subsection 1.2.2 in the low curvature regime (compared to Planck curvature). The predictions made by these two approaches should be in agreement in this regime. In the following, we will concentrate on the case of black holes. We will start by presenting in the first section two main notions of potentials in QFT. The notion of scattering potential associated with the scattering of plane waves, and the notion of static potential associated with the interaction of static sources. In the second section, we will review how these quantities have been computed for gravity. In the third section we will discuss the fact that in classical general relativity it is much easier to find a quantity corresponding to a static interaction potential than to a scattering potential. We will write this quantity explicitly and compute it for the case where there are two static point sources, one of which is much heavier than the other. This will be equivalent to computing the interaction potential of a static test particle in a Schwarzschild metric. We will then write down the most general modified Schwarzschild metric so that this interaction potential matches the one presented in the second section. As before, we will be paying particular attention to the way the gauge is fixed in these computations since, if we want to compare these results to those obtain in the previous part, it will be important to do so in the same gauge. This metric will be first written in the harmonic gauge completed with the boundary conditions mentioned in section 1.1.2, and then in the gauge using the area radius as the radial coordinate (the latter being the most common choice). In the last section we will illustrate how this result can be compared with popular quantum black hole models, namely the Hayward metric as well as some generalizations of this metric. We will see that it can be used to test which non-perturbative quantum black hole models correctly reproduce the perturbative ones, and also how it can help to construct such non perturbative models.

2.1 Potentials in quantum field theory

It is well known that in quantum field theory, the notions of force and interaction potential between particles are not fundamental, but emerge from more fundamental concepts such as fields and interaction Lagrangians. Depending on the physical situation of interest, there are several ways of deriving a quantity that can be interpreted as an interaction potential. In this section, we recall how to obtain two of these notions of potential. The first is the scattering potential, this is the most commonly studied one and is obtained from the computation of scattering amplitude. This quantity is well described in most quantum field theory textbooks (see [72] for the case of QED, the author derive the formula for the Coulomb potential in this way). In a second step we will introduce the notion of static potential, which is the quantity we will be interested in next, and which has been extensively studied in the case of QCD in order to study quark confinement [73].

2.1.1 Scattering potential

In this subsection, we recall how in QFT a scattering potential can be derived from the computation of the scattering amplitude of quantum field excitations. In order to do so, we will need to review how, in non-relativistic quantum mechanics, it is possible to obtain the differential cross section of a particle scattered on a potential. As these are standard results found in most reference textbooks on the subject [62, 72, 74], we will focus on the physical considerations and approximations used, rather than on the technical details. We will then see how, in QFT, it is possible by an inverse reasoning to obtain the expression of the scattering potential from the differential cross section. Let us start by writing the Schroedinger equation in the following way

$$-\frac{\hbar^2}{2m}\vec{\nabla}^2\psi(\vec{r}) + V(\vec{r})\psi(\vec{r}) = E\psi(\vec{r}), \tag{2.1}$$

where $V(\vec{r})$ is the potential term assumed to be known, and going to 0 in the limit $r \to +\infty$ rapidly enough. In the most general case the solution to such an equation can be written as follow

$$\psi(\vec{r}) = \psi_0(\vec{r}) + \frac{2m}{\hbar^2}\int d^3\vec{r'}G(\vec{r}-\vec{r'})V(\vec{r'})\psi(\vec{r'}), \tag{2.2}$$

where

$$(\vec{\nabla}^2 + k^2)\psi_0(\vec{r}) = 0 \quad \text{and} \quad (\vec{\nabla}^2 + k^2)G(\vec{r}) = \delta(\vec{r}) \quad \text{with} \quad k^2 = \frac{2mE}{\hbar^2}. \tag{2.3}$$

We are interested in the situation of a plane wave propagating towards the center of the scattering potential and then being scattered by it. It is therefore natural to take $\psi_0(\vec{r}) = e^{i\vec{k_i}.\vec{r}}$ representing the incident plane wave with wave vector $\vec{k_i} = k\vec{u_i}$, $\vec{u_i}$ being the direction of propagation of this plane wave. On the other hand, we retain only the retarded Green's function corresponding to an outgoing scattered wave. It is further assumed that the potential is only significant in a region L, and we are interested in the form of the wave function for $r \gg L$. The general solution (2.2) therefore takes the following form [74]

$$\psi(\vec{r}) = e^{i\vec{k_i}.\vec{r}} + \frac{e^{ikr}}{r}f(\theta,\phi) \quad \text{with} \quad f(\theta,\phi) = -\frac{m}{2\pi\hbar^2}\int d^3\vec{r}e^{-ik\vec{u}.\vec{r}}V(\vec{r})\psi(\vec{r}) \quad \text{and} \quad \vec{u} = \frac{\vec{r}}{r}. \tag{2.4}$$

As expected, the second term in the right hand side descries a spherical outgoing wave This solution is not analytic since the function f depends on ψ. One could replace this ψ by the entire right hand side and repeat this procedure infinitely. From there the usual approximation, called the Born approximation, consists of taking into account only the lowest order term in V, leading to the following approximate solution

$$f(\theta,\phi) = -\frac{m}{2\pi\hbar^2}\int d^3\vec{r}e^{-ik(\vec{u}-\vec{u_i}).\vec{r}}V(\vec{r}). \tag{2.5}$$

One can then express the differential cross section in term of (2.5). To do so, remember that the differential cross section $\sigma(\theta,\phi)$ is defined as

$$dn = \sigma(\theta,\phi)F_i d\Omega, \tag{2.6}$$

where F_i is the incident flux of particle and dn is the number of particle per second scattered in the solid angle $d\Omega$ centered around θ and ϕ. It is then possible to compute dn and F_i from the solution (2.4). One can conclude that the differential cross section is given by [74]

$$\sigma(\theta,\phi) = |f(\theta,\phi)|^2 = \left| \frac{m}{2\pi\hbar^2} \int d^3\vec{r} e^{-ik(\vec{u}-\vec{u_i}).\vec{r}} V(\vec{r}) \right|^2 . \tag{2.7}$$

Let us now turn to the study of scattering processes in QFT. In this context, there is no quantity such as $V(r)$ known a priory. It is however possible to compute transition amplitudes between an initial and a final state of fields. This quantity is generally referred to as $\mathcal{M}$ and is obtain perturbatively as a sum of many terms $\mathcal{M} = \sum_i \mathcal{M}_i$, each of which is associated with a Feynman diagram. It turns out that the differential cross section of the scattering process considered can be reconstructed from this quantity using the following formula [62]

$$\sigma(\theta,\phi) = \frac{|\mathcal{M}|^2}{64\pi^2 E_{CM}^2}, \tag{2.8}$$

where E_{CM} is the total energy in the center of mass. Considering the non-relativistic limit (i.e. that the momentum of the incident waves is non-relativistic), it is expected that the predictions made in this way should correspond to the non-relativistic reasoning presented above. By replacing the expression for the differential cross section (2.7) in the result (2.7) and then performing an inverse Fourier transform, one can define a notion of scattering potential in QFT given by the following expression

$$V(\vec{r}) = \frac{\hbar^2}{4mE_{CM}} \int e^{i\vec{k}.\vec{r}} |\mathcal{M}| d^3k. \tag{2.9}$$

The transition amplitude $\mathcal{M}$ is usually written as a power series of the coupling constant between the fields (e.g. the fine structure constant α in QED). Therefore, the scattering potential can be computed at different order with respect to the coupling constant. In QED, the dominant term correspond to the Coulomb potential, one can perform the computation at next order with α and would fine quantum corrections [72]. Let us conclude this section by pointing out that the scattering potential introduced here is an approximate quantity (since it is based on the Born approximation), and that it is associated with scattering processes. There is, however, no simple quantity in classical gravity describing the process of plane-wave scattering. It will therefore be complicated to compare the result 2.9 in the case of gravity with the result we would obtain in classical general relativity. This is why, in the next subsection, we will look at another notion of interaction potential with a clear physical meaning and a simple classical analog in general relativity.

2.1.2 Static potential

The potential presented in the previous section is relevant for scattering processes, i.e. for dynamical situations. We will now introduce a notion of static potential describing the interaction of two static point sources. The advantage of this quantity is that, in the case of general relativity, there is a simple quantity describing the exact same physical situation which can then be compared with the quantum corrected one. This notion of static potential has been widely used in QCD to study

the confinement of quarks [73]. We will briefly present how this quantity can be derived and, in a second time, illustrate how it can be used in the case of massive QED. Let us start by noting J the source term that describes the interacting objects. We will then denote $|n\rangle_J$ the eigenstates of the Hamiltonian containing a source term $H(J)$, associated with the eigenvalues $E_n(J)$. The vacuum state when the source is switched off is denoted $|0\rangle$ and has zero energy. We assume that the source is switched on at $t = -\frac{T}{2}$ and off at $t = \frac{T}{2}$. The transition amplitude from vacuum to vacuum between these two instants is evaluated as follows

$$\langle 0| e^{-\frac{i}{\hbar}H(J)T} |0\rangle = \frac{Z(J)}{Z(J=0)}. \tag{2.10}$$

By introducing the identity, one has

$$\frac{Z(J)}{Z(0)} = \sum_n \langle 0| e^{-\frac{i}{\hbar}H(J)T} |n\rangle_{JJ} \langle n| 0\rangle = \sum_n |\langle 0 |n\rangle_J|^2 e^{-\frac{i}{\hbar}E_n(J)T}. \tag{2.11}$$

One can then perform the change $T \to T(1+i\epsilon)$, with $\epsilon \ll 1$ a regulator, and take the limit $T \to +\infty$. This enables to isolate the first term of the sum, by removing the regulator ϵ we obtain

$$E_0(J) = \lim_{T\to+\infty} \frac{i\hbar}{T} \log \frac{Z(J)}{Z(0)}. \tag{2.12}$$

The quantity thus obtained corresponds to the minimum of energy due to the presence of the source J. If we choose static sources, this energy will be there self-energy as well as their energy of interaction. This formula is of great use in QCD, for example, since it shows that the energy of interaction between quarks contains a linear term depending on the distance separating them, responsible for confinement [62, 73]. In order to illustrate the usefulness of (2.11), we will quickly review how it can be applied in the case of massive QED, i.e. for a massive vector field (cf [75] for more details). The action of a massive vector field A_μ coupled to a source J_μ is

$$S[A_\mu] = \int dx^4 \left(-\frac{1}{4} F^{\mu\nu} F_{\mu\nu} + \frac{1}{2} m^2 A_\mu A^\mu + A_\mu J^\mu \right) \tag{2.13}$$

with $F_{\mu\nu} = \partial_\mu A_\nu - \partial_\nu A_\mu$. The partition function obtained from this action is

$$Z(J) = \int DA_\mu e^{\frac{i}{\hbar}\int dx^4 (A^\mu B_{\mu\nu} A^\nu + A^\mu J_\nu)} \tag{2.14}$$

where $B_{\mu\nu} = (\partial^2 + m^2)\eta_{\mu\nu} - \partial_\mu\partial_\nu$ is the heat kernel directly obtained from (2.13). It is possible to rewrite this Gaussian integral as follows

$$Z(J) = Z(0) e^{-\frac{i}{2\hbar}\int d^4x d^4y J^\mu(x) D_{\mu\nu}(x-y) J^\nu(y)} \tag{2.15}$$

We introduced the field propagator $D_{\mu\nu} = B^{-1}_{\mu\nu}$, which in this case admits the following expression

$$D_{\mu\nu}(x) = \int \frac{d^4k}{(2\pi)^4} \frac{k_\mu k_\nu/m^2 - \eta_{\mu\nu}}{k^2 - m^2} e^{ik^\mu x_\mu}. \tag{2.16}$$

We then choose a source representing two static particles, one positively charged at the origin and the other negatively charged at $\vec{R}$, more formally one has

$$J^\mu(x) = \left[\underbrace{ev^\mu \delta(\vec{x})}_{J_p^\mu(x)} - \underbrace{ev^\mu \delta(\vec{x}-\vec{R})}_{J_n^\mu(x)} \right] \Pi(x^0) \qquad \text{with} \qquad v^\mu = (1,0,0,0). \tag{2.17}$$

The first term in the right hand side represent the positive particle, and the second one the negative one. This source is switched on at $x^0 = -\frac{T}{2}$ and off at $x^0 = \frac{T}{2}$, hence the presence of the function Π equal to 1 when $-\frac{T}{2} \leq x^0 \leq \frac{T}{2}$ and 0 otherwise. By inserting (2.16) and (2.17) in (2.15), and by noticing that the current conservation implies $k_\mu J^\mu = 0$, one can show that

$$\frac{Z(J)}{Z(0)} = e^{\frac{i}{2\hbar}\int d^4x d^4y \frac{d^4k}{(2\pi)^4} \frac{\eta_{\mu\nu}(J_p^\mu(x)J_p^\nu(y) + J_n^\mu(x)J_n^\nu(y) - J_p^\mu(x)J_n^\nu(y) - J_n^\mu(x)J_p^\nu(y)}{k^2-m^2} e^{ik^\mu(x_\mu - y_\mu)}}. \tag{2.18}$$

Using (2.12) would lead to a relation between the argument of this exponential and the energy introduced by the source (2.17), namely the self energy of the two particles as well as there energy of interaction. Since we are only interested by the energy of interaction between the two sources, we will only take into account the two last term in the exponential, the two others representing the self energy of the sources. One can show that the part of(2.18) we are interested in can be written as follows

$$e^{-\frac{i}{2\hbar}\int \frac{d^4k}{(2\pi)^4} dxdy \frac{J_p^\mu(x)J_{n\mu}(y) + J_n^\mu(x)J_{p\mu}(y)}{k^2-m^2} e^{ik(x-y)}} = e^{\frac{iTe^2}{8\pi\hbar|\vec{R}|}e^{-m|\vec{R}|}}. \tag{2.19}$$

One can finally deduce by using (2.12) that the energy of interaction of the sources is

$$V_{\text{int}} = -\frac{e^2}{4\pi|\vec{R}|}e^{-m|\vec{R}|}. \tag{2.20}$$

This is the Yukawa potential, which is the expected result for a massive vector field such as that describing pions, for example. Note also that in the limit $m \to 0$, we recover the Coulomb potential, which is not surprising since the photon field is a massless vector field. In this section, we have introduced two different notions of potential, a scattering potential and a static potential which is actually more an energy than a potential, we shall therefore refer to it in the following as static energy of interaction. In the next section, we will show how general relativity, although non renormalizable, can be treated as an effective field theory, and how these potentials can be computed in this case.

2.2 Perturbative quantum gravity

We will now review some of the main step of the effective field theory treatment of general relativity (for a more complete review of the topic, see [3,4]). We will recall what are the quantum corrections to the Newton's potential this approach enable to predict. First in the case of scattering phenomena [8] and then in the case of interaction between static objects [10,76]. We will see that these results allow us to deduce certain properties about the quantum properties of black holes in the low energy regime. We will be paying particular attention to the way in which the gauge is fixed in these

computations, since our aim is to compare these results with those obtained by describing a black hole with a (modified) Schwarzschild metric.

2.2.1 1 loop correction to the scattering potential

We will now sketch out the quantization of linearized gravity. This is an approach initiated long ago by t'Hooft and Veltmann in [1], a more pedagogical presentation can be found in [63]. The aim is to present the minimal formalism needed to understand how graviton corrections to Newton's potential can be obtained when studying scattering processes and then in the case of static sources. The first step is to add a gauge fixing and a ghost term to the Einstein Hilbert action, leading to the following pure gravity action

$$\mathcal{S}_{\text{PG}} = \int d^4x \left[\underbrace{\sqrt{-g}\frac{2}{\kappa^2}R}_{\mathcal{L}_{\text{EH}}} + \underbrace{\frac{1}{\xi}\sqrt{-g}\left(\partial^\nu h_{\mu\nu} - \frac{1}{2}\partial_\mu h\right)^2}_{\mathcal{L}_{\text{gf}}} + \underbrace{\sqrt{-g}\eta^{*\mu}\partial^\lambda\partial_\lambda\eta_\mu}_{\mathcal{L}_{\text{ghost}}} \right], \tag{2.21}$$

where ξ is usually taken to be 1, and η is the gauge field, which is a fermionic vector field. One can then couple gravity to a matter source. As the aim is to compute the potential introduced in the subsections 2.1.1 and 2.1.2, different source terms will have to be considered.

In order to determine the scattering potential introduced in subsection 2.1.1, we start by adding to the action (2.21) the following Lagrangian density corresponding to two massive scalar fields that while be scattered

$$\mathcal{L}_{\text{scalar field}} = \frac{1}{2}\sqrt{-g}\sum_{i=1,2}\left(D^\mu\phi_i D_\mu\phi_i - m_i^2\phi_i^2\right). \tag{2.22}$$

The two fields interact via exchanges of gravitons and the scattering amplitude of an plane wave of ϕ_1 with one of ϕ_2 can be perturbatively computed. The computation can in principle be done at any order in G in the low energy regime, without the non renormalizability of general relativity being a problem [3]. In practice, the computation of this scattering amplitude was performed at one loop (i.e. at order G^2), and it was then possible to estimate the first graviton correction to Newton's potential via the formula (2.9). After several attempts and self-corrections [5–7], the established result is the following one [8]

$$V_{\text{scat}}(R) = -\frac{Gm_1m_2}{R}\left(1 + 3\frac{G(m_1+m_2)}{R} + \frac{41}{10\pi}\frac{G\hbar}{R^2}\right) + \mathcal{O}(G^3), \tag{2.23}$$

where the sub-index "scat" refers to the fact that this quantity is related to a scattering process. This is the best known result in the effective field theory treatment of general relativity, and it is notably this result that is compared with non perturbative black hole models [53–55]. However, this quantity is related to the scattering of plane waves, and therefore of completely delocalized objects. It is hard to conceive that this prediction can be directly used to describe the quantum behavior black holes, which are localized objects. It is sometimes argued that by taking the limit $m_1 \gg m_2$, the result (2.23) describes the interaction of a test object (of mass m_2) with a black hole (of mass m_1). But this limiting case still corresponds to the interaction of two delocalized objects.

2.2.2 1 loop correction to the energy of interaction

On the other hand, it is possible to use the notion of static energy of interaction, introduced in subsection 2.1.2, to determine the first graviton correction to the energy of interaction of two static and localized sources. To do so, we consider that the sources involved are described by the following energy momentum tensor

$$T^{\mu\nu}(x) = m\delta_0^\mu\delta_0^\nu\delta^{(3)}(x-x_1) + M\delta_0^\mu\delta_0^\nu\delta^{(3)}(x-x_2). \tag{2.24}$$

This tensor corresponds to two static and point-like, one with mass m at $x_1 = (t_1, \vec{0})$ and the other with mass M at $x_2 = (t_2, \vec{R})$. This energy momentum tensor corresponds to adding the following term to (2.21)

$$S_{\text{static}} = -m\int_0^T dt\sqrt{g_{tt}(t,\vec{x}_1)} - M\int_0^T dt\sqrt{g_{tt}(t,\vec{x}_2)}. \tag{2.25}$$

The formula (2.12) can then be used to perturbatively compute the energy of interaction the sources considered. Here Again the computation can theoretically be performed at any order in G in the low energy regime. The first quantum correction was computed in [10] and is given by

$$V_{\text{static}} - \frac{GmM}{R}\left(1 - \frac{G(m+M)}{2R} + \frac{17G\hbar}{20\pi R^2}\right). \tag{2.26}$$

As can be seen, the expressions (2.23) and (2.26) differ. This should not be surprising since, as we have already mentioned, these two quantities describe completely different physical situations and therefore have no reason to coincide. Note also that in the classical limit $\hbar \to 0$, the two results do not coincide either. Indeed, the expressions (2.23) and (2.26) have different post-Newtonian (PN) corrections. This should not worry us either, since there are also several notions of potential in general relativity, corresponding to different physical situations and containing different post-Newtonian corrections. In the next section, we will focus on static interactions in the regime where one of the first objects is much heavier than the second (i.e. $M \gg m$). In this case, the potential (2.26) becomes

$$V_{\text{static}} = -\frac{GmM}{R}\left(1 - \frac{GM}{2R} + \frac{17G\hbar}{20\pi R^2}\right) + \mathcal{O}(G^3). \tag{2.27}$$

This system, of two static objects in gravitational interaction with one of the two objects much heavier than the second, corresponds classically to a static test particle in a Schwarzschild metric. In the following section, we will present the formula giving the energy of interaction of such a static particle in a Schwarzschild metric. We will then generalize the computation for a modified metric with quantum terms and see under which conditions the result (2.27) is reproduced.

2.3 Comparison with modified Schwarzschild spacetime

In this section, we will start by deriving the formula for the energy of interaction of a static test particle in a Schwarzschild metric. In particular, it will be important to write this formula in the same gauge as that used in the subsection 1.1.1. It will then be possible to observe that the formula

thus obtained agrees with (2.27) in the classical limit. We will then use a generalized version of this formula to show that the Hayward metric, which is one of the most common modified Schwarzschild metrics, does not allow us to recover (2.27). We will close the section by writing the most general modified metric that reproduces the perturbative result.

2.3.1 Static potential in general relativity

Let use consider a test particle of mass m, for now not necessarily static, evolving in a Schwarzschild metric of mass M. The Lagrangian of such a particle is

$$L = -m\frac{d\tau}{dt}, \tag{2.28}$$

where τ is the proper time of the test particle and t is the proper time of a static observer at infinity. We then consider that the point particle is moving in a Schwarzschild geometry and following a radial trajectory. The proper time is given by the following expression

$$d\tau^2 = \left(1 - \frac{2M}{r}\right) dt^2 - \frac{dr^2}{1 - \frac{2M}{r}}. \tag{2.29}$$

We introduce the velocity $v = \frac{dr}{dt}$, and by using (2.29) the Lagrangian 2.28 becomes

$$L_{\text{Sch}} = -m\left[1 - \frac{2M}{r} - \frac{v^2}{1 - \frac{2M}{r}}\right]^{1/2}. \tag{2.30}$$

The sub index "Sch" indicates that this is the expression of the Lagrangian for a particle in a Schwarzschild spacetime. The next step is to perform a Legendre transformation to obtain the Hamiltonian of this test particle. The conjugate moment is obtained directly from (2.28), and the expression for the Hamiltonian follows from this.

$$p = \frac{\partial L}{\partial v} = m\frac{\frac{v}{1-\frac{2M}{r}}}{\left[1 - \frac{2M}{r} - \frac{v^2}{1-\frac{2M}{r}}\right]^{1/2}} \quad \text{and} \quad H_{\text{Sch}} = m\frac{1 - \frac{2MG}{r}}{\left[1 - \frac{2MG}{r} - \frac{v(p)^2}{1-\frac{2MG}{r}}\right]^{1/2}}. \tag{2.31}$$

Since we are interested in a situation where the interacting objects are static, we impose $v = 0$. And since we want to compare this result with the one loop computation presented in subsection 2.27, we can expand this Hamiltonian to order G^2

$$H_{\text{Sch}} = m + V_{\text{int}}^{\text{Sch}} \quad \text{with} \quad V_{\text{int}}^{\text{Sch}} = -\frac{GMm}{r}\left(1 + \frac{GM}{2r^2}\right) + \mathcal{O}(G^3) \tag{2.32}$$

We directly recognize the usual Newtonian potential term in the expression of the energy of interaction, together with a term of order G^2 which is a PN correction. There is obviously no quantum corrections in (2.32) since the Schwarzschild spacetime is purely classical. We will consider in what follows other black hole metrics, modified by quantum terms. In order to test which of these metrics

are able to reproduce the correct quantum correction, we need to generalize the previous computation to the case of a general static and spherically symmetric spacetime, i.e. for metrics of the form

$$ds^2 = g_{tt}dt^2 + g_{rr}dr^2 + r^2 d\Omega^2. \tag{2.33}$$

In this case, the Lagrangian of a particle moving only radially is $L = -m\sqrt{g_{tt} - g_{rr}v^2}$. The previous canonical analysis can be reproduced leading to the following Hamiltonian

$$H = m\frac{g_{tt}}{\sqrt{g_{tt} - g_{rr}v^2}}. \tag{2.34}$$

One can then require the test particle to be static, and by removing the energy of mass one can deduce the generalized expression for the energy of interaction.

$$V_{\text{int}} = m(\sqrt{g_{tt}} - 1). \tag{2.35}$$

Before using this result for modified Schwarzschild metric, we will see how to switch from the area radius gauge used in (2.33) (and in most of the modified black hole models one can find in the literature) to the harmonic gauge used in section 2.2.

2.3.2 The harmonic gauge for spherically symmetric and static spacetime

The energy of interaction (2.27) was obtained by imposing the harmonic gauge (1.7) and some additional boundary conditions listed in subsection (1.1.2). The quantity R appearing in (2.27) is therefore the harmonic radial coordinate defined by

$$R = \sqrt{X_1^2 + X_2^2 + X_3^2}, \tag{2.36}$$

where X_1, X_2 and X_3 satisfy (1.6). This is not a common gauge choice when working with modified black hole metrics. The area radius r is often preferred. In order to compare (2.27) with (2.32) and (2.35), we shall rewrite these results in the harmonic gauge supplemented by the boundary conditions of subsection 1.1.1. The analysis that follows is similar to what has been done in [77]. It can be shown that in a static, spherically symmetric spacetime, the harmonic gauge (1.6) imposes the following condition between R and r [78]

$$\frac{d}{dr}\left[r^2\sqrt{\left|\frac{g_{tt}}{g_{rr}}\right|}\frac{dR}{dr}\right] - 2R\sqrt{|g_{tt}g_{rr}|} = 0. \tag{2.37}$$

Let us start by considering the case of the Schwarzschild metric. In this situation, the previous equation admits the following solution

$$R(r) = C_1\,(r - MG) + C_2\left(\frac{1}{2}\,(r - m_1 G)\log\left|\frac{1}{1 - \frac{2MG}{r}}\right| - m_1 G\right). \tag{2.38}$$

This solution contains two constants of integration C_1 and C_2, as (2.37) is a second order differential equation. The presence of these two constants, which we are free to choose as we wish, reveals that

the harmonic gauge is not a complete gauge fixing. We can impose the same fall off conditions on R that we considered in subsection 1.1.1 to completely fix the gauge. On the one hand, condition **(1)** requiring harmonic coordinates to be bounded everywhere imposes that $C_2 = 0$. On the other hand according to condition **(2)**, the harmonic coordinates must coincide with the Cartesian coordinates at infinity. This is equivalent to requiring that $R(r) \xrightarrow{r\to+\infty} r$, in other words, imposing $C_1 = 1$. With these choices the solution (2.38) simplifies and becomes unique, the Schwarzschild line element can be written in the harmonic gauge as follows

$$ds^2 = \frac{R-MG}{R+MG}dt^2 - \frac{R+MG}{R-MG}dR^2 + (R+MG)^2 d\Omega^2 \quad \text{with} \quad R = r - MG. \tag{2.39}$$

In this gauge, the result (2.32) becomes

$$V_{\text{int}}^{\text{Schw}} = -\frac{GMm}{R}\left(1 - \frac{GM}{2R}\right) + \mathcal{O}(G^3). \tag{2.40}$$

As one can see, this result contains the same PN correction as (2.27). We can conclude that, in addition to having the same physical meaning, the two results (2.40) and (2.27) coincide in the classical limit. In the next subsection, we will discuss the possibility of recovering the same quantum correction as in (2.27) by choosing an appropriate modified Schwarzschild metric.

2.3.3 The most general metric

From the previous subsection, we have a way to test whether a modified quantum Schwarzschild metric in the low-energy regime is consistent with the effective treatment of general relativity. We conclude this section by going one step further and writing the most general metric that reproduces this perturbative prediction. To do this, we look for the metric such that, by inserting its g_{tt} component written in the harmonic gauge into (2.35) and expanding to order G^2, the result coincides with (2.27). This is achieved for

$$g_{tt} = 1 - \frac{2GM}{R} + \frac{2G^2M^2}{R^2} - \frac{17G^2\hbar M}{10\pi R^3} + \mathcal{O}\left(G^3\right). \tag{2.41}$$

This is the most general metric enabling the perturbative prediction to be reproduced. It is important to note that this result was obtained using the harmonic gauge (as well as some boundary conditions mentioned in subsection 1.1.1). The R coordinate is not the area radius but the harmonic radius. In order to translate the condition (2.41) into the radial gauge, which is the most commonly used gauge, we need to solve the equation (2.37). This would lead to a relation between R and r, which would allow to rewrite (2.41) with r. However, no condition is imposed on g_{rr}, which means that the equation (2.37) is implicit and cannot be solved in full generality. However, we want to make predictions at the order G^2. Moreover, as we saw in the section 2.2, one-loop results are of order $\hbar$. It is therefore natural to consider the following anzats for the solution of the equation (2.37), as well as for the g_{tt} and g_{rr} components of the metric

$$r = R + GM + a_1\frac{G\hbar}{R} + a_2\frac{G^2M^2}{R} + a_3\frac{G^2M\hbar}{R^2} + \mathcal{O}(G^3) + \mathcal{O}(\hbar^2), \tag{2.42}$$

$$g_{tt} = 1 - \frac{2GM}{r} + b_1\frac{G\hbar}{r^2} + b_2\frac{G^2M^2}{r^2} + b_3\frac{G^2M\hbar}{r^3} + \mathcal{O}(G^3) + \mathcal{O}(\hbar^2), \tag{2.43}$$

$$g_{rr} = -\left(1 - \frac{2GM}{r} + c_1\frac{G\hbar}{r^2} + c_2\frac{G^2M^2}{r^2} + c_3\frac{G^2M\hbar}{r^3}\right) + \mathcal{O}(G^3) + \mathcal{O}(\hbar^2). \tag{2.44}$$

At this stage it is assumed that the solution (2.37) can be written as (2.42). We will now see how to fix the coefficients $a_1, a_2, a_3, b_1, b_2, b_3, c_1, c_2$ and c_3 so that the equation (2.37) and the condition (2.41) are satisfied. Using the uniqueness theorem as in 2.3.2, it will be possible to assert that (2.37) is the only solution to (2.42). We start by inserting (2.42) into (2.43) and obtain

$$g_{tt} = 1 - \frac{(2MR - b_1\hbar)G}{R^2} + \frac{(2+b_2)G^2M^2}{R^2} + \frac{(2a_1 - 2b_1 + b_3)G^2M\hbar}{R^3} + \mathcal{O}(G^3) + \mathcal{O}(\hbar^2). \tag{2.45}$$

For this expression to be consistent with (2.41), one must impose

$$b_1 = b_2 = 0 \quad \text{and} \quad a_1 = -\frac{17}{20\pi} - \frac{b_3}{2}. \tag{2.46}$$

On the other hand, one can invert the relation (2.42) to have an expression of R in terms of r. This can be done by solving (2.42), which is an order 3 polynomial equation in R. The analytic solution is rather tedious, and since we are interested in relations at the order G^2 and $\hbar$, it will be easier to directly consider the following expression for R.

$$R = r - GM + \alpha_1\frac{G\hbar}{r} + \alpha_2\frac{G^2M^2}{r} + \alpha_3\frac{G^2M\hbar}{r^2} + \mathcal{O}(G^3), \tag{2.47}$$

where $(\alpha_1, \alpha_2, \alpha_3)$ are numerical factors that can be expressed in terms of (a_1, a_2, a_3) by solving (2.42). In fact, by inserting (2.42) into (2.47) and taking into account (2.46), one gets

$$R = R - \frac{(10\pi b_3 - 20\pi\alpha_1 + 17)G\hbar}{20(\pi R)} + \frac{G^2M^2(a_2+\alpha_2)}{R} + \frac{G^2M\hbar(a_3 - \alpha_1 + \alpha_3)}{R^2} + \mathcal{O}\left(G^3\right) + \mathcal{O}\left(\hbar^2\right). \tag{2.48}$$

For consistency, we therefore need to impose the following relations

$$\alpha_1 = \frac{b_3}{2} + \frac{17}{20\pi}, \quad \alpha_2 = -a_2 \quad \text{and} \quad \alpha_3 = \frac{b_3}{2} + \frac{17}{20\pi} - a_3. \tag{2.49}$$

One can then insert (2.48), (2.43) and (2.44) in (2.37) and show that

$$\frac{d}{dr}\left[r^2\sqrt{\left|\frac{g_{tt}}{g_{rr}}\right|}\frac{dR}{dr}\right] - 2R\sqrt{|g_{tt}g_{rr}|} = -\frac{(\frac{17}{10\pi} + (c_2 + b_3))G\hbar}{r} - \frac{G^2M^2(c_1 + 2\alpha_2 - 4)}{r} - \frac{G^2M\hbar(\frac{17}{10\pi} + \frac{1}{2}(5b_3 - 2c_2 + c_3))}{r^2} + \mathcal{O}(G^3) + \mathcal{O}(\hbar^2). \tag{2.50}$$

Since we want the right hand side of this equation to be 0 at order G^2 and $\hbar$, one must impose

$$\alpha_2 = 2 - \frac{c_1}{2}, \quad b_3 = -\frac{17}{10\pi} - c_2 \quad \text{and} \quad c_3 = \frac{51}{10\pi} + 7c_2. \tag{2.51}$$

In summary, we can see from (2.46), (2.49) and (2.51) that all parameters introduced in this section can be expressed in terms of a_3, c_1 and c_2. The most general relation between r and R satisfying (2.37) and taking into account (2.41) is

$$r = R + GM - \frac{17}{20\pi} + \frac{1}{2}\left(\frac{17}{10\pi} + c_2\right)\frac{G\hbar}{R} + \left(\frac{c_1}{2} - 2\right)\frac{G^2M^2}{2R} + a_3\frac{G^2\hbar M}{R^2} + \mathcal{O}(G^3) + \mathcal{O}(\hbar^2), \tag{2.52}$$

and the most general metric components written in the area radius gauge and satisfying (2.41) are

$$g_{tt} = 1 - \frac{2GM}{r} - \left(\frac{17}{10\pi} + c_2\right)\frac{G^2\hbar M}{r^3} + \mathcal{O}(G^3) + \mathcal{O}(\hbar^2) \tag{2.53}$$

$$g_{rr} = -\left(1 - \frac{2GM}{r} + c_1\frac{G\hbar}{r^2} + c_2\frac{G^2M^2}{r^2} + \left(\frac{51}{10\pi} + 7c_2\right)\frac{G^2\hbar M}{r^3}\right) + \mathcal{O}(G^3) + \mathcal{O}(\hbar^2) \tag{2.54}$$

One can notice that the relation between r and R given by (2.52) satisfies the boundary conditions mentioned in the subsection 2.3.2 and is therefore the unique solution at this order in G and $\hbar$. Moreover it can be noted that the fact that this relation, as well as the expressions of the metric component (2.53), depend on three free parameters is consistent with the fact that in the harmonic gauge, only g_{tt} is constrained by (2.41) and not g_{RR}. Indeed, at order G^2 and $\hbar$, the latter can be written as

$$g_{RR} = -\left(1 + \frac{2GM}{R} + \kappa_1\frac{G\hbar}{R^2} + \kappa_2\frac{G^2M^2}{R^2} + \kappa_3\frac{G^2M\hbar}{R^3}\right) + \mathcal{O}(G^3) + \mathcal{O}(\hbar^2), \tag{2.55}$$

and also depends on three parameters κ_1, κ_2 and κ_3. In order to reproduce the modified metric (2.41) proposed by the perturbative approach, it is therefore necessary to modify both g_{tt} and g_{rr} in the area radius gauge. We can also note that the relations (2.53) impose that

$$g_{tt} \neq -\frac{1}{g_{rr}}. \tag{2.56}$$

In the next subsection, we will look at some of the modified black hole models proposed in the literature and discuss their ability to reproduce the result (2.41).

2.3.4 Testing modified Schwarzschild metrics with the perturbative approach

We now have everything we need to test which non perturbative quantum black hole models correctly reproduce the perturbative result presented in subsection 2.2.2. To do this, we simply have to write down the metric we want to test in the harmonic gauge and compare its g_{tt} component with (2.41). Or, and it will often be more convenient, we can write the metric in the area radius gauge and compare its g_{tt} and g_{rr} components with (2.53). Let us illustrate this procedure with the Hayward metric [11], expressed as follows

$$g_{\mu\nu}dx^\mu dx^\nu = \left(1 - \frac{2MGr^2}{r^3 + 2MG^2\hbar}\right) dt^2 - \frac{dr^2}{1 - \frac{2MGr^2}{r^3+2MG^2\hbar}} - r^2 d\Omega^2. \tag{2.57}$$

This metric is written in the area radius gauge and one can easily expand its g_{tt} and g_{rr} components at order G^2 and $\hbar$

$$g_{tt} = 1 - \frac{2MG}{r} + \mathcal{O}(G^3) + \mathcal{O}(\hbar^2) \tag{2.58}$$

$$g_{rr} = -\left(1 + \frac{2MG}{r} + \frac{4G^2M^2}{r^2}\right) + \mathcal{O}(G^3) + \mathcal{O}(\hbar^2). \tag{2.59}$$

It is straightforward to see that it is impossible to choose the free parameters appearing in (2.53) to obtain the previous expansion of the Hayward metric components. The Hayward metric is therefore not consistent with the perturbative computation presented in section 2.2. We could have reached the same conclusion by noting that this metric does not satisfy (2.56). We also note that it is not possible to modify only the g_{tt} component of the Hayward metric to reproduce (2.53), despite what was suggested in [55]. This subsection clearly illustrates how the perturbative result (2.53) can be used to test the relevance of some non perturbative modified black hole models. We will see in chapter 4 (cf subsection 4.4.3) how the perturbative result can be used in a more constructive way by fixing some ambiguities that can appear in the construction of non perturbative modified black hole models.

2.4 Conclusion

Despite the non renormalizability of general relativity, treating it as an effective field theory in a perturbative way enables finite and reliable predictions at low energy (i.e. in regimes where the curvature is small compared to the Planck curvature). Predictions made in this way are independent of the complete underlying quantum gravity theory, as yet unknown, and must therefore be reproduced by the latter at low energy. In a similar way that general relativity had to be in agreement with Newton's theory of gravitation in the non-relativistic limit of low curvature. In this chapter, we reviewed two of the main predictions made by this perturbative approach, which are quantum corrections to the scattering potential and to the energy of interaction of two static sources. The question addressed here is how to use these results to constrain non perturbative quantum gravity theories. In the absence of such a complete theory, we have focused on the case of black holes. In the literature, there are a large number of quantum black hole models formulated as modified Schwarzschild metrics. Although the main interest of such models is to propose a scenario in the Planckian curvature region and address the singularity problem, they have to agree with perturbative predictions in the low curvature regime. We have seen that the quantum correction to the energy of interaction of two static sources obtained by the perturbative approach can, in the case where one of the two objects is much more massive than the other, be interpreted as a quantum correction to the energy of interaction of a static test particle in a black hole. This computation provides a clear prediction of the quantum modifications of the Schwarzschild black hole in the low energy regime. We have also seen how, given a modified Schwarzschild metric, the energy of interaction of a static particle in such a metric is related to the expression of the metric components. It

was then possible to write down the most general metric reproducing the correct expression for the energy of interaction. In order to compare modified Schwarzschild metrics with the perturbative predictions, we had to be careful to treat the gauge freedom in the same way in both cases. In the perturbative approach, it is necessary to fix the gauge in order to obtain the graviton propagator. This is usually done by imposing the harmonic gauge and a number of boundary conditions. We have seen how to fix the same gauge in the non perturbative approach. We have also seen how this most general metric can be written in the radius gauge area. Finally, we have ended this chapter by showing that in the case of the Hayward metric, the perturbative prediction is not reproduced, calling into question the validity of this model. On the other hand, it was possible to use the perturbative results to fix certain ambiguities inherent in the construction of non perturbative models, here the polymer black hole models. In particular, we have seen that the usual choice for these ambiguities, i.e. the sine function for polymerization functions, does not allow us to recover the perturbative prediction. We will end this section by pointing out that effective theories such as gravitation have the advantage of clearly revealing their limitations. Indeed, these theories naturally introduce an energy scale (in the case of gravitation, this corresponds to the Planck scale), and are only valid for energies lower than the Planck scale, since they require the higher derivative terms in the Lagrangian to be subdominant. For gravity, this means that the effective treatment is no longer predictive at the Planck scale, so this perturbative approach is notably not suitable for studying the quantum effects of geometry at singularities such as those present at the big bang or at the center of black holes. In the rest of this thesis, we will explore other non-perturbative approaches to studying these high-energy regimes.

Part II

Black holes in Loop Quantum Gravity

Our focus in this part will be on non-perturbative quantum gravity models, motivated by loop quantum gravity, to study Planck energy regimes. An emblematic problem of quantum gravity arising in these regimes is to understand the fate of the black hole singularity predicted by general relativity. Aside from extremely simplified 2d models, see e.g. [79, 80], explicit calculations are not within current reach, and this motivates the study of models simplified by symmetry considerations, known as minisuperspace or symmetry reduced models, to shed useful light on the qualitative aspects of the process.

In loop quantum gravity, minisuperspace models are constructed using the key input from the full theory that the fundamental quantum operators are holonomies of the Ashtekar-Barbero connection. These are defined in a representation which lacks weak-continuity, thus making the models unitary inequivalent to those based on metric variables. We will present this construction in more detail in chapter 3. As we will see in this same chapter, a compelling result of this approach is the generic singularity-avoidance [81], with the minisuperspace dynamics predicting a bounce occurring at a critical energy or curvature density. This is valid in both cosmological [81,82] and black hole [83–87] models. One key aspect of the construction is that the resulting quantum corrections can be equally predicted using an effective classical dynamics, where the original Hamiltonian is modified in a precise way [88]. This step is known as polymerization, and enables a simple description of the system and independent exploration of this type of effective models, known as polymer models. In spite of the compelling singularity resolutions, these models are only a first step towards a clear understanding of the non-perturbative quantum gravitational effects.

To move forward, it is important to address their limitations and shortcomings, which will be done as a conclusion to the first chapter. One of the limitations is that the polymerization procedure is a regularization of the classical dynamics. The phase space variables are replace in the classical Hamiltonian by functions of these variables. These functions, called the polymerization function, are not identified a priori from fundamental principles or deductions from the full theory; but rather reconstructed a posteriori requiring a good semiclassical limit at large scales, and there is no uniqueness about the procedure used [89]. The polymerization functions used are typically picked to be a sine. This is supposed to represent working with the holonomy in the fundamental representation in full loop quantum gravity. However it has been known for a while that there may be quantization ambiguities associated with this choice already in the full theory [90].[3] These ambiguities affect models like [93] in which the polymerization scheme is derived from the full theory taking expectation values with respect to symmetry-reduced coherent states. The effect of such ambiguities where recently analyzed in the context of quantum cosmology in [89], showing that they strongly affect the physics. In chapter 4, we will study how changes in the choice of polymer function affect static and spherically symmetric black hole models. The content of this chapter is strongly based on [44].

[3] It has been recently pointed out in [91] that some of the ambiguities can be reduced by a new quantization of the Hamiltonian constraint of the full theory; nonetheless, ambiguities of the type analyzed here remain in the part of the Hamiltonian constraint responsible for non-trivial propagation [92].

On the other hand, those simple effective models are nice as they illustrate possibly generic features of the general situation. However, they carry the drawback of being often removed, by the very symmetry assumptions that simplify them, from the realistic physical situations about which one would like to gain non-trivial insights. Moreover, when it comes to black holes, most of the studies have focused on effective dynamical descriptions [4] , while quantum dynamics has received less attention due to its often insurmountable complexity even in simple models. For instance, concerning the first drawback we know that real black holes are not time translational invariant due to the expected presence of Hawking evaporation (in contrast with the static nature of many of the quantum black hole models) and that all symmetry assumptions must fail near the singularity when the backreaction of Hawking particles correlated with the outside radiation would be properly taken into account (see [50] for further discussion of this issue). When it comes to the second drawback, even when effective descriptions can provide the dynamical evolution of the spacetime geometry with matter fields on it, its classical nature precludes the analysis of genuine quantum phenomena such as entanglement and other quantum information issues of highest interest from the perspective of Hawking's evaporation (e.g. the longstanding information puzzle or the question of the fate of unitarity in black hole evaporation). Although this does not resolve the first limitation, we will present a model in chapter 5 that we believe represents a humble step in the right direction. Concerning the second, we will see that the quantum dynamics is fully accessible in our simple model opening the road for exact computations in the quantum realm.

From now and for the rest of the thesis, we use the signature $(-1, 1, 1, 1)$. We will also use the convention $c = \hbar = G = 1$ in order to work in Planck units.

3 From LQG to polymer quantum black holes

The aim of this section is to outline the construction of quantum models of black holes inspired by LQG, namely the polymer black hole models. It will also allow us to introduce some of the notations and definitions that will be used in the rest of this part. We will give a short but self consistent presentation of these models. To this end, it will be necessary to start with a brief introduction to the main ideas on which LQG is based. We shall show how general relativity can be formulated as a gauge theory, thanks to the Ashtekar-Barbero variables. We will then see how these variables are smeared to form the so-called holonomy-flux algebra. We will not, however, enter into the details of the quantization of this algebra, the construction of the kinematic Hilbert space, the construction of the operator associated with the Hamiltonian constraint or the construction of the area and volume operators. Nevertheless, we will mention that the latter admit discrete spectra. This is why it is commonly claimed that LQG predicts a discreteness of space. The second step will be to reproduce the same construction for symmetry reduced models, i.e. models for which symmetries of the geometry are assumed before proceeding to quantization. More precisely, we will start by looking at the FRLW cosmological model, for which spacetime is considered homogeneous and isotropic. We will see how Ashtekar-Barbero variables can be used to formalize the classical dynamics of such a system. This dynamics is obviously the same as the one obtained with the usual

[4] The word effective refers here to the fact that these models are formalized as a trajectory in a phase space generated by a modified Hamiltonian, an effective Hamiltonian. There is no reference to the effective treatment of general relativity presented in the previous part.

geometrodynamic variables. We will discuss the possibility of applying the canonical quantization method to this formulation (with Ashtekar-Barbero variables or with geometrodynamic variables), leading to the Wheeler-DeWitt quantum cosmology. It is well known, however, that this approach fails to remove the classical singularity predicted at the first moment of the universe. In the second section, we present the main steps in the construction of LQC, which consist in reproducing that of LQG. After having smeared the Ashtekar-Barbero variables in the case of cosmology, we will present the new algebra satisfied by the smeared phase space variables, analogous to the holonomy-flux algebra in LQG. From this point on, it will be possible to study the quantum dynamics, and we will review how the latter naturally leads to a resolution of the classical singularity. In the last subsection, we present the so-called polymerization procedure, resulting more directly in the resolution of the singularity. This method leads to an effective description in the sense that the classical Hamiltonian is modified by terms important only at the Planck scale. In particular, we will discuss how the validity of this method is usually supported in the literature. Finally, we will present how this polymerization procedure has been applied to the case of black holes in recent years, and how the models thus constructed provide a solution to the problem of singularity at their centers. Finally, we will mention a number of problems that these models present, which will serve to motivate the rest of this part.

3.1 General relativity as a gauge theory

Two results from LQG are necessary in order to construct LQC. One is the discreteness of space, initially suggested in [94] by developing a volume and surface operator acting on the kinematic Hilbert space of LQG. In the following, this result will be admitted without review. The second ingredient is the formulation of general relativity as a gauge theory. This is made possible by the Ashtekar-Barbero variables and the holonomy-flux algebra that can be derived. Let us start with the latter.

3.1.1 Ashtekar-Barbero variables

For the sake of brevity, we will limit ourselves to a brief description of the construction of the Ashtekar-Barbero variables. Several pedagogical reviews on the subject can be found in the literature, such as [95] or [96]. The starting point will be Holst's action in the tetrad formalism

$$S(e,\omega) = \int \left(\frac{1}{2}\epsilon_{IJKL} + \frac{1}{\gamma}\delta_{IJKL}\right) e^I \wedge e^J \wedge F^{KL}, \tag{3.1}$$

where γ is the so called Immirzi parameter, ϵ is the Levi-Civita symbol, e the tetrad, ω the spin connection and F the curvature associated to this connection defined by $F^{IJ} = d\omega^{IJ} + \omega^I{}_K \wedge \omega^{KJ}$. For a more detailed presentation of the tetrad formalism, see [97]. In the following, we will only be interested in the canonical approach, which requires a 3+1 splitting of the spacetime. Spacetime is assumed to be hyperbolic, which means it can be decomposed into a hypersurface space like of dimension 3 that we'll call Σ (parametrized by a set of coordinates x^a, with $a = 1, 2$ or 3) and a timelike direction (parametrized by a coordinate t). The ADM variable is the one usually used to describe the geometry of this decomposition, with N the lapse function, N^a the shift vector and

q_{ab} the metric induced on the hypersurface. A pedagogical and more developed introduction to the ADM formalism can be found in [95]. The normal vector to this hypersurface is usually denoted n^μ. Since tetrads exhibit gauge invariance corresponding to Lorentz transformations in internal space (labeled by the capital Latin superscript), this normal vector can be used to partially fix a gauge by imposing the condition $e^I_\mu n^\mu = \delta^I_0$. This allows to introduce the triad e^i_a with a corresponding to spatial indices and $i = 1, 2$ or 3 to internal indices. Once this partial gauge fixing, called time gauge, has been achieved, it is then possible to introduce the densitized triad

$$E^a_i = \frac{1}{2}\epsilon_{ijk}\epsilon^{abc}e^j_b e^k_c \tag{3.2}$$

as well as the Ashtekar connection

$$A^i_a = \gamma K^i_a + \Gamma^i_a, \tag{3.3}$$

where K^i_a is obtain from the densitized triad and the extrinsic curvature K_{ab} of the spacelike hypersurface Σ, And Γ^i_a is an $so(3)$ connection given in term of the triad. There expressions are respectively

$$K^i_a = \frac{1}{\sqrt{\det(E^{ai})}}K_{ab}E^b_j\delta^{ij} \quad \text{and} \quad \Gamma^i_a = -\frac{1}{2}\epsilon^{ij}_k e^b_j(\partial_{[a}e^k_{b]} + \delta^{kl}\delta_{ms}e^c_l e^m_a \partial_b e^s_c). \tag{3.4}$$

The densitized triad (3.2) and the Ashtekar-Barbero connection (3.3), called the Ashtekar-Barbero variables, present two major interests. The first is that they are a set of conjugate variables, satisfying the following relations

$$\{E^{bj}(x), A_{ai}(x)\} = \kappa\gamma\delta^b_a\delta^j_i\delta^3(x-y), \quad \{E^{bj}(x), E^{ai}(x)\} = 0 \quad \text{and} \quad \{A_{bj}(x), A_{ai}(x)\} = 0. \tag{3.5}$$

Several ways of obtaining these Ashtekar-Barbero variables and showing that they satisfy the commutation relations (3.5) are proposed in the literature [17, 96, 98]. The second interest of these variables stems from the fact that the densitized triad E^i is a vector in internal space and the Ashtekar-Barbero connection A_i is a $su(2)$ connection, thus providing a gauge-theoretic formulation of general relativity. Indeed, this is analogous to QED, where the electric field E, which is a 1 dimensional vector in internal space, and the gauge field A, which is a $u(1)$ connection, are conjugate variables. We shall see in the next subsection how it is possible to reproduce lattice gauge theory (LGT) techniques with this formulation of general relativity. Let us continue by giving the expression of the total Hamiltonian of the system. Details on obtaining the latter are not presented here, but can be found in [17, 95, 96]. With the Ashtekar Barbero variables, the Holst action (3.1) takes the following form

$$S(A, E, N, N^a) = \frac{1}{\gamma}\int dt \int_\Sigma d^3x[\dot{A}_{ai}E^{ai} - A^i_0 D_a E^a_i - NH - N^a H_a]. \tag{3.6}$$

The Hamiltonian density can be read off this action and admit the following expression

$$H = N\mathcal{H} + N^a\mathcal{H}_a + g_i G^i_{rot}, \tag{3.7}$$

Where $\mathcal{H}$, $\mathcal{H}_a$ and G^i are first class constraints generating gauge transformations and can be written as follow

$$\mathcal{H} = \frac{E^{ai}E^{bj}}{\sqrt{E}}(\epsilon_{ijk}F^k_{ab} - 2(1+\gamma^2)K^i_{[a}K^j_{b]}) \tag{3.8}$$

$$\mathcal{H}_a = E^{bi}F_{bai} - (1+\gamma^2)K^i_a G_i \tag{3.9}$$

$$G^i = D_a E^{ai} := \partial_a E^{ai} + \epsilon_{ijk}A_{aj}E^{ak}, \tag{3.10}$$

where $F_{ab} = \partial_a A^i_b - \partial_b A^i_a + \epsilon^i{}_{jk}A^j_a A^k_b$ is the curvature associated to the Ashtekar-Barbero connection A. Furthermore, $\mathcal{H}$ is called the Hamiltonian constraint, $\mathcal{H}^a$ the space-diffeomorphisms constraints and G_i the Gauss constraint. It is well known that the first produces diffeomorphisms in the t direction, while the second produces diffeomorphisms in the spacelike hypersurface. It is easier to see this directly from there expression in the ADM formalism, by computing there Poisson brackets with the ADM variables [95]. The main difference with the tetrad, and then with the Ashtekar-Barbero variables, is that there is an additional symmetry in an internal space, labeled with Latin lowercase $(i, j, k, l...)$, and described by the group $SO(3)$ after fixing the time gauge. Since this group is characterized by the same constant structure as $SU(2)$, it will be equivalent to work with the latter. This is the usual choice, which simplifies the coupling to fermions described also as representations of $SU(2)$. As shown in [95], G_i are the generators of this $SU(2)$ symmetry, since they satisfy the following algebra

$$\{G(\Lambda_1), G(\Lambda_2)\} = \frac{\gamma}{2}G([\Lambda_1, \Lambda_2]) \quad \text{with} \quad G(\Lambda) = \int d^3x G_i(x)\Lambda^i(x). \tag{3.11}$$

Moreover, the Ashtekar-Barbero variables transform in the following way under the action of this generator

$$\{G(\Lambda), E^a_i(y)\} = \gamma\epsilon_{ijk}\Lambda^j(y)E^{an}(y) \quad \text{and} \quad \{G(\Lambda), A^i_a(y)\} = \gamma\partial_a\Lambda^i(y) + \gamma\epsilon_{mji}\Lambda^j(y)A^m_a(y). \tag{3.12}$$

This explicitly illustrates what we mentioned earlier, i.e. that E^{ai} transforms as components of a vector, while A_{ai} transforms as components of a connection on the principal fiber bundle $F = (M, SO(3))$.

In summary, this reformulation of general relativity in terms of the Ashtekar-Barbero variables achieves the key result that the theory can be formulated as a gauge theory with a compact SU(2) group. From there, it is possible to apply non perturbative quantization techniques coming from lattice gauge theory in the present case, which is the starting point of loop quantum gravity.

3.1.2 Regularization of Ashtekar-Barbero variables : the holonomy-flux algebra

At this stage it seems natural to propose to proceed to the canonical quantization of the formalism presented in the previous subsection, i.e. to replace A and E by operators satisfying the algebra (3.5), and the constraints (3.8) by operators to be solved in order to have access to the physical Hilbert space. However, there is a direct obstacle to this procedure coming from the fact that A is a $su(2)$ Lie algebra of valued one form, meaning that the associated operator would act on a space of

functions defined on the Lie algebra $su(2)$. If one wants, for example, to normalize these functions, it will be necessary to integrate them on $su(2)$, which requires a measure on this algebra. However, no such measure exists, which prevents the definition of such an operator $\hat{A}$. To get around this problem, one can take some inspiration from lattice gauge theory. In this approach, a cubic lattice of constant dimension is introduced and the connection field A is integrated along the edges of this lattice to form the so-called parallel transporter from one point in space to another. This object will describe how a vector defined on the fiber bundle changes as it moves between the two points. The main difference with our situation is that we do not have a background metric to define such a lattice. We will therefore integrate the Ashtekar-Barbero connection along an edge called $e \in \Sigma$. This quantity is called holonomy and is given by

$$h_e[A] = P \exp\left(-\int_e A\right), \tag{3.13}$$

where P denotes the path ordered exponential. It is standard in lattice gauge theory to take such an ordering, details of this construction can be found in [96, 99]. This ordering is necessary because the integrand A evaluated at one point does not usually commute with itself evaluated at another point. In the case of the symmetry reduced models we will consider below, they will be simple enough to commute. Therefore the path ordering will be trivial in what follows, and we will not give more details on the construction of these holonomies. The main point is that the holonomies h thus defined are elements of the group $SU(2)$ which admits a measure, the Haar measure. It is now possible to associate an operator to the holonomy. The way to do this is to introduce the so-called cylindrical functions, which are the building blocks of the kinematic Hilbert space in LQG. We consider a graph Γ on Σ composed of L edges, i.e. $\bigcup_{i=1}^{L} e_i = \Gamma \in \Sigma$. The cylindrical functions are written $\psi_{\Gamma,f}$ so that $f : SU(2)^L \to \mathbb{C}$ and satisfy

$$\psi_{\Gamma,f} := f(h_{e_1[A]}, ...h_{e_L}[A]). \tag{3.14}$$

One can then define an holonomy operator $\hat{h}_e[A]$ as a multiplication operator

$$\hat{h}_e[A]\psi_{\Gamma,f} = \begin{cases} h_{e[A]}\psi_{\Gamma,f} & \text{if there is an } i \text{ such that } e = e_i \\ 0 & \text{otherwise.} \end{cases} \tag{3.15}$$

On the other hand, it is possible to define an operator associated with the electric field E^{ai}. The procedure is to construct a two form from this quantity by considering $E^{ai}\epsilon_{abc}$. The main reason to do this is that since the holonomy is defined via a 1 dimensional integral, it is natural to integrate this quantity on a 2 dimensional surface, noted S, so that we will get ride of the Dirac delta in the right hand side of the Poisson bracket (3.5). The resulting quantity, called flux in analogy to the electric flux in electromagnetism, is

$$E^i[S] = \int_S E^i, \tag{3.16}$$

with n_a the normal to S. The algebra formed by the holonomies and the fluxes is called the holonomy-flux algebra. One can naturally associate an operator to (3.16) by choosing E^a_i to act by derivation on the cylindrical functions. The details of the definition of this operator are not

important in what follows and will be omitted here. The main reason for mentioning this operator is that it helps to define an area operator. Indeed, it is possible to show [95] that the area of a surface S in classical General Relativity in terms of the Ashtekar-Barbero variables is

$$A(S) = \int_S \sqrt{E_i E^i}. \tag{3.17}$$

Various ways of regularizing this quantity have been proposed in order to define an area operator acting on the space of cylindrical functions. The operators thus obtained are expressed in terms of flux operators and have the property of having a discrete spectrum. It is also possible to define in a similar way a volume operator which also has a discrete spectrum. The historical definition of these operator has been done in . The main properties of these operator is to have a discrete spectrum. Let us present a simple derivation of this property for the area operator, inspired from [100]. We start by introducing the following generalization of the electric flux (3.16)

$$E(\tilde{S}, \alpha) = \int_{\tilde{S}} \alpha_i E^i. \tag{3.18}$$

$\tilde{S}$ is chosen such that it enclose a volume V and contain S. On the other hand α_i is a test function equal to 1 on S and quickly decaying to zero on the rest of the domain of integration such that it would be equivalent to integrate only over S. The interest of integrating over $\tilde{S}$ is that it is now possible to use the Stokes theorem

$$E(\tilde{S}, \alpha) = \int_V d(\alpha_i E^{ai}) = \int_V D(\alpha_i E^{ai}) \approx \int_V E^{ai} D\alpha_i. \tag{3.19}$$

The second equality comes from the fact that $\alpha_i E^i$ is a scalar, it is therefore possible to use the covariant derivative introduced in (3.10). The third equality is obtain after using the Gauss constraint. By combining (3.19) with (3.5), one can show the key relation

$$\{E(\tilde{S}, \alpha), E(\tilde{S}, \beta)\} \approx \kappa\gamma E(\tilde{S}, [\alpha, \beta]) \quad \text{with} \quad [\alpha, \beta]_i = \epsilon_{ijk}\alpha^j \beta^k. \tag{3.20}$$

The $E(\tilde{S}, \alpha)$ form a representation of the $su(2)$ Lie algebra. We can therefore associate to these quantity operators having the same spectrum than the usual angular momentum operators, which is discrete. In particular, one has the Casimir operator acting on eigenstate $|\psi_j\rangle$ as follow

$$\hat{E}(\tilde{S}, \delta_i)\hat{E}(\tilde{S}, \delta^i) |\psi_j\rangle \approx \kappa\gamma j(j+1) |\psi_j\rangle , \tag{3.21}$$

where δ_i is the smeared function for which only its ith component is equal to 1, all the others being 0. The eigenstates $|\psi_j\rangle$ are called spin networks and are related to the cylindrical function in a way that we will not discuss here (cf [16, 95] for more details) Finally, one can define a volume operator by decomposing the integral expression of (3.17) into a sum over infinitesimal coordinate regions S_k

$$\hat{A}(S) |\psi_j\rangle \approx \sum_k S_k \sqrt{\hat{E}_i(S_k)\hat{E}^i(S_k)} \approx \sum_k \sqrt{\hat{E}(S_k, \delta_i)\hat{E}(S_k, \delta^i)}. \tag{3.22}$$

Its precise action on the spin networks requires a better description of the latter. However, since this operator is a sum of operator having a discrete spectrum, it will also have a discrete spectrum.

The upshot of this quantization program is that spacetime acquires a quantum nature in which the geometry itself is discretized and probabilistic. This has potentially far-reaching consequences. Among them is the possibility of resolving the classical singularities associated with the Big Bang and black holes. In the next section, we will address these issues in the context of symmetry reduced models. We will now conclude this section by presenting how cosmology can be formulated in terms of the Ashtekar-Barbero variables.

3.1.3 Ashtekar-Barbero variables in cosmology

Let us conclude this section by showing how one can impose symmetry conditions, here isotropy and homogeneity, on the Hamiltonian formulation of general relativity written in terms of Ashtekar-Barbero variables (introduced in 3.1.1) in order to obtain the FLRW model of cosmology. In addition, we will add to this symmetric spacetime a massless scalar field minimally coupled to gravity. Let us start by writing down the most general metric with the symmetries mentioned above

$$g_{\mu\nu}dx^\mu dx^\nu = -N^2(t)dt^2 + a^2(t)(dx^2 + dy^2 + dz^2). \tag{3.23}$$

It is natural to choose a spacelike foliation corresponding to the t = constant hypersurfaces, the induced metric of such a foliation will be

$$q_{ab}dx^a dx^b = a^2(t)(dx^2 + dy^2 + dz^2) \tag{3.24}$$

Moreover, it is standard to introduce the associated fiducial metric

$$\mathring{q}_{ab}dx^a dx^b = dx^2 + dy^2 + dz^2. \tag{3.25}$$

A first problem that appears is the fact that the domain of spatial integration that we use to compute the action can lead to divergences. In fact, considering the case $k = 0$, two topologies are acceptable for the space. The first is that of a torus $\mathbb{T}^3$, which has a finite volume with respect to the induced metric, and thus does not pose a problem. The second is $\mathbb{R}^3$, which has an infinite volume with respect to the induced metric. To regularize the spatial integrals, we consider a cubic integration cell denoted C whose edges are parallel to the x, y, z directions. It has a volume V_0 with respect to the fiduciary metric and a physical volume $V = a^3V_0$ with respect to the induced metric. In the following we will assume that the space has the topology of $\mathbb{R}^3$. Therefore, we will replace the integrals over the whole space by integrals over the cell C. However, we have to make sure that the resulting physics does not depend on the choice of this cell. On the other hand, one can show that the induced metric (3.24) is equivalent to the following choice of a triad

$$e^{ai}\tau_i\partial_a = a(t)(\tau_1\partial_x + \tau_2\partial_y + \tau_3\partial_z), \tag{3.26}$$

and the fiducial metric (3.25) can be reconstructed with the following fiducial triad

$$\overset{\circ}{e}^{ai}\tau_i\partial_a = \tau_1\partial_x + \tau_2\partial_y + \tau_3\partial_z \tag{3.27}$$

It is then possible to determine the expressions of the Ashtekar-Barbero variables. First, we can see from (3.2) that the electric field is

$$E^{ai} = a(t)\overset{\circ}{e}^{ai}. \tag{3.28}$$

Concerning the connection, one can first notice that E^{ai} is independent of the spatial coordinates, which implies from (3.4) that $\Gamma^i_a = 0$. On the other hand, we know that $K_{ab} = \frac{1}{2}\mathcal{L}_{\frac{\partial}{\partial t}} q_{ab} = a(t)\dot{a}(t)\delta_{ab}$. From (3.4) we can conclude that $K^i_a = \dot{a}(t)\overset{\circ}{e}^i_a$. So in the end we have

$$A_{ai} = \gamma\dot{a}(t)\overset{\circ}{e}_{ai}. \tag{3.29}$$

For convenience, it is standard to introduce the following notations

$$c = V_0^{1/3}\gamma\dot{a}, \quad p = V_0^{2/3}a^2 \quad \text{such that} \quad E^{ai} = V_0^{-2/3}p\overset{\circ}{e}^{ai}, \quad A^i_a = V_0^{-1/3}c\overset{\circ}{e}_{ai}. \tag{3.30}$$

One can now write down the Einstein-Hilbert action as well as the action of a massless scalar field coupled to gravity. For the former, it is possible to start from (3.6), since the system is homogeneous, it is not hard to show that the space-diffeomorphism constraints are trivially equal to zero. This is also the case for the Gauss constraint, since we have chosen a particular orientation for the triad that breaks gauge invariance. The only constraint left is the Hamiltonian constraint. By adding the action of a massless scalar field

$$S_\phi = -\frac{1}{2}\int d^4x\sqrt{-g}g^{\mu\nu}\partial_\mu\phi\partial_\nu\phi, \tag{3.31}$$

and by assuming that this matter field has the same symmetry as the spacetime, one can show that the total action obtained after integration with respect to x, y and z is

$$S = \int dt\left[\dot{\phi}p_\phi - \frac{3}{8\pi\gamma}c\dot{p} - N\left(\frac{p_\phi^2}{2p^{3/2}} - \frac{3c^2\sqrt{p}}{8\pi\gamma^2}\right)\right] \tag{3.32}$$

From this expression one can see that N is a Lagrange multiplier. In the following, we will work in the harmonic gauge which is obtained for $N = p^{3/2}$. The Hamiltonian is a constraint given by

$$H_{\text{total}} = \frac{p_\phi^2}{2} - \frac{3c^2p^2}{8\pi\gamma^2} \approx 0. \tag{3.33}$$

Furthermore, the phase space variables are c, p, ϕ and p_ϕ and satisfy the following Poisson brackets

$$\{c, p\} = \frac{8\pi\gamma}{3} \quad \text{and} \quad \{\phi, p_\phi\} = 1 \tag{3.34}$$

The main motivation for defining c and p the way we did in (3.30) is to have Poisson brackets independent of V_0, which is not a physically meaningful quantity. We will end this subsection by introducing the following canonical transformation

$$v = \frac{p^{3/2}}{2\pi} \quad \text{and} \quad b = \frac{c}{\sqrt{p}}. \tag{3.35}$$

With these new variables, the Hamiltonian constraint (3.33) becomes

$$H_{\text{total}} = \frac{p_\phi^2}{2} - \frac{3\pi v^2 b^2}{2\gamma^2} \approx 0, \tag{3.36}$$

and the Poisson brackets (3.34) lead to

$$\{b, v\} = 2\gamma \quad \text{and} \quad \{\phi, p_\phi\} = 1. \tag{3.37}$$

By combining (3.30) and (3.35), one can see that v is, up to a factor 2π, the physical volume of the fiducial cell C, and b is proportional to the Hubble rate. It is then possible to study the classical dynamics of this system. A key observation that can be made from (3.36) is that $\frac{p_\phi^2}{2}$ is a constant of motion. This directly implies that ϕ is proportional to the harmonic time and can be used as a clock [5]. It will be very convenient in the next section to use it as a clock. On the other hand, one can also deduce that $\frac{3\pi v^2 b^2}{2\gamma^2}$ is also a constant of motion and is equal to $\frac{p_\phi^2}{2}$ on shell. One can show that

$$\frac{dv}{d\tau} = 2\sqrt{3\pi} p_\phi v, \tag{3.38}$$

where τ is the harmonic time. This differential equation is solved by $v(\tau) = v_0 e^{2\sqrt{3\pi} p_\phi \tau}$. In the limit $\tau \to 0$ this quantity vanishes. This corresponds to the classical singularity, where both the scale factor and the volume of any fiducial cell go to zero. Moreover, since the energy density of the matter field is given by $\frac{p_\phi^2}{4\pi v}$, the instant when v goes to zero also corresponds to a divergence of this energy density. It is possible to check that this happens in a finite time for a co-moving observer. Indeed, the co-moving time t is related to the harmonic one by

$$dt = N(\tau) d\tau = 2\pi v(\tau) d\tau. \tag{3.39}$$

This equation leads to

$$t(\tau) - t(0) = \frac{\sqrt{\pi}}{\sqrt{3} p_\phi} (e^{2\sqrt{3\pi} p_\phi \tau} - 1). \tag{3.40}$$

The harmonic time $\tau = -\infty$ is therefore accessible in a finite amount of proper time for a co-moving observer, which means that the singularity is physically accessible.

One can expect that this singularity should be removed by quantum corrections when the energy density of the matter field becomes too large and the spacetime is contracted enough. One can proceed to the Wheeler-DeWitt quantization, which is the canonical quantization of the phase space described above. However, the singularity is not removed in this approach, i.e. the physical Hilbert space thus obtained contains states for which the expectation value of the volume operator

[5] Let us mention that a formulation of the dynamics is possible within the framework of unimodular gravity, which allows us to work with a natural time and to have a Hamiltonian identical to that of a particle in a $\frac{1}{r}$ potential [101].

(i.e. the operator associated with the variable v) vanishes at early time [22]. In the next section we will mimic the regularization of the Ashtekar-Barbero variables, presented at the beginning of this section, in the case of cosmology. We will also see how the idea of discreetness of geometry proposed in LQG can be implemented in the quantization of this system.

3.2 Loop quantum cosmology

The main questionable claim of the above mentioned Wheeler-DeWitt quantization is the direct assignment of operators to the phase space variables b and v. But according to LQG it should not be allowed to associate an operator with the connection variable b. Indeed, we mentioned in subsection 3.1.2 that the Ashtekar-Barbero connection takes value in the Lie algebra $su(2)$, which has no measure allowing to perform integration, preventing to associate an operator to this variable. We have also seen in this subsection that in the complete theory this problem leads us to adapt new variables, instead of working with the connection and the dense triad, we use respectively the holonomy of the former and the flow of the latter. We will follow a similar construction in the case of cosmology, i.e. we will replace the connection by its holonomy along a line γ, which will be chosen as an edge of the fiducial cell. We will explicitly show what the expression of this holonomy is for the edge oriented in the x direction, but we could generalize the result for arbitrary directions thanks to isotropy. Moreover, the position of this line in space is not important, since in our model the universe is homogeneous. Finally, we choose a line of physical length $l = \mu V^{1/3}$, where μ may be a phase space variable. We will see how to choose this quantity later in this section. We will then define the kinematic Hilbert space of LQC and define the action of the operators associated with the holonomy and the flux on this Hilbert space. The next step will be to regularize the Hamiltonian constraint (3.33), or (3.36), in order to express it in terms of holonomies. We will see how we can implement the idea of discreetness suggested in LQG in this regularization procedure. This will lead to a quantum equation. After briefly presenting the solutions to this equation, we will be able to study the spectrum of the operator associated with the volume of the fiducial cell and the energy density of the scalar field. This will allow us to examine whether the singularity is resolved in this approach.

3.2.1 Kinematic Hilbert space of LQC

As motivated above, our first task is to compute the holonomy of A along a curve γ oriented in the x direction. In addition, we will consider that this curve has a physical length $l = \mu V^{1/3}$, so its coordinate length with respect to x is $l_0 = \mu V_0^{1/3}$. Using the expression (3.30) for the Ashtekar-Barbero connection, we get

$$h_\gamma = \exp\left(\int_\gamma A_x^i \tau_i dx\right) \tag{3.41}$$

$$= \exp\left(\int_0^{\mu V_0^{1/3}} c V_0^{-1/3} \tau_1 dx\right) \tag{3.42}$$

$$= \exp(\mu c \tau_1) \tag{3.43}$$

$$= \cos(\mu c/2)\mathbb{I} + 2\sin(\mu c/2)\tau_1 \tag{3.44}$$

We see that the holonomy, which could be used as a new variable instead of c, can be completely expressed in terms of the function $\exp(i\mu c/2)$. It is therefore natural to choose the latter as our new variable instead of c. The second step is to replace the densitized triad by its flow through one of the faces of the cell C (again, it does not matter which face we use, since we are considering a homogeneous and isotropic universe). It is not complicated to show that this quantity is p. In summary, our new variables are p and $N_\mu(c) = e^{i\mu c/2}$. Using the same Poisson brackets as before (cf. (3.34)), we can show that

$$\{N_\mu(c), p\} = \frac{8\pi i\gamma\mu}{6} N_\mu(c), \quad \{N_\mu(c), N_{\mu'}(c)\} = 0 \quad \text{and} \quad \{p, p\} = 0. \tag{3.45}$$

This algebra is the analog of the holonomy-flux algebra mentioned in subsection (3.1.2).

The next step, which has not been presented here in the case of full LQG, is to proceed to the canonical quantization of this algebra. The phase space variables p and $N_\mu(c)$ are replaced by operators and the Poisson brackets (3.45) are replaced by the following commutation relation

$$[\hat{N}_\mu(c), \hat{p}] = -\frac{8\pi\hbar\gamma\mu}{6} \hat{N}_\mu(c), \quad [\hat{N}_\mu(c), \hat{N}_\mu(c)] = 0 \quad \text{and} \quad [\hat{p}, \hat{p}] = 0. \tag{3.46}$$

In the Wheeler-DeWitt quantization, the kinematic Hilbert space is the space $L^2(\mathbb{R})$ equipped with the usual inner product $\langle f, g \langle = \int_{-\infty}^{+\infty} f(x)\overline{g(x)}dx$, where f and $g \in L^2(\mathbb{R})$. As we said, this Wheeler-DeWitt quantization does not resolve the singularity. Moreover, by Stone's Von Neumann theorem [22], all representations of the commutation relation (3.45) are related to that of the Wheeler-DeWitt quantization by a unitary transformation and are therefore all physically equivalent. If we want to construct a theory that has a chance of removing the classical singularity, we need to break one of the hypotheses of the Stone von Neumann theorem. In addition, we also want a representation where there is no operator associated with c, the component of the Ashtekar connection. We will see that these two requirements come together in LQC. The way to achieve them is to consider a different Hilbert space for which the operator $N_\mu(c)$ is not weakly continuous, which is one of the conditions for the applicability of the theorem. We will see what it means for an operator not to be weakly continuous. The Hilbert space in LQC is the one formed by the almost periodic function, i.e. the function of the form

$$\Psi(c) = \sum_{n=1}^{N} \alpha_n \exp(i\mu_n c/2) \quad \text{with} \quad \alpha_n \in \mathbb{C} \quad \text{and} \quad \mu_n \in \mathbb{R} \quad \forall n \in \mathbb{N}, \tag{3.47}$$

where N is finite, and having a finite norm

$$||\Psi||^2 = \lim_{D\to+\infty} \frac{1}{2D} \int_{-D}^{D} dc \bar{\Psi}(c)\Psi(c) = \sum_{n=1}^{N} |\alpha_n|^2. \tag{3.48}$$

This vector space is denoted by $L^2(\mathbb{R}_{\text{Bohr}}, d\mu_{\text{Bohr}})$, where $\mathbb{R}_{\text{Bohr}}$ is the Bohr compactification of the real line and $d\mu_{\text{Bohr}}$ is the Haar measure. Furthermore, to form a Hilbert space, this vector space is equipped with the following inner product

$$\langle \Psi_1 | \Psi_2 \rangle = \lim_{D\to+\infty} \frac{1}{2D} \int_{-D}^{D} \bar{\Psi}_1(c)\Psi_2(c) dc = \sum_{n=1}^{N} |\alpha_n|^2. \tag{3.49}$$

Now that we have a kinematic Hilbert space, we can define the action of the operator $\hat{N}_\mu(c)$ corresponding to the variable $N_\mu(c)$ on this Hilbert space. It is usually defined as the action by multiplication

$$\hat{N}_\mu(c)\Psi(c) = \exp(i\mu c/2)\Psi(c), \tag{3.50}$$

and by using the commutation relation between $\hat{N}_\mu(c)$ and $\hat{p}$, the operator $\hat{p}$ is

$$\hat{p}\Psi(c) = -\frac{8\pi i\hbar\gamma}{3} \frac{d\psi}{dc}. \tag{3.51}$$

Notice that by using the inner product (3.49) we have

$$\langle N_\mu(c), N_{\mu'}(c) \rangle = \langle e^{i\mu c/2}, e^{i\mu' c/2} \rangle = \delta_{\mu,\mu'}, \tag{3.52}$$

where the right side is not a Dirac distribution as usual, but a Kronecker symbol. This is a crucial difference that makes the $\hat{N}_\mu(c)$ operator not weakly continuous. Indeed, one can show that

$$\langle N_\mu(c) | \hat{N}_\sigma(c) | N_\mu(c) \rangle = \begin{cases} 0 & \text{if } \sigma \neq 0 \\ 1 & \text{if } \sigma = 0 \end{cases} \tag{3.53}$$

And therefore

$$\lim_{\sigma\to 0} \langle N_\mu(c) | \hat{N}_\sigma(c) | N_\mu(c) \rangle = 0 \neq \langle N_\mu(c) | N_\mu(c) \rangle. \tag{3.54}$$

This result implies, by the definition of weak continuity, that the operator $\hat{N}_\mu(c)$ is not weakly continuous. The Stone von Neumann theorem does not hold for this representation of the commutation relation, and can therefore lead to different physical predictions than for the Wheeler DeWitt representation. Note also that the result (3.54) implies that it is impossible to right a well-defined operator $\hat{c} = \lim_{\sigma\to 0} \frac{\hat{N}_\sigma(c) - \mathbb{I}}{i\sigma}$. The impossibility to form a connection operator in LQG is thus reverted to LQC. Moreover, according to the commutation relations (3.46), such an operator $\hat{c}$ would act as an infinitesimal translation operator in the p representation. Recall that p corresponds to the surface of the fiducial cell (cf. (3.30)). The fact that there is no operator $\hat{c}$ means that it is not possible to continuously change the value of the surface of this region. There is only a finite change allowed, which is generated by the operator $N_\mu(c)$. This feature corresponds to a discreteness of the geometry, as proposed in LQG. In short, the circumvention of the Stone von Neumann theorem, the impossibility of forming an operator associated with the Ashtekar-Barbero connection, and the

discreteness of the geometry are properties that all come together with the previous choice for the kinematic Hilbert space.

As we have just said, the operator $N_\mu(c)$ produces a finite shift of the wave function in the p representation, and the step of this shift is μ. Historically, this regulator μ, introduced in (3.41) to define holonomies, was taken as a constant. It was quickly realized that this regularization scheme, called the μ_o scheme, led to physical inconsistencies, and an improved parameter, called the $\bar{\mu}$ scheme [81], was rapidly proposed. It is defined as follows

$$\bar{\mu} = \frac{\lambda}{\sqrt{p}} \quad \text{with} \quad \lambda = l_p\sqrt{2\sqrt{3}\pi\gamma}. \tag{3.55}$$

We will come back to this choice in the next section. Since the regulator is now phase space dependent, we need to identify the action of $\hat{N}_{\bar{\mu}}(c)$ on the Hilbert space. Let us work in the p representation. We note $|p\rangle$, the eigenvector of the operator $\hat{p}$. The action of $\hat{N}_\mu(c)$ on these states was simply $\hat{N}_\mu(c)\,|p\rangle = |p+\mu\rangle$, i.e. it generates a translation μ in the p direction of the phase space. The action of $\hat{N}_{\bar{\mu}}(c)$ will be simpler if we proceed to the canonical transformation (3.35). In fact, this was one of the main reasons for introducing these variables. Since there is a bijection between p and v (recall that $v = \frac{p^{3/2}}{2\pi}$), we can associate each state $|p\rangle$ with a state $|v\rangle$ on which the operator $\hat{v}$ acts by multiplication. Finally, since $\hat{N}_{\bar{\mu}}(c) = \hat{N}_\lambda(b) = \widehat{e^{i\lambda b/2}}$ and since b and v are conjugated, we have

$$\hat{N}_\lambda(b)\,|v\rangle = |v - \lambda\gamma l_p^2\rangle\,. \tag{3.56}$$

Regarding the (ϕ, p_ϕ) part of the phase space, it is quantized using the usual Schroedinger representations, i.e. the Poisson bracket satisfied by these two variables (3.34) is replaced by the commutation relation $[\hat{\phi}, \hat{p}_\phi] = i\hbar$, ϕ acts by multiplication and p_ϕ by derivation on $L^2(\mathbb{R})$ functions (in the ϕ representation, and the opposite in the p_ϕ representation). Therefore, the total kinematic Hilbert space, denoted by $\mathcal{H}_{\text{kin}}$, is defined as the vector space $L^2(\mathbb{R}_{\text{Bohr}}, d\mu_{\text{Bohr}}) \otimes L^2(\mathbb{R})$ equipped with the following inner product

$$\langle\Psi_1|\Psi_2\rangle = \lim_{D\to+\infty} \frac{1}{2D}\int_{-\infty}^{+\infty}\int_{-D}^{D} \bar{\Psi}_1(c,\phi)\Psi_2(c,\phi)dcd\phi. \tag{3.57}$$

We will not further comment on the properties of this Hilbert space in this section. We will however come back to it in chapter 4 when details will be needed (like the expression of the wave functions (3.47) in the conjugate representation, or the description of subspaces conserved by the dynamics, etc).

The next step is to express the regularization of the Hamiltonian constraint (3.36) with the holonomy and flux variables introduced in this subsection. It will then be possible to obtain a quantum equation for the dynamics by replacing these variables by the corresponding quantum operators $\hat{v}$ and $\widehat{e^{i\lambda b/2}}$ we have just defined.

3.2.2 The equation of motion, a difference equation

The main point of the last subsection was to construct a representation of the commutation relations (3.45) for which there is no operator $\hat{c}$, or $\hat{b}$. Therefore, it is also impossible to directly quantize the Hamiltonian constraint (3.33), or (3.36). To overcome this problem, we go back to the initial expression of the Hamiltonian constraint (3.8), which we recall here

$$H = \int d^3x N\mathcal{H} = \int d^3x N \frac{E^{ai}E^{bj}}{16\pi\sqrt{E}}(\epsilon_{ijk}F^k_{ab} - 2(1+\gamma^2)K^i_{[a}K^j_{b]}) \tag{3.58}$$

It is not hard to show that the second term of this expression vanishes in the cosmological setting we are considering. Moreover, using the expression of E^{ai} given in (3.30), one can show that

$$H = -\int d^3x \frac{\mathring{e}^a_i \mathring{e}^b_j p^2}{16\pi\gamma^2 V_0^{1/3}} \epsilon^{ij}{}_k F^k_{ab}, \tag{3.59}$$

where again we have fixed the lapse to be $N = p^{3/2}$. The gravitational part of the constraint (3.33) was obtained from this expression by computing F^k_{ab} (using its definition given below (3.8)). Instead, we will mimic the LQG approach by regularizing this quantity in terms of holonomies. This regularization is inspired by what is done in lattice gauge theories, where the curvature is computed from the holonomies of the connection around a closed loop. We will consider a square loop symbolically denoted $\Box_{ij}$ in the i-j plane, where i and j are associated with the space direction x, y, or z (in the same way that internal indices are associated with space indices via (3.26)). We will assume that each side of this plaquette has a fiducial length (i.e., a length with respect to the fiducial metric) $l_0 = \bar{\mu}V_0^{1/3}$, where $\bar{\mu}$ is a phase space function whose exact expression will be discussed in a moment. We know from lattice gauge theories that the curvature can be expressed in terms of the holonomy along such a plaquette, noted $h_{\Box_{ij}}$, in the following way [99]

$$F_{ab} = \lim_{\mu\to 0} \frac{h_{\Box_{ij}} - \mathbb{1}}{(\bar{\mu}V_0^{1/3})^2} \mathring{e}^i_a \mathring{e}^j_b, \tag{3.60}$$

In this cosmological setting, it is not too difficult to obtain the expression of $h_{\Box_{ij}}$ by combining the result (3.41) to reproduce the integration contour $\Box_{ij}$. After some manipulations [15], one can show that

$$F^k_{ab} = \lim_{\mu\to 0} \epsilon_{ij}\, {}^kV_0^{-2/3} \mathring{e}^i_a \mathring{e}^j_b \left(\frac{\sin^2(\mu c)}{\bar{\mu}^2}\right) \tag{3.61}$$

One can check that by taking the limit $\bar{\mu} \to 0$ and inserting (3.61) into (3.59), we recover the gravitational part of the Hamiltonian constraint (3.33). However, the regulator is kept finite in the following, so that the c dependence of the curvature appears through a sine function. This sine function can be expressed as a complex exponential which, as we saw in the previous subsection, can be associated with a well-defined operator. The fact that the regulator $\bar{\mu}$ remains finite is motivated by the discreteness of the geometry in LQG. Indeed, the limit $\bar{\mu} \to 0$ can be taken in the case of a continuous geometry, since this corresponds to a continuous shrinking of the integration contour $\Box_{ij}$ until it forms a single point. In LQG, however, the geometry is discrete and there is

a smaller area equal to $\lambda^2 = 2\sqrt{3}\pi\gamma l_p^2$. In LQC, this discreteness is added by hand, assuming that the physical length of each edge of the integration contour is $l = al_0 = \lambda$. And since $l_0 = \bar{\mu}V_0^{1/3}$, one can conclude that

$$\bar{\mu} = \frac{\lambda}{\sqrt{p}}. \tag{3.62}$$

This expression of $\bar{\mu}$ coincides with the one we assumed in (3.55). It is then possible to associate the following operator to the curvature (3.61)

$$\widehat{F}^k_{ab} = \epsilon_{ij}\ {}^kV_0^{-2/3}\,{}^\circ e^i_a\,{}^\circ e^j_b \left(\widehat{\frac{\sin\bar{\mu}c}{\bar{\mu}}}\right)^2 \tag{3.63}$$

The sine operator can be decomposed as a sum of exponential operators, and we now understand why it was necessary to define the operator $\widehat{e^{i\bar{\mu}c/2}}$ with $\bar{\mu} \propto \frac{1}{\sqrt{p}}$ (cf. (3.56)). One can then determine the quantum operator associated with the gravitational part of the Hamiltonian constraint by combining (3.63) and (3.59).

$$\hat{H} = -\frac{3}{8\pi\gamma^2}\sqrt{\hat{p}}\left(\widehat{\frac{\sin(\bar{\mu}c)}{\bar{\mu}}}\right)\hat{p}\left(\widehat{\frac{\sin(\bar{\mu}c)}{\bar{\mu}}}\right)\sqrt{\hat{p}}. \tag{3.64}$$

As usual, there is an ambiguity in the choice of ordering of operators. The one chosen is the simplest, which guarantees that $\hat{H}$ is self adjoint. On the other hand, we saw in the previous subsection that the action of $\widehat{e^{i\bar{\mu}c/2}}$, and thus of $\widehat{\sin(\bar{\mu}c)}$, on the kinematical Hilbert space is simpler when the variables v and b are used. Using this change of variables, the operator (3.64) becomes

$$\hat{H} = -\frac{3\pi}{2\gamma^2}\sqrt{\hat{v}}\left(\widehat{\frac{\sin\lambda b}{\lambda}}\right)\hat{v}\left(\widehat{\frac{\sin\lambda b}{\lambda}}\right)\sqrt{\hat{v}}. \tag{3.65}$$

Finally, the matter contribution must be added to obtain the Hamiltonian of the total system. This contribution was made explicit in the previous subsection and leads to the following total Hamiltonian

$$\hat{H}_{\text{total}} = \frac{\hat{p}_\phi^2}{2} - \frac{3\pi}{2\gamma^2}\sqrt{\hat{v}}\left(\widehat{\frac{\sin\lambda b}{\lambda}}\right)\hat{v}\left(\widehat{\frac{\sin\lambda b}{\lambda}}\right)\sqrt{\hat{v}}. \tag{3.66}$$

Since classical dynamics is given by the cancellation of the Hamiltonian constraint, it is natural to ask that quantum dynamics is given by the subset of $\mathcal{H}_{\text{kin}}$ that cancels the operator (3.66), i.e. the physical Hilbert space is defined as

$$\mathcal{H}_{\text{phys}} = \{|\Psi\rangle \in \mathcal{H}_{\text{kin}},\ \hat{H}_{\text{total}}\,|\Psi\rangle = 0\}. \tag{3.67}$$

We know from the previous subsection how the operators appearing in (3.66) act on the kinematic Hilbert space. It is not difficult to show that the wave functions belonging to the physical Hilbert space must satisfy the following difference equation

$$\partial_\phi^2\Psi(v,\phi) = \frac{3\pi l_p^4}{\gamma^2\lambda^2}v\left((v+2\lambda\gamma l_p^2)\Psi(v+4\lambda\gamma l_p^2,\phi) - 2v\Psi(v,\phi) + (v-2\lambda\gamma l_p^2)\Psi(v-4\lambda\gamma l_p^2,\phi)\right) \tag{3.68}$$

As mentioned in the subsection 3.1.3, it is common to use the scalar field ϕ as a clock. This equation has been studied numerically [81]. It has been shown that there are solutions for which $\langle\hat{v}\rangle$ never cancels out, suggesting that quantum dynamics governed by (3.66) resolve the classical singularity. On the other hand, it is possible to obtain analytic expressions for wave functions in physical Hilbert space, which we will discuss in the next subsection.

3.2.3 Solvable Loop Quantum Cosmology

We will now see how the difference equation (3.68) can be transformed into a differential equation that can be solved analytically. The framework we will introduce is sometimes referred to as solvable loop quantum cosmology (sLQG). The first step is to switch from the v representation used in the previous subsection to the b representation. This is done as usual by a Fourier transformation. From (3.68) we know that v takes values in a countable support such that $v = 4n\lambda\gamma l_p^2 + \epsilon$. Therefore, like a particle in a circle, the conjugate variable, here b, is expected to be periodic with a period $\frac{\pi}{\lambda}$. The transition from one representation to the other is achieved by the following Fourier transformations

$$\Psi(b,\phi) = \sum_{v=4n\lambda} e^{ivb/2}\Psi(v,\phi) \quad \text{and} \quad \Psi(v,\phi) = \frac{\lambda}{\pi}\int_0^{\pi/\lambda} e^{-ivb/2}\Psi(b,\phi)db. \tag{3.69}$$

By introducing

$$\chi(v,\phi) := \frac{\lambda}{\pi v}\Psi(\nu,\phi), \tag{3.70}$$

then by taking the Fourier transform of (3.68) and finally by defining

$$x = \frac{1}{\sqrt{12\pi G}}\log\left(\tan\frac{\lambda b}{2}\right) \quad \text{such that} \quad x \in (-\infty,+\infty), \tag{3.71}$$

It is possible to show [102] that the difference equation (3.68) reduces to the following differential equation

$$\partial_\phi^2\chi(x,\phi) = \partial_x^2\chi(x,\phi) =: -\Theta\chi(x,\phi). \tag{3.72}$$

The phase space variables ϕ are used as a clock, which allows (3.72) to be interpreted as a familiar wave equation. The solution space can be decomposed into right- and left-hand modes, corresponding to the expanding and contracting universe, respectively. A careful analysis of the general expression of the solutions as well as the computation of the expectation value of the volume operator $\hat{v}$ can be found in [102]. The main result is that for generic states χ solving (3.72) the expectation of the volume operator at any time ϕ satisfies

$$\langle\chi(\phi)|\,\hat{v}\,|\chi(\phi)\rangle \geq v_{\min}, \tag{3.73}$$

where the minimum volume $v_{\min}$ as well as the time ϕ_{bounce} at which this minimum is reached depends on the choice of the initial state. Furthermore, one can define an operator related to the energy density of the scalar field

$$\hat{\rho}_\phi = \frac{\hat{v}^{-1/2}\hat{p_\phi}\hat{v}^{-1/2}}{4\pi}. \tag{3.74}$$

This quantity can be computed analytically, and its dependence on the initial state can be studied. In particular, it can be concluded that the energy density reaches a maximum value ρ_{bounce} at the bounce (i.e. when $\langle\hat{v}\rangle = v_{\text{min}}$). This maximum value is given by

$$\rho_{\text{bounce}} = \frac{\sqrt{3}}{32\pi^2\gamma^3 G^2\hbar} = 0.41\rho_{\text{Planck}}, \tag{3.75}$$

which is independent of the choice of the initial state. Let us mention that these predictions were compared with the numerical prediction made in [81] from the difference equation (3.68), and agreed [102].

On the other hand, people have devoted some interest to the study of the evolution of coherent states, noticed χ_{coh}. More precisely, they have studied the evolution of sharply peaked states around given values of the phase space variables. In particular, they showed that such states remain sharply peaked throughout their evolution, even in strongly quantum regions (when the scalar field energy density becomes Planckian). This means that the relative fluctuations of the operators associated with the phase space variables remain small and can be ignored. The main feature of the dynamics is therefore contained in the evolution of the mean values of these operators. This observation led to the polymerization procedure, which allows the main features of quantum dynamics to be captured by a simple modification of the classical Hamiltonian. The aim of the following subsection is to present this procedure in more detail and to see how it has been used to generalize the study to the case of black holes.

3.3 Polymerization and quantum black holes

The aim of this section is to outline the polymerization procedure and discuss the reasons for its validity. We will then look at how this procedure has been applied to black holes. As we shall see, there is no single way of applying the polymerization procedure. This is why we will not, at this stage, discuss in detail the physical predictions made by black models constructed in this way. We will, however, mention some of the main and common predictions of these models. We will end this section by discussing some problems and ambiguities induced by the polymerization procedure, which will serve to motivate the remainder of this manuscript.

3.3.1 Polymerization and effective dynamics

In subsection 3.2.2 we presented how the Hamiltonian constraint operator (3.66) is constructed in LQC. With some hindsight, we can see that this operator could have been obtained more directly by replacing the connecting variable c in (3.33) by $\frac{sin(\bar{\mu}c)}{\bar{\mu}}$. It would then have been necessary to replace the latter by an operator whose action is defined by the Poisson bracket between itself and the electric field variable p (as was done in the subsection 3.2.1). This shortening is called polymerization. The choice of the sine as the regularization function was motivated in subsection 3.2.1 and follows from the regularization of the connection by its holonomy written in the fundamental representation of the $SU(2)$ group (to which it belongs, cf. subsection 3.1.2). It should be noted, however, that the choice of the fundamental representation, and thus of the sine function, has no reason to be privileged and will be questioned in chapter 4. Moreover, this polymerization

procedure does not specify how to choose the quantum parameter $\bar{\mu}$. And as we have seen in the case of LQC, this parameter cannot be a simple constant, as this would change the physics in low density regimes (compared to Planck density). This quantity must be phase space dependent, and its exact expression, established in subsection 3.2.2, requires additional inputs not given by the polymerization procedure. This procedure thus allows for a rather quick regularization of the Hamiltonian constraint, but does not give all the instructions for carrying out this regularization. Note, however, that before associating operators with phase space variables, this procedure leads to a modified classical dynamics, commonly called effective dynamics, which is generated by the following effective Hamiltonian constraint

$$H^{(\text{eff})}_{\text{total}} = \frac{p_\phi^2}{2} - \frac{3}{8\pi\gamma^2 V_0}\left(\frac{\sin(\bar{\mu}c)}{\bar{\mu}}\right)^2 p^2 \tag{3.76}$$

$$= \frac{p_\phi^2}{2} - \frac{3\pi}{2\gamma^2}\left(\frac{\sin(\lambda b)}{\lambda}\right)^2 v^2 \approx 0. \tag{3.77}$$

It is then possible to derive effective equations of motion for the phase space variables and show that they lead to a singularity-free spacetime. This observation can be derived more directly from (3.76). Indeed, we can see that $\frac{sin(\lambda b)}{\lambda} v$ is a constant of motion. And since $\sin(\lambda b)$ is bounded, v cannot tend to 0. So the volume of the reference cell cannot tend to zero, and the energy density of the scalar field cannot diverge.

However, it is not clear whether this effective description is a "good" description of the dynamics. More precisely, one might ask whether it is possible to derive this effective dynamics from the quantum one presented in 3.2.2 and 3.2.3. As it happens, several people have studied the evolution of the mean value of operators associated with phase space variables for an initially sharply peaked state around a classical solution. Such a quantum state can be written, for example, as

$$\psi(v,\phi) = A e^{-\frac{(v-v_0)^2}{2\sigma_v^2}} e^{ivb_0} e^{-\frac{(\phi-\phi_0)^2}{2\sigma_\phi^2}} e^{i\phi p_{\phi 0}}, \tag{3.78}$$

where A is a normalization constant and $(v_0, b_0, \phi_0, p_{\phi 0})$ are initial values for phase space variables corresponding to a classical geometry (i.e., a geometry for which the curvature and energy density are small compared to the Planck scale). Let us assume that the relative fluctuations in v and p_ϕ are initially small. It has been shown for states of this form [103], as well as for more general states [104], that these relative fluctuations remain small on the other side of the bounce when the curvature and energy density become small again. This means that the bounce does not induce significant fluctuations after it has occurred. However, this says nothing about the value of these fluctuations at the moment of the bounce. On the other hand, there is a more general argument, which does not require any particular choice of the expression for the wave function in the initial state (we will not develop this argument here, but it can be found in [105]), which says that these fluctuations can be made as small as desired at any time by modifying the choice of V_0. Thus, it seems to be well established in LQC that fluctuations are negligible, and an effective description of the dynamics allows to quickly capture certain predictions of this theory, such as the resolution of the singularity. In the next subsection we will apply this polymerization technique to the case of Schwarzschild black holes and assume that an effective description is also possible. Although the

latter claim has never been proven, several models of effective black holes have been proposed in recent years based on this hypothesis.

3.3.2 Polymerization applied to black holes

In the remainder of this section, we will focus on the case of Schwarzschild black holes. In this subsection, we will present the main line of the Hamiltonian formulation of this system and show how the polmerization procedure is usually applied in this case. The first step is to write down the most general spherically symmetric and static line element, namely

$$ds^2 = -f(R)dt^2 + h(R)dR^2 + |p_c(R)|d\Omega^2. \tag{3.79}$$

In order to obtain a Hamiltonian formulation of the problem, we need to choose a foliation. Since the geometry is static and spherically symmetric, the metric component depends only on the R coordinate, so it is natural to choose a $R =$ constant foliation. The Hamiltonian thus obtained will be the generator of the evolution in the R direction. It then requires some technical manipulations, which we will not present here (but which can be found in [25]), to obtain the following expressions for the Ashtekar-Barbero variables

$$E^a_i\tau^i\partial_a = p_c\sin(\theta)\tau^3\partial_t + \frac{p_b}{L_o}\sin(\theta)\tau^2\partial_\theta - \frac{p_b}{L_o}\tau^1\partial_\phi \tag{3.80}$$

$$A^i_a\tau_i dx^a = \frac{c}{L_o}\tau_3 dx + b\tau_2 d\theta - b\sin(\theta)\tau_1 d\phi + \cos(\theta)\tau_3 d\phi, \tag{3.81}$$

where L_o is an infrared regulator, analogous to V_o in LQC, needed to regularize the integration of the Lagrangian in the t direction (which is a non compact direction and on which the Lagrangian does not depend). We also introduced $p_b = L_o\sqrt{-fp_c}$, and b and c are conjugate to p_b and p_c, i.e.

$$\{b, p_b\} = \gamma \quad \text{and} \quad \{c, p_c\} = 2\gamma. \tag{3.82}$$

Let us also mention that in order to obtain the expressions (3.80) and (3.81), the Gauss constraint has been solved [25]. With these phase space variables, the line element (3.79) can be rewritten as follows

$$g_{\mu\nu}dx^\mu dx^\nu = -N(R)^2dR^2 + \frac{p_b(R)^2}{L_o|p_c(R)|}dt^2 + |p_c(R)|d\Omega^2, \tag{3.83}$$

where N is the lapse function. One can then compute and check that the space-diffeomorphism constraint (3.8) trivially vanishes, which is not surprising since the geometry is homogeneous on each slice. On the other hand, it can be shown that the Hamiltonian constraint takes the following expression

$$H = N\mathcal{H} = -\frac{8\pi N\text{sign}(p_c)b}{\gamma^2\sqrt{|p_c|}p_b}(2cp_cbp_b + (b^2+\gamma^2)p_b^2) \approx 0. \tag{3.84}$$

A standard choice for the lapse is $N = \frac{\gamma\text{sign}(p_c)\sqrt{|p_c|}}{16\pi b}$. It is not difficult to generate the equations of motion for the phase space variables and solve them [25], which leads to the Schwarzschild spacetime as expected.

One can then proceed with the polymerization procedure, presented in the previous subsection, to try to obtain a modified dynamics free of singularities. The first step is to identify the phase space variables corresponding to the components of the Ashtekar-Barbero connection. Here these are b and c, as indicated by (3.81). We then introduce a regulator, called a quantum parameter, for each of these components, denoted δ_b and δ_c, respectively. All we have to do then is perform the following substitution in (3.84)

$$b \to \frac{\sin(\delta_b b)}{\delta_b} \quad \text{and} \quad c \to \frac{\sin(\delta_c c)}{\delta_c}, \tag{3.85}$$

which leads to the following expression for the effective Hamiltonian

$$H_{\text{eff}} = -\frac{1}{2\gamma}\left(2\frac{\sin(\delta_c c)}{\delta_c}\frac{\sin(\delta_b b)}{\delta_b}p_c + \left(\left(\frac{\sin(\delta_b b)}{\delta_b}\right)^2 + \gamma^2\right)p_b\right) \approx 0. \tag{3.86}$$

As mentioned in 3.3.1, the polymerization procedure does not constrain the choice of the quantum parameters δ_b and δ_c. Similarly to the cosmological case, these parameters can be phase space dependent and several choices can be envisaged, motivated by different physical considerations. we will not present all possible choices investigated in the literature, it is possible to find a summary of the different schemes envisaged in [31]. However, let us present an extremely general argument, analogous to the one discussed for LQC in 3.1.3, which shows that these polymer models should lead to a singularity resolution. It can be seen from (3.84), and with the choice of lapse function made below, that cp_c is a Dirac observable. A solution of the classical equation of motion would show that $\frac{cp_c}{\gamma L_o}$ is the mass of the black hole. On the other hand, one can see from (3.86) that if δ_b (or δ_c) is a constant or a function only of b and p_b (or a function only of c and p_c), then $\frac{\sin(\delta_c c)}{\delta_c}p_c$ is again a Dirac observable. It is natural to expect that this quantity is finite and non zero, since in the classical regime (i.e. for $\delta_c \to 0$) it should correspond to the black hole mass. Furthermore, we know that p_c is the surface radius squared. This quantity cannot go to zero in the effective setting, since c has been replaced by $\frac{\sin(\delta_c c)}{\delta_c}$, which is bounded in contrast to c in the classical case. Therefore, the surface $p_c = 0$ containing the classical singularity does not exist in the effective dynamics. In the next section we will discuss in more detail one regularization scheme in particular corresponding to the BMM [86] model, which leads to a singularity free metric. At the end of this section, we will keep our discussion general and discuss the advantages of such models as well as the problems they pose.

3.3.3 Interests and issues of these models

In this subsection, we will discuss the reasons why these models have attracted and continue to attract great interest. On the other hand, these models are not without their problems, some of which we will attempt to address in the remainder of this chapter. We have already begun to discuss the great diversity of polymer black hole models in the previous subsection, associated with the many possible choices of the quantum parameters δ_b and δ_c. Although the exact structure of the metric varies from model to model, they all lead to the resolution of the classical singularity. In fact, these models are technically simple enough to be studied either analytically or numerically. For all of them it is possible to show that the Kretschmann scalar never diverges, thus eliminating

what is sometimes called the scalar singularity. In fact, as we suggested in the previous subsection, it is possible to show in more detail that the surface radius can no longer cancel in these models and that there exists a surface where the surface radius takes a minimum value. This surface is generally of the order of the Planck surface and lies in a region where the curvature is Planckian. It is called a transition surface because it separates a trapped region, which corresponds to the interior of the black hole and which also exists classically, from an anti-trapped region, which does not exist classically. This transition is sometimes called the black to white hole transition, or bounce, because the interior of a black hole is isometric to a homogeneous and anisotropic cosmological model (Kantowschi-Sachs model), and the transition surface is analogous to the bounce in the LQC.

Moreover, these models restore the geodesic completeness of spacetime that was lost in the case of a classical black hole. In this way, they solve the singularity problem suggested by Penrose's theorems. An object falling into such a black hole will not stop at the transition surface, but will continue beyond it into a white-hole-like region, and escape into a region whose exact geometry depends on the details of the model, such as the expression of the quantum parameters used. For all these reasons, these models are of great interest. However, despite the compelling singularity resolutions, these models are only a first step towards a clear understanding of non-perturbative quantum gravitational effects. To move forward, it is important to address their limitations and shortcomings.

We will now mention some of these problems, starting with the most general and ending with the most specific. The idea is not to criticize and reject these models out of hand, but rather to point out their weaknesses, which need to be addressed, and which we will attempt to do in the remainder of this manuscript. The first criticism that can be made, in the context of the first part of this manuscript, is that these models ignore one of the main lessons of the EFT treatment of general relativity. Indeed, the latter suggests that the metric is an effective description that is valid only at a scale of curvature below the Planck curvature. A metric description below this scale does not seem possible, and other d.o.f, whose exact nature is still unknown, must be taken into account. Polymer black hole models ignore this fact by assigning a metric to the Planck curvature regime without attempting to describe these additional d.o.f that are expected to be relevant at this scale.

Another problem we want to mention is the absence of matter. There is however a class of models that describe the collapse of matter into a black hole. Here, too, the polymerization process is used, which avoids the formation of a classical singularity. However, it is even less clear that an effective description is sufficient for this class of systems. In fact, there is no general procedure for renormalizing fluctuations of the energy-momentum tensor in curved spacetime. The latter are likely to become important near the singularity and thus generate significant geometric fluctuations. We will return to this problem in more detail in the final part of this thesis, when we turn our attention to the information loss paradox, for which it will be crucial to consider the effects of ingoing Hawking radiation.

One the other, there is no purely quantum description of the geometric d.o.f for these models. This means that, in contrast to LQC, the structure of the physical Hilbert space and the operator algebra is not known. This makes it impossible to describe the geometry in terms of a wave function, which may be in a superposition of states or even entangled with an external system. However, this is necessary to study entanglement with additional matter if one want to study the information loss paradox. This issue motivated a quantum black hole model that we elaborated and will present in

chapter 5. Moreover, the effective description obtained by the polymerization procedure in LQC emerged from the quantum description. Since we do not have such a quantum description for black holes, the effective description is assumed but not justified.

We could also mention the presence of a Cauchy horizon in these models, which leads to the loss of predictability or instability of spacetime. However, this problem goes beyond these models, since it is also present in classical Kerr or Reissner-Nordstrom solutions, so we will not develop it further here (see [106] for a discussion of this issue in the case of loop quantum black hole models). Moreover, these models rely on a specific foliation. In fact, as mentioned in the subsection 3.3.2, it is common to consider a foliation $R =$ constant. However, it is not obvious whether a different choice would lead to different physical predictions. In fact, it has been shown in [107–110] that foliation independence is lost for this class of effective models. Although it is important to keep in mind the existence of these problems, we will not have much to say about these two issues, and we will focus on those mentioned above, starting with the ambiguities in the polymerization scheme.

The last issue we would like to mention, which is the one we will address in the next part, is the following one : the choice of the polymerization scheme (i.e. the use of the sine function and the choice of the quantum parameters δ_b and δ_c) is not identified a priori from fundamental principles or deductions from full LQG. Rather, it is motivated by the polymerization procedure derived from LQC (cf. 3.3.1) and adapted a posteriori, requiring a good classical limit at large scales. But there is nothing unique about the procedure used. Indeed, as presented in 3.2.1, the use of the sine function is supposed to represent working with the holonomy in the fundamental representation in full LQG. However, it has been known for some time that there may be quantization ambiguities associated with this choice even in the full theory [90]. These ambiguities affect models such as [93] in which the polymerization scheme is derived from the full theory taking expectation values with respect to symmetry-reduced coherent states. The effect of such ambiguities has recently been analyzed in the context of quantum cosmology in [89], showing that they strongly influence the physics. [89]. It will be the task of the next chapter to discuss the role of this ambiguity in the context of black holes.

4 Regularization ambiguities

In this part, we will study the physical consequences of the change of the polymerization scheme, presented in 3.3.1 and applied to black holes in 3.3.2, on the physics of polymer black holes (the results presented in this chapter is strongly based on [44]). To that end, we focus on a specific polymer black hole model, the one proposed in [86] that we refer to as the BMM (Bodendorfer, Mele, Münch) model from here on. The model is a spherically symmetric black hole, with a four-dimensional phase space. The two configuration variables correspond to a time and an angular component of the metric. As we will see, the use of this specific choice of variables allows to realize a so-called $\bar{\mu}$-scheme on the Ashtekar-Barbero variables. We will not touch these choices. We will instead investigate what happens if the sine functions used in the polymerization [86] are replaced by *arbitrary* functions. We expect that our techniques and the implications of our results can be applied to models of polymer quantum black holes such as [85, 86, 111–130] other than BMM. It turns out that many properties of the polymer black holes are accessible without making an explicit choice for these functions. This remarkable fact is due to the simplicity of the model, in particular the fact that one of the two Dirac observables remains simple even after polymerization. The second does not, and it makes some of ours formulas implicit, without however hindering our considerations. We show first of all that the configuration variables of [86] produce a $\bar{\mu}$-scheme for any choice of polymer functions. Requiring the correct semiclassical limit at spatial infinity imposes a condition on the first derivatives of both polymer functions, but also a condition on the second derivative of the angular polymer function. Regularity of both functions avoids singularities, and replaces them with bounces. The number of bounces turns out to be determined by the angular function alone; whereas the number of horizons is determined by the time function alone. Their relative location depends on both the chosen functions and the solution considered. We provide a general graphical analysis to deduce these properties without committing to specific choices, but our analysis and formulas can be of help also in studying a specific model that one may be interested in. Our results shows that there is a valuable richness in the class of polymer black holes, and that considerable mathematical control can be kept also relaxing the standard choice of sine polymer functions. We hope that some of this control can be used to address some of the limitations and help constructing more robust models.

4.1 From the classical black hole to a polymerized black hole

We will review the classical Schwarzschild solution, based on the Hamiltonian formulation, in order to introduce the notations commonly used in the literature. More precisely, after giving the general expression of the line element compatible with the symmetry considered (i.e. spherical symmetry and staticity) in term of the geometrodynamic variables. Then we will recall how the problem can be reformulated in terms of Ashtekar-Barbero variables and how this reformulation can lead to a new convenient set of variables, the (v, P) variables. From there, we will quickly recall the general ideas of the BMM polymerisation model which will be useful in the next part. We will highlight the main result of this model like the resolution of the singularity but we will also insist on the limitation of this model caused by the particular choices on which it is built.

4.1.1 Minisuperspace black hole model

We consider the following spherically symmetric and static ansatz

$$ds^2 = -\bar{a}(r)dt^2 + \frac{\bar{n}(r)}{\bar{a}(r)}dr^2 + \bar{b}^2(r)d\Omega^2. \tag{4.1}$$

The spatial diffeo constraint vanishes identically, and we eliminated the shift vector via our choice for the coordinates t, θ and ϕ. On the other hand, we have not fixed the r coordinate to be the area radius, and there is still a non-trivial Hamiltonian constraint to be solved associated with this reparametrization. Plugging this ansatz into the Einstein's equations, one finds

$$\bar{n}(r) = c_1^2\dot{\bar{b}}(r)^2, \qquad \bar{a}(r) = c_1^2\left(1 - \frac{c_2}{\bar{b}(r)}\right). \tag{4.2}$$

The solution space is thus parametrized by two constants of integration, and $\bar{n}(r)$ is arbitrary. However only one of the constants has a geometrical interpretation, since c_1 can always be reabsorbed by rescaling the coordinate t. The metric in this form can be recognized to be the Schwarzschild solution, with

$$M = \frac{c_2}{2}, \tag{4.3}$$

asymptotic unit proper time $\tau := c_1 t$ and area radius b. We can freely choose a constant $\bar{n}(r) \equiv c_1^2$, and this will make r the area radius. In other words, one constant of integration is the black hole's mass, another is a rescaling of the asymptotic time, and $\bar{n}$ is the freedom of r-reparametrizations.

The symmetry reduction makes the Einstein-Hilbert action, as well as the ensuing Poisson structure, divergent on a open topology. In the following, we will study the canonical structure of the foliation by hypersurfaces of constant r. This is because r is a time-like coordinate inside the horizon, and we are ultimately interested in the dynamics near the singularity. To regularize the action, one introduces a fiducial cell for the coordinates $x := (t, \theta, \phi)$ given by $C := [0, \ell_0] \times S^2$. The physical size L_0 of the fiducial cell is r-dependent. Taking for instance spatial infinity as reference, we have

$$L_0 := \int_0^{\ell_0} \sqrt{|g_{tt}(r=\infty)|}dt = \ell_0|c_1| \tag{4.4}$$

on-shell. Then,

$$S[C] = \frac{1}{16\pi}\int dr \int_C d^3x\sqrt{-g}R + \text{boundary term} = \int dr\, L, \tag{4.5}$$

where

$$L := \frac{\ell_0\sqrt{\bar{n}}}{2}\left(\frac{\dot{\bar{a}}\dot{\bar{b}}\bar{b}}{\bar{n}} + \frac{\bar{a}\dot{\bar{b}}^2}{\bar{n}} + 1\right). \tag{4.6}$$

The boundary term to be added to the action is the Gibbons-Hawking-York term, which takes care of eliminating derivatives on lapse and shift. For the interested reader, details are reported in Appendix B. It is convenient to reabsorb the coordinate length ℓ_0 changing variables to:

$$\sqrt{a} := \ell_0\sqrt{\bar{a}}, \qquad b := \bar{b}, \qquad \sqrt{n} := \ell_0\sqrt{\bar{n}}, \tag{4.7}$$

Notice that $\sqrt{a}$ is the physical length of the fiducial cell in the t direction as a function of r. We end up with the following Lagrangian,

$$L(a,b,n) = \frac{\sqrt{n}}{2}\left(\frac{\dot{a}\dot{b}b}{n} + \frac{a\dot{b}^2}{n} + 1\right) \tag{4.8}$$

which will give a well-defined phase space.

At this point the spherical black hole minisuperspace model is effectively being described by a point-particle mechanical system.[6]

The solution space is the same as before, in particular

$$a = \ell_0^2 c_1^2 \left(1 - \frac{c_2}{b}\right). \tag{4.9}$$

However, there is an important difference about the physical interpretation of the solutions: in the point-particle description we have no longer access to the coordinate t, hence it is not possible to reabsorb c_1 with a time diffeomorphism. In other words, fiducial cells of different physical size (4.4) correspond to physically distinct points in the solution space.

Turning c_1 from an irrelevant constant to a physical one is clearly an artefact of the regularization, but it is also natural in the following sense. In the full space space, the Schwarzschild solution is a one-parameter trajectory. The smallest phase space in which this family can be embedded is 2-dimensional, hence we expect a second variable to be present and to be conjugated to the mass, and c_1 plays this role. The role of the regularization in defining this two-dimensional phase space can also be nicely understood looking at the symplectic potential obtained from the on-shell variation of (4.5), which in the area-radius gauge gives

$$\theta = -\frac{1}{2}\ell_0 \left(c_1 dc_2 + 2c_2 dc_1 - 2r dc_1\right), \tag{4.10}$$

with symplectic structure

$$\omega = \frac{\ell_0}{2} dc_1 \wedge dc_2. \tag{4.11}$$

Removing the regulator taking $\ell_0 \to \infty$ gives a divergent symplectic structure. One can also see that the commutation relation $\{c_1, c_2\} = 2/\ell_0$ has a vanishing limit, and interpret this as a sign that one of the coordinates loses its dynamical role, c_1 in this case, and can be reabsorbed into the redefinition of asymptotic time .[7]

We now review the Hamiltonian of the system associated with the foliation by r =constant hypersurfaces. The signature of this foliation is not fixed, being time-like outside the horizon, null at the horizon, and space-like inside. No issues arise from this fact, thanks to the symmetry reduction the dynamics is well-defined for all values of r. The lapse function in the interior is

$$N(r) = \frac{\sqrt{n(r)}}{\sqrt{-a(r)}}. \tag{4.12}$$

[6] And it is part of a class of minisuperspace models described by the motion of point particles in a given supermetric, which in this case reads

$$G = \frac{2\sqrt{n}}{b}\begin{pmatrix} -a/b & 1 \\ 1 & 0 \end{pmatrix}.$$

See e.g. [131] for a description in these terms of generic spherical black holes and Bianchi models.

[7] This is the same observation already made at the quantum level in [132].

Inspection of the Lagrangian shows that one can freely trade between N and n as Lagrange multipliers. With this choice of time, the conjugate momenta with respect to this global time parameter are

$$p_a = \frac{\partial L}{\partial \dot{a}} = \frac{b\dot{b}}{2\sqrt{n}}, \qquad p_b = \frac{\partial L}{\partial \dot{b}} = \frac{2a\dot{b} + \dot{a}b}{2\sqrt{n}}, \qquad p_n = \frac{\partial L}{\partial \dot{n}} = 0. \tag{4.13}$$

The last equation gives a primary constraint, that should be added to the Legendre transform of the Lagrangian. Upon doing so, one finds the primary Hamiltonian

$$H(n) = \sqrt{n}\left(\frac{2p_a p_b}{b} - \frac{2ap_a^2}{b^2} - \frac{1}{2}\right) + \lambda p_n, \tag{4.14}$$

where λ is a Lagrange multiplier. Stabilizing the primary constraint, i.e. imposing $\dot{p}_n \approx 0$, leads to the secondary constraint

$$\psi := \frac{2p_a p_b}{b} - \frac{2ap_a^2}{b^2} - \frac{1}{2} \approx 0. \tag{4.15}$$

This is the Hamiltonian constraint generating r-diffeomorphisms. It is automatically stable, and no further constraints arise in the analysis. We thus obtain a 2-dimensional physical phase space, in agreement with the two-parameter family of solutions (4.2). Moreover $\dot{n} = \lambda$, hence we can treat $\sqrt{n}$ as a Lagrange multiplier, remove the pair (n, p_n) from the phase space and set $\lambda = 0$ without any loss of generality. Then we have a 4d kinematical phase space with Hamiltonian constraint $H(n) = \sqrt{n}\psi$. We will use this formulation from now on.

Consider now the following canonical transformation [86],

$$v_1 := \frac{2}{3}b^3, \qquad P_1 := \frac{p_b}{2b^2} - \frac{ap_a}{b^3} = \frac{\dot{a}}{4\sqrt{n}b}, \tag{4.16a}$$

$$v_2 := 2ab^2, \qquad P_2 := \frac{p_a}{2b^2} = \frac{\dot{b}}{4\sqrt{n}b}, \tag{4.16b}$$

$$\{v_i, P_j\} = \mathrm{d}_{ij}. \tag{4.16c}$$

It is the generalization to the black hole model of a similar transformation used in loop quantum cosmology, and it will be relevant to construct the effective quantum model below. In terms of the new variables the Hamiltonian constraints becomes

$$H(n) = \sqrt{n}\left(12v_1P_1P_2 + 4v_2P_2^2 - \frac{1}{2}\right), \tag{4.17}$$

and generates the dynamical equations

$$\dot{v}_1 = 12\sqrt{n}v_1P_2, \tag{4.18a}$$

$$\dot{v}_2 = 12\sqrt{n}v_1P_1 + 8\sqrt{n}v_2P_2, \tag{4.18b}$$

$$\dot{P}_1 = -12\sqrt{n}P_1P_2, \tag{4.18c}$$

$$\dot{P}_2 = -4\sqrt{n}P_2^2. \tag{4.18d}$$

Notice that the equations for P_i are decoupled. It is also possible to easily identify two constants of motion. The first can be deduced by inspection of the Hamiltonian, and it is given by

$$K_1 = v_1P_1. \tag{4.19}$$

The second can be found taking the ratio of (4.18c) and (4.18d) and integrating, giving

$$K_2 = \ln|P_1| - 3\ln|P_2|. \tag{4.20}$$

In performing the integration we fix the integration constants so that the two contributions to K_2 vanish when $P_1 = 1$ and $P_2 = 1$. The two constants of motion turn out to be canonically conjugated functions, $\{K_1, K_2\} = 1$, and commute with the Hamiltonian constraint by construction. Therefore they provide two Dirac observables for the system.

It is instructive to derive the Schwarzschild solution from this formulation of the dynamics, because it will help comparison with the polymerized model below. To solve the equations, let us fix its gauge freedom imposing $n = n_o$ constant, Then, (4.18d) is solved by

$$P_2(r) = \frac{1}{4\sqrt{n_o}r}, \tag{4.21}$$

up to a constant of integration that can always be absorbed by a shift of the r coordinate. This solution is valid provided $r \neq 0$. We restrict the domain to $r > 0$, hence $b > 0$. Then, using (4.20) directly leads to

$$P_1(r) = \mathrm{sign}(P_1)\frac{e^{K_2}}{(4\sqrt{n_0}r)^3}. \tag{4.22}$$

From this, (4.19), and the fact that $v_1 = \frac{2}{3}b^3 > 0$, we derive that

$$P_1(r) = \frac{\mathrm{sign}(K_1)e^{K_2}}{(4\sqrt{n_0}r)^3} \quad \text{and} \quad v_1(r) = (4\sqrt{n_o})^3|K_1|e^{-K_2}r^3, \tag{4.23}$$

Finally, from the vanishing of the Hamiltonian constraint (4.17) we derive that

$$v_2(r) = 4\sqrt{n_o}\left(\frac{1}{2}\sqrt{n_o} - \frac{3K_1}{r}\right)r^2. \tag{4.24}$$

This general solution is of course equivalent to (4.2) found earlier. To see this explicitly, we can reconstruct the metric. Let us do so in terms of the unbarred quantities (4.7), in terms of which it reads

$$\mathrm{d}s^2 = -\frac{a(r)}{\ell_0^2}\,\mathrm{d}t^2 + \frac{n(r)}{a(r)}\,\mathrm{d}r^2 + b(r)^2\,\mathrm{d}\Omega^2. \tag{4.25}$$

Inverting (4.16), we obtain

$$a = \frac{e^{2K_2/3}}{16}\left(\frac{2}{3|K_1|}\right)^{2/3}\left(1 - \frac{24\left(\frac{3}{2}\right)^{1/3}K_1|K_1|^{1/3}e^{-K_2/3}}{b}\right), \tag{4.26}$$

$$b = 4\sqrt{n_o}\left(\frac{3|K_1|}{2}\right)^{1/3}e^{-K_2/3}r. \tag{4.27}$$

where

$$M = 2^{5/3}3^{4/3}K_1|K_1|^{1/3}e^{-K_2/3}. \tag{4.28}$$

We see that the metric describes the Schwarzschild solution with mass M, area radius b, and asymptotic time

$$t_S := \frac{e^{K_2/3}}{4\ell_0}\left(\frac{2}{3|K_1|}\right)^{1/3}t. \tag{4.29}$$

The solution space is spanned by all values $K_i \in \mathbb{R}^2$. Each point in this space describes a Schwarzschild black hole (with given mass—positive or negative—asymptotic time and area radius), except the line $K_1 = 0$ which describes a degenerate spacetime. The zero-mass limit corresponds to the limit $K_i \to (0^{\pm}, -\infty)$.

The last equation (4.27) shows that if one wants to fix the gauge $b = r$, then the constant n_0 has to be chosen in a phase-space dependent manner (note that we had already stumbled upon this fact below equation (4.3))[8]. For convenience, we also report the relation between the K_i's and the c_i's,

$$K_1 = \frac{\ell_0 c_1 c_2}{6} \qquad K_2 = \log\left|16\ell_0^4 c_1^4 c_2\right| = \log\left|16\ell_0^4 c_1 c_2\right| + 3\log|c_1|. \tag{4.30}$$

From these relations we recover the results of the previous section, in particular the expression (4.3) for the mass, and c_1 being the only parameter that enters the rescaling of the asymptotic time.

Let us add a few remarks useful in the following.

- On the interpretation of the P_i variables. Using the on-shell values (4.21) and (4.23) and the relation between b and r (4.27), one finds [86]

$$P_1(b) = \frac{M}{b^3}\left(\frac{2}{3|K_1|}\right)^{1/3}\frac{e^{K_2/3}}{8}, \qquad P_2(b) = \frac{1}{b}\left(\frac{3|K_1|}{2}\right)^{1/3} e^{-K_2/3}. \tag{4.31}$$

  Thus P_1 is proportional to the (square root of the) Kretschmann scalar, and P_2 to the inverse area radius of the Schwarzschild black hole.

- Any phase space function that is monotonic in r will be a good clock for our Hamiltonian evolution. From the general solution, we see that all variables except v_2 are monotonic functions of r. Therefore, all of them provide good internal clocks. If we choose P_2 in particular, we can rewrite the metric in a lapse-independent way,

$$\begin{aligned} ds^2 =& -\frac{1}{16}\left(\frac{2e^{K_2}}{3K_1}\right)^{2/3}(1-24K_1P_2)\,\mathrm{d}\tau^2 \\ &+\left(\frac{3K_1\lambda_1}{2\lambda_1 P_1}\right)^{2/3}(1-24K_1P_2)^{-1}\,{\lambda_2}^2\,\mathrm{d}{P_2}^2 + \left(\frac{3K_1\lambda_1}{2\lambda_1 P_1}\right)^{2/3}\mathrm{d}\Omega^2, \end{aligned} \tag{4.32}$$

$$\tau := \frac{t}{\ell_0} \tag{4.33}$$

  This is the form of the metric that we will write below for the polymerized model.

[8] There is a subtlety about n_0, not relevant for the following, but useful to make contact with a discussion made in [86]. Under a change of fiducial cell $\ell_0 \mapsto \alpha\ell_0$, the function n rescales as $n \mapsto \alpha^2 n$. Under a time diffeomorphism $t \mapsto t'(t)$, it is invariant—this follows from its definition

$$\sqrt{n} := \ell_0\sqrt{\bar{n}} = \int_0^{\ell_0}\sqrt{-g_{tt}g_{rr}}dt$$

which makes it akin to a volume quantity. Therefore, also the constant n_0 has to be chosen in an ℓ_0-dependent way in order to preserve this properties.

4.1.2 Ashtekar-Barbero variables

The first step towards polymerisation is a canonical transformation to Ashtekar-Barbero variables,

$$A^i_a := \Gamma^i_a + \gamma K^i_a, \qquad E^a_i = \frac{1}{2}\epsilon_{ijk}\epsilon^{abc}e^j_b e^k_c, \tag{4.34}$$

where γ is the Immirzi parameter. For the interior of a spherically symmetric and static spacetime we can take them to be [85, 116, 121][9]

$$A^i_a \tau_i dx^a = \frac{c(r)}{\ell_0}\tau_3 dt + d(r)\tau_2 d\theta - d(r)\tau_1 \sin\theta d\phi + \tau_3 \cos\theta d\phi, \tag{4.35}$$

$$E^a_i \tau^i \partial_a = p_c(r)\tau_3 \sin\theta \partial_t + \frac{p_d(r)}{\ell_0}\tau_2 \sin\theta \partial_\theta - \frac{p_d(r)}{\ell_0}\tau_1 \partial_\phi, \tag{4.36}$$

where $\tau_i = (-i/2)\sigma_i$ and σ_i are the Pauli matrices. The map to the previous variables is given by

$$\mathrm{sign}(p_c)\, c = -2\gamma\left(\frac{p_b}{2b} - \frac{a p_a}{b^2}\right) = -2\gamma P_1 \left(\frac{3v_1}{2}\right)^{1/3}, \tag{4.37a}$$

$$\mathrm{sign}(p_d)\, d = 2\gamma \frac{\sqrt{-a}p_a}{b} = 4\gamma P_2 \sqrt{-\frac{v_2}{2}}, \tag{4.37b}$$

$$\mathrm{sign}(p_c)\, p_c = b^2 = \left(\frac{3v_1}{2}\right)^{2/3}, \tag{4.37c}$$

$$\mathrm{sign}(p_d)\, p_d = \sqrt{-a}b = \sqrt{-\frac{v_2}{2}}. \tag{4.37d}$$

The overall sign ambiguity is the usual global parity freedom in the triad, whereas the relative sign ambiguity is a consequence of the symmetry reduction, and cannot be eliminated [25]. This map is a canonical transformation, with non vanishing Poisson brackets given by

$$\{c, p_c\} = 2\gamma, \qquad \{d, p_d\} = \gamma, \tag{4.38a}$$

and Hamiltonian constraint

$$H(N) = -\frac{Nd}{2\gamma^2 \,\mathrm{sign}(p_c)\sqrt{|p_c|}}\left(2cp_c + \left(d + \frac{\gamma^2}{d}\right)p_d\right). \tag{4.39}$$

As before lapse is related to our choice of Lagrange multiplier n by (4.12), a redefinition which does not affect the equations of motion.[10]

4.1.3 BMM polymerisation

The BMM model [86] is based on the (v_i, P_i) phase space variables we reviewed above. There are two key observations made in [86] that motivate the use of these variables. The first is that as we observed above, P_1 is related to the Kretschmann scalar and P_2 to the inverse area radius.

[9] With the renaming $b(r) \mapsto d(r)$ to avoid confusion with our $b(r)$ defined in (4.1) and (4.7).

[10] Hamilton's equations are modified by the addition of a term proportional to the constraint and thus zero on-shell.

Hence we could intuitively expect that replacing these variables by bounded functions should remove the classical divergences of the dynamics. The second is that polymerizing these variables with a non-dynamical regulator induces a $\bar{\mu}$-scheme on the Ashtekar-Barbero variables, compatible with the Hamiltonian. Hence these variables are the analogue of the (v, b) variables in loop quantum cosmology. To see this, consider the replacement

$$P_i \to \frac{\sin(\lambda_i P_i)}{\lambda_i}, \qquad i = 1, 2, \tag{4.40}$$

where λ_1 and λ_2 are a priori independent polymerisation scales (i.e. the scale at which the modification of the dynamic will be important). We take them to be constants, and of Planckian order. From (4.37) we have that

$$\lambda_1 P_1 = \delta_c c, \qquad \delta_c := -\text{sign}(p_c)\frac{\lambda_1}{2\gamma\sqrt{|p_c|}}, \tag{4.41}$$

$$\lambda_2 P_2 = \delta_d d, \qquad \delta_d := \text{sign}(p_d)\frac{\lambda_2}{4\gamma|p_d|}. \tag{4.42}$$

Hence the replacement (4.40) is equivalent to

$$c \to \frac{\sin(\delta_c c)}{\mathrm{d}_c}, \qquad d \to \frac{\sin(\mathrm{d}_d d)}{\mathrm{d}_d d}, \tag{4.43}$$

where the quantum parameters δ_c and δ_d have a phase-space dependance given by (4.41). This phase-space dependence can be used to introduce the area-gap of the full theory, thus defining a $\bar{\mu}$-scheme for the Ashtekar-Barbero variables. The replacement (4.40) leads to the modified Hamiltonian constraint

$$H_{\text{eff}}(n) = \sqrt{n}\mathcal{H}_{\text{eff}} \quad , \quad \mathcal{H}_{\text{eff}} = 12v_1\frac{\sin(\lambda_1 P_1)}{\lambda_1}\frac{\sin(\lambda_2 P_2)}{\lambda_2} + 4v_2\frac{\sin(\lambda_2 P_2)^2}{\lambda_2^2} - \frac{1}{2} \approx 0. \tag{4.44}$$

On the other hand, the polymerization of the Ashtekar-Barbero Hamiltonian (4.39) under (4.43) gives

$$H_{\text{eff}}(N) = -\frac{N\sin(\delta_d d)}{\delta_d 2\gamma^2\,\text{sign}(p_c)\sqrt{|p_c|}}\left(2\frac{\sin(\delta_c c)}{\delta_c}p_c + \left(\frac{\sin(\delta_d d)}{\delta_d} + \frac{\gamma^2\delta_d}{\sin(\delta_d d)}\right)p_d\right).$$

Inserting (4.41), (4.37) and (4.12) in the latter recovers the former, therefore the polymerization (4.40) is consistent with the $\bar{\mu}$-scheme also at the dynamical level.

The dynamics generated by the polymerized Hamiltonian is expected to capture the mean field quantum corrections [88] and it is thus referred to as effective dynamics. This effective dynamics is obtained from (4.44) and the original Poisson brackets (4.16c), giving

$$\dot{v}_1 = 12\sqrt{n}v_1\cos(\lambda_1 P_1)\frac{\sin(\lambda_2 P_2)}{\lambda_2}\ , \tag{4.45a}$$

$$\dot{v}_2 = 12\sqrt{n}v_1\frac{\sin(\lambda_1 P_1)}{\lambda_1}\cos(\lambda_2 P_2) + 8\sqrt{n}v_2\frac{\sin(\lambda_2 P_2)}{\lambda_2}\cos(\lambda_2 P_2)\ , \tag{4.45b}$$

$$\dot{P}_1 = -12\sqrt{n}\frac{\sin(\lambda_1 P_1)}{\lambda_1}\frac{\sin(\lambda_2 P_2)}{\lambda_2}\ , \tag{4.45c}$$

$$\dot{P}_2 = -4\sqrt{n}\frac{\sin(\lambda_2 P_2)^2}{\lambda_2^2}\ , \tag{4.45d}$$

$$\mathcal{H}_{\text{eff}} = 3v_1\frac{\sin(\lambda_1 P_1)}{\lambda_1}\frac{\sin(\lambda_2 P_2)}{\lambda_2} + v_2\frac{\sin(\lambda_2 P_2)^2}{\lambda_2^2} - \frac{1}{8} = 0\ . \tag{4.45e}$$

It was shown in [86] that the equations can be solved analytically, and the following properties ensue:

1. The singularity at $b = 0$ is removed.
2. There are two asymptotic spacetime regions, both approaching a Schwarzschild geometry.
3. There is a space-like surface at some $b_{min} \neq 0$ inside the horizon, which is the a global minimum of the area radius b and corresponds to a black-to-white hole transition.
4. There are two independent Dirac observables, which can be physically interpreted as the masses of the separate asymptotic Schwarzschild regions, namely of the black and of the white hole masses respectively.
5. The horizon is slightly smaller than the classical result (for black hole masses large w.r.t. the polymerisation scales).
6. For black hole masses comparable or smaller of the polymerisation scales, there are large quantum effects at the horizon scale.
7. There is an upper bound to the curvature, as measured for instance by the Kretschmann scalar, and this value is obtained at the transition surface and depends on the black holes mass (as well as the white hole mass), unlike in the prior polymerization scheme of [85] or in other models of non-singular black hole [39]

This model has the nice feature that shows how an LQG–inspired quantization can lead to a resolution of the singularity and its explicit replacement by a (non-necessarily symmetric) black-hole-to-white-hole transition, a scenario suggested in [133]. A possible shortcoming of the model is that the scale at which quantum effects become large depends on the parameters, and a certain restriction on the masses is necessary if one wants to confine this scale to inside the horizon.[11] On the other hand, the model is based on several arbitrary choices:

(i) A specific foliation of the spacetime has been fixed, given by the level sets of the r coordinate in Schwarzschild coordinates, and it has been shown that different foliations can give different physical results [134].

(ii) A specific $\bar{\mu}$-scheme, based on the polymerisation of the two P_i variables, neither more nor less.

(iii) The polymerisation function for both variables is a sine function, in analogy with LQC models.

These choices are common, and indeed motivated by, the literature (see e.g. [85, 112–114, 116]). However, more general recent proposals exist, see e.g. [121]. Testing the robustness of the results with different choices, and conversely identifying choices that reduce the shortcomings, is crucial to move forward in the study of such models. In the rest of this chapter we focus on (iii), and study the effect of changing the polymerization function.

[11] This situation arises in other proposals as well [118]. An attempt to improve this situation has been made in [118, 119].

4.2 Generalised polymerisation

4.2.1 Presentation of the setup

To preserve the LQG-inspired idea of a polymer quantisation, it is sufficient to restrict the polymerisation function to a generic function (for a general discussion of this ambiguity see [90], for its study in quantum cosmology see [89]). Consequently, we consider a generic replacement

$$P_i \to \frac{f_i(\lambda_i P_i)}{\lambda_i}, \tag{4.46}$$

where f_1 and f_2 are real, bounded, C^1 and periodic functions of periodicity 2π, and such that $f_i(x) = x + o(x)$, that is

$$f_i(0) = 0, \tag{4.47a}$$
$$f_i'(0) = 1, \tag{4.47b}$$

with the notation $f_i' = \frac{\mathrm{d}f_i(\lambda_i P_i)}{\mathrm{d}(\lambda_i P_i)}$. Below in Section 4.4.1 we will prove that these conditions are necessary in order to recover the Schwarzschild solution in the large distance limit, but not sufficient: one further needs $f_2''(0) = 0$. This additional condition however does not affect qualitatively the short distance structure, hence we will only introduce it when needed explicitly. Following this replacement, the new polymerized Hamiltonian is given by

$$H_{\text{eff}} = \sqrt{n}\mathcal{H}_{eff}, \qquad \mathcal{H}_{\text{eff}} := 12v_1 \frac{f_1(\lambda_1 P_1)}{\lambda_1}\frac{f_2(\lambda_2 P_2)}{\lambda_2} + 4v_2 \frac{f_2^2(\lambda_2 P_2)}{\lambda_2^2} - \frac{1}{2} \approx 0, \tag{4.48}$$

In the limit $\lambda_i P_i \to 0$ we recover the classical Hamiltonian, thanks to the required linear behaviour around the origin.

The polymerized dynamical equations are

$$\dot{v}_1 = 12\sqrt{n}v_1 f_1' \frac{f_2}{\lambda_2}, \tag{4.49a}$$
$$\dot{v}_2 = 12\sqrt{n}v_1 \frac{f_1}{\lambda_1} f_2' + 8\sqrt{n}v_2 \frac{f_2}{\lambda_2} f_2', \tag{4.49b}$$
$$\dot{P}_1 = -12\sqrt{n}\frac{f_1}{\lambda_1}\frac{f_2}{\lambda_2}, \tag{4.49c}$$
$$\dot{P}_2 = -4\sqrt{n}\frac{f_2^2}{\lambda_2^2}, \tag{4.49d}$$
$$\mathcal{H}_{\text{eff}} = 3v_1 \frac{f_1}{\lambda_1}\frac{f_2}{\lambda_2} + v_2 \frac{f_2^2}{\lambda_2^2} - \frac{1}{8} \approx 0. \tag{4.49e}$$

They generalize (4.45) in a straightforward way. Remarkably, it is possible to solve these equations in full generality without specifying the functions f_i, even though in a partially implicit way. The knowledge of the implicit general solution will be sufficient to describe a large number of features of the modified spacetime generated by f_1 and f_2. The first step to construct this solution is to identify the Dirac observables.

4.2.2 Dirac observables

Dirac observables are gauge independent quantities, namely they Poisson-commute with all the constraints. The only constraint of our model is $\mathcal{H}_{\text{eff}}$ (cfr. Eq. (4.48)), which also generates the dynamics. Dirac observables will coincide with constants of motion, thus their identification leads immediately to the general solution of the equations of motions. More precisely, the expressions for the Dirac observables plus the constraints provide sufficient implicit relations to determine all phase space variables in terms of a chosen internal clock.

As the kinematical phase space is four-dimensional and we have one first class constraint, there are at most two independent Dirac observables. These were referred to as K_i in the non-polymerized case, and we keep the same notation. They can be identified proceeding as in the non-polymerized case. The first can be found by inspection of the Hamiltonian constraint (4.48) to be

$$K_1 := v_1 \frac{f_1}{\lambda_1}. \tag{4.50}$$

Recall further, that v_1 is closely related to the area radius b (cfr. Eq. (4.16)). Therefore, this Dirac observable will be useful to analyse the area radius as a function of P_1 and to make statements about possible bounces and black-to-white hole transitions (see Sec. 4.3.2 below). For the second Dirac observable again we divide (4.49c) by (4.49d) and integrate, obtaining as before

$$K_2\left(P_1, P_2\right) = \lambda_1 \int_1^{P_1} \frac{\mathrm{d}P_1}{f_1(\lambda_1 P_1)} - 3\lambda_2 \int_1^{P_2} \frac{\mathrm{d}P_2}{f_2(\lambda_2 P_2)}. \tag{4.51}$$

This constant of motion is well-defined for any choice of polymer function. However its explicit form can only be accessed once the functions are specified. The choice of lower bound in the integrals is made once and for all and it is needed to fix the freedom of constant shifts of Dirac observables. Here we picked 1 in agreement with the choice made in (4.20).

4.2.3 General expression of the metric

To solve the dynamics in terms of the Dirac observables, we will start by noticing that the Hamiltonian constraint (4.48) imposes that f_2 can never vanish on solutions. Consequently, the equation (4.49d) implies that P_2 is a strictly decreasing function of r. It is thus a good internal clock, and we use it to deparametrise the equations of motion,[12] and rewrite the metric coefficients as $a(P_2)$ and $b(P_2)$. Notice that with this choice the metric will be independent of the lapse, see (4.32). The coordinate r and P_2 are related via (4.49d)

$$dr = -\frac{\lambda_2^2}{4\sqrt{n} f_2^2} dP_2. \tag{4.52}$$

Next, we want to determine the metric coefficients in (4.25) as functions of P_2. To that end, b can be expressed in terms of P_1 using the first Dirac observable (4.50) and (4.16a), leading to

$$b(P_1) = \left(\frac{3\lambda_1 K_1}{2 f_1}\right)^{1/3}. \tag{4.53}$$

[12] Note that this is possible at the effective level as here we have access to P_2 directly. At the polymer quantum level P_2 is not available and this de-parametrisation would have to be reconsidered.

This can be turned into a function of P_2 using the implicit relation $P_1 = P_1(\lambda_2 P_2, K_2)$ determined by picking a specific value K_2 for the second Dirac observable (4.51). To make this step clear, we will use the following notation,

$$f_1\big(\lambda_1 P_1(\lambda_2 P_2, K_2)\big) = g_1(\lambda_2 P_2, K_2)\ . \tag{4.54}$$

To determine a, we use the Hamiltonian constraint (4.48) to write

$$v_2 = \frac{\lambda_2^2}{8 f_2^2} - \frac{3K_1\lambda_2}{f_2}. \tag{4.55}$$

Plugging this expression in (4.16) we find

$$a = \left(\frac{2f_1}{3\lambda_1 K_1}\right)^{2/3}\left(\frac{\lambda_2^2}{16 f_2^2} - \frac{3K_1\lambda_2}{2f_2}\right). \tag{4.56}$$

This way all metric components are expressed in terms of the Dirac observables K_i and the internal clock P_2, and the metric (4.25) reads[13]

$$\begin{aligned} ds^2 = &-\left(\frac{2g_1}{3K_1\lambda_1}\right)^{2/3}\left(\frac{\lambda_2}{4f_2}\right)^2\left(1-\frac{24K_1 f_2}{\lambda_2}\right)\mathrm{d}\tau^2 \\ &+\left(\frac{3K_1\lambda_1}{2g_1}\right)^{2/3}\left(1-\frac{24K_1 f_2}{\lambda_2}\right)^{-1}{\lambda_2}^2\,\mathrm{d}{P_2}^2 + \left(\frac{3K_1\lambda_1}{2g_1}\right)^{2/3}\mathrm{d}\Omega^2\ , \end{aligned} \tag{4.57}$$

with $\tau = t/\ell_0$ as before.

Note that the Dirac observable K_1 appears explicitly in this line element, while K_2 enters only implicitly via the definition of g_1, see Eq. (4.54). Once the polymer functions f_i have been specified, one can compute the integrals (4.51) and obtain $P_1(P_2)$. This will make g_1 explicit and thus the metric. It is quite remarkable that one can write the metric line element for completely arbitrary polymer functions, albeit with the limitation of an implicit function explained above. It means that one can deduce a great deal of the properties of the models without committing to specific choices too soon, and this is what we investigate next. As a sanity check, replacing the polymer functions by their arguments recovers the metric (4.32), namely the Schwarzschild solution. The polymerized metrics on the other hand are obviously not solutions of the Einstein's equations, and as we show in the next Section, describe spacetimes with a varying number of horizons and bounces, depending on the polymer functions as well as the Dirac observables. A feature that remains from the unpolymerized model is that $K_1 = 0$ describes metrics everywhere degenerate. In the following Section 4.4.1, we will show that even if the metrics do not describe a classical black hole, the Schwarzschild metric is recovered in the large radius limit, provided the condition $f_2''(0) = 0$ is satisfied.

In order to do so, it is convenient to express the metric using the area radius as coordinate, as opposed to P_2. However, the polymerization makes $b(P_2)$ a non-monotonic function. This is known already for the sine functions [86], and will become clear during the analysis of (4.49) in the next

[13] Note that all factors of n dropped out, which was expected as this is a pure gauge freedom specifying the coordinate r, which was replaced by the intrinsic clock P_2.

Section. The area radius coordinate will have to be independently defined in different branches. On each of these branches, we have

$$\mathrm{d}s^2 = -\frac{1}{b^2}\left(\frac{\lambda_2}{4f_2}\right)^2\left(1-\frac{24K_1f_2}{\lambda_2}\right)\mathrm{d}\tau^2 + \frac{1}{f_1'^2}\left(1-\frac{24K_1f_2}{\lambda_2}\right)^{-1}\mathrm{d}b^2 + b^2\,\mathrm{d}\Omega^2 \tag{4.58}$$

In other words, (4.57) is the maximal extension, and (4.58) the expression valid in each area radius patch.

4.3 Generic features of the dynamics

In this Section we study the geometry of the polymer spacetime (4.57). We show that it is possible to work out several features such horizons, bounces, and singularity resolution without specifying the polymerisation functions. We start by analysing the equations of motion as a dynamical system, in order to identify the asymptotic regions and relative locations of the spacetime features.

4.3.1 Evolution and fixed points

We proceed as follows. First, we eliminate the v_i variables using respectively K_1 and the Hamiltonian constraint. We then focus on the restricted space spanned by P_i, with equations of motion (4.49c) and (4.49d). Notice that $P_2 \neq 0$, otherwise the Hamiltonian constraint is violated as a consequence of (4.47). We also exclude $P_1 = 0$, because again from (4.47) it implies $K_1 = 0$ and as shown earlier these points describe degenerate metrics.

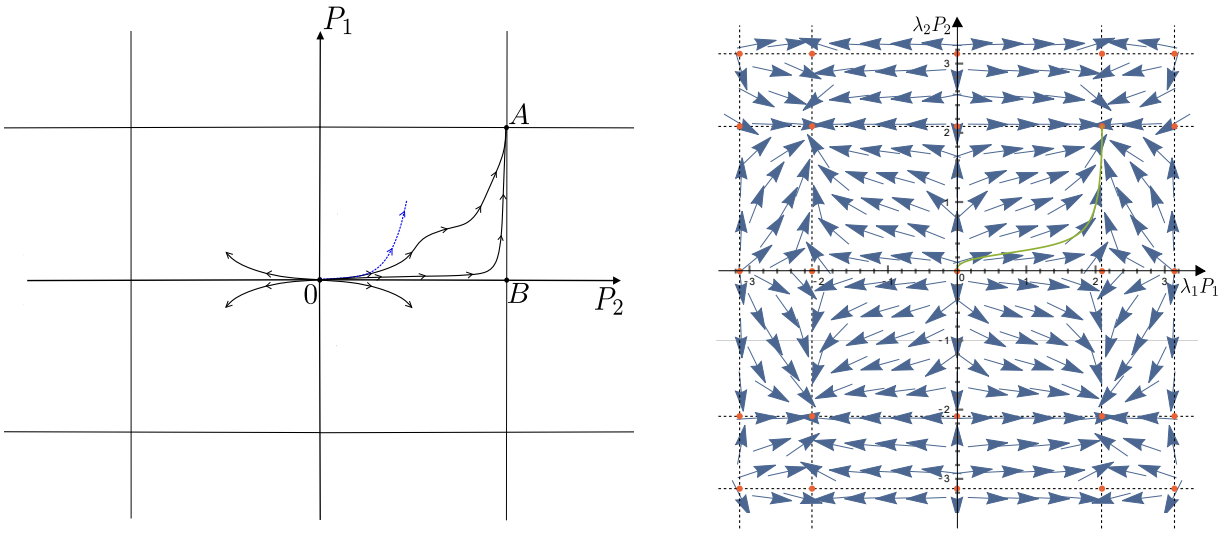
To study the restricted space of the dynamics of the P_i's, it is convenient to fix the lapse to

$$\sqrt{n} = \frac{\lambda_2}{4f_2}, \tag{4.59}$$

because it decouples the equations of motion. This gauge choice is always accessible, as the Hamiltonian constraint (4.48) implies $f_2(\lambda_2 P_2) \neq 0$ throughout the evolution. The dynamical flow is then described by the simple vector field

$$V(P_1, P_2) = \begin{pmatrix}\dot{P}_1\\ \dot{P}_2\end{pmatrix} = \begin{pmatrix}-3f_1/\lambda_1\\ -f_2/\lambda_2\end{pmatrix}. \tag{4.60}$$

We have already argued that f_2 can never vanish on solutions, because otherwise the Hamiltonian constraint is violated. On the other hand f_1 can vanish, but if it does, $K_1 \equiv 0$, and the motion is then confined on points which describe only degenerate metrics. Excluding degenerate metrics, the polymer functions can never vanish along the solutions. This key property implies that there are no fixed points to the dynamical system, and that the P_i's plane is partitioned into a check-board given by the zeros of the f_i's, with the dynamics being trapped inside each square. See Fig. 1, left panel, for an illustration. Notice that what matters is the zeros, not the period, of the f_i's. If there are zeros before the period, one obtains an irregular check-board with some squares smaller than others, see the right panel of the figure. Furthermore, the evolution of the P_i's is *monotonic* between the extrema allowed. This allows us to get a pretty clear qualitative picture of the dynamics. We focus on the four squares of the check-board connected to the origin, since they are the only ones



(a) (b)

Figure 1: (a) Qualitative picture of generic dynamics. The horizontal and vertical straight lines are the zeros of f_1 and f_2 respectively. The trajectories are monotonic in both variables within each square. The vertices of the check-board are alternatively repulsive and attractive asymptotic fixed points, like the origin and the point A, or unstable points like B. For reference, the blue dashed line is the relation in the case of the classical Schwarzschild solution. (b) Flow generated by the vector field V with $f_1(x) = f_2(x) = (\sin(x) + \sin(2x))/3$. In this example, an additional zero is present inside one period of each polymer function, hence the check-board of confined evolution has squares smaller than the period, and of different sizes. The (asymptotic) fixed points are marked with red dots.

that contain the classical regime $\lambda_i P_i \ll 1$. Even though the origin in itself is not an allowed configuration, it plays the role of an asymptotic fixed point, as we now show.

Near the origin the f_i's have a linear behaviour, hence (4.60) gives $\mathrm{sgn}(P_i) = \mathrm{sgn}(\dot{P}_i)$. Not only the evolution is monotonic, but it is also tied to the sign of P_i. Therefore if we trace it backwards it will tend towards the origin, whichever of the 4 squares we are on. The origin must thus be a repulsive fixed point. It is actually an asymptotic fixed point, since the point itself is excluded from the phase space. The monotonic evolution without fixed points then forces the system to reach the farthest corner (across the diagonal of the square) for each square, see again Fig. 1. These corners are thus attractive asymptotic fixed points.

The above description can be completed with an explicit perturbative expansion around the (asymptotic) fixed points. To that end, we posit

$$P_i(r) = \overset{\circ}{P}_i + \delta P_i(r), \tag{4.61}$$

where $\overset{\circ}{P}_i$ are zeros of f_i, and we Taylor-expand the polymer functions for $\lambda_i \delta P_i \ll 1$ around $\overset{\circ}{P}_i$. At leading order, (4.60) simplifies to

$$\delta\dot{P}_1 = -3\overset{\circ}{f}{}'_1 \delta P_1, \qquad \delta\dot{P}_2 = -\overset{\circ}{f}{}'_2 \delta P_2, \tag{4.62}$$

whose solutions are

$$\delta P_1 = \delta\overset{\circ}{P}_1 e^{-3\overset{\circ}{f}{}'_1 r}, \qquad \delta P_2 = \delta\overset{\circ}{P}_2 e^{-\overset{\circ}{f}{}'_2 r}. \tag{4.63}$$

From conditions (4.47b) we conclude that the exponents are negative, meaning that the classical regime is reached for $r \to \infty$. Conversely, the farthest corner must have negative derivatives (because it is the next zero of the function), hence it is reached for $r \to -\infty$. The remaining two corners of each square are unstable fixed points with one positive and one negative derivative.

This analysis can also be used to show that the area radius is not a monotonic function of P_2, and therefore not of r. In fact, we see from (4.53), and the periodicity of f_1, that b is not a monotonic function of P_1, and the monotonicity of the P_i as a function of r implies that also $P_1(P_2)$ is monotonic. Therefore, the inversion $P_2(b)$ can only be done for each of the branches, as illustrated in Fig. 2.

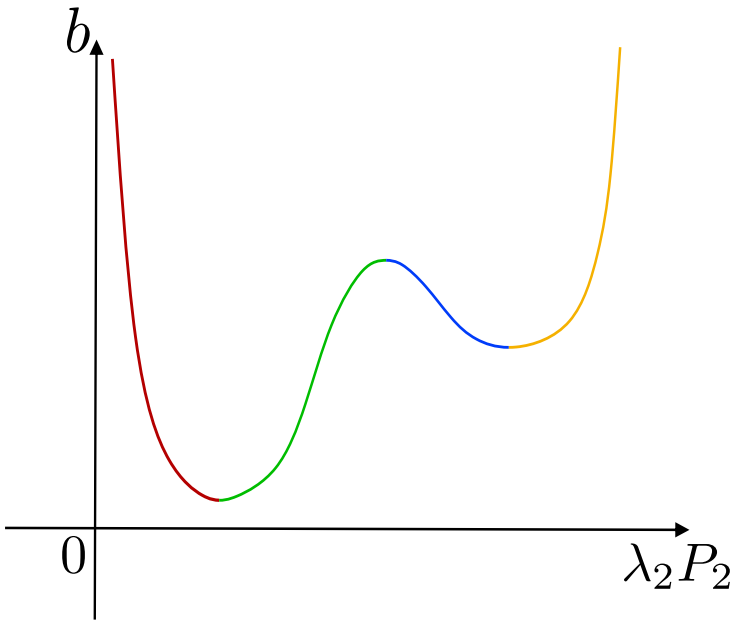


Figure 2: Plot of the area radius as a function of $\lambda_2 P_2$. Different colours are used to separate the branches where the function $b(\lambda_2 P_2)$ is invertible.

4.3.2 Bounces and singularity resolution

The notion of bounce can be visualized if we keep in mind the parallel between a black hole and a Kantowski-Sachs cosmological spacetime: a bounce is associated to a local minimum of the area radius $b(r)$. We will see in this Section that the location and number of bounces depends only on f_1. In the next Section we will see that the location and number of Killing horizon is determined by f_2 instead.

The evolution equation for the area radius given by (4.49a) is monotonic until we hit an extremum of f_1, namely a point such that

$$f_1' = 0, \qquad f_1'' \neq 0. \tag{4.64}$$

At this point the evolution turns around, and we have a bounce if it was initially decreasing, and a anti-bounce or turning point if it was increasing. Existence of at least one such point is

guaranteed by the requirement of periodicity of f_1. So the bounce is guaranteed, but we can have as many bounces and counter-bounces (or turning points) as we want, choosing the appropriate f_1. Furthermore, boundness of f_1 implies that that $b = 0$ is only accessible for the solutions with vanishing K_1 and those are everywhere degenerate. Therefore the bounce must occur before reaching zero area radius. This suggests that the Schwarzschild singularity is resolved. To look into the question of singularities more precisely, one can evaluate the Kretschmann scalar associated with (4.57). This can be done explicitly with the aid of an algebraic manipulator like Mathematica or Maple. The result has the following form,

$$R^2_{\mu\nu\rho\sigma} = \frac{F(g_1, f_2)}{f_2^4 g_1^{8/3}}, \tag{4.65}$$

where F is a six-order polynomial in g_1, f_2 and their first and second derivatives. If we take polymerisation functions that are periodic and C^2, the numerator in the previous expression is finite. The only divergences can arise from zeros of g_1 or f_2. These do occur, but at points that we have identified as the asymptotes for $r \to \pm\infty$. Let us examine them separately. The first of these is the origin in P_i space (see Fig. 1) where we know that the solution describes the Schwarzschild metric at $r \to \infty$ with finite (indeed vanishing) Kretschmann invariant. For the opposite corners, we don't have a general argument for finiteness. However these points correspond to $r \to -\infty$, therefore in so far as this limit describes the post-bounce behaviour of another asymptotically flat spacetime, it will be non-singular. We conclude that the only singularities allowed by these polymer models with smooth f_i's are big-rip-type singularities, and require polymer functions such that the curvature diverges at $r \mapsto -\infty$.

Of course in the case where the spacetime is also a Schwarzschild spacetime around this fixed point, the Kretschmann scalar will be finite also near this fixed point. This case is particularly interesting since it corresponds to a black to white hole transition. We will see in the following how to choose the polymerization functions f_1 and f_2 to obtain this situation. This type of argument can in principle be extended to other curvature scalars and it is an indication of the absence of singularities away from asymptotic points in these models.

4.3.3 Horizons

The number of horizons depends on f_1 alone, and their location on both f_i. From the general form (4.25) of the metric, we know that ∂_t is a Killing vector, therefore there is a Killing horizon whenever $a = 0$. From (4.16b) and the fact that $b \neq 0$ everywhere, this condition is equivalent to $v_2 = 0$. Using then the Hamiltonian constraint (4.48), this translates to

$$f_2 = \frac{\lambda_1\lambda_2}{24 v_1 f_1} = \frac{\lambda_2}{24 K_1}. \tag{4.66}$$

It is clear that it is possible to get any number of horizons, depending on the choice of f_2 and the value of K_1. Fig. 3 shows an example of polymer function admitting four horizons. Since f_2 is bounded, there always exist values of K_1 for which there are no horizons. The bound in order to have at least one horizon is

$$K_1 \geq \frac{\lambda_2}{24 \max f_2}. \tag{4.67}$$

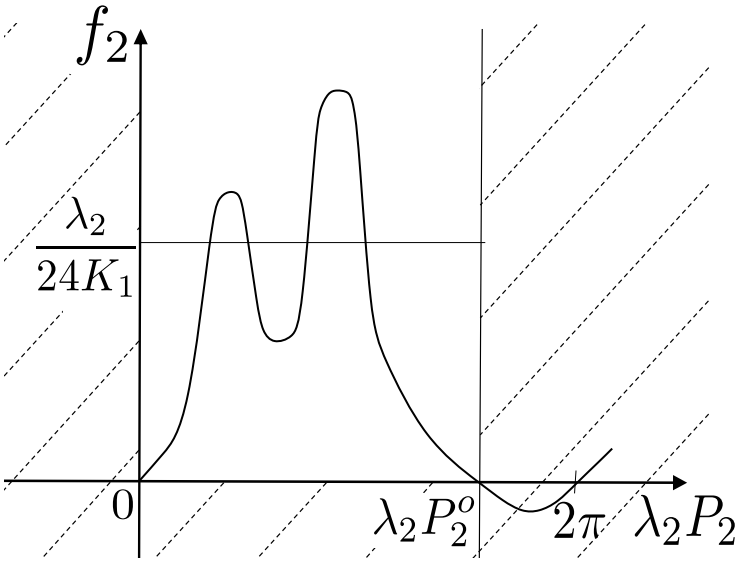


Figure 3: Sketch of an arbitrary example polymerisation function for f_2. Only the non-shaded region between $\lambda_2 P_2 = 0$ and $\lambda_2 P_2^o$ is relevant for the dynamics. The horizons correspond to the intersection of the function f_2 and the horizontal line $\frac{\lambda_2}{24K_1}$, explicitly depends on the chosen solution and the value K_1.

It follows that while the unpolymerized solution space describes always Schwarzschild black holes, of different mass and asymptotic time, the polymerized solution space always contains (non-singular) black holes as well as spacetimes without horizons (or exotic quantum stars).

These model polymers are not dynamical, and so cannot be used to describe the evaporation process suggested by Hawking. However, one may wonder how their horizons would evolve as their mass decreases. Similarly to the subsection 4.1.1, we will show in the subsection 4.4.1 that $K_1 \propto M$, where M is the mass of the black hole. K_1 therefore decreases when M decreases. Graphically, this means that the horizontal line on figure 3 corresponding to $f_2 = \frac{\lambda_2}{24K_1}$ will move upwards as M decreases, until it no longer intersects the $f_2(\lambda_2 P_2)$ curve. At that point, there is no horizon, and the black hole is no longer able to radiate. This simple analysis of these models, which are obviously far too simplistic to describe the full complexity of the evaporation process, especially at the end of the black hole's life, suggests a possible scenario where evaporation ceases before the black hole has completely disappeared. We will see in subsection 4.4.1, when we have the relationship between K_1 and M, that this happens when the black hole reaches the Planck mass.

A non-singular black hole scenario well considered in the literature is the black-to-white transition [86, 116, 133, 135, 136], in which two event horizons sit on either side of a bounce. Sine polymer functions realize this scenario already [86]. One can then ask the question if the realization of this scenario imposes interesting restrictions on the polymer functions, and how much the scenario can be generalized allowing arbitrary polymer functions. From the analysis just done, we see that the black-to-white transition corresponds to having a maximum of $f_1(P_1(P_2))$ between two intersections of $f_2(P_2)$ with K_2. No further requirement is needed. Therefore the freedom/ambiguity in the polymer functions cannot significantly be constrained by requiring that such scenario be realized. Conversely, all sorts of modifications of the scenario are possible by playing with global features of the regularization functions. The simplest qualitative novelty that can be introduced changing

f_i from the sine function is an asymmetry between the contracting phases. More in general, it is possible to combine multiple bounces and multiple horizons.

In all cases, the relative location of bounces and horizons is not fixed, and will depend on both the choice of polymer functions and initial conditions. If the system is explicitly solved, the relative location can straightforwardly be determined from the functions $P_i(r)$. Interestingly, it is possible to find the relative location of bounces and horizons even without knowing the explicit solutions $P_i(r)$. This follows from the fact that the trajectories must satisfy the identity

$$3\int_{\lambda_2 P_2(r_0)}^{\lambda_2 P_2(r)} \frac{dx}{f_2(x)} = \int_{\lambda_1 P_1(r_0)}^{\lambda_1 P_1(r)} \frac{dx}{f_1(x)}, \tag{4.68}$$

as it follows from the constancy of the Dirac observable K_2 defined in (4.51). Given two reference values $P_i(r_0)$, this equation can be used to find the value of say $P_2(r)$ as a function of $P_1(r)$. To show how this is done in practise, consider the example of one bounce and two horizons, with polymer functions depicted in Fig. 17. We want to establish if the bounce occurs in between the horizons, or outside. To bring out the dependence on the initial conditions, we can choose a value for r_0 in the classical domain, so that an approximate explicit solution is known, given by (4.21) and (4.23). Equation (4.68) fixes in this way $P_2(r_b)$ as a function of $P_1(r_b)$ and classical inputs and can be used to determine the position of the bounce with respect to the horizons present in the effective geometry, as illustrated on Fig. 5. All this depends explicitly on the choice of the polymer functions and Dirac observables K_1 and K_2. The analysis holds for multiple bounces and multiple horizons.

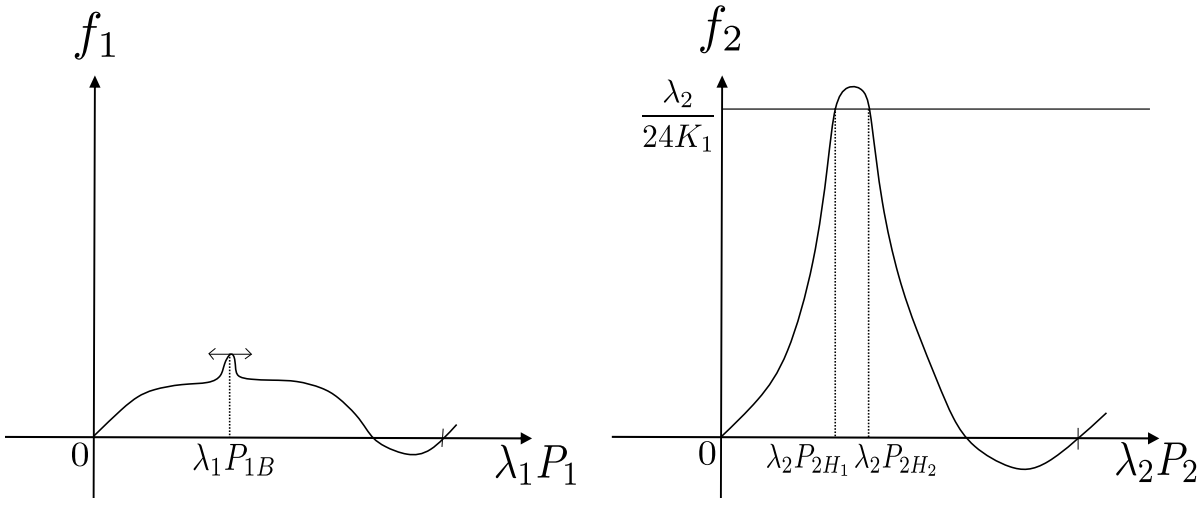
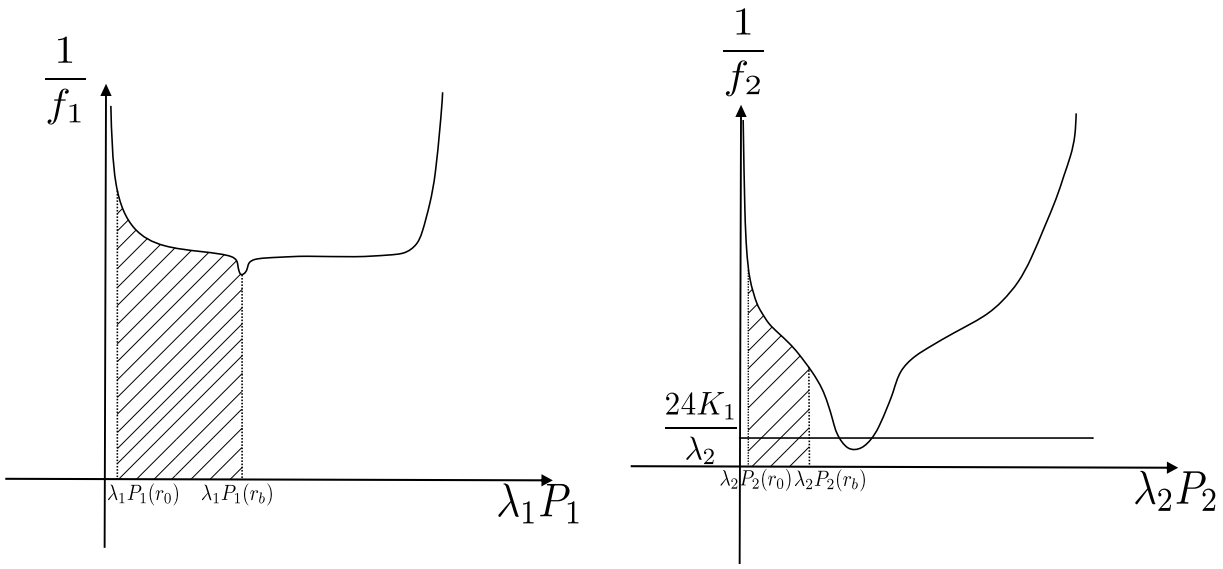


Figure 4: (a) Plot of a specific polymerisation function for f_1 with only one local maximum between its two first zeros, i.e. only one bounce can appear (b) Plot of a specific polymerisation function for f_2 with only one local maximum between its two first zeros. Depending on the choice made for the Dirac observable K_1, at most two horizons will appear.



(a) (b)

Figure 5: Plot of the inverse of the polymerisation functions where the dashed area correspond to the integrals in (4.68).

	$\text{sign}(\dot{b}) = -$	$\text{sign}(\dot{b}) = +$
$\text{sign}(a) = -$	Anti-trapped	Trapped
$\text{sign}(a) = +$	Free	Free

Table 1: Summary of the causal structure of a region in term of the sign of a and b. These results come from (4.69) and (4.70)

4.3.4 Trapped and anti-trapped regions

In a black-to-white hole transition, the bounce separates a trapped and anti-trapped region between the two corresponding horizons. We now show that the nature of the trapping or anti-trapping region turns out to be very simply determined by the sign of f_1'. More general cases, for instance if both horizons are on the same side of the bounce, would require a systematic analysis.

To see this, we recall that the outgoing and incoming expansions of null geodesic congruences for the spherical metric (4.1) are given by (see e.g. [86, 116])

$$\theta_+ = \sqrt{-\frac{2}{N}}\frac{\dot{b}}{b}\text{sign}(a), \tag{4.69}$$

$$\theta_- = -\sqrt{-\frac{2}{N}}\frac{\dot{b}}{b}. \tag{4.70}$$

The sign of a and $\dot{b}$ determine if the region is trapped, anti-trapped or free. We can summarize the possibilities in Table 1. At this point, we now that regions outside the horizon ($a > 0$) are generically free regions. Similarly, regions inside the horizon ($a < 0$) are trapped or anti-trapped, as illustrated on Fig. 6. The sign of a is determined uniquely by the sign of v_2, see (4.16b), and the

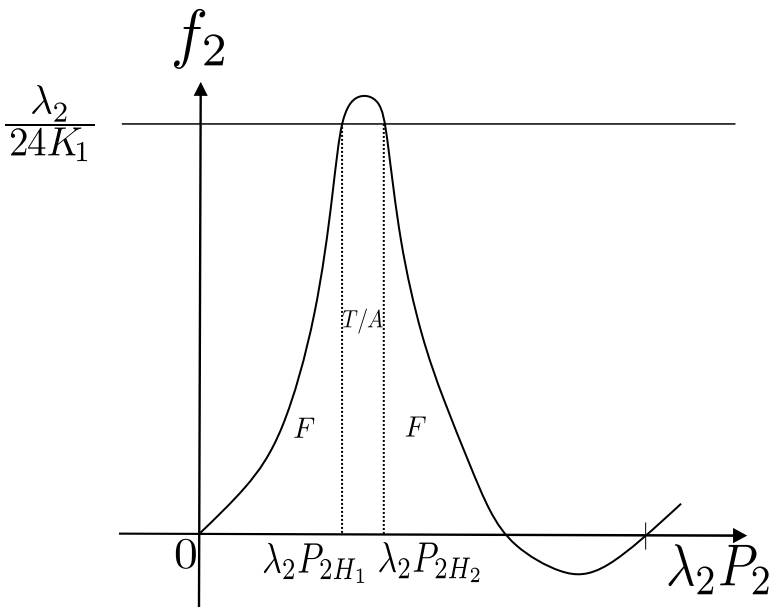


Figure 6: Plot of the polymerisation function f_2 chosen in Fig. 17. The horizontal line marks the threshold below which the region is free, and above which it is trapped/anti-trapped (T/A) depending on the sign of $\dot{b}$ as shown in Table 1. The intersections correspond to two horizons. If f_1 is chosen so to have a single bounce, three situations can occur. Starting from the asymptotic region at $r \to +\infty$, namely, $\lambda_2 P_2 = 0$, the region between the horizon will be trapped (respectively anti-trapped) if the bounce occurs after the horizon (respectively before the horizon). If it occurs between the horizons, this region will be trapped and then anti-trapped.

latter is positive for all P_2 such that

$$f_2 < \frac{\lambda_2}{24K_1}. \tag{4.71}$$

However, which of both is the case, i.e. if the interior region is trapped or anti-trapped or if a transition happens as this depends on the position of the bounce relative to the horizons and thus the polymer functions and the Dirac observables K_1 and K_2. To determine if the region between the horizon is trapped or anti-trapped, we have to look at f_1. We recall that since $\dot{v}_1 = 2\dot{b}b^2 = 12\sqrt{n}v_1 f_1' \frac{f_2}{\lambda_2}$, and since $f_2 > 0$ we have $\text{sign}(\dot{b}) = \text{sign}(f_1')$.

So in this specific case, since $f_1' < 0$ between the horizons (cf Fig. 7), which means that $\dot{b} < 0$. So referring to Table 1, we deduce that the region between the horizons is anti-trapped. On the other hand, if we had chosen C such that the bounce lies within the horizons, the bounce surface would have been a transition surface between a trapped and an anti-trapped region. In this case, a proper black-to-white hole transition appears.

4.4 Large distance behaviour

We have seen that the polymerized black holes present many non-classical features, such as multiple horizons and bounces. However, we would still like these solutions to reproduce the standard Schwarzschild black hole at large distances. This was the motivation to restrict the polymer functions to satisfy (4.47). These restriction were based on experience with loop quantum cosmology and with the standard polymer black hole. In this section we derive these conditions showing that

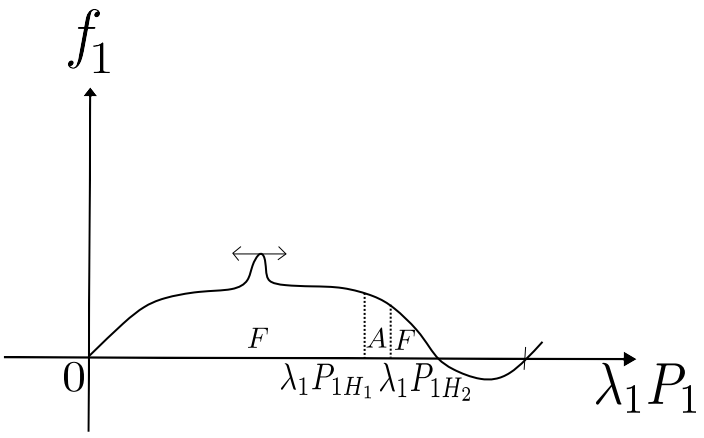


Figure 7: Plot of the polymerisation function f_1 chosen at the beginning of this section.The property free (F), trapped (T) or anti-trapped (A) of the spacetime is summarized on this plot.

they are indeed necessary in order to recover the Schwarzschild solutions at large scales. However, it turns out that they are not sufficient. One needs a further condition, given by $f_2'' = 0$ which is satisfied by the sine polymerization, for instance.

Even thought this condition was not explicitly required in the analysis of the previous Section, a quick inspection shows that it was not used anywhere, hence all the results there presented apply to the class of polymer functions correctly reproducing Schwarzschild metric's at large distances. The analysis presented in this Section is also somewhat heavier and requires additional notation, which is our reason to leave it for the end. It will also allows us to identify the mass of the black hole described by the generic solution (4.58).

An independent reason to study the large scale behaviour of the solutions concerns the interpretation of the spacetime *after* the bounce. If asymptotic flatness is recovered in that limit as well, it then becomes meaningful to talk about the mass of the white hole, and discuss the physics of the bouncing process in terms of asymptotic charges.

Let us now come to the technical aspects. The area radius is given by the variable b, hence the large scale limit is $b \to \infty$. However, while we can freely switch between r and P_2 as time variables, $b(\lambda_2 P_2)$ is not a monotonic function, recall analysis of Section 4.2.3 and Fig. 2.[14] Therefore, we have to restrict our analysis to each branch of invertibility. Since we are interested in the asymptotic behaviour, we can focus on the two branches connected to the $r \to \pm\infty$ limits which corresponds to $b \to \pm\infty$. To study this, we will proceed with a perturbative expansion of the polymer functions with respect to $1/b$. Since the polymer functions depend implicitly on b via the solution $P_i(b)$, this will be a nested perturbative expansion that requires the use of the equations of motion.

[14]The origin of this is that $b(r)$ is no longer monotonic. This is why one can have b inverting behaviour going through a bounce while r runs smoothly over the whole real axis. Notice also that the value r_{bounce} can occur for either positive or negative values, depending on the polymer function and the parameters of the solution.

4.4.1 Asymptotic behaviour

Let us consider the regions in P_i-space connected to the origin $P_i = 0$ (see Fig. 1). We denote $P_i^\pm$ the two asymptotic fixed points reached in the limit $r \to \pm\infty$ respectively (we assume that in the $r \to \infty$ limit we flow to the semiclassical regime, hence $P_i^+ = 0$). We introduce the following notation,

$$x := \frac{1}{b} \,, \tag{4.72a}$$

$$z^\pm(x) := \lambda_1 P_1 - \lambda_1 P_1^\pm, \tag{4.72b}$$

$$y^\pm(x) := \lambda_2 P_2 - \lambda_2 P_2^\pm, \tag{4.72c}$$

so to have $y^\pm$ and $z^\pm$ vanish at the two fixed points of each trajectory. We denote the fixed points $x = 0^\pm$. To treat them at once with a single perturbative expansion we redefine the functions $f_i(\lambda_i P_i) \mapsto f_i(\lambda_i P_i - \lambda_i P_i^\pm)$, such that $f_i(0^\pm) = 0$. In the following, we will drop the superscript $\pm$ from y and z to further lighten the notation.

In terms of these variables, the relevant components of (4.58) read

$$g_{\tau\tau}(x) = -\, x^2 \left(\frac{\lambda_2^2}{16 f_2 \left(y(x)\right)^2} - \frac{3K_1\lambda_2}{2 f_2\left(y(x)\right)} \right) \,, \tag{4.73a}$$

$$g_{xx}(x) = g_{bb}(x)/x^4 \,. \tag{4.73b}$$

$$g_{bb}(x) = -\, \frac{\lambda_2^2 x^2}{16 f_1'(z(x))^2 f_2\left(y(x)\right)^2 g_{\tau\tau}(x)} \,, \tag{4.73c}$$

After some computations that can be found in Appendix C, one can show that these metric components at first order in x are

$$g_{\tau\tau} = -\frac{\lambda_2^2}{16 f_2'(0^\pm)^2 y'(0^\pm)^2} \left(1 - \frac{2y'(0^\pm)\left(12K_1 f_2'(0^\pm)^2 + \lambda_2 f_2''(0^\pm)\right)}{\lambda_2 f_2'(0^\pm)} x \right) + O(x^2) \,, \tag{4.74a}$$

$$1/g_{bb} = f_1'(0^\pm)^2 \left(1 - \frac{24K_1 f_2'(0^\pm) y'(0^\pm)}{\lambda_2} x \right) + O(x^2) \,. \tag{4.74b}$$

Since we have already fixed the area radius as coordinate, asymptotic flatness imposes

$$f_1'(0^\pm) = \pm 1. \tag{4.75}$$

Next, we still have the freedom fo rescaling τ, which we use to reabsorb the prefactor in $g_{\tau\tau}$, so to have asymptotic flatness in the new time variable without restrictions on the polymer functions. On the other hand, area radius also requires that the time and radial components are the inverse of one another. Inspection of the above equations shows that this occurs if and only if

$$\frac{y'(0^\pm) f_2''(0^\pm)}{f_2'(0^\pm)} = 0 \qquad \Rightarrow \qquad f_2''(0^\pm) = 0 \tag{4.76}$$

by the previous conditions. In that case, the mass of the black hole is given by

$$M = \frac{12K_1 f_2'(0^\pm) y'(0^\pm)}{\lambda_2} \,. \tag{4.77}$$

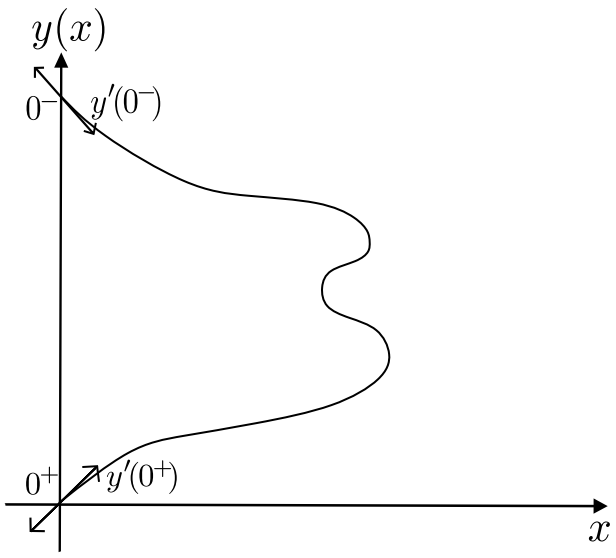


Figure 8: Sketch of the parametric solution $y(x)$. $y'_-(0^\pm)$ uniquely fixes the trajectory $y(x)$ and thus the final derivative $y'_+(0^\pm)$.

Notice that it depends on K_2 via $y'(0^\pm)$, since K_2 appears in the relation between P_2 and b.[15]

Consider now separately the two solutions for $r \to \pm\infty$. The corresponding values of M will generically be different, because $f_2'(0^\pm)$ and $y'(0^\pm)$ can take different values. Since $f_2'(0^\pm)$ and $y'(0^\pm)$ are both positive (respectively negative) in the black hole side (respectively in the white hole side), then the sign of the mass is only determined by the sign of K_1, as in the unpolymerized case.

In summary, in order to obtain the Schwarzschild solution asymptotically at the fixed point, we need to impose the conditions (C.5), (4.75) and (4.76), i.e.

$$f_1'(0^\pm) = f_2'(0^\pm) \quad \text{and} \quad f_1'(0^\pm)^2 = 1 \quad \text{and} \quad f_2''(0^\pm) = 0\,. \tag{4.78}$$

This fixes of the three of the four derivatives of f_1 and f_2 up to the second order expansion. Note that in the case of the sine polymerisation, these conditions are automatically satisfied.

If we impose (4.78) at both fixed points, we obtain an evolution from an asymptotic Schwarzschild region to another asymptotic Schwarzschild region. Let us call the masses in the two regions M_{BH}

[15] One may ask how this mass enters the Kretschmann scalar, given schematically by (4.65). The complexity of that expression makes it however hard to answer this question, even for the simplest choices of polymer functions.

and M_{WH}.[16] They are given by

$$M_{BH} = \frac{12K_1 f_2'(\lambda_2 P_2^-) y'(0^\pm)}{\lambda_2} \quad , \quad M_{WH} = \frac{12K_1 f_2'(\lambda_2 P_2^+) y'(0^\pm)}{\lambda_2} \,. \tag{4.79}$$

From (4.78) we see that $\left|f_2'(\lambda_2 P_2^-)\right| = \left|f_2'(\lambda_2 P_2^+)\right| = 1$. The evolution studied in Sec. 4.3.1 is such that no zeros of f_2 are crossed. Therefore, $f_2'(\lambda_2 P_2^-) = -f_2'(\lambda_2 P_2^+)$ and

$$\frac{M_{WH}}{M_{BH}} = -\frac{y'(0^\pm)}{y'(0^\pm)}. \tag{4.80}$$

Moreover, as it is illustrated in Figure 8, $y'(0^\pm)$ is positive in the black hole side and negative in the white hole side. This implies that the black hole mass and the white hole mass have the same sign. It is also possible to locally[17] change coordinates in phase space from K_i to (M_{BH}, M_{WH}).

Because the two asymptotic regions are disconnected, different asymptotic masses does not mean a violation of energy conservation: it only means that the time-like Killing vector cannot be normalized to one at both asymptotes. If one were interested in solutions with matching masses, one would be looking at a 1-dimensional subspace of the 2-dimensional phase space, determined by (4.80) once the polymer functions are chosen.

4.4.2 Taming quantum gravity effects outside the horizon

An obvious issue with non-singular black holes is to contain the deviations from general relativity not to spoil the macroscopic behaviour. To that end, we look at the next order term in the expansion (4.74a), and impose bounds on it. This requires $y^{(3)}(0^\pm)$, which can be computed as before from the equation of motion (C.3b) and taking the limit $x \to 0$. This leads to an recursive relation with $y^{(3)}(0^\pm)$ on both sides, which can be solved to obtain

$$y^{(3)}(0^\pm) = \frac{y'(0^\pm)^3 f_2^{(3)}(0^\pm)}{2 f_2'(0^\pm)}, \tag{4.81}$$

where we use explicitly the condition $f_2''(0^\pm) = 0$. We then find

$$g_{\tau\tau} = -\frac{\lambda_2^2}{16 f_2'(0^\pm)^2 y'(0^\pm)^2} \left(1 - 2Mx - \text{sign}\left(f_2'(0^\pm)\right) \frac{y'(0^\pm)^2 f_2^{(3)}(0^\pm)}{2\lambda_2} x^2\right) + O\left(x^3\right). \tag{4.82}$$

The $O(x^2)$ term of $1/g_{bb}$ vanishes, as a consequence of $z''(0^\pm) = 0$ (cf (C.1)) and using the condition $f_2''(0^\pm) = 0$.

[16] These names have absolutely no meaning in terms of a black or white hole. Both asymptotic regions are Schwarzschild so both of these regions contain both, a black and a white hole. However, for the initial region, the black hole lies in the future and for the final region the white hole lies in the past. Depending on where the bounce is located w.r.t. the horizons (see the discussion in Sec. 4.3.4), an observer falling radially and freely starting in the initial region, will experience a black hole first, then see a transition from a trapped to an anti-trapped region, which the observer would call a white hole region until, she finds herself in an asymptotic exterior region of a Schwarzschild spacetime. This motivates the given notation, but there is no deeper physical meaning.

[17] The change of coordinates is given by (4.79) (recall that $y'(0^\pm)$ depends on K_2), and this may not be globally bijective. Consequently, we are limited to saying that this change of coordinates exists locally.

To keep the quantum corrections small outside of the horizon, we need the third term to be much smaller than the second for $b = x^{-1} \geq 2M$, namely

$$\frac{y'(0^{\pm})^2 f_2^{(3)}(0^{\pm})}{8\lambda_2 M^2} \ll 1. \tag{4.83}$$

This means that for given polymer functions, the condition is always satisfied for large enough black holes. Moreover, the expansion (4.82) allows us to obtain a criterion on the value of the area radius for which the deviations from the Schwarzschild metric become order one, given by

$$b \leq \sqrt{\left| \frac{y'(0)^2 f_2^{(3)}(0)}{2\lambda_2} \right|}. \tag{4.84}$$

A more precise characterization of the quantum corrections can be obtained studying the violations of the energy conditions, like for example in [40].

4.4.3 Constraining ambiguities with the EFT approach

We will conclude this section by showing how one can use the results from the EFT treatment of gravity presented in the previous part to set some additional constraints on the polymer functions f_1 and f_2. Let us first recall that this approach allows us to write down the most general metric that reproduces the correct expression for the energy of two point-like and static sources, one of which is much heavier than the other. To make this subsection easier to read, we rewrite this metric using the area radius as the radial coordinate

$$g_{tt} = -\left(1 - \frac{2GM}{r} - \left(\frac{17}{10\pi} + c_2\right)\frac{G^2\hbar M}{r^3}\right) + \mathcal{O}(G^3) + \mathcal{O}(\hbar^2) \tag{4.85}$$

$$g_{rr} = 1 - \frac{2GM}{r} + c_1\frac{G\hbar}{r^2} + c_2\frac{G^2M^2}{r^2} + \left(\frac{51}{10\pi} + 7c_2\right)\frac{G^2\hbar M}{r^3} + \mathcal{O}(G^3) + \mathcal{O}(\hbar^2), \tag{4.86}$$

where c_1 and c_2 are arbitrary numeric parameters. On the other hand, we know from (4.73) that the metric can be expressed in full generality as follows

$$ds^2 = -x\left(\frac{\lambda_2^2}{16 f_2\left(y(x)\right)^2} - \frac{3K_1\lambda_2}{2 f_2\left(y(x)\right)}\right)d\tau^2 + \frac{\lambda_2^2 x^2}{16 f_1'(z(x))^2 f_2\left(y(x)\right)^2 g_{\tau\tau}(x)}dr^2 + \frac{1}{x^2}d\Omega^2, \tag{4.87}$$

We have also seen in the previous subsection that the $g_{\tau\tau}$ component of (4.87) admits the following expansion in the low-curvature regime corresponding to $x \to 0$ (expanding the metric components in x is equivalent to expanding them in G or $\hbar$, since both cases correspond to the weak-field regime)

$$g_{\tau\tau} = -\frac{\lambda_2^2}{16 f_2'(0^{\pm})^2 y'(0^{\pm})^2}\left(1 - 2Mx - \text{sign}\left(f_2'(0^{\pm})\right)\frac{y'(0^{\pm})^2 f_2^{(3)}(0^{\pm})}{2\lambda_2}x^2\right) + O\left(x^3\right). \tag{4.88}$$

Moreover, by a similar computation that the one leading to (4.88), it can be seen shown that the g_{rr} component of (4.87) admits the following series expansion

$$g_{rr} = -1 + 2Mx + \mathcal{O}(x^3). \tag{4.89}$$

It is not hard to see that (4.89) is compatible with (4.85) by taking $c_1 = c_2 = 0$, and no conditions need to be imposed on the polymer functions. On the other hand, for (4.88) to be compatible with (2.53) one must impose

$$f_2^{(3)}(0) = 0. \tag{4.90}$$

It is interesting to note that the sine function, which is the usual choice for the polymerization procedure, does not satisfy this condition. Remember that we cannot impose $P_2'(0) = 0$, since the black hole mass is proportional to this quantity. We will end this section by insisting on the fact that the choice of the sine function as the polymerization function, besides being arbitrary, does not lead to predictions in agreement with the perturbative approach. This subsection also clearly illustrates how the perturbative result (2.53) can be used to help in the construction of non perturbative modified black hole models by fixing part of the ambiguities. One can expect that obtaining quantum corrections at higher orders would bring more constraints on the polymerization functions. But since higher order corrections requires to know the irrelevant coupling constants of gravity, this clearly illustrates that the non renormalizability of general relativity is in correspondence with the problem of ambiguity in polymer black hole models.

4.5 Conclusion

We have shown that it is possible to investigate generic features of effective models describing spherically symmetric black hole models inspired by loop quantum gravity taking into account the large freedom in choosing the polymerization functions. Most of the relevant global features of the solutions, as the location of horizons and the existence of bounces, are directly related to global features of the polymerization functions and the values of some Dirac observables or constants of motion. More precisely, the features of the polymerization function f_1 encode the physics of bounces, while f_2 and its relation to certain constants of motion determines the location of the Killing horizons. Consistency with the classical regime does not strongly restrict the infinite dimensional ambiguity in the polymerization procedure. However, it is worth pointing out that in addition to the usual requirements on $f_i(0^{\pm})$ and $f_i'(0^{\pm})$ that are derived from the naive continuum limit, our asymptotic analysis shows that in addition one needs to have $f_2''(0^{\pm}) = 0$. The number of bounces and the number of horizons can be freely specified by tuning the polymer functions and suitably choosing constants of motion. With respect to the list of properties of the BMM model (listed in Section 4.1.3) we conclude that all of them hold for an arbitrary polymerization except the shrinking of horizon. The deformation of the horizon can be freely controlled playing with the choice of polymer function. We notice in passing that the model also allows for solutions with no horizons at all, where quantum effects produce violations of the classical Einstein's equations that can be seen as quantum stars made of 'matter' of an entirely quantum nature. A naive analysis of these model also suggested that a black hole that loses some mass through Hawking radiation tends to see its horizons disappear. Without an horizon, the black hole would no longer produce radiation and its mass would no longer evolve, leaving a Planck mass remnant. Finally, We ended this chapter by

showing that the results obtained in chapter 2 could impose certain constraints on this ambiguity. In particular, we found that the choice of sine functions, which is usually made, fails to recover the quantum correction of the energy of interaction derived from the perturbative approach and presented in chapter 2. Indeed we showed that the latter imposes constraints on the possible choice for the polymer function. Moreover, we argued that this problem of ambiguities is connected to the non renormalizability of gravity. The existence of such a large ambiguity in the construction of these models should not be surprising on general grounds [89, 90]. On the upper side this freedom could prove useful in the investigation of off-shell hypersurface deformation algebra [137–139]. Our analysis can also be applied to specific choices of non-sine polymer functions. It would be interesting to see whether it could be extended to different $\bar{\mu}$-schemes like the one proposed in [93], and then be able to study analytically the behaviour of the geometry post-bounce [87].

5 A quantum black hole model

We have so far focused on polymer black hole models without matter. As mentioned in 3.3.3, the latter hypothesis is not realistic, as black holes are produced by the collapse of matter and then emit matter after their formation by Hawking radiation. The complete formation and evaporation of these objects cannot therefore be described by the models previously studied. Moreover, these models are effective in the sense that they are formalized as a trajectory in a phase space generated by a modified Hamiltonian. As a result, geometric d.o.f cannot be described in a quantum way. In particular, they cannot be in a superposition of states, or entangled with external d.o.f such as the d.o.f of matter. In this section, we present a model that addresses both these problems, i.e. a black hole model that includes matter d.o.f, and whose geometry and matter are described quantum mechanically. In order to do so, let us start by recalling that the interior region $r < 2M$ of a Schwarzschild black hole of mass M can be seen as a homogeneous anisotropic cosmological model where the r=constant surfaces (in the usual Schwarzschild coordinates) are Cauchy surfaces of homogeneity where any two arbitrary points can be connected along orbits of the isometry group that involves spacelike translations along the staticity Killing field $\xi = \partial_t$ and the rotations associated to spherical symmetry. Models with these isometries will be refereed to as Kantowski-Sachs (KS) models [140]. They include not only the Schwarzschild black hole interior geometry (vacuum case) but also the Reissner-Nordstrom black hole interior geometry (in the Einstein-Maxwell case) and other solutions depending of the type of matter that one decides to couple to the system. In this chapter we would like to emphasize the fact that Kantowski-Sachs models, with a coupled massless scalar field, define a natural toy model capturing some aspects of the dynamics and back-reaction of matter near the singularity of realistic black holes that Hawking radiate and evaporate. The model can certainly not replace the full dynamical description of a generic gravitational collapse in the full theory as it remains a toy model with finitely many d.o.f. However, we will argue, it can handle in a simplistic way some dynamical aspects that might be relevant when discussing questions in the context of evaporating black holes.

5.1 Scalar excitations falling inside a Schwarzschild black hole: the deep interior regime

Let us consider a free test point particle (with no angular momentum) falling into the interior of a Schwarzschild black hole. As the particle approaches the singularity—in a description on an r equal constant slicing of the interior—one expects its wave function to become better and better approximated by a translational invariant wave function since the expansion in the spacelike Killing direction $\xi = \partial_t$ diverges for $r \to 0$. If this conclusion is correct then it means that zero angular momentum test particles can be approximated by the type of excitations that can be accommodated in the dynamical framework of the KS cosmologies (at least in the sense of a near singularity approximation). One can be quantitative about this intuition as follows: free test particles with four wave vector k^a on the Schwarzschild background are associated with the conserved Killing energy $\mathcal{E} \equiv -k^a\xi_a$. We are assuming that the particle has zero angular momentum which implies that its wave function is already translational invariant in the directions transversal to ξ^a on the r-slices. The wave function can only vary in the direction of the Killing ξ^a and the component of

the physical momentum in this direction is given by

$$p_\xi \equiv \frac{k^a \xi_a}{\sqrt{\xi \cdot \xi}} = -\mathcal{E}\sqrt{\frac{r}{2M-r}}, \tag{5.1}$$

which vanishes in the limit $r \to 0$. The wave length of such a particle diverges, and thus particles without angular momentum are better and better represented by translational invariant excitations as one approaches the singularity. These are precisely the kind of homogeneous configurations that can be described in the KS framework.

This simple implication deduced from the idealized notion of test particle can be made more precise by looking at the analogous features of scalar field excitations (solutions of the Klein-Gordon equation). Indeed, the simplistic argument given here can be made precise in the field theoretical context as we will show in what follows.

5.1.1 Solutions of the Klein-Gordon equation in the deep interior region

Here we argue that the Kantowski-Sachs model (described in detail in Section 5.2) coupled to a massless scalar field faithfully captures the dynamics of a Klein-Gordon excitation falling into the deep interior region of a Schwarzschild black-hole. We will do this by analysing the behaviour of solutions of the Klein-Gordon equation on the Schwarzschild background in the $r \ll 2M$ regime. We will focus on the spherically symmetric solutions and show that they become homogeneous on r=constant surfaces as $r \to 0$ and thus can be accommodated in the framework of KS configurations. This implies that the KS system can be used to model the dynamics and (most importantly) the back-reaction of such (zero angular momentum) scalar configurations falling into the deep interior region of spherically symmetric black holes.

Let us first start by approximating the Schwarzschild metric in the deep interior region $r \ll 2M$ as

$$ds^2 = \frac{2M}{r}dt^2 - \frac{r}{2M}dr^2 + r^2 d\Omega^2. \tag{5.2}$$

We will choose coordinates such that the time-radial part of the metric is conformally flat. Remarkably, in the deep interior region, this is achieved by switching to area variables $a = 4\pi r^2$ (the well known tortoise coordinate r_* is actually proportional to r^2 near the singularity). With these variables the metric becomes

$$ds^2 = \frac{1}{16\pi\sqrt{a_{\rm H} a}}\left(d\tau^2 - da^2\right) + \frac{a}{4\pi}d\Omega^2, \tag{5.3}$$

with $a_{\rm H} = 16\pi M^2$, $\tau = \sqrt{16\pi a_{\rm H}}t$, and $a = 4\pi r^2$. The Klein-Gordon equation for a massless scalar field then reads

$$\Box\Phi = \frac{1}{\sqrt{-g}}\partial_\mu\left(\sqrt{-g}g^{\mu\nu}\partial_\nu\Phi\right) = 0 \tag{5.4}$$

$$\iff \left(-\frac{\partial^2\Phi}{\partial a^2} - \frac{1}{a}\frac{\partial\Phi}{\partial a} + \frac{\partial^2\Phi}{\partial\tau^2} + \frac{1}{4\sqrt{a_{\rm H} a}\,a}\left(\frac{1}{\sin\theta}\frac{\partial\left(\sin\theta\frac{\partial\Phi}{\partial\theta}\right)}{\partial\theta} + \frac{1}{\sin^2\theta}\frac{\partial^2\Phi}{\partial\varphi^2}\right)\right) = 0. \tag{5.5}$$

To solve it, we make the usual ansatz

$$\Phi_{\ell m} = e^{i\omega t} Y_{lm}(\theta,\varphi)\phi_l(a) = e^{i\frac{\omega\tau}{\sqrt{16\pi a_{\rm H}}}} Y_{lm}(\theta,\varphi)\phi_l(a) \tag{5.6}$$

which reduces the Klein-Gordon equation to

$$\phi_l'' + \frac{\phi_l'}{a} + \left(\frac{\omega^2}{16\pi a_{\rm H}} + \frac{l(l+1)}{4\sqrt{a_{\rm H} a}a}\right)\phi_l = 0. \tag{5.7}$$

For the spherical modes $l = 0$ one obtains

$$\phi_0(a) = c_1 J_0\left(\frac{\omega a}{\sqrt{16\pi a_{\rm H}}}\right) + c_2 Y_0\left(\frac{\omega a}{\sqrt{16\pi a_{\rm H}}}\right), \tag{5.8}$$

with J_0 and Y_0 Bessel functions and c_1 and c_2 constants. As we will prove in Section 5.2 that these solutions match nicely with solutions of the KS model (mentioned at the end of the introduction). This follows from two complementary properties of the solutions of the Klein-Gordon equation. On the one hand, the near singularity limit of the quantity (simply related to the KS momentum variable as we will see in Section 5.2)

$$\lim_{a\to 0} a\frac{\partial\phi_0}{\partial a} = -\frac{2c_2}{\pi} \tag{5.9}$$

is finite and independent of ω. On the other hand, the t dependence of the Klein-Gordon solutions is 'ironed' by the infinite expansion of the geometry in the ∂_t direction: the region $\ell_0 \equiv \Delta t = 2\pi\omega^{-1}$ where the solution has a significant (order-one) change corresponds to a length scale $\Delta d \approx 2\pi\omega^{-1}\sqrt{M/r}$ (in agreement with the infinite redshift effect captured in equation (5.1)). Therefore, in a length scale $\ell_p \ll \ell \ll \Delta d$ along the background Killing field direction $\xi = \partial_t$, and in the deep interior region $a \ll M^2$, the solutions of the Klein-Gordon equations can be considered as homogeneous and therefore compatible with initial data that would be admissible in the KS model.

We will see in Section 5.2 that the momentum variable p_ϕ in the KS model is simply related to the quantity whose limit was considered in the previous paragraph as it is defined as

$$\mathrm{p}_\phi \equiv -8\pi M\ell_0 r\frac{\partial\Phi_{00}}{\partial r} = -\ell_0 a_{\rm H} a\frac{\partial\Phi_{00}}{\partial a}, \tag{5.10}$$

where the pre-factors arise form the hamiltonian analysis of Section 5.2 and ℓ_0 is an IR cutoff scale naturally associated in the previous discussion to the scale $\Delta t = 2\pi\omega^{-1}$. It follows from the previous considerations that

$$\lim_{a\to 0} \mathrm{p}_\phi = \text{constant} \tag{5.11}$$

in the region of interest. One can relate the previous quantity to the average 'energy density' on the r=constant hyper-surfaces as one approaches the singularity (this will be simply related to the KS Hamiltonian that will be defined in the following section). Namely,

$$\frac{1}{\ell_0}\int_{t_0}^{t_0+\ell_0} dt\left(\int d\theta d\varphi\left(\sqrt{|g|}T_{\mu\nu}\partial_r^\mu\partial_r^\nu\right)\right) = \frac{\mathrm{p}_\phi^2}{64\pi M^2\ell_0^2}, \tag{5.12}$$

where the scale ℓ_0 enters the definition of the average in the time direction. For concreteness one can match ℓ_0 to the wavelength $2\pi\omega^{-1}$ of the excitation and the previous result will already hold (of course it holds for $\ell_0 > 2\pi\omega^{-1}$).

For completeness we give the limiting behaviour of solutions in the non-spherical case. For the non-spherical modes, one can neglect the term containing the frequency in equation (5.7) in analysing the small a behaviour of solutions. If we do so, we obtain for $l \neq 0$

$$\phi_l(a) = c_1 J_0\left(\sqrt[4]{\frac{a}{\pi}}\sqrt{\frac{l(l+1)}{M}}\right) + 2c_2 Y_0\left(\sqrt[4]{\frac{a}{\pi}}\sqrt{\frac{l(l+1)}{M}}\right). \tag{5.13}$$

Solutions diverge logarithmically (as $\log[a]$) for $a \to 0$. This holds both for spherically symmetric as well as for non spherically symmetric solutions as it follows from the asymptotic behaviour of the Bessel functions or from the finiteness of p_ϕ in the spherical case. The mild character of the divergence was emphasized in [141, 142] as an attractive possibly interesting property when one considers the definition of the associated quantum operators in quantum field theory (in view of a possible definition of semiclassical gravity). Here we simply point out that such simple behaviour allows for bridging to a solvable KS model to understand aspects of the back-reaction of classical (as well as quantum) excitations falling into a spherically symmetric black hole.

5.2 The Kantowski-Sachs spacetime coupled with a massless scalar field

In this section we revisit the construction of the phase space of the KS model by perforing the canonical analysis of the associated symmetry reduced model where staticity and spherical symmetry are imposed from the onset (in Section 5.2.1). To improve the clarity of the presentation we simply start from the vacuum case—whose solutions are isomorphic to the interior Schwarzschild solutions—and later couple the system to a scalar field without mass. We express variables in terms of the usual Schwarzschild-like coordinates. In Section 5.2.2 we present a truncation of the Hamiltonian and show, in Section 5.2.3, that it defines a tractable approximation of the dynamics in the $r \ll M$ region of the interior of physically realistic black holes. We call this regime the *deep interior dynamics*. In Section 5.2.4 we show that the regime of applicability of the model includes the physically interesting situation of Hawking scalar excitations with zero angular momentum falling inside of the black hole.

5.2.1 Symmetry reduced covariant phase space

It is well known that for a spherically symmetric and static spacetime, the line element can be written without any loss of generality as

$$ds^2 = -f(r)dt^2 + h(r)dr^2 + r^2 d\Omega^2 \ . \tag{5.14}$$

It follows that the Eintein-Hilbert action (with the appropriate boundary term that renders it differentiable) becomes

$$S_{\text{geo}} = \frac{1}{16\pi}\left[\int_R d^4x\sqrt{-g}R + 2\int_{\partial R} K\right] = \frac{\ell_0}{2\ell_p^2}\int dr\left(\sqrt{fh} + \sqrt{\frac{f}{h}} + \frac{\dot{f}r}{\sqrt{fh}}\right), \tag{5.15}$$

where the dot denotes the derivative with respect to r and ℓ_0 is a cut-off in the non compact spacelike ∂_t direction that regularizes the dynamical system. The cut-off will be associated a natural meaning

in modelling the fate of zero angular momentum excitations falling inside the black hole. In the deep interior region $r \ll M$ and we will take $\ell_0 \sim \omega^{-1}$ for $\omega \approx 1/M$ (the typical frequency in the Hawking spectrum of a macroscopic black hole of mass M). One can easily verify that the variations of the action lead to the Schwarzschild solutions

$$ds^2 = -\mathrm{p}_M^2 \left(1 - \frac{2M}{r}\right) dt^2 + \frac{dr^2}{\left(1 - \frac{2M}{r}\right)} + r^2 d\Omega^2, \tag{5.16}$$

and the symplectic potential (stemming from the on-shell evaluation of the action variation)

$$\theta = -\frac{\ell_0}{\ell_p^2}(c_1 dM + 2M d\mathrm{p}_M - 2d\mathrm{p}_M r), \tag{5.17}$$

and symplectic structure

$$\omega = \frac{\ell_0}{\ell_p^2} d\mathrm{p}_M \wedge dM. \tag{5.18}$$

Instead of working directly with the physical phase space parametrized by the Dirac observables p_M and M it will be convenient for us to work with kinematical variables and constraints for the moment. This is because of the usual difficulty in linking the timeless physical phase space with a classical intuition based on spacetime geometry. To avoid such difficulties we would like to have a notion of parametrized 'time evolution' which in our context will take the form of an area radius evolution. Thus we take the integrand of (5.15) as the Lagrangian $\mathscr{L}_{\mathrm{geo}}$ of the spacetime subsystem

$$\mathscr{L}_{\mathrm{geo}} = \frac{\ell_0}{2\ell_p^2}\left(\sqrt{fh} + \sqrt{\frac{f}{h}} + \frac{r\dot{f}}{\sqrt{fh}}\right). \tag{5.19}$$

On the other hand, we will couple the system to a massless scalar field by adding the matter action

$$S_m = -\frac{1}{2}\int_R d^4x\sqrt{-g}\partial_a\phi\partial^a\phi = -2\pi\ell_0\int dr r^2\dot{\phi}^2\sqrt{\frac{f}{h}}. \tag{5.20}$$

The conjugate momenta to f, h and ϕ are given by

$$\mathrm{p}_f = \frac{\ell_0}{2\ell_p^2}\frac{r}{\sqrt{fh}} \quad , \quad \mathrm{p}_h = 0 \quad \text{and} \quad \mathrm{p}_\phi = -4\pi r^2\ell_0\sqrt{\frac{f}{h}}\dot{\phi}, \tag{5.21}$$

and the primary Hamiltonian, defined by $H = \dot{f}\mathrm{p}_f + \dot{h}\mathrm{p}_h + \dot{\phi}\mathrm{p}_\phi - \mathscr{L}_\phi - \mathscr{L}_{\mathrm{geo}}$, becomes

$$\mathrm{H}_1 = -\frac{\ell_0}{2\ell_p^2}\frac{f(h+1)}{\sqrt{fh}} - \frac{h\mathrm{p}_\phi^2}{8\pi r^2\ell_0\sqrt{fh}}\,. \tag{5.22}$$

From the expression of the conjugate momenta (5.21) we identify the constraints

$$\xi \equiv \mathrm{p}_f - \frac{\ell_0}{2\ell_p^2}\frac{r}{\sqrt{fh}} = 0 \quad \text{and} \quad \mathrm{p}_h = 0, \tag{5.23}$$

and the secondary Hamiltonian

$$\mathrm{H}_2 = \mathrm{H}_1 + \lambda\xi + \eta\mathrm{p}_h\,, \tag{5.24}$$

where λ and η are Lagrange multipliers. One can show that the stability of the two constraints (5.23) can be ensured by fixing the associated Lagrange multipliers, i.e., the constraints (5.23) are second class and can be explicitly solved leading to

$$\mathrm{p}_h = 0 \quad \text{and} \quad h = \frac{\ell_0^2}{4\ell_p^4}\frac{r^2}{f\mathrm{p}_f^2}. \tag{5.25}$$

Thus, the secondary Hamiltonian (5.24) reduces to

$$\mathrm{H}_2 = -\frac{1}{r}\left(f\mathrm{p}_f + \frac{1}{16\pi\ell_p^2}\frac{\mathrm{p}_\phi^2}{f\mathrm{p}_f} + \frac{\ell_0^2}{4\ell_p^4}\frac{r^2}{\mathrm{p}_f}\right) . \tag{5.26}$$

The previous encodes the KS dynamics of geometry coupled to a massless scalar field. The relevant solutions for physical applications correspond to small departures from the vacuum Schwarzschild solutions representing macroscopic black holes with scalar field perturbation falling inside. We will further simplify the system by focusing on, what we call, the deep interior region $r \ll M$ where M is the mass scale defined by the corresponding black hole solution perturbed (in the sense of Sections 5.2.3 and Section 5.2.4) by the presence of matter. It is in this regime where the solutions of the KS system faithfully describe the dynamics of a spherically symmetric scalar perturbation (representing for instance a Hawking particle) as it falls towards the interior singularity. The KS Hamiltonian evolution matches, in this sense, the test-field evolution (the Klein-Gordon solutions on the Schwarzschild background fixed non dynamical background) and incorporates, as a simplified model, aspects of the back-reaction that are expected to become more important as one approaches the singularity.

5.2.2 The deep interior dynamics

We are interested in the dynamical evolution in the $r \ll 2M$ regime. In addition we will use the present dynamical system to model (in a suitable approximation) the back-reaction of a Hawking quantum falling into a black hole singularity. Hawking particles do not correspond to static excitations as the one we can model with the symmetry assumptions of the present section. However, as argued in Section 5.1, when spherically symmetric, these particles look more and more static as seen by a radially freely falling observer in the limit $r \to 0$. This is the reason why we are interested in such regime of the present dynamical system. In the next section we will study the classical solution of the model using perturbation theory in the parameter p_ϕ^2/M^2—as p_ϕ^2 will be assumed to be much smaller to M^2 in applications—and show that the dynamics simplifies in the deep interior region. The simplification occurs due to the negligible effect of the last term in the expression of the hamiltonian (5.26): more precisely, in the deep interior region, the Hamiltonian is well approximated by

$$\mathrm{H}_{\mathrm{di}} = -\frac{1}{r}\left(f\mathrm{p}_f + \frac{1}{16\pi\ell_p^2}\frac{\mathrm{p}_\phi^2}{f\mathrm{p}_f}\right). \tag{5.27}$$

This toy theory reflects the dynamics of the leading order in an expansion near $r = 0$. Order $\mathscr{O}(r)$ effects could be included in perturbation theory near $r = 0$ in which case the term we dropped would correspond to the perturbation Hamiltonian. The consistency of this truncation will be shown in Section 5.2.3.

The system we are dealing with has no gauge symmetries as the radial reparametrization symmetry has been gauged fixed with the metric ansatz (5.14) by choosing the area radius as time. In order to recover the structure of a gauge theory, with a clear analogy with the full theory of LQG, it will be convenient 'reparametrize' the system by promoting the area radius r to a d.o.f with conjugate momentum p_r and add a scalar constraint $\mathrm{C} = \mathrm{p}_r - \mathrm{H}_2 = 0$. The phase space is therefore extended to $(f, \mathrm{p}_f, r, \mathrm{p}_r, \phi, \mathrm{p}_\phi)$, and the number of d.o.f is preserved by the inclusion of the Hamiltonian constraint

$$\mathrm{C}_r = \mathrm{p}_r - \frac{1}{r}\left(f\mathrm{p}_f + \frac{\mathrm{p}_\phi^2}{16\pi\ell_p^2 f \mathrm{p}_f}\right) \approx 0. \tag{5.28}$$

In this approximation one can show that we have the following Dirac observables

$$\mathrm{D}_1 = f\mathrm{p}_f \quad , \quad \mathrm{D}_2 = f r^{-\frac{\mathrm{p}_\phi^2}{4f\mathrm{p}_f^2}+1} \quad , \quad \mathrm{D}_3 = \mathrm{p}_\phi \quad \text{, and} \quad \mathrm{D}_4 = \phi + \frac{\mathrm{p}_\phi \log(r)}{2f\mathrm{p}_f}. \tag{5.29}$$

It will be convenient to make the following canonical transformation and thus introduce what we call the *deep interior variables*

$$m = -f\mathrm{p}_f \quad \text{and} \quad \mathrm{p}_m = -\log(-f) \ , \tag{5.30}$$

and—in trying to introduce the kinematical structure proper to loop quantum gravity—to adopt the area a of the surfaces of constant r, namely

$$a = 4\pi r^2 \quad \text{and} \quad \mathrm{p}_a = \frac{\mathrm{p}_r}{8\pi r} \ , \tag{5.31}$$

as new dynamical variables. With this choice the phase space is described by the geometric variables m, p_m, a and p_a with Poisson brackets

$$\{m, \mathrm{p}_m\} = 1 \ , \quad \{a, \mathrm{p}_a\} = 1 \ ,$$

and by the matter variables ϕ and p_ϕ for which

$$\{\phi, \mathrm{p}_\phi\} = 1, \tag{5.32}$$

with all the other Poisson brackets equal to zero. In the new variables the deep interior dynamics Hamiltonian constraint (5.28) becomes

$$\boxed{\mathrm{C}_a = \mathrm{p}_a + \frac{1}{2a}\left(m + \frac{\mathrm{p}_\phi^2}{16\pi\ell_p^2 m}\right) \approx 0.} \tag{5.33}$$

The previous constraint is central in the rest of this chapter. We will see that it leads to a fully controllable dynamics both at the classical as well as the quantum level. Indeed, the dynamics is exactly solvable in the vacuum case while it can be dealt with in perturbation theory for the case where the scalar field is excited. In the next section we will justify the truncation that took us from (5.26) to (5.27) (and finally to the constraint (5.33)) using perturbation theory. In Section 5.2.4 we will show that the perturbative regime is consistent with the conditions that make our model applicable to the description of a spherically symmetry Hawking particle falling into a Schwarzschild black hole during evaporation.

5.2.3 Perturbative solutions in p_ϕ/M and the dynamics in the deep interior region

Exact KS solutions with scalar fields have been studied in the past (see for instance [143]). KS coupled to scalar fields does not lead necessarily to (asymptotically flat) back hole spacetimes globally speaking. However, we will show here that solutions can be interpreted in terms of perturbations of a vacuum Schwarzschild solution in the deep interior region $r \ll 2M$ in the regime where $\mathrm{p}_\phi/M \ll 1$. We will also show that in that regime the Hamiltonian (5.26), and the equations it generates, can be well approximated by (5.27). This will lead to a simple solvable system, both at the classical and quantum levels, which can be used to model aspects of the physics of (zero angular momentum) scalar particles falling into a spherically symmetric black hole (possibly useful in view of describing aspects of Hawking radiation). We will analyze the system in first order perturbation theory in p_ϕ/M.

In order to best organise the perturbative equations we replace p_ϕ^2 by $\epsilon^2\mathrm{p}_\phi^2$ where ϵ is a smallness parameter. We introduce the following expansion of the relevant dynamical quantities

$$f(r) = f_0(r) + \epsilon^2 f_1(r) + \mathscr{O}(\epsilon^4), \tag{5.34}$$
$$\mathrm{p}_f(r) = \mathrm{p}_{f0}(r) + \epsilon^2 \mathrm{p}_{f1}(r) + \mathscr{O}(\epsilon^4)\ , \tag{5.35}$$

and write the equations of motion for them by keeping terms up to order ϵ^2. Starting from

$$\begin{aligned}\dot{f} &= \{f, \mathrm{H}_2\} = -\frac{f(r)}{r} + \frac{\epsilon^2\mathrm{p}_\phi^2}{16\pi\ell_p^2 r f(r)\mathrm{p}_f(r)^2} + \frac{\ell_0^2 r}{4\ell_p^4 \mathrm{p}_f(r)^2},\\ \dot{\mathrm{p}}_f &= \{\mathrm{p}_f, \mathrm{H}_2\} = \frac{\mathrm{p}_f(r)}{r} - \frac{\epsilon^2\mathrm{p}_\phi^2}{16\pi\ell_p^2 r f(r)^2\mathrm{p}_f(r)},\end{aligned} \tag{5.36}$$

with H_2 given in equation (5.26), one can solve the equations order by order with solutions

$$f_0(r) = \mathrm{p}_M^2\left(1 - \frac{2M}{r}\right), \qquad f_1(r) = -\frac{\ell_p^2\mathrm{p}_\phi^2}{8\pi r\ell_0^2 M^2}\left(2M + (M-r)\log\left(\frac{r}{2M-r}\right)\right), \tag{5.37}$$

$$\mathrm{p}_{f0}(r) = \frac{\ell_0}{4\ell_p^2\mathrm{p}_M} r, \qquad \mathrm{p}_{f1}(r) = -\frac{\mathrm{p}_\phi^2 r}{32\pi\ell_0 M^2\mathrm{p}_M^3}\left(\frac{2M}{2M-r} + \log\left(\frac{r}{2M-r}\right)\right). \tag{5.38}$$

The function $h(r)$, is recovered from the constraint (5.23) and gives

$$h_0(r) = \frac{1}{1-\frac{2M}{r}}, \quad h_1(r) = -\frac{\ell_p^2\mathrm{p}_\phi^2 r\log\left(\frac{r}{2M-r}\right)}{8\pi\ell_0^2\mathrm{p}_M^2 M(2M-r)^2}\ . \tag{5.39}$$

Note that the Schwarzschild solution with mass M and conjugate momentum p_M—as in (5.16)—is recovered in the leading order. Consistency of the perturbative treatment requires the ratio of first-to-leading order contributions to remain small, namely

$$\begin{aligned}\frac{f_1(r)}{f_0(r)} &= \frac{\ell_p^2\mathrm{p}_\phi^2}{32\pi\ell_0^2 M^2\mathrm{p}_M^2}\log\left(\frac{r^2}{4M^2}\right) + \mathscr{O}\left(\frac{r}{M}\right) \ll 1,\\ \frac{h_1(r)}{h_0(r)} &= \frac{\ell_p^2\mathrm{p}_\phi^2}{32\pi\ell_0^2 M^2\mathrm{p}_M^2}\log\left(\frac{r^2}{4M^2}\right) + \mathscr{O}\left(\frac{r}{M}\right) \ll 1\end{aligned} \tag{5.40}$$

in the regime $r < M$. The logarithmic behaviour of the right hand side of the previous equations is not a threat, as the classical solutions are not to be trusted for r near the Planck scale. Therefore, assuming $r > \ell_p$, we conclude that our analysis is consistent as long as

$$\frac{\ell_p^2 \mathrm{p}_\phi^2}{32\pi\ell_0^2 M^2 \mathrm{p}_M^2} \log\left(\frac{\ell_p^2}{4M^2}\right) \ll 1 \tag{5.41}$$

which is always valid in the usual macroscopic black hole regime $\ell_p/M \ll 1$. Similarly, note that the ratio of the last term in the Hamiltonian (5.26) to the leading first term is exactly $h(r)$ which in the same regime is $\mathscr{O}(\ell_p^2/M^2 \log(\ell_p/M))$ as seen from (5.39). This suggests that one can simplify the dynamics (if interested in the deep interior region $r \ll M$) and use the Hamiltonian

$$\mathrm{H}_{\mathrm{di}} = -\frac{1}{r}\left(f\mathrm{p}_f + \frac{1}{16\pi\ell_p^2}\frac{\mathrm{p}_\phi^2}{f\mathrm{p}_f}\right). \tag{5.42}$$

This expectation is confirmed by the analysis of the Hamiltonian flow generated by H_{di} in the relevant regime. One might be slightly uncomfortable with the UV cut-off used in devising conditions such as (5.41), after all the classical equations predict a singular evolution when $r \to 0$ and in this limit the right hand sides of the equations (5.40) actually blows up invalidating in appearance the perturbative analysis. We will see that the quantum dynamics across the classical singularity is actually well defined. Moreover, we will also see that there are exact effective equations describing the evolution of the expectation value of semiclassical states across $r = 0$ as well. These equations imply that the counterpart of the right hand side of (5.40) not only does not diverge but rather tends to zero when quantum effects are included.

5.2.4 Validity of perturbation theory in view of applying the model to Hawking pairs

Here we argue for the validity of the perturbation theory analysis of the previous section in the context of applications of the KS model to the quantum dynamical description of scalar field excitations falling inside a Schwarzschild black hole during Hawking evaporation. The assumptions here are: First the usual assumption that the gravitational collapse has formed a spherical black hole with mass $M \gg m_p$. Second, that the Hawking pairs produced by such a macroscopic black hole can be described as test field excitations on a stationary Schwarzschild geometry far away from the singularity. Finally, we restrict our attentions to spherically symmetric Hawking pairs which are the only that can be mapped to the spherically symmetric KS configurations. This is not a serious restriction given that most of the Hawking radiation is emitted in such modes [144].

The following discussion can be framed in the context of figure 9 where Hawking pairs are represented by the red arrows. The stationarity of the background implies that the (test field) current $j_a \equiv T_{ab}\xi^b$ is conserved, where ξ^a is the stationarity Killing field that in the adapted coordinates that we use here is simply given by $\xi = \partial_t$ and T_{ab} is the energy momentum tensor of the scalar field[18]. Conservation of energy leads to the expectation that when a Hawking particle is detected at $\mathscr{I}^+$ with a given energy $\mathcal{E} = \omega$ (which coincides with the associated Killing conserved

[18]The Hawking effect is a quantum process and the relavant state describing it is a quantum state that corresponds to the vacuum in the far past idealized by $\mathscr{I}^-$. Such state can be viewed in the interior as a superposition of particles. Actual particles appear inside in the hypothetical situation of the detection of a partner at $\mathscr{I}^+$ which, according to

quantity), a Hawking partner with (Killing) energy $-\omega$ falls into the black hole singularity reducing the mass of the black hole by ω. A more precise field theoretical expression of this is that the flux of the (expectation value of) the energy-momentum current j_a at infinity in the state of the field after the detection of the particle at $\mathscr{I}^+$ equals minus the flux of the same current on (for instance) a constant $r < 2M$ hyper-surface Σ_r. Namely,

$$\int_{\Sigma_r} j_a n^a dV^{(3)} \quad = \quad -\omega. \tag{5.43}$$

Using our coordinates to write explicitly the integrand in the left hand side while pushing Σ_r to the region where comparison with the KS regime is possible (a constant r such that $r \ll 2M$) we get

$$8\pi M \int_0^{\ell_0} T_{r0}(t,r) r dt = 8\pi M \int_0^{\ell_0} \partial_t\phi\partial_r\phi r dt = \frac{\omega \mathrm{p}_\phi^2}{16\pi M \ell_0}\log(r) + \mathscr{O}(1) = -\omega, \tag{5.44}$$

where the right hand side of the last equality comes from the evaluation of the energy flux of a Hawking particle, while in the evaluation of the left hand side we used that for $r \ll 2M$ (see for instance (5.11)) the scalar field behaves like

$$\begin{aligned} \phi \quad &= \quad \mathrm{Re}\left[e^{-i\omega t}\left(\phi_0 - \frac{\mathrm{p}_\phi}{8\pi M\ell_0}\log(r)\right)\right] + \mathscr{O}\left(\frac{r}{M}\right) \\ &= \quad \cos(\omega t)\left(\phi_0^R - \frac{\mathrm{p}_\phi^R}{8\pi M\ell_0}\log(r)\right) + \sin(\omega t)\left(\phi_0^I - \frac{\mathrm{p}_\phi^I}{8\pi M\ell_0}\log(r)\right) + \mathscr{O}\left(\frac{r}{M}\right). \end{aligned} \tag{5.45}$$

The result in (5.44) follows also from the assumption that $\ell_0 > \omega^{-1} \approx M$. By pushing the integral to its largest possible value when $r \to \ell_p$, we conclude that energy conservation (encoded in (5.44)) implies the bound

$$\frac{\mathrm{p}_\phi^2}{16\pi M^2}\log\left(\frac{\ell_p}{M}\right) < 1, \tag{5.46}$$

which is consistent with the condition for the validity of perturbation theory (5.40). We see that the physical context provided by the problem of Hawking evaporation precisely justifies the simplifying assumptions that led to (5.33). Notice also that the fiducial length scale ℓ_0 acquires in such a physical situation an operational meaning as well.

A generalization of the analysis of the present Sections 5.2 to a wider class of close to stationary black holes is certainly very appealing. Even though it is clear that the tools employed here would not apply to black hole spacetimes with angular momentum (due to the breaking of spherical symmetry), one could entertain the possibility of including an electric charge without leaving the general framework of this work. However, such an apparently simple extension will reserve challenging new aspects. The first qualitative new feature is that the singularity becomes timelike in the unperturbed black hole. However, when a scalar field perturbation is added its back reaction is expected to produce the phenomenon of mass inflation [145] near the Cauchy horizon of the unperturbed background. This completely changes the global features of a realistic charged black hole

the standard interpretation of quantum mechanics, will produce a collapse of the vacuum to a new state containing an actual particle falling into the black hole. The situation after such collapse is the semiclassical situation that we model here with our classical language. A precise description of such a situation in quantum terms is a question that can only be addressed in a full theory of quantum gravity. We argue here that our little solvable model goes a humble little step into that direction.

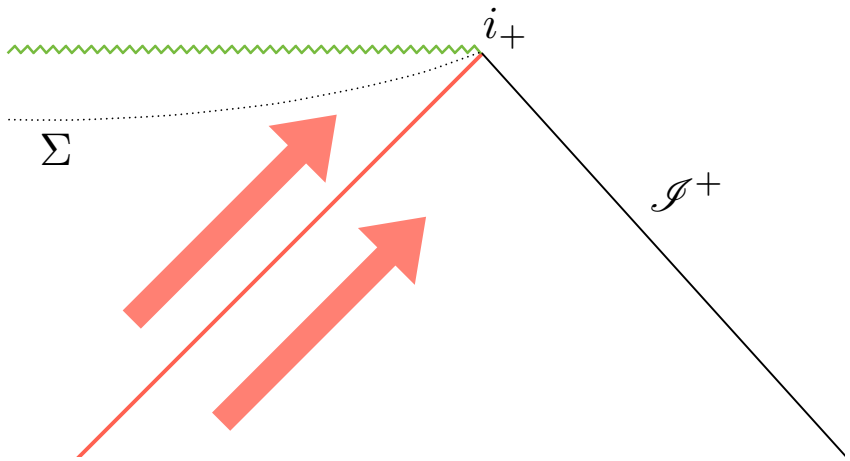


Figure 9: Hawking pairs (red arrows) produced in a black hole spacetime with $M \gg m_p$ are described as test field excitations on a background spacetime that is idealized by a stationary black hole solution in the region of the Penrose diagram away from the collapsing matter and containing i_+. Stationarity implies the existence of a conserved energy-momentum current used, in this chapter, to relate the value of p_ϕ in the KS model to the frequency of the emitted particle at $\mathscr{I}^+$ and (via Hawking temperature) to the black hole mass M. The surface Σ represents an r=constant surface in the interior (denoted Σ_r in the main text).

.

interior in a way that would seem to preclude the applicability of the present methods. More precisely, if we use the Reissner-Nordstrom background black hole geometry as a basis for the present discussion—noting that the presence of mass inflation already implies that strong deviations from the Reissner-Nordstrom interior solution are to be expected—the true would-be-singularity should materialize near the location of the Cauchy horizon. However, close to the Cauchy horizon scalar field modes with frequency ω are expected to be infinitely blue shifted precluding the type of approximation available in the present case. This makes such exploration highly non-trivial even when certainly interesting.

5.3 A natural polymer quantization of the deep interior dynamics

In previous sections we have shown that the Hamiltonian constraint (5.33) describes the deep interior dynamics of scalar excitations without angular momentum falling into a macroscopic Schwarzschild black hole. The approximations used are based on assumptions that are satisfied by the (spherically symmetric) Hawking excitations produced during black hole evaporation. Thus, the simplified dynamics in the deep interior region, which will turn out to be analytically solvable (both at the quantum and classical level), offers a toy scenario to analyze key questions of black hole evaporation in a controlled scenario. We will show in this section that there is natural polymer quantization of the deep interior dynamics with remarkable simple properties such as: (like in the full theory of LQG) the discreteness of the area of constant area surfaces, a well defined quantum dynamics across the singularity, an effective classical description, and a direct (to our knowledge novel) link with the continuum representation. The polymer quantization we propose does not suffer from the usual ambiguities associated to the so-called holonomy corrections [89] as the Hamiltonian constraint evolution has (in our simple model) a clear-cut geometric interpretation that allows for

a unique polymerization that is compatible with the continuum limit (defined by the Schroedinger representation). This special geometric property arises from the fact that the Hamiltonian constraint is linear in the momentum conjugate to the area of the spheres whose spectrum is discrete in our polymer representation. Ambiguities remain in the form of the so-called inverse volume corrections which are necessary if one defines the quantum dynamics across the singularity.

5.3.1 Sketch of the Schrodinger quantization

In the standard Schrodinger representation one would quantize the phase space of Section 5.2.1 by promoting the variables $a, m, \mathrm{p}_a, \mathrm{p}_m$ to self adjoint operators

$$\widehat{m}\ \psi(m,\mathrm{p}_\phi,a) = m\psi(m,\mathrm{p}_\phi,a), \qquad \widehat{a}\ \psi(m,\mathrm{p}_\phi,a) = a\psi(m,\mathrm{p}_\phi,a), \qquad \widehat{\mathrm{p}}_\phi\psi(m,\mathrm{p}_\phi,a) = \mathrm{p}_\phi\psi(m,\mathrm{p}_\phi,a)$$
$$\widehat{\mathrm{p}}_m\psi(m,\mathrm{p}_\phi,a) = -i\partial_m\psi(m,\mathrm{p}_\phi,a), \qquad \widehat{\mathrm{p}}_a\psi(m,\mathrm{p}_\phi,a) = -i\partial_a\psi(m,\mathrm{p}_\phi,a), \qquad \widehat{\phi}\ \psi(m,\mathrm{p}_\phi,a) = i\partial_\phi\psi(m,\mathrm{p}_\phi,a)$$

in the kinematical Hilbert space is $\mathscr{H}_{\mathrm{S}} = \mathscr{L}^2(\mathbb{R}^3)$, equipped with the usual inner product

$$\langle\psi_1,\psi_2\rangle = \int_{-\infty}^{+\infty}\int_{-\infty}^{+\infty}\int_{-\infty}^{+\infty}\overline{\psi_1(m,\mathrm{p}_\phi,a)}\psi_2(m,\mathrm{p}_\phi,a)dmd\mathrm{p}_\phi da, \tag{5.47}$$

where we have chosen the momentum representation for the scalar field for convenience (as p_ϕ is one of the constants of motion of the system). Eigenstates of the $\widehat{a}$ operator are interpreted as distributions (they are not in the Hilbert space) and one usually writes

$$\widehat{a}\,|a\rangle = a\,|a\rangle \tag{5.48}$$

with $a \in \mathbb{R}$ and form an orthonormal basis

$$\langle a,a'\rangle = \delta(a,a'). \tag{5.49}$$

The dynamics is imposed by solving the Hamiltonian constraint (5.33) which, in the present representation, takes the precise form of a Schrodinger equation in the area variable a, namely

$$\left[-i\hbar\frac{\partial}{\partial a} + \frac{1}{2a}\left(m + \frac{\mathrm{p}_\phi^2}{16\pi\ell_p^2 m}\right)\right]\psi(m,\mathrm{p}_\phi,a) = 0. \tag{5.50}$$

As usual, solutions of the constraint are certainly not square integrable in the a-direction, thus physical states are outside of the kinematical Hilbert. The physical Hilbert space is defined as the space of square integrable functions of m and p_ϕ at fixed time a—$\mathscr{H}_{\mathrm{phys}} = \mathscr{L}^2(\mathbb{R}^2)$—with inner product

$$\langle\psi_1(a),\psi_2(a)\rangle_{\mathrm{phys}} = \int_{-\infty}^{+\infty}\int_{-\infty}^{+\infty}\overline{\psi_1(m,\mathrm{p}_\phi,a)}\psi_2(m,\mathrm{p}_\phi,a)dmd\mathrm{p}_\phi, \tag{5.51}$$

which is preserved, i.e. it is independent of a, by the Schrodinger equation (evolution is unitary in a).

Two important remarks are in order: First note that we are formulating in detail the dynamics of the system in the near singularity approximation. The physical reason for this is that (as argued previously) it is only in this approximation that the system can be compared with a (spherically symmetric) black hole with spherically symmetric excitations falling inside. A side gain is also

the simplification of the dynamics which will allow us for a simpler quantization and the analysis of the possibility of a well defined dynamics across the singularity when we undergo the LQG inspired quantization. One could however consider the quantization of the minisuperspace system without the near singularity approximation. In that case one would need to write a Schroedinger equation using the Hamiltonian (5.26), now genuinely time-dependent (r-dependent), for which unitary evolution would involve path ordered exponentials (as the Hamiltonian does not commute with itself at different r values). In addition one would need to work with either $r, f, \mathrm{p}_r, \mathrm{p}_f$ variables or $a, f, \mathrm{p}_a, \mathrm{p}_f$ variables without the luxury of the simplifications introduced by the use of the near singularity variables (5.30).

5.3.2 The polymer quantization

We define now a representation of the phase space variables that incorporates a key feature of the full theory of LQG: the area quantization. Such representation closely mimics the structure of the quantum theory in the fundamental theory in such a way that the area variable a acquires a discrete spectrum. Mathematically, this is achieved by replacing the $\mathscr{L}^2$ structure of the inner product in the variable p_a by the inner product of the Bohr compactification of the p_a phase space dimension. More precisely one substitutes the kinematical inner product in the Schroedinger representation (5.47) by

$$\langle \psi_1, \psi_2 \rangle = \lim_{\Delta \to +\infty} \frac{1}{2\Delta} \int_{-\Delta}^{+\Delta} \left(\int_{-\infty}^{+\infty} \overline{\psi_1(m, \mathrm{p}_\phi, \mathrm{p}_a)} \psi_2(m, \mathrm{p}_\phi, \mathrm{p}_a) dm d\mathrm{p}_\phi \right) d\mathrm{p}_a \ . \tag{5.52}$$

With this inner product, periodic functions of p_a with arbitrary period are normalizable and the conjugate a-representation acquires the property of discreteness in a way that closely mimics the structure of the fundamental theory of loop quantum gravity [22]. In particular eigenstates of $\widehat{a}$ exist

$$\widehat{a} \, |a\rangle = a \, |a\rangle \tag{5.53}$$

with $a \in \mathbb{R}$. These state form an orthonormal basis with inner product

$$\langle a, a' \rangle = \delta_{a,a'}, \tag{5.54}$$

in contrast with (5.49). Discreteness of the spectrum of $\widehat{a}$ comes at the prize of changing the kinematical Hilbert space structure in a way that precludes the infinitesimal translation operator $\widehat{\mathrm{p}}_a$ to exist. Instead only finite translations (quasi periodic functions of p_a) can be represented as unitary operators in the polymer Hilbert space. Their action on the a-basis is given by

$$\widehat{e^{i\lambda \mathrm{p}_a}} \psi(m, \mathrm{p}_\phi, a) = \psi(m, \mathrm{p}_\phi, a + \lambda \ell_p). \tag{5.55}$$

Eigenstates of the finite translations (or shift operators) exist and are given by wave functions supported on discrete a-lattices. Namely,

$$\psi_{k,\epsilon}(a) \equiv \begin{cases} \exp(ika) & \text{if} \quad a \in \Gamma_{\epsilon,\lambda} \equiv \{(\epsilon + n\lambda)\ell_p^2 \in \mathbb{R}\}_{n \in \mathbb{Z}} \\ 0 & \text{otherwise} \end{cases} \tag{5.56}$$

where the parameter $\epsilon \in [0, \lambda) \in \mathbb{R}$. The discrete lattices denoted $\Gamma_{\epsilon,\lambda}$ are the analog of the spin-network graphs in LQG with the values of a on lattice sites the analog of the corresponding spin labels. With all this one has (using (5.55)) that

$$\widehat{e^{i\lambda \mathrm{p}_a}}\psi_{k,\epsilon}(a) = e^{i\lambda k}\psi_{k,\epsilon}(a). \tag{5.57}$$

Note that, unlike the Schroedinger representation where the eigen-space of the momentum operator is one dimensional, the eigen-spaces of the translation operator (labelled by the eigenvalue $e^{i\lambda k}$) are infinite dimensional and non separable. This is explicit from the independence of the eigen-values of the continuous parameter $\epsilon \in [0, \lambda)$ labelling eigenstates. Such huge added degeneracy in the spectrum of the shift operators is a general feature of the polymer representation. We will show that this degeneracy can show up in Dirac observables of central physical importance such as the mass operator in Section 5.4.3.

5.3.3 Quantum dynamics

The dynamics is dictated by the quantization and imposition of the constraint (5.33). As the operator corresponding to p_a does not exist in our kinematical Hilbert space we introduce a polymerized version. Traditionally, this is achieved by replacing the infinitesimal translation operator

$$\lambda\widehat{\mathrm{p}}_a \quad \underset{\text{traditional}}{\longrightarrow} \quad \widehat{\sin \lambda \mathrm{p}_a}. \tag{5.58}$$

The rule consists of making some 'minimal' substitution of p_a by a periodic regularization satisfying that in the limit $\lambda \to 0$ the functional choice will approximate the original function. Such rule is intrinsically ambiguous and, it opens in general the door for an infinite set of possibilities. Such choices are to be interpreted as quantization ambiguities of the Hamiltonian constraint with potential quantitative dynamical consequences (for a general discussion see [90]). Dynamical implications of these ambiguities have been discussed in the previous chapter.

In the full theory a new perspective on the regularization issue has been introduced motivated by the novel mathematical notion of generalized gauge covariant Lie derivatives [146] and their geometric interpretation allowing for the introduction of a natural regularization (and subsequent) anomaly free quantization of the Hamiltonian constraint [147]. Even when the procedure does not eliminate all ambiguities of quantization (choices are available in the part of the quantum constraint responsible for propagation [92]), the new technique reduces drastically some of them in the part of the Hamiltonian that is more stringently constrained by the quantum algebra of surface deformations.

What we want to emphasize here is that the analogous procedure in the case of our symmetry reduced Hamiltoinian has a similar effect. Indeed, because our classical Hamiltonian constraint is linear in the variable p_a (whose associated Hamiltonian vector field has a crystal-clear geometric interpretation of infinitesimal translations in a), one has an unambiguous choice of quantization: the obvious choice to replace infinitesimal translations (which do not exist in the polymer representation) by finite translations or shifts. From this geometric perspective the right polymerization is the regularization that make the replacement

$$\lambda\widehat{\mathrm{p}}_a \quad \longrightarrow \quad \widehat{e^{i\lambda \mathrm{p}_a}}. \tag{5.59}$$

In other words the differential time evolution in the Schrodinger equation must be represented in the polymer Hilbert space by a finite translation with a polymerization scale λ. However, as such an action is associated with a clear geometric meaning, the geometric compatibility with the Schrodinger equation can be preserved if the second term in the classical Hamiltonian (5.33) is exponentiated too in order to produce the well known unitary evolution operator that produces finite area evolution. Disregarding for the moment quantum corrections that will have to be included near the $a = 0$ region (see Section 5.4.1), the quantum constraint is taken to be

$$\underbrace{\exp(i\lambda \mathrm{p}_a)}_{\substack{\text{finite areatime}\\ \text{translation}}} |\psi\rangle - \overbrace{\exp\left(\frac{i}{2}\log\left(\frac{a+\lambda}{a}\right)\left(m+\frac{\mathrm{p}_\phi^2}{16\pi G m}\right)\right)}^{\substack{\text{finite areatime}\\ \text{unitary evolution operator}}} |\psi\rangle = 0, \tag{5.60}$$

whose action is well defined in the polymer representation and whose solutions are easily found (by acting on the left with $\langle m, \mathrm{p}_\phi, a|$) to be wave functions satisfying the discrete dynamics given by

$$\psi(m, \mathrm{p}_\phi, a + \lambda\ell_p^2) = e^{\frac{i}{2}\log\left(\frac{a+\lambda\ell_p^2}{a}\right)\left(m+\frac{\mathrm{p}_\phi^2}{16\pi\ell_p^2 m}\right)}\psi(m, \mathrm{p}_\phi, a). \tag{5.61}$$

The physical Hilbert space is defined via the usual inner product at fixed (discrete) time a via

$$\langle\psi_1(a), \psi_2(a)\rangle_{\text{phys}} = \int_{-\infty}^{+\infty}\int_{-\infty}^{+\infty}\overline{\psi_1(m, \mathrm{p}_\phi, a)}\psi_2(m, \mathrm{p}_\phi, a)dmd\mathrm{p}_\phi, \tag{5.62}$$

which independent of the lattice sites as required (a property that we could identify with the intrinsic unitarity of the quantum constraint kernel). More precisely the physical inner product is a constant of the quantum motion associated to the full history represented by the lattice $\Gamma_{\epsilon,\lambda}$ as implied by unitarity. Explicitly one has

$$\langle\psi_1(a), \psi_2(a)\rangle_{\text{phys}} = \langle\psi_1(a+\lambda), \psi_2(a+\lambda)\rangle_{\text{phys}} \quad \forall \quad a \in \Gamma_{\epsilon,\lambda}. \tag{5.63}$$

Ambiguities of regularization that are usually associated with the polymerization procedure are thus completely absent in this model. The reason is the linear dependence of the Hamiltonian constraint in the polymerized variable which allows for a regularization fixed by the geometric interpretation of the classical Hamiltonian vector field associated to the corresponding variable. However, ambiguities remain when one studies the evolution across the *would-be-singularity* of the Kantowski-Sachs model at $a = 0$. We will study this in the next section.

Now we would like to concentrate on the evolution when we are away from the $a = 0$. In such regime the one step evolution (5.61) can be composed to produce the arbitrary initial to final area evolution

$$\psi(m, \mathrm{p}_\phi, \epsilon + n\lambda) = \left(\frac{\epsilon + n\lambda}{\epsilon + q\lambda}\right)^{\frac{im}{2}\left(1+\frac{\mathrm{p}_\phi^2}{16\pi\ell_p^2 m^2}\right)}\psi(m, \mathrm{p}_\phi, \epsilon + q\lambda), \tag{5.64}$$

for arbitrary integers $n, q > 1$. Evolving across the $a = 0$ point will be discussed later.

5.4 The continuum versus the polymer dynamics

The polymer dynamics that arises from the geometric action of the quantum constraint (5.60) enjoys of the appealing feature of being closely related to the dynamics that one would obtain in the continuum Schroedinger representation. This statement can be made precise as follows: any solution of the Schroedinger equation (5.50) induces on any given lattice $\Gamma_{\epsilon,\lambda}$ a solution of (5.60). Conversely, physical states of the polymer theory represent a discrete sampling of the continuum solutions of (5.50). However, the Schroedinger evolution is ill defined at the singularity $a = 0$ due to the divergence of the $1/a$ factor in front of the second term of (5.50). The polymer representation allows for a well defined evolution across the singularity thanks to the deviations from the $1/a$ behaviour introduced by the analog of the 'inverse-volume' corrections (see next section). Nevertheless, with the appropriate modification of the $1/a$ factor in the Schroedinger equation the correspondence between the discrete and continuum continues to hold.

5.4.1 Quantum evolution across the classical singularity

Quantum evolution in a for all values of a including the singularity is dictated by the quantum corrected version of the constraint (5.60) given by

$$\psi(m, \mathrm{p}_\phi, a) = e^{\frac{i}{2}\left[\int_{a_0}^{a} \left[\frac{1}{a}\right]_q da\right]} \left(m + \frac{\mathrm{p}_\phi^2}{16\pi\ell_p^2 m}\right) \psi(m, \mathrm{p}_\phi, a_0) \tag{5.65}$$

$$= e^{\frac{i}{2}[\tau(a)-\tau(a_0)]} \left(m + \frac{\mathrm{p}_\phi^2}{16\pi\ell_p^2 m}\right) \psi(m, \mathrm{p}_\phi, a_0), \tag{5.66}$$

where

$$\left[\frac{1}{a}\right]_q \tag{5.67}$$

denotes the quantum corrected expression for the operator a^{-1} (the analog of inverse volume correction in cosmology) that can be implemented in various ways due to inherent ambiguities associated to the polymer quantization. In general this will give deviations of the a^{-1} behaviour in the region $a \sim \ell_p^2$. This modifies the integral of a^{-1} in a way charaterized by the (to a large extend arbitrary [89]) function $\tau(a)$ introduced in the second line. One, among the many possibilities, is the one that follows from the so-called Thiemann's trick whose most elementary form is (see [22] for its application in cosmology, see [89] for a discussion of the multiplicity of variants)

$$\left[\frac{1}{a}\right]_{\mathrm{Thm}} \equiv \mathrm{sign}(a) \left(\frac{\sqrt{|a+\ell_p^2|} - \sqrt{|a-\ell_p^2|}}{\ell_p^2}\right)^2 = \frac{1}{a} + \mathscr{O}\left(a^{-3}\right). \tag{5.68}$$

Integration leads to the following $\tau(a)$ function in (5.65)

$$\tau(a) = \begin{cases} |a|\left(|a| - \sqrt{|a|^2-1}\right) + \log\left(\sqrt{|a|^2-1} + |a|\right) - \frac{\pi}{2} + 1 & 1 \le |a| \\ -|a|\left(\sqrt{1-|a|^2} - 2\right) - \sin^{-1}(|a|) & |a| \le 1 \end{cases}, \tag{5.69}$$

whose graph is presented in Figure 10.

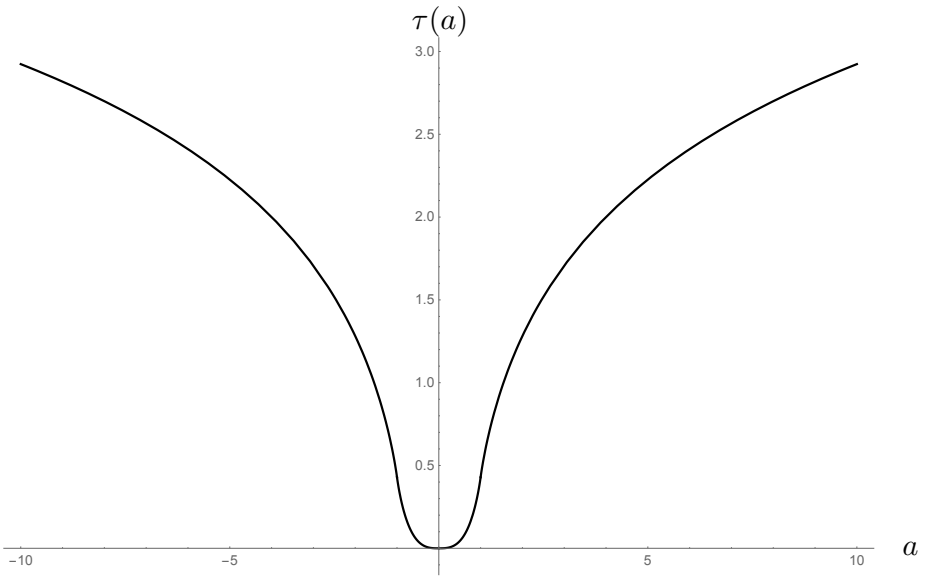


Figure 10: The dynamics across the singularity is regular due to inverse volume corrections. In this picture we show the function $\tau(a)$, defining the dynamical evolution across the singularity, in the case of Thiemann's regularization of the inverse-area-operator.

.

The classical theory does not fix the evolution uniquely in this high curvature regime where quantum geometry effects cannot be neglected. Quantum geometry effects regularize the dynamics near the $a = 0$ singularity; one way of seeing this is that the factor $\log(a)$ in the quantum evolution away from the singularity in (5.60) receives inverse volume quantum geometry corrections. As discussed in [89] these corrections are ambiguous (as fact that should not be surprising given the expectation that the classical theory cannot guide us all the way to the deep UV in QFT). Instead of proposing one particular UV extension, as in the example shown where Thiemann regularization was used, one might simply keep all possibilities open and assume that the corresponding operator is regularized in the relevant region by some arbitrary function $\log(a) \to \tau(a)$. In regions where $\tau(a) = \log(a)$ the quantum evolution leads to semiclassical equations that match exactly Einstein's equations in the KS sector (more details in Section 5.4.2)

5.4.2 Dynamics of semiclassical states and tunelling across the singularity

Let us first consider the vacuum $\mathrm{p}_\phi = 0$ case. This case is important because it should correspond to the Schrwarzschild interior in the region $r \ll M$ (or $a \ll M^2$). The dynamical evolution (5.65) becomes

$$\psi(m, a) = e^{\frac{i}{2}m(\tau(a)-\tau(a_0))}\psi(m, a_0). \tag{5.70}$$

In the p_{m} representation the previous equation simply reads

$$\psi(p_{\mathrm{m}}, a) = \psi(p_{\mathrm{m}} + \frac{\tau(a) - \tau(a_0)}{2}, a_0), \tag{5.71}$$

i.e., a simple translation in momentum space. Such dynamical evolution in a implies in an obvious manner that semiclassical states peaked at classical values $(\overline{m}, \overline{\mathrm{p}}_m)$ at area a_0 with some given fluctuations will be simply evolved into the translated state with the very same fluctuation properties peaked at $(\overline{m}, \overline{\mathrm{p}}_m + (\tau(a) - \tau(a_0))/2)$ at area a. This is a remarkable property of the quantum system: independently of the quantum gravity effects encoded in the precise form of $\tau(a)$, expectation values satisfy well defined effective dynamical equations which are exact (not an approximation), and semiclassical states are not spread by the dynamical evolution (as in the simple case of the harmonic oscillator). Notice that the validity of effective dynamical equations in the context of black hole models have remained a conjecture in other formulations [31].

In regions where $\tau(a) = \log a$ the previous evolution gives

$$\overline{\mathrm{p}}_m(a) = \log(r) + \overline{\mathrm{p}}_m(a_0), \quad \overline{m}(a) = \overline{m}(a_0). \tag{5.72}$$

From the definitions (5.30) we have that $f\mathrm{p}_f = m(a)$ and $f = -\exp[-\mathrm{p}_m(a)]$. The constraint (5.25), gives us $h(r)$ and the metric becomes

$$ds^2 = e^{-\mathrm{p}_m(a)} dt^2 - \frac{\ell_0^2}{(4\ell_p)^4\pi^2} \frac{e^{-\mathrm{p}_m(a)}}{m(a)^2} da^2 + \frac{a}{4\pi} d\Omega^2 \tag{5.73}$$

which corresponds to the Schrwarzschild solution with the two Dirac observables M and p_M given in terms of the initial conditions by

$$M = \frac{2\sqrt{4\pi}\ell_p^4}{\ell_0^2\sqrt{a_0}} m(a_0)^2 e^{\mathrm{p}_m(a_0)}, \qquad \mathrm{p}_M = \frac{\ell_0\sqrt{4\pi}}{2\ell_p\sqrt{a_0}} \frac{e^{-\overline{\mathrm{p}}_m(a_0)}}{\overline{m}(a_0)}. \tag{5.74}$$

When quantum inverse volume corrections are taken into account then the quantum evolution is perfectly well defined across the classical singularity. The evolution of the mean values of a semiclassical state is also well defined and given by

$$\overline{\mathrm{p}}_m(a) = \overline{\mathrm{p}}_m(a_0) + \frac{1}{2}(\tau(a) - \tau(a_0)), \quad \overline{m}(a) = \overline{m}(a_0). \tag{5.75}$$

Such solutions can also be obtained from the Hamiltonian constraint given that one replaces the operator a^{-1} by its quantum regularization (effective equations are in this sense exact). The metric for all values of $|a| \ll M^2$ but otherwise arbitrary becomes

$$ds^2 = \exp\left[-\overline{\mathrm{p}}_m(a_0) - \frac{1}{2}(\tau(a) - \tau(a_0))\right] \left(dt^2 - \frac{\ell_0^2}{(4\ell_p)^4\pi^2} \frac{da^2}{\overline{m}(a_0)^2}\right) + \frac{a}{4\pi} d\Omega^2. \tag{5.76}$$

Since the Thiemann regularization produces a $\tau(a) \sim a^2 \sim r^4$ near $a = 0$ we see that the previous metric is just given by a two dimensional Minkowski metric fibrated with two dimensional sphere with time dependent radius r. The shrinking of the spheres leads to a singularity at $a = 0$ where the spheres collapse and the spacetime geometry (as described by the effective line element) becomes a two dimensional flat one at the singularity in the a-t plane. Despite the singular nature of the effective metric the fundamental quantum evolution is well defined across the singularity.

In the presence of matter the situation is a bit more involved due to the factor p_ϕ/m appearing in matter contribution to the Hamiltonian constraint (5.60). However, in the spirit of applying this analysis to macroscopic black holes and modelling the dynamics of a weak scalar excitation (a

Hawking particle) falling into the singularity, it is natural to focus on semiclassical states (Gaussian) peaked on values such that $\overline{m} \gg \mathrm{p}_\phi$ with fluctuations $\sigma_m \ll \overline{m}$. As in the vacuum case $\overline{m} = \overline{m}_0$, i.e., $\overline{m}$ is a constant of motion as well as its spread σ_m. The dynamics of the conjugate variable (the mean value $\overline{\mathrm{p}}_m$ of the variable p_m) can be evaluated using stationary phase methods and the result is

$$\overline{\mathrm{p}}_m(a) = \overline{\mathrm{p}}_m(a_0) + \frac{1}{2}(\tau(a) - \tau(a_0)) \left[1 + \frac{\mathrm{p}_\phi^2}{\overline{m}(a_0)^2}\left(1 + \frac{3}{4}\frac{\sigma_m^2}{\overline{m}(a_0)^2}\right)\right] + \mathscr{O}\left(\frac{\sigma_m^3}{\overline{m}(a_0)^3}\right), \tag{5.77}$$

which can be seen to correspond to the classical solutions found in Section 5.2.3. Notice that, as expected from the form of the matter coupling, there are here quantum corrections characterized by terms proportional to $\sigma_m^2/\overline{m}(a_0)^2$. The spread in the variable p_m is not time independent if we take into account higher order corrections, namely

$$\overline{\sigma}^2_{\mathrm{p}_m}(a) = \frac{1}{\sigma_m^2} + \frac{\sigma_m^2 \mathrm{p}_\phi^4}{4\overline{m}(a_0)^4}(\tau(a) - \tau(a_0))^2. \tag{5.78}$$

The previous equations are derived assuming that the scalar field is in an eigenstate of the momentum p_ϕ. This is an idealization that simplifies the analysis of the dynamical evolution of the geometry. Similarly, if we assume that the geometry state was in an eigenstate of m then we can easily analyze the dynamics of the scalar field assuming that it is initially in a gaussian semiclassical state picked about $\overline{\mathrm{p}}_\phi(a_0)$ and $\overline{\phi}(a_0)$. In accordance with the classical solutions we get

$$\begin{aligned} \overline{\mathrm{p}}_\phi(a) &= \overline{\mathrm{p}}_\phi(a_0) \\ \overline{\phi}(a) &= \overline{\phi}(a_0) + (\tau(a) - \tau(a_0))\,\frac{\overline{\mathrm{p}}_\phi(a_0)}{16\pi\ell_p^2 m}. \end{aligned} \tag{5.79}$$

One way to quickly derive these equations by inspection is to realize that the Hamiltonian constraint (5.33) is that of a non relativistic point particle with mass proportional to our geometric variable m evolving in $d\tau = [1/a]_q da$. Note that (5.77) implies that the back-reaction of the scalar field enters only through a simple modification of the exponential conformal factor in front of the 2-metric in the a-t 'plane' in equation (5.76).

Unlike the geometry d.o.f, the fluctuations in the scalar field grow as one approaches the would-be-singularity: for a given geometry semiclassical state picked around the mass M, the spread of the scalar field σ_ϕ in an initially eigenstate of ϕ at area a grows to a maximum value close to the would-be-singularity such that

$$M\sigma_\phi < \sqrt{\frac{M\log\left(a/\ell_p^2\right)}{16\pi\ell_0}}, \quad \sigma_{\mathrm{p}_\phi} < \sqrt{\frac{16\pi M}{\ell_0 \log\left(a/\ell_p^2\right)}} \tag{5.80}$$

which are small in the interior if we take $\ell_0 \gg M$ as expected from appearance of ℓ_0 in the fundamental commutation relations [132]. Note that, if we take into account inverse volume corrections of the type suggested by LQG (see Figure 10), the scalar field reaches a critical point at $a = 0$ where its area velocity vanishes.

5.4.3 The mass operator (in the vacuum case)

In this section we concentrate in the vacuum case for simplicity as the mass can be directly read off the form of the metric in this case via a simple comparison with the classical Schwarzschild solution. In this case the result is

$$M = \frac{2\sqrt{4\pi}\ell_p^4}{\ell_0^2\sqrt{a}} m^2 e^{\mathrm{p}_m}. \tag{5.81}$$

where we used the vacuum solution (5.16) (in its $r \ll M$ approximation) and (5.30). It is easy to verify that the previous is indeed a Dirac observable by showing that it commutes with Hamiltonian constraint (5.33). Its non linear dependence on the basic variables anticipates factor ordering ambiguities when it comes to promoting the mass to a quantum operator. Here we focus on the choice

$$\widehat{M} = \alpha(\widehat{a}) \left[\widehat{m} e^{\widehat{\mathrm{p}}_m} \widehat{m}\right], \tag{5.82}$$

where $\alpha(a) \equiv 2\sqrt{4\pi}\ell_p^4/(\ell_0^2\sqrt{a})$. The eigenstates equation

$$\widehat{M}|\phi_M\rangle = M|\phi_M\rangle, \tag{5.83}$$

turns into the differential equation

$$\alpha(a) e^{\mathrm{p}_m} \frac{\partial \phi_M(\mathrm{p}_m, a)}{\partial \mathrm{p}_m} + \alpha(a) e^{\mathrm{p}_m} \frac{\partial^2 \phi_M(\mathrm{p}_m, a)}{\partial \mathrm{p}_m^2} + M\phi_M(\mathrm{p}_m, a) = 0, \tag{5.84}$$

if we expand the eigenstate in the p_m, a basis, namely

$$|M\rangle = \sum_{a \in \Gamma_{\epsilon,\lambda}} \int \phi_M(\mathrm{p}_m, a) |\mathrm{p}_m\rangle |a\rangle d\mathrm{p}_m, \tag{5.85}$$

where the sum runs over the discrete lattice $\Gamma_{\epsilon,\lambda}$ defined in (5.56) when introducing the dynamical constraint (5.60). This differential eigenvalue equation is solved by

$$\phi_M(\mathrm{p}_m, a) \equiv \langle \mathrm{p}_m, a | M\rangle = \sqrt{\frac{2\sqrt{M}}{\alpha(a)}} e^{-\mathrm{p}_m/2} J_1\left(2\sqrt{\frac{M}{\alpha(a)}} e^{-\mathrm{p}_m/2}\right), \tag{5.86}$$

where J_1 is a Bessel function. One can explicitly verify that the quantum dynamics (5.60) preserves the eigenstates by explicitly showing that the evolution between arbitrary lattice points $a_1, a_2 \in \Gamma_{\lambda,\epsilon}$ sends the wave function of the eigenstate at the a_1 lattice point to the a_2 lattice point (as expected for a Dirac observable); or equivalently, the eigenstates of the mass are physical states solving (5.60). Explicitly,

$$\widehat{e^{\frac{i}{2}(\log(a_2)-\log(a_1))m}} \phi_M(\mathrm{p}_m, a_1) = \phi_M\left(\mathrm{p}_m + \frac{1}{2}(\log(a_2) - \log(a_1)), a_0\right) = \phi_M\left(\mathrm{p}, a_2\right). \tag{5.87}$$

Now the evolution across $a = 0$ requires inverse volume corrections which modifies the previous dynamical law by replacing $\log(a) \to \tau(a)$. The mass Dirac observable still exists once inverse volume corrections are turned on. It corresponds to the modification of (7.16) via the substitution $\widehat{a} \to \exp(\widehat{\tau}(a))$. Eigenstates are also obtained by the same substitution in (5.86) and satisfy the

expected Dirac observable condition (which now holds for lattice points at different sides across the singularity)

$$e^{\frac{i}{2}\widehat{(\tau(a_2)-\tau(a_1))m}}\phi_M(\mathrm{p}_m, a_1) = \phi_M\left(\mathrm{p}_m + \frac{1}{2}(\tau(a_2)-\tau(a_1)), a_0\right) = \phi_M\left(\mathrm{p}, a_2\right). \tag{5.88}$$

When supported on the same lattice, one can show that they satisfy the orthogonality relation

$$\langle M|M'\rangle_{\mathrm{phys}} = \delta(M, M'), \tag{5.89}$$

where the inner product is computed with the physical inner product (5.62). Thus the spectrum of the mass operator is continuous. It was argued in the context of the full LQG theory in [50, 148, 149] that the eigenspaces of the mass should be infinite degenerate due to the underlying discrete structure of the fundamental theory and the existence of defects that would not be registered in the ADM mass operator. Interestingly, the conjectured property is illustrated explicitly in our simple toy model as the eigenvectors (5.85) for a given eigenvalue M there are infinitely many and labelled by a continuum parameter. More precisely they are associated with wave functions of the form (5.86) supported on lattices with different values of ϵ. Thus eigenstates of the mass should then be denoted $|M, \epsilon\rangle$ with orthogonality relation

$$\langle M, \epsilon|M', \epsilon'\rangle_{\mathrm{phys}} = \delta(M, M')\delta_{\epsilon,\epsilon'}, \tag{5.90}$$

where $\delta_{\epsilon,\epsilon'}$ is the Kronecker delta symbol. The existence of such a large degeneracy is a generic feature of the polymer representation. Even when this is a toy model of quantum gravity, this feature is likely to reflect a basic property of the representation of the algebra of observables in the full LQG context. Here we are showing that the mass operator is hugely degenerate suggesting that the usual assumption of the uniqueness of the vacuum in background dependent treatments of quantum field theory might fail in a full loop quantum gravity context.

Alternative factor orderings of the quantum operator M could be treated similarly (some simple choices lead to slightly different eigenvectors written also in terms of Bessel functions). Such an ambiguity is not relevant for our purposes (and it does not change the key fact that the spectrum of M is infinitely degenerate) as the aim of the model is not to construct any quantitative physical prediction but rather to use it as a toy model to investigate possibly sufficiently generic features that could actually survive in the full theory. The large degeneracy of the mass spectrum is, in our view, an interesting example of one such feature.

5.5 Conclusion

We have shown that test field solutions of the Klein-Gordon equation with zero angular momentum behave like solutions of the KS symmetry reduced model in the deep interior region $r \ll M$ defined in terms of the background Schwarzschild spacetime. This implies that, spherically symmetric scalar matter falling into a spherical black hole can be modeled by the KS solutions near the singularity. Despite the expected limitations of symmetry reduced models in capturing the full physics in the UV regime, the model includes backreaction of the scalar matter. Focusing in the deep interior region and using perturbation theory in p_ϕ/M we show that it is possible to interpret the solutions of KS with matter as Schwarzschild solutions with matter excitations falling towards the $r = 0$

singularity (this interpretation is not global but it is shown to be correct in the deep interior region). The Hamiltonian dynamics simplifies considerably in that regime becoming tractable both at the classical as well as the quantum level. Perturbation theory applies (we have shown) to the situation involving Hawking particles falling into the singularity.

In close analogy to LQG, we define a quantization of the system describing the deep interior region where the area of the r =constant spheres has a discrete spectrum. This leads to the polymer representation of the area of the orbits of the rotation group and its conjugate momentum that allows for a well defined quantum evolution across the singularity if one introduces customary 'inverse-volume' corrections to the quantum scalar constraint. The Hamiltonian constraint admits a simple geometric interpretation in the to-be-polymerized sector due to the linearity of the Hamiltonian constraint in the momentum variable conjugated to the area of the r =constant spheres. The geometric nature of the action of the classical constraint allows for the introduction of a unique polymerization prescription respecting this action at the quantum level. This reduces the ambiguity usually associated to the procedure of quantization of the dynamical constraints for reasons that resonate with the ones that lead to similar advantages in the full theory [146]. Remarkably, the dynamics is exactly solvable at the quantum level. In the vacuum case, the mass operator is a Dirac observable that we quantize and whose spectrum is given explicitly. Semiclassical states dynamics leads to effective evolution equations that can be characterized exactly in the vacuum case and using suitable stationary phase approximations in the case where matter is present. These effective equations coincide with Einsteins equations in regions where the inverse volume corrections can be neglected.

An important formal aspect of the model is that it presents a concrete example of violation of the 'unicity of the vacuum' assumption that permeates discussions of Hawking's information puzzle for over 40 years. In loop quantum gravity the discrete structure of the theory at the Planck scale suggests that a given ADM mass configuration need not correspond to a unique quantum state. High degeneracy due to the contribution of planckian d.o.f is expected but hard to prove at the present stage. This leads to a certain degree of disagreement on the status of such statements in the field at large. Although, a key instance where such degeneracy is accepted with little controversy is in the loop quantum gravity models designed to calculate black hole entropy (for reviews and references see [150, 151]) where the statistical origin of the entropy lies precisely in the large multiplicity of underlying planckian states. Our simple model might still be too simple to represent definite evidence in this direction. Nevertheless, the results of Section 5.4.3 do provide a toy model to eventually study the implications of the large degeneracy of the mass spectrum in discussion of the fate of information in black hole evaporation.

The model we introduce here is simple and workable, we hope it could provide potentially useful insights in dealing with qualitative questions concerning black hole evaporation. The investigation of these interesting possibilities is left for chapter 7.

Part III

The information loss puzzle

The discussion surrounding Hawking's information puzzle in black hole formation and evaporation [152] holds significant importance as it serves as a testing ground for ideas aimed at establishing a coherent framework for quantum gravity. It is indeed generally accepted that the solution to this problem could come from a quantum description of gravity, playing a role either at the horizon for some, or in the Planckian curvature region for others. The aim of this section is to present recent developments suggesting that the Planckian d.o.f of geometry, from which the familiar notion of a metric emerges, could play a crucial role in restoring the purity of the system at the end of evaporation. In particular, we shall see that this scenario is supported by the results presented in the previous parts of this thesis.

The aim of chapter 6 is to recall the formalism and assumptions behind the historic result predicting the evaporation of black holes. Although the most famous result is Hawking's [46], we emphasize that Wald and Parker's is more complete [47, 48], partly because it allows to directly re derive the former. In addition, it clearly shows that Hawking's radiation is purified by ingoing partners falling into the black hole. At this point, it is therefore clear that there is no loss of information. Next, we will examine how these results predict the evaporation of black holes, and why this appears to lead to a breakdown in unitarity, thus to a loss of information. Several assumptions are necessary to reach these conclusions. In particular, it is assumed that the geometry is unaffected by the quantum field responsible for Hawking radiation (absence of backreaction) and that the geometry can be treated classically (semi-classical approach). We will explain why these effects cannot be neglected in two cases: when the black hole reaches planckian size, and for field modes heading towards the region of Planckian curvature. As this part of the field contains all the information needed to purify Hawking radiation, we will argue that it is crucial to understand its evolution in the strong quantum gravity regime in order to restore unitarity in black hole evaporation.

A complete description of this evolution is still beyond reach since we still lack a full theory of quantum gravitation. However, simplified symmetry reduced models can make this scenario more concrete. This is the purpose of chapter 7. To do so, we will use the model introduced in chapter 5 where we demonstrated that Kantowski-Sachs models (with a massless scalar field coupling) serve as a natural toy model for studying the dynamics and backreaction of matter near black hole singularities that radiate and evaporate. This model was quantized in the LQG framework, revealing certain planckian d.o.f that are not apparent to coarse observers. The existence of this hidden sector, or quantum hair, plays a crucial role in the proposed scenario for purifying Hawking radiation. Using this simple black hole model, we will show how quantum correlations between matter and these d.o.f inevitably develop during evolution. It implies that planckian physics is essential in the discussion of unitarity since they may contain the information needed to purify Hawking radiation at the end of evaporation. The results presented in this chapter are strongly inspired by [49].

The black hole is therefore expected to radiate almost all its mass, with the possible exception of a remnant of Planck mass since at this stage it is not guaranteed that the evaporation con-

tinues. In order to respect the conservation of energy, the planckian d.o.f present at the end of the evaporation process, responsible for purifying the radiation, must not store any energy since its is entirely contained in the Hawking radiation. The latter is, according to Hawking, Wald and Parker's computation, in a mixed state. Looking at the whole process of formation and evaporation, we can conclude that the matter field, initially pure and collapsing to form a black hole, evolves towards a mixed state while retaining almost all its energy. The field thus undergoes decoherence, but without dissipation. Although some have argued that this type of evolution is impossible [153], we will present in chapter 8 a QFT model that demonstrates its realizability. Although this model is too simplified to properly describe the formation and evaporation of a black hole, it provides a faithful analogy for many aspects of this process. The results presented in this chapter are strongly inspired by [154]

6 The essence of the puzzle and possible resolutions

This chapter provides a concise introduction to the problem of information loss, in order to set the framework for the original work carried out in this thesis, which will be detailed in subsequent chapters. We begin by recalling the historical results of Hawking, Wald and Parker, showing how they lead to the conclusion that black holes evaporate, which seems to induce information loss. We will then outline various proposed solutions to this problem. Finally, we will present our approach, which is based in part on the flaws observed in Hawking, Wald and Parker's computations, as well as in existing solutions.

6.1 A brief derivation of the problem

We begin by outlining the reasoning behind the conclusion that black holes evaporate. This will involve a review of the historical results of Hawking, Wald and Parker. We shall not go into the details of the computations that can be found in the literature. The original thermal radiation computation is performed by Hawking in [46]. The expression of the density matrix after black hole formation is obtained by Wald and Parker in [47, 48]. This section is based on the following pedagogical and modern reviews [155, 156]. We will then recall how these results seem to predict a loss of information. We will end by discussing to the assumptions on which they are based and discuss possible weaknesses that might point to a solution to the problem of information loss.

6.1.1 Hawking, Wald and Parker result

Hawking, Wald and Parker's results are obtained using the formalism of quantum field theory in curved spacetime. In this formalism, the notion of both particle and vacuum becomes observer dependent. In particular, their computations show how the vacuum seen by an observer before the formation of a black hole (on $\mathscr{I}^-$) is perceived by an observer after the black hole has formed (on $\mathscr{I}^+$). The demonstration is based on a semi classical description of gravitation. This is a description in which spacetime is considered classical, while matter is quantized. Such a description is given by Einstein's semi classical equations.

$$G_{\mu\nu} = 8\pi G \langle T_{\mu\nu} \rangle. \tag{6.1}$$

We will come back to the validity of this description in the next sub-section. A second assumption, to which we will also return, is the absence of backreaction. It means that the geometry is considered fixed, and the quantum fields evolving on top of it do not change the geometry. To simplify the discussion, we consider a massless scalar field, denoted ϕ, evolving on a geometry corresponding to a Schwarzschild black hole. It is essential, however, that this black hole is not stationary, i.e. that there is no timelike Killing vector field. Otherwise it would be possible to have a universal notion of vacuum, as argued in [155]. No radiation could be spontaneously created from the vacuum. We will therefore consider one of the simplest dynamical black hole models, namely the Vaidya Vaidya model, which describes the collapse of a light-like shell of matter leading to a Schwarzschild metric. The Penrose diagram of such a model is given in figure 11, and is described by the following line element

$$ds^2 = -\left(1 - \frac{2M(v)}{r}\right) dv^2 + 2dvdr + r^2 d\Omega^2 \tag{6.2}$$

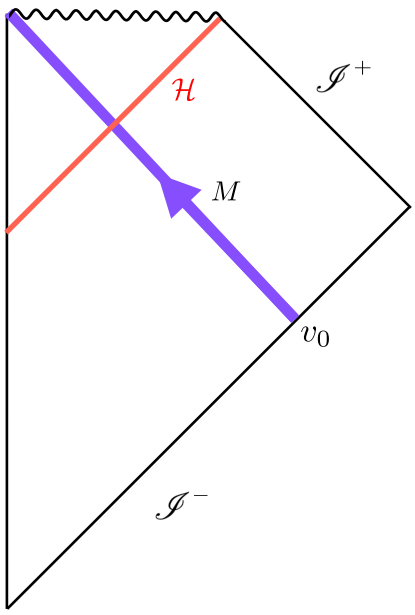


Figure 11: Penrose diagram of a Vaidya spacetime form by the collapse at advanced time v_0 of a null shell of mass M.

This metric is a solution of Einstein's equations for an energy momentum tensor of the form $T_{vv} = \frac{1}{4\pi r^2}\frac{dM(v)}{dv}$ and corresponds to the Schwarzschild metric for constant M. For further simplification, we consider here that the mass distribution is given by $M(v) = M\theta(v - v_0)$, where θ is the Heaviside function, meaning that the black hole is formed by the collapse of a shock wave at the advanced time $v = v_0$, as shown in figure 11. The metric is Minkowski for $v < v_0$ and Schwarzschild for $v > v_0$. Let us add the scalar field, which, assuming no back-reaction, does not modify the geometry just

described. It can be decomposed on $\mathscr{I}^-$ into positive and negative frequency modes with respect to advanced time as follows

$$\phi_{\text{in}} = \int d\omega [a_\omega^{\mathscr{I}^-} u_\omega^{\mathscr{I}^-} + a_\omega^{\mathscr{I}^-\dagger} u_\omega^{\mathscr{I}^-*}] \tag{6.3}$$

where $u_\omega^{\mathscr{I}^-}$ and $u_\omega^{\mathscr{I}^-*}$ correspond to the positive and negative frequency mode on $\mathscr{I}^-$. And $a_\omega^{\mathscr{I}^-}$ and $a_\omega^{\mathscr{I}^-\dagger}$ are the ladder operators of these modes on $\mathscr{I}^-$. In the following, we will assume that this field is in the vacuum state. It will be denoted $|0^{\mathscr{I}^-}\rangle$ and will satisfy the relation $a_\omega^{\mathscr{I}^-} |0^{\mathscr{I}^-}\rangle = 0$ far any ω. The aim of Hawking, Wald and Parker's computation is to determine the state of the field after the formation of the black hole. $\mathscr{I}^-$ being a Cauchy surface, it is natural to be interested in the state of the field on a posterior Cauchy surface in order to have a unitary evolution. It's standard to consider the union of the $\mathcal{H}$ horizon and $\mathscr{I}^+$. The field on this surface will be denoted ϕ_{out} and will be decomposed as follows

$$\phi_{\text{out}} = \int d\omega [a_\omega^{\mathscr{I}^+} u_\omega^{\mathscr{I}^+} + a_\omega^{\mathscr{I}^+\dagger} u_\omega^{\mathscr{I}^+*} + a_\omega^{\mathcal{H}} u_\omega^{\mathcal{H}} + a_\omega^{\mathcal{H}\dagger} u_\omega^{\mathcal{H}*}], \tag{6.4}$$

where $u_\omega^{\mathscr{I}^+}$ and $u_\omega^{\mathscr{I}^+*}$ (respectively $u_\omega^{\mathcal{H}}$ and $u_\omega^{\mathcal{H}*}$) correspond to the positive and negative frequency modes on $\mathscr{I}^+$ (respectively on $\mathcal{H}$) with respect to retarded time (respectively Killing time). And $a_\omega^{\mathscr{I}^+}$ and $a_\omega^{\mathscr{I}^+\dagger}$ (respectively $a_\omega^{\mathcal{H}}$ and $a_\omega^{\mathcal{H}\dagger}$) are the ladder operators for modes on $\mathscr{I}^+$ (respectively on $\mathcal{H}$). As explained earlier, the notion of positive and negative frequency is not the same on this Cauchy surface as on $\mathscr{I}^-$. But since $u_\omega^{\mathscr{I}^-}$ and $u_\omega^{\mathscr{I}^-*}$ form a complete family of solutions, it is possible to use them to express the modes forming ϕ_{out}. Such a transformation is called a Bogolubov transformation and is given by

$$u_\omega^{\mathscr{I}^+} = \int d\omega [\alpha_{\omega\omega'} u_{\omega'}^{\mathscr{I}^-} + \beta_{\omega\omega'} u_{\omega'}^{\mathscr{I}^-*}] \quad \text{and} \quad u_\omega^{\mathcal{H}} = \int d\omega [\gamma_{\omega\omega'} u_{\omega'}^{\mathscr{I}^-} + \eta_{\omega\omega'} u_{\omega'}^{\mathscr{I}^-*}] \tag{6.5}$$

or equivalently

$$a_\omega^{\mathscr{I}^+} = \int d\omega [\alpha^*_{\omega\omega'} a_{\omega'}^{\mathscr{I}^-} - \beta^*_{\omega\omega'} a_\omega^{\mathscr{I}^-\dagger}] \quad \text{and} \quad a_\omega^{\mathcal{H}} = \int d\omega [\gamma^*_{\omega\omega'} a_{\omega'}^{\mathscr{I}^-} - \eta^*_{\omega\omega'} a_\omega^{\mathscr{I}^-\dagger}] \tag{6.6}$$

where $\alpha_{\omega\omega'}, \beta_{\omega\omega'}, \gamma_{\omega\omega'}$ and $\eta_{\omega\omega'}$ are the so called Bogolubov coefficients. The interest in knowing these coefficients becomes explicit if we want, for example, to estimate the number of excitations in the ω mode that an observer on $\mathscr{I}^+$ will detect if the field is in the vacuum state at $\mathscr{I}^-$. This is equivalent to computing $\langle 0_{\text{in}}| N_\omega^{\text{out}} |0_{\text{in}}\rangle = \int d\omega' |\beta_{\omega\omega'}|^2$, with $|0_{\text{in}}\rangle$ the void at $\mathscr{I}^-$. It is possible to compute the Bogolubov coefficients concerned for the (6.2) metric, and it turns out that they diverge. This is because plane waves are not a normalized solution set with respect to the usual Klein-Gordon scalar product. It is therefore more natural to work with wave packets localized in space. We call them $u_{j,n,\epsilon}$ and they are formed from the u_{omega} modes so that they can be normalized (cf [156] for details of this relationship). These wave packets are constructed so that they are localized around $u = \frac{2\pi n}{\epsilon}$ with a spread of $\frac{2\pi}{\epsilon}$, frequency centered around $\omega_j = j\epsilon$ and with spectral width ϵ. The Bogolubov transformation 6.5 can be replaced by

$$u_{j,n,\epsilon}^{\mathscr{I}^+} = \int d\omega [\alpha_{(j,n,\epsilon),\omega'} u_{\omega'}^{\mathscr{I}^-} + \beta_{(j,n,\epsilon),\omega'} u_{\omega'}^{\mathscr{I}^-*}] \quad \text{and} \quad u_{j,n,\epsilon}^{\mathcal{H}} = \int d\omega [\gamma_{(j,n,\epsilon),\omega'} u_{\omega'}^{\mathscr{I}^-} + \eta_{(j,n,\epsilon),\omega'} u_{\omega'}^{\mathscr{I}^-*}], \tag{6.7}$$

or equivalently

$$a^{\mathscr{I}^+}_{j,n,\epsilon} = \int d\omega[\alpha^*_{(j,n,\epsilon),\omega'} a^{\mathscr{I}^-}_{\omega'} - \beta^*_{(j,n,\epsilon),\omega'} a^{\mathscr{I}^-\dagger}_{\omega}] \quad \text{and} \quad a^{\mathcal{H}}_{j,n,\epsilon} = \int d\omega[\gamma^*_{(j,n,\epsilon),\omega'} a^{\mathscr{I}^-}_{\omega'} - \eta^*_{(j,n,\epsilon),\omega'} a^{\mathscr{I}^-\dagger}_{\omega}]. \tag{6.8}$$

In addition to having a clear physical meaning for the wave packets $u^{\mathscr{I}^+}_{j,n,\epsilon}$ and $u^{\mathcal{H}}_{j,n,\epsilon}$, this allows to define Bogolubov coefficients that will be finite. From now on, we will consider n and ϵ to be fixed and will no longer explicitly write these indices. In a completely general way, two vacuum states with mode decompositions linked by a Bogolubov transformation (in our case, the vacuum on $\mathscr{I}^-$ denoted $|0^{\mathscr{I}^-}\rangle$ and the vacuum on $\mathscr{I}^+$ and $\mathcal{H}$ denoted $|0^{\mathscr{I}^+,\mathcal{H}}\rangle$) satisfy the following relation

$$|0^{\mathscr{I}^-}\rangle = \langle 0^{\mathscr{I}^+,\mathcal{H}}|\, 0^{\mathscr{I}^-}\rangle \exp\left(-\frac{1}{2}\sum_{i,j} V_{ij} a_i^{\mathscr{I}^+\dagger} a_i^{\mathcal{H}\dagger}\right) |0^{\mathscr{I}^+,\mathcal{H}}\rangle\,, \tag{6.9}$$

where V_{ij} is a matrix whose components are expressed in terms of Bogolubov coefficients. The tour de force achieved by Hawking, Wald and Parker was to compute the Bogolubov coefficients (6.7) and deduce the expression of V_{ij} in the case of a black hole collapse. We will not present the details of the calculation here, only the result (see [156] or [155] for a pedagogical presentation of this calculation). In order to estimate these coefficients, it is necessary to solve the Klein Gordon equation $\Box\phi = 0$. Neglecting the potential term in this equation and taking the late time limit, i.e. $n \to +\infty$, we can show that

$$|0^{\mathscr{I}^-}\rangle = \bigotimes_j \sqrt{1 - e^{-}8\pi M\omega_j} \sum_{N=0}^{+\infty} e^{-4\pi N M\omega_j} |N_j^{\mathscr{I}^+}\rangle \otimes |N_j^{\mathcal{H}}\rangle\,. \tag{6.10}$$

This is the main result illustrating how the formation of a black hole transform the vacuum into an excited state and is due to Wald and Parker [47, 48]. In the next section we will see how one can interpret this result, more precisely we will describe what an observer at $\mathscr{I}^+$ and at late time will see. We will then see how this result seems to lead to the so called information loss paradox.

6.1.2 Loss of information

We can, from (6.10), reproduce Hawking's historic result [46] by computing what an observer located at $\mathscr{I}^+$ would see. To do this, we need to trace out the d.o.f. of the modes falling inside the black hole. Considering the density matrix of the total system described by (6.10), then tracing on the $\mathcal{H}$ part we obtain

$$\rho_{\mathscr{I}^+} = \mathrm{Tr}_{\mathcal{H}}\left(|0^{\mathscr{I}^+}\rangle\langle 0^{\mathscr{I}^+}|\right) = \bigotimes_j (1 - e^{-8\pi M\omega_j}) \sum_{N=0}^{+\infty} e^{-8\pi N M\omega_j} |N_j^{\mathscr{I}^+}\rangle\langle N_j^{\mathscr{I}^+}|\,. \tag{6.11}$$

From this density matrix, it is possible to compute the quantity $\langle 0^{\mathscr{I}^-}|\, N_j^{\mathscr{I}^+}\, |0^{\mathscr{I}^-}\rangle = \langle 0^{\mathscr{I}^-}|\, a_j^{\mathscr{I}^+\dagger} a_j^{\mathscr{I}^+}\, |0^{\mathscr{I}^-}\rangle$ which according to the definition of $a_j^{\mathscr{I}^+}$ and $a_j^{\mathscr{I}^+\dagger}$ given in the previous subsection, corresponds to the number of particles of frequency $\omega_j \pm \epsilon$ that an observer on $\mathscr{I}^+$ would detect at $u = frac2\pi n\epsilon$ for a duration $\frac{2\pi}{\epsilon}$ if the field were in the vacuum state at $\mathscr{I}^-$. We find

$$\langle 0^{\mathscr{I}^-} | \, N_j^{\mathscr{I}^+} \, |0^{\mathscr{I}^-}\rangle = \frac{1}{e^{\hbar\omega_j/k_bT_h}-1} \quad \text{with} \quad T_h = \frac{\hbar}{8\pi k_b M}. \tag{6.12}$$

The spectrum of particles measured by such an observer is therefore thermal with a temperature T_H called the Hawking temperature. In the paper [46], Hawking derives this result without computing the state of the total system (6.10). The choice here is to emphasize that the outgoing radiation, although in a mixed state, is completely purified by the ingoing one, as can be seen via (6.10). At this stage there is no non-unitary evolution and therefore no loss of information.

One the other hand, since Hawking radiation contains energy, the black hole must, by energy conservation, lose some. This process therefore leads to the evaporation of black holes. However, the above computations assume the absence of backreaction. In order to determine whether this is a good approximation, one can proceed to the following dimensional analysis: the characteristic length scale of a black hole is the Schwarzschild radius, so the wavelength of a Hawing particle should be of this order too, i.e. $\lambda_H = M$. The characteristic energy of a particle is therefore $E_H = 1/M$, and the characteristic emission time is $t_H = 1/E_H = M$. More rigorous reasoning can lead to the same result [156]. In short, a macroscopic black hole takes a very long time to emit a particle containing very little energy. This justifies that the quantum field backreaction is negligible. On the other hand, according to this estimate, a Planckian mass black hole will emit very energetic particles very quickly. It would then be necessary to take backreaction into account, and the results of Hawking, Wald and Parker would no longer be justified. We will come back to the importance of backreaction in more detail in the next subsection. Thus, for a macroscopic black hole, evaporation can be seen as a quasi-static process in which its mass is constantly decreasing. It would evolve from one equilibrium state to another, and the previous derivation of Hawking radiation is valid at each of these stages. In the seminal paper [152], Hawking concludes that this process leads to a loss of the information initially available on $\mathscr{I}^-$ and thus to a breakdown of unitarity. The problem pointed out by Hawking, then reformulated by others [157], can be summarized as follows: a black hole disappears completely by emitting a thermal radiation, leaving only this radiation behind. The initially pure system thus evolves into a mixed state, breaking the unitarity of quantum mechanics. So we need to explain where the information that allows Hawking's radiation to be purified has gone, in order to restore unitarity. But as explained above, as soon as the black hole reaches Planck's mass, there is no guarantee that it will continue to radiate. The problem is not yet solved, however, since we still need to explain how a black hole of Planck mass, which contains very little energy, can contain enough information to purify Hawking radiation, which can have an arbitrarily large entropy. Indeed, the latter depends on the mass of the initial black hole, which can be arbitrarily big.

6.1.3 Assumptions and robustness of the result

We will now return to the various assumptions made to obtain the result (6.10) (in the order in which they are mentioned in the previous subsection). We will see that some of them represent weaknesses likely to play a role in solving the information loss problem. Others, on the other hand, can be modified without profoundly changing the result, which tends to demonstrate its robustness.

1. The semi classical treatment of gravity is valid, i.e. the quantum effects of gravity are

negligible.

It is indeed expected that a classical description of spacetime is possible for curvature scales that are small compared to the Planck curvature. This being the case outside a macroscopic black hole, it is expected that the quantum effects of gravity play no role in this region (we will nevertheless present in the next paragraph a qualitative argument suggesting that the backreaction of Hawking radiation induces quantum fluctuations of the geometry long before the black hole reaches the Planck mass). There are however certain regimes during the evaporation of a black hole for which the semi classical description is no longer possible. Indeed, a macroscopic black hole should radiate in the way suggested by (6.12) and thus see its mass decrease until it reaches a Planckian mass for which the curvature is Planckian at the horizon. From this point on, the semi classical treatment, and therefore (6.12), is no longer valid. There is currently no consensus on what will happen at that point. However, it seems clear that a quantum theory of gravity is needed to describe what will be happening to such an object. Furthermore, this semi classical framework is unable to describe the fate of the falling matter field inside the black hole, which will inexorably reach a zone where the curvature becomes Planckian. As we see in (6.10), this part of the field contains all the information needed to purify Hawking radiation. It is therefore essential to explain what happens to it as it falls towards the black hole, in order to propose a solution to the problem of information loss. And it seems that this can only be done with the help of a quantum gravitational theory that can describe the Planckian d.o.f. of the geometry of this region and their interactions with the ingoing modes.

2. We can consider a fixed metric and neglect the backreaction of the quantum field.

It is argued in [155], by considerations on the components of the Riemann tensor for a particular class of observer, that the energy density of Hawking radiation should indeed not significantly modify the geometry. We justified this more intuitively in the previous subsection by presenting an order of magnitude computation predicting that a particle of energy $E_H = 1/M$ is emitted every $t_H = M$ by a black hole of mass M. The conclusion was that for a macroscopic black hole, this time is sufficiently long, and this energy sufficiently low, to consider that the effect of this radiation on the black hole's geometry is not significant. For a Planckian mass black hole, on the other hand, this reasoning tends to show that the backreaction of the quantum field is no longer negligible. It therefore seems reasonable to consider that neglecting the backreaction is a good approximation as long as the black hole is macroscopic. However, it is interesting to mention an old result obtained by Don Page in [158]. In this paper, Page suggests by way of a qualitative argument that the backreaction of Hawking radiation would be important long before the black hole becomes Planckian, and would lead to significant quantum fluctuations of the geometry. Page's argument is based on the conservation of momentum: the black hole, by emitting a Hawking particle, will recoil. As each particle is in a superposition of states, the black hole will also find itself in a superposition of momentum and therefore of position. Page has shown that this effect induces a dispersion in black hole position of the order of the initial black hole size (i.e. $\Delta x \sim M$) after the latter has radiated a fraction $f \sim \frac{1}{M^{2/3}}$ of its mass. To give an example, a solar mass black hole will be spread by this mechanism over a region as large as its Schwarzschild radius after it has radiated 10^{-25} times its mass. This computation seems to indicate that the backreaction is not negligible long before the black hole reaches Planck mass, and that it induces considerable geometric fluctuations. This does not, however, completely invalidate Hawking, Wald and Parker's result, since it is conceivable that their reasoning could apply in any of the superposition states. Nevertheless, it does suggest

that quantum fluctuations in geometry are present throughout the entire evaporation process. To neglect them is to ignore part of the total system, which could be at the root of the information loss problem. A complete theory of quantum gravitation capable of describing the backreaction of matter on geometry, as well as the fluctuations of the latter, is therefore needed to fully describe the evaporation of a black hole. In the absence of such a theory, we will present a perspective on the problem of information loss that takes into account, in a simplified way, the role of quantum fluctuations of the geometry.

3. The background metric is a Vaidya type collapse model and the matter field is a massless scalar field.

It is completely possible to reproduce previous results for more general metrics as well as for other matter fields. In particular, it is discussed in [156] that the result (6.10) is also valid for more general collapsing models (as was originally done in [46–48]). Moreover, people have been able to show that this result generalizes to the case of charged and rotating black holes (cf [156] for a review). Even if the result (6.10) as well as (6.12) will be modified, the radiation seen by an observer at $\mathscr{I}^+$ is still in a mixed state. The reasoning of the previous subsection leading to the problem of loss of information therefore remains valid. Finally, it is possible to show that a black hole does not radiate only scalar field excitations. It is also possible to obtain a similar result to (6.10) for higher spin fields. One of the main differences is that for fermionic fields, the radiation will be given by a Fermi-Dirac distribution rather than a Bose Einstein distribution as is the case for whole-spin fields. Page has notably estimated the proportion of particles of different kinds in Hawking radiation [159, 160]. Here again, the radiation seen by an observer at $\mathscr{I}^+$ will still be in a mixed state, and the problem of information loss persists.

4. The potential appearing in the Klein Gordon equation whose scalar field is the solution is neglected.

It is also possible to generalize (6.12) by taking into account the potential term in the Klein-Gordon equation. Although the computations allowing these are not trivial, there is no conceptual difficulty. The result (6.12) will be modified as follows

$$\langle 0^{\mathscr{I}^-} |\, N_j^{\mathscr{I}^+} \,| 0^{\mathscr{I}^-} \rangle = \frac{\Gamma_{\omega_j,l}}{e^{\hbar\omega_j/k_b T_h} - 1}, \tag{6.13}$$

where l is the angular momentum of each mode and $\Gamma_{omega_j,l}$ is called the grey body factor (see [156] for its derivation). Since the potential depends on the angular momentum l of the modes, the grey body factor will also depend on l. The latter takes into account the fact that some modes heading towards $\mathscr{I}^+$ are backscattered towards the black hole by the potential. Taking this effect into account, Hawking radiation is no longer thermal, but remains in a mixed state.

5. Considering very high frequency modes (transplanckian) is allowed.

Recall that the result (6.12) describes the radiation measured by an observer at $\mathscr{I}^+$ at late time. In Hawking, Wald and Parker's computation, it is necessary to consider that the observer is at late time. Otherwise, it can be shown that there is no particle creation (cf [156] for a more detailed discussion of this aspect of Hawking radiation). Furthermore, the modes detected by this observer come from a region infinitely close to the horizon (there is no particle creation far from the horizon [156]).

Because of the geometry in this region, these modes are infinitely redshifted as they arrive at $\mathscr{I}^+$. This requires them to have an infinite frequency close to the horizon, so that they do not have zero energy at $\mathscr{I}^+$. The contribution of such modes is therefore necessary to achieve the results (6.10) and (6.12). The problem is that the backreaction of such energetic modes cannot be negligible, and quantum gravity effects on these modes with wavelengths arbitrarily shorter than the Planck length are expected. We have little to say about this problem, except that it reinforces the idea that a quantum theory of gravitation that takes account of the backreaction of matter on geometry is needed to properly describe the evaporation of black holes, as well as the problem of information loss.

6.2 Some attempt of resolution

The aim of this section is to present the main scenarios that have been studied to solve the problem of information loss. We begin by examining the holographic scenarios, based on the so called central dogma, according to which all the information contained in a black hole is stored on its horizon. We will explain why we think this assumption is incorrect, and why it is essential to understand what happens inside the black hole as it evaporates. Next, we will look at remnant scenarios, which are not based on a holographic view of information. However, we will show how these models neglect certain aspects of quantum gravity discussed in the first two parts of this thesis. Finally, we will present our own perspective on the problem, partly motivated by the limitations of previous approaches.

6.2.1 Holographic scenarios

Let us start by discussing the class of scenarios referred to as holographic. We will not discuss each one in detail, as there are many of them and I have no deep understanding of them. We will, however, discuss what earns them the name holographic, the ideas on which they are based and the criticisms that can be leveled at them. This approach is mainly studied in the string theory community, and has had a revival with the AdS/CFT correspondence.

In this approach, the thermodynamic entropy of black holes $S_{\text{thermo}} = \frac{A}{4}$ (with $A = 4M^2$ the area of the horizon of a black hole of mass M) computed by Bekeinstein [161] is interpreted as the total number of microstates of a black hole of mass M. In other words, in a quantum description of gravity, there would be $\frac{A}{4}$ states corresponding to a black hole of mass M. This interpretation of Bekeinstein's result is known as the central dogma. The term holographic refers to the fact that, in this approach, all the information of such a system is encoded on a two dimensional surface. On the other hand, we have seen that a black hole radiates a thermal radiation which has a zero Von Neumann entropy $S_{\text{VN}}^{\text{rad}}$ when the black hole is formed, and which increases as it evaporates. If the total system is pure before the black hole radiates, this implies that $S_{\text{VN}}^{\text{rad}}$ is equal to the Von Neumann entropy of the black hole $S_{\text{VN}}^{\text{BH}}$, i.e. $S_{\text{VN}}^{\text{rad}} = S_{\text{VN}}^{\text{BH}} = S_{\text{VN}}$. In this approach, the thermodynamic entropy of black holes $S_{\text{thermo}} = \frac{A}{4}$ (with $A = 4M^2$ the area of the horizon of a black hole of mass M) computed by Bekeinstein [161] is interpreted as the total number of microstates of a black hole of mass M. In other words, in a quantum description of gravity, there would be $\frac{A}{4}$ states corresponding to a black hole of mass M. This interpretation of Bekeinstein's

result is known as the central dogma. The term holographic refers to the fact that, in this approach, all the information of such a system is encoded on a two dimensional surface. On the other hand, we have seen that a black hole radiates a thermal radiation which has a zero Von Neumann entropy $S_{\rm VN}^{\rm rad}$ when the black hole is formed, and which increases as it evaporates. If the total system is pure before the black hole radiates, this implies that $S_{\rm VN}^{\rm rad}$ is equal to the Von Neumann entropy of the black hole $S_{\rm VN}^{\rm BH}$, i. e. $S_{\rm VN}^{\rm rad}$ is equal to the Von Neumann entropy of the black hole $S_{\rm VN}^{\rm rad}$. e. $S_{\rm VN}^{\rm rad} = S_{\rm VN}^{\rm BH} = S_{\rm VN}$. The latter therefore has a Von Neumann entropy $S_{\rm VN}$ which is initially zero, and which increases as it evaporates. On the other hand, as its surface area decreases, its thermodynamic entropy also decreases. However for any system, the Von Neumann entropy must always be greater than the thermodynamic entropy. But according to this analysis, there exists a time, called Page time and denoted $t_{\rm Page}$, for which $S_{\rm thermo} < S_{\rm VN}$. Since this is not allowed (with the interpretation of the thermodynamic entropy of a black hole presented above), supporters of the central dogma have devised mechanisms to purify Hawking radiation in such a way that $S_{\rm VN}$ decreases from $t > t_{\rm Page}$ so that it follows the so called Page curved [162]. More precisely, these mechanisms ensure that $S_{\rm VN}^{\rm rad}$ increases for $t < t_{\rm Page}$ and then decreases until it cancels out at the end of the evaporation process. Note that $t_{\rm Page}$ is much smaller than the total evaporation time, so the black hole is far from Planckian in size at this point. The mechanisms thus imagined for this early purification require significant modification to the computations of Hawking, Wald and Parker in a regime where none was expected. This is why this approach is sometimes referred to as non conservative [163]. We will not discuss in detail the various mechanisms devised to reproduce the Page curve. But we can mention some of these approaches which do not necessarily agree in their details but all share a certain common ground. Examples range from works that give a fundamental status to Bousso type of entropy bounds [164], works in the context of the ADS-CFT correspondence [165], to t'Hooft's [166] and Susskind's ideas on complementarity [167].

We will not be taking any further interest in this approach. The reason is that we do not share the interpretation of thermodynamic entropy proposed by the central dogma. There is no clear argument that all the d.o.f. of a black hole is encoded on its horizon. There is, however, a simple argument to the contrary. The latter is a direct consequence of the generalized second law. Let us consider a Schwarzschild black hole on which evolves any matter field described by a density matrix ρ (see figure 12). We note A_a and $\rho_a^{\rm out}$ (respectively A_b and $\rho_b^{\rm out}$) the area of the black hole at the Cauchy surface a (respectively at the Cauchy surface b) and the density matrix on the sub region of a (respectively on the sub region of b) outside the black hole. Then the following inequality applies

$$\frac{A_a}{4} + S_{\rm VN}(\rho_a^{\rm out}) < \frac{A_b}{4} + S_{\rm VN}(\rho_b^{\rm out}). \tag{6.14}$$

This is the generalized second law. Moreover, if we consider that the state is pure on a, it will also be pure on b, and thus $S_{\rm VN}(\rho_a^{\rm in}) = S_{\rm VN}(\rho_a^{\rm out})$ and $S_{\rm VN}(\rho_b^{\rm in}) = S_{\rm VN}(\rho_b^{\rm out})$ with $\rho_a^{\rm in}$ (respectively $\rho_b^{\rm in}$) the density matrix of the subsystem of a (respectively of b) inside the black hole. The generalized second law thus naturally becomes

$$\frac{A_a}{4} + S_{\rm VN}(\rho_a^{in}) < \frac{A_b}{4} + S_{\rm VN}(\rho_b^{in}). \tag{6.15}$$

This inequality clearly shows that it is not the area of the black hole that is increasing, but that the entropy of the matter field inside it must also be taken into account. The area therefore does not

correspond to the entropy associated with the horizon and what is inside a black hole (it is possible to generalize this argument to the case where the matter field on a and b is in a mixed state by using the sub additivity of the Von Neumann entropy).

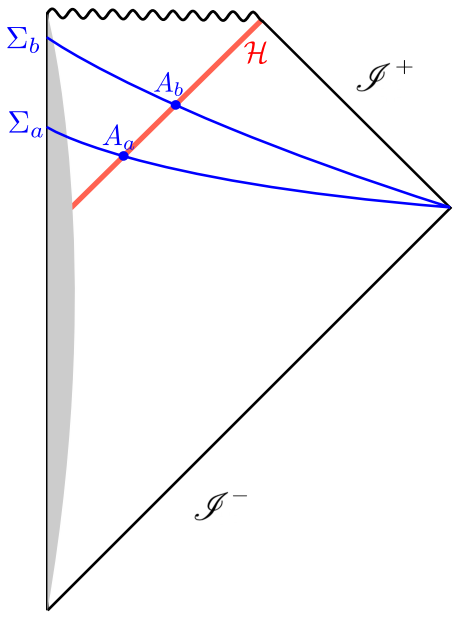


Figure 12: Penrose diagram of a black hole with some matter fields illustrating the generalized second law.

Another criticism of this holographic approach stems from the fact that any convincing resolution must in our view involve the strong quantum gravity regime since this is where the ingoing modes purifying the Hawking radiation end up. Perhaps with the exception of the fuzzball scenario [168], holographic approaches frequently dismiss the question of the quantum dynamics near the singularity as if it were a non-existent matter [169–171].

6.2.2 Remnant scenarios

We will now present a class of scenario which take into account the criticisms made in the previous subsection. Namely that the internal d.o.f of a black hole, and more precisely the ingoing modes of (6.10), are not encoded on the horizon. It is crucial to dynamically depict there fate as they evolve towards the strong Planckian regime near the singularity since they are the carriers of the information that preserve unitarity (according to (6.10)).

An interesting possibility arises if we remember that Hawking, Wald and Parker's computations cease to be valid for a black hole reaching a planckian size. There is therefore no reason to believe that such a black hole would continue to radiate. It is conceivable that what is left contains all the information contained in the ingoing modes, and therefore all the information needed to purify Hawking's radiation. One major concern about this 'remnant scenario' which has been rapidly raised is that the existence of such particle-like entities with high entropy, which would give rise to significant pair production amplitudes for these exotic objects which would impact quantum

processes at low energies (see [172] and references therein). The perceived issue stems from the assumption that remnants can be effectively described in the framework of effective field theory, a premise that becomes highly questionable when considering the extremely vast internal universes that lie beyond the horizons of old black holes from a general relativity perspective [173]. However, this scenario does not explain what happened to the ingoing modes and the information they carry. It simply states that the information is contained in this remnant, but provides no insight into how this information is stored.

Another proposal, known as Wheeler's bag-of-gold [174], is closely related to the previous one and has the advantage of proposing a scenario for what happens to the information contained in the remnant. Here the remnant is presumed to harbor the purifying d.o.f within a vast internal 'universe.' These d.o.f would gradually escape into the nearly flat external spacetime as extremely low-energy particles after the black hole has completed its evaporation. However, there are significant challenges associated with this proposal. If a black hole begins with a macroscopic mass M and undergoes evaporation through standard Hawking radiation, following semiclassical expectations until its mass nears the Planck mass m_p, energy conservation dictates that the individual components of the purifying radiation emitted by the remnant possess energies smaller than m_p^3/M^2 for a remnant of Planckian dimensions. At the superficial level it is already difficult to conceive how such long-wavelength particles could be emitted from an object that appears Planckian from an external perspective. At a deeper level, and despite some recent interest [175] in the context of loop quantum gravity, simple entropic considerations make such a proposal highly improbable within a theory that incorporates fundamental discreteness. Specifically, as mentioned before (and illustrated in Figure 14), the Hawking partners that were initially correlated with the Hawking radiation are forced to hit the strong Planckian regime near the singularity residing within and thus interact with a new enormous number of planckian d.o.f: the atomistic structure of spacetime in such a theory. From an entropic standpoint, this would necessitate an exceedingly delicate conspiracy for these excitations to reorganize into extraordinarily long-wavelength particles within quantum field theory as they emerge from the remnant (for further discussion, see [50]).

6.2.3 Other scenarios

The literature explores several additional possibilities worth considering. One such possibility is that the internal universe of the remnant remains causally disconnected from the external universe where black hole evaporation occurs, without any leakage of particles (cf for example [176] and references therein). This scenario would effectively break unitarity for the outside world. Another possibility is that when gravity is incorporated, quantum mechanics may require modifications wherein unitarity ceases to be a fundamental law (as discussed in Surdarsky's perspective in [50] and related references). Furthermore, it is conceivable that certain aspects of the semiclassical language employed to describe the problem are inadequate, and the final state of evaporation may preclude a meaningful mean field spacetime representation (as highlighted in [158, 177] and more recently in [178–181]). In such cases, the non-local nature of quantum mechanics and gravity could blur the distinction between the inside and outside regions [182]. Presently, there are no substantial objections to these possibilities. To ensure clarity in presenting our specific proposal, we have chosen to relegate the discussion of these aspects to a secondary role, with the hope that readers can obtain

a more comprehensive understanding from the contributions of other authors in this special issue.

6.2.4 A resolution based on the presence of planckian d.o.f

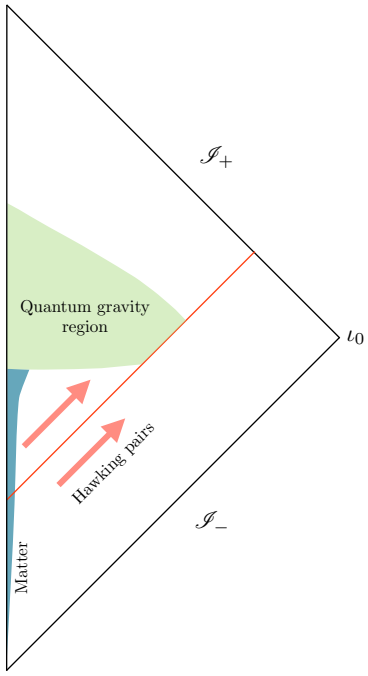


Figure 13: The Ashtekar-Bojowald paradigm: the inside singularity is replaced by a quantum gravity region where no semiclassical or spacetime description is possible. Geometric observables (as well as matter d.o.f) cannot not be represented in terms of smooth field theoretic notions. Evolution across this region is expected to be well defined in the fundamental theory into a future where geometry and matter fields a well described (in a mean field sense) by a nearly flat spacetime geometry in vacuum.

The perspective we are about to discuss offers a straightforward and intuitive resolution of the paradox. It aligns with other well established descriptions of standard physical systems (like standard matter in statistical mechanics, or even in the context of analogue gravity [183]) in which information is degraded, yet not lost, due to the presence of planckian d.o.f [148]. It is a conservative resolution of the problem, in contrast with the non conservative approaches discussed in subsection 6.2.1. It is however in sharp contrast with the standard remnant scenario mentioned in subsection 6.2.2, as the planckian d.o.f purifying the Hawking radiation are not necessarily localized within a particle-like object. Indeed one of the main lesson of EFT was that the description of spacetime in terms of metric will not hold at the Planck scale. The geometry in and around a planckian remnant is therefore not correctly described by a metric. Instead, more fundamental d.o.f will characterize the geometry of this planckian curvature region, and nothing force them to be localized inside the remnant and can eventually leaks out the quantum gravity region. In this way our proposal avoids the objections raised against standard remnants mainly because we are explicitly claiming that an EFT description is not appropriate.

This possibility is based on the assumption that there is a quantum evolution across the singularity (in the context of loop quantum gravity the paradigm was first put forward in [184] and

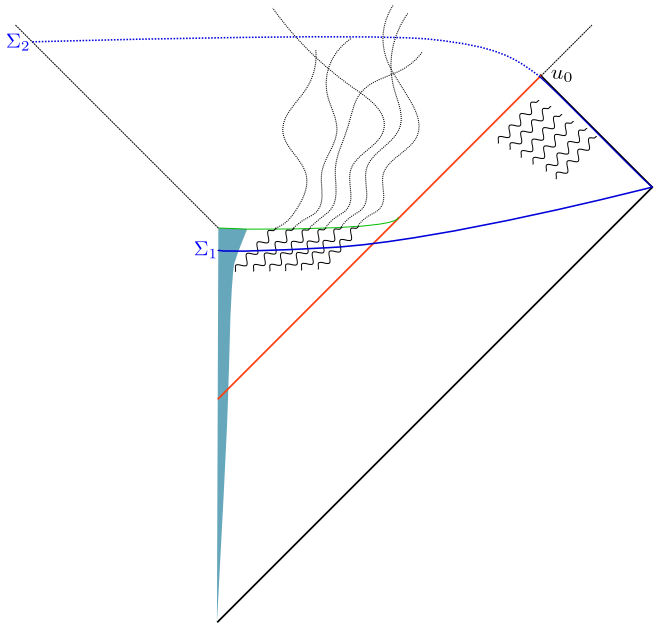


Figure 14: Inside Hawking partners (initially maximally correlated with the Hawking radiation emitted to $\mathscr{I}^+$) fall into the quantum gravity region where they are dynamically forced to interact with the planckian d.o.f of the geometry. Near the singularity matter excitations are infinitely blue shifted into the Planckian regime. Such interactions transfer the entanglement from the initial field theoretic d.o.f in the Hawking partner to defects at the Planck scale. Defects emerge in the future of the quantum gravity region and their entanglement with the Hawking radiation purifies the final state. As the defects do not weight (the mean field flat geometry is degenerate) the process is compatible with energy conservation.

.

includes more recent black to white hole transition models [185]). The physical situation representing black hole formation and evaporation, of what we call the Ashtekar-Bojowald paradigm, is illustrated by the Penrose diagram shown in Figure 13 where the singularity is replaced by a region where no spacetime description is possible and a full quantum gravity treatment becomes mandatory. However, this representation assumes the possibility of a metric description of the geometry in the region of planckian curvature, as well as after the black hole has finished evaporating. We propose here an alternative that avoids making such an assumption. We know that the ingoing radiation will travel towards the center of the black hole until it reaches a region of Planckian curvature. As mentioned above, other Planckian d.o.f. will intervene and interact with this ingoing radiation. To describe this interaction precisely, and what will result from it, we need a non perturbative theory of quantum gravity. Since we do not have such a theory, we will simply say that what is in the future light cone of the Planckian curvature region cannot be precisely described, and cannot a priori be described in terms of a metric. It is therefore not possible to associate a Penrose diagram with this region. A pictorial representation of the scenario for purification that we propose is given in figure 14. Entanglement between the Hawking radiation going to infinity at $\mathscr{I}^+$ and inside partners maintain unitarity in the semiclassical quantum field theory description that is expected to be valid while the black hole is macroscopic. In our illustration we assume this is so around the instant defined by the Cauchy surface Σ_1. Inside partners (wavy lines on the left

of the horizon) fall into the quantum gravity region and transfer their entanglement to defect-like Planckian d.o.f that cannot be described in an effective field theory framework. These defects are represented by dotted lines in the quantum gravity region. The evolution between Σ_1 and Σ_2 in the full quantum gravity theory should includes the Planckian d.o.f and is thus unitary. In contrast with fuzzballs, the amount of information that can be coded in these defects grows with the number of defects involved—which can be arbitrary depending on the internal extension of the black hole, e.g., one per Planck volume—and hence is by no means bounded by the area of the corresponding horizon. Information would seem to be lost in any effective description that neglects such Planckian defects. We shall see in chapter 7 how this mechanism for transferring information contained in ingoing modes to planckian geometric d.o.f. can be illustrated using the symmetry reduced model presented in chapter 5. Although this model will not describe what happens at the end of a black hole's life, we will see how it suggests that at the end of evaporation, the Hawking radiation which is in a mixed state, is in fact entangled and therefore purified by the Planckian geometric d.o.f present in the dotted part of Σ_2.

Now, for the scenario to be consistent with energy conservation, the Bondi mass of the system for retarded times after u_0 (retarded time of complete semiclassical evaporation) must be close to zero or about the Planck mass. This is possible if the subsystem corresponding to the dotted part of Σ_2 is degenerate, i.e, is described as a superposition of many inequivalent configurations at the Planck scale having zero or planckian energy[19]. This means that the d.o.f. present on the dotted part of Σ_2 must contain a large amount of information to purify Hawking radiation, but cannot contain energy. To sum up, in this scenario a field containing M energy is pure on $\mathscr{I}^-$, and at the end of the evaporation process, Hawking radiation contains all the energy (with the possible exception of a Planckian mass remnant) but is no longer in a pure state. Part of the system containing all the energy has therefore decohered, but without dissipation. The possibility of such an evolution in quantum mechanics has been the subject of several debates in the literature. In chapter 8, we propose a QFT model where such an evolution is possible. In our model, this is notably made possible by the presence of a bath with a degenerate vacuum and is therefore in this sense analogous to the d.o.f present on the dotted part of Σ_2.

For a more detailed presentation of this viewpoint, which will be defended in the remainder of this thesis, the reader is referred to the following bibliography : [50, 149, 151]. The aim here is not to repeat what has already been said in these articles, but to present new results illustrating the paradigm previously described.

[19]This is a feature expected to be present in certain approaches to quantum gravity. In the case of LQG such property is precisely the one that explains the origin of black hole entropy in the semiclassical regime [186–189] (for reviews see [150, 151] for more discussion of this specific feature see [50])

7 The fate of the information in a symmetry reduced model

A fundamental description of the previous mechanism remains out of reach at the present time. However, it is possible to make the scenario presented in subsection 6.2.4 concrete in simplified models. The aim of this chapter is to show how the symmetry reduced model presented in chapter 5 can be used to achieve this. We recall that the model is base on the fact that the interior region $r < 2M$ of a Schwarzschild black hole of mass M can be seen as a homogeneous anisotropic cosmological model where the r=constant surfaces (in the usual Schwarzschild coordinates) are Cauchy surfaces of homogeneity. We showed that such Kantowski-Sachs models (with a massless scalar field coupling) define a natural toy model capturing aspects of the dynamics and backreaction of matter near the singularity of black holes that Hawking radiate. The model was quantized *á la loop* and it was shown that certain planckian d.o.f (not relevant for coarse observers) arise as a consequence of peculiar representation of the algebra of observables used. Such, at first appearance exotic, representation is indeed the natural one when it comes to the construction of the background independent quantization of gravity in loop quantum gravity [190]. The presence of planckian d.o.f that remain hidden at low energies is an expected generic feature in the full quantum gravity regime [20].

The existence of such a hidden sector (which represents a sort of quantum hair) is central in the scenario for purification of the Hawking radiation in black hole evaporation proposed in subsection 6.2.4. In the present chapter we will use this simple black hole model to illustrate some key ingredients of the general scenario. Namely, we will show how quantum correlations between matter excitations and such planckian d.o.f develop unavoidably during dynamical evolution. This suggests that the planckian physics does play an important role in discussions about the fate of unitarity in black hole formation and evaporation, and that any effective field theory approach to the unitarity question that avoids confronting the details of the dynamics near the singularity misses a central aspect. And thus cannot provide a complete picture of the resolution of the puzzle.

The chapter is organized as follows. In Section 7.1 we use the simplified setup to construct a minimalistic model of the dynamics of a Hawking pair on our simplifies black hole setup. The back reaction of the ingoing partner is suitably taken into account as it approaches the strong field regime near the singularity where the coupling between geometry and matter becomes most important. The outside partner dynamics is assumed to be trivial (idealizing the weak back reaction for wave packets evolving toward infinity; completely neglected in the framework of the Hawking effect) and the full dynamics is unitary. In Section 7.3 we present how the correlations between the different subsystem change with the dynamics, in a way allowing to support our claims.

[20] Even when the continuum limit remains an open issue in the framework of loop quantum gravity, there are various potential sources of planckian degeneracy in the structure of the theory. For instance, consistent regularizations of the Hamiltonian constraint all seem to share the property of being insensitive to certain planckian details of the quantum states that could code information. These defect-like structures are related to the fundamental degeneracy of the quantum geometry at the Planck scale. There are studies showing that in the emergent low energy regime some d.o.f would decouple as they would appear as highly massive [191–193].

7.1 Model of a Hawking pair on our quantum geometry

Outgoing Hawking excitations detected in normalizable wave packets at future null infinity are expected to evolve unitarily—independently of the inside d.o.f—when they become sufficiently separated from the black hole. These excitations are however entangled with the ingoing partner. The backreaction of the inside partner on the quantum geometry is expected to be strong as the particle falls toward the singularity. Instead, the back reaction of the outside partner is expected to be weak as the evolution happens in the weak gravitational field region (the back reaction is completely neglected in the original Hawking computation for these reasons). The setup we introduce in this section incorporates a simplified version for the backreaction for the inside partner (based on the model of chapter 5). The dynamical evolution for the outside partner is simplified by assuming it to be trivial: the outside Hamiltonian vanishes. The key feature is however the entanglement in the initial state and the transfer of information to the planckian structure of the quantum geometry which will be shown in Section 7.3.

7.1.1 Construction of the initial state

In order to simplify as much as we can the description of the matter part, we will consider that the *inside* matter can be in two different orthogonal states $|+\rangle$ or $|-\rangle \in \mathscr{H}_{in}$ (with subscript *in* standing for the *inside* Hilbert space of the scalar d.o.f) which are eigenvector of $\hat{\mathrm{p}}_\phi$ of eigenvalue p_+ and p_- respectively. On the other hand, we will consider that the outgoing part of the matter can be in two different orthogonal states $|+\rangle$ or $|-\rangle \in \mathscr{H}_{out}$ (with subscript *out* standing for the *outside* Hilbert space of the scalar d.o.f). As the outside outgoing partner evolves in regions of low curvature where the type of effects we are focusing on should be very small, we model such evolution by a trivial Hamiltonian. This simple description of the matter is sufficient to write down a state for the total matter where the ingoing particle and the outgoing one are initially maximally entangled, and to study how the dynamic modifies these correlations. We can now write down the total Hilbert space describing the geometrical and the matter d.o.f. It can be written as

$$\mathscr{H}_{total} = \underbrace{\mathscr{H}_m \otimes \mathscr{H}_\epsilon}_{\text{geometry}} \otimes \overbrace{\mathscr{H}_{in} \otimes \mathscr{H}_{out}}^{\text{matter}} , \tag{7.1}$$

where we have organized the Hilbert space of geometry as the tensor product of normalizable functions $\mathscr{H}_m$ of the configuration variable m, defined in (5.30), on a given lattice times the separable truncation $\mathscr{H}_\epsilon = \mathbb{C}^{n_\epsilon}$ of the epsilon sector where we assume that a finite number n_ϵ of lattices $\Gamma_{\epsilon,\lambda}$—introduced in (5.56)—are allowed. Concretely, and for simplicity, we will take $n_\epsilon = 2$ with two alternative values $\epsilon_\pm$. With such simple choices we have that $\mathscr{H}_\epsilon = \mathscr{H}_{in} = \mathscr{H}_{out} = \mathbb{C}^2$, i.e., with the exception of $\mathscr{H}_m$ that is infinite dimensional, the other quantum numbers have been truncated to standard q-bits. Thus, a basis of this Hilbert space is defined by the set of vectors $|m, \varepsilon, i, o\rangle$ with $m \in \mathbb{R}^+$, ε (encoding the planckian ϵ sectors), i (encoding the *inside* particle state) and o (encoding the *outside* state) spin-like quantum numbers taking values $\pm$. The inner product between basis states is

$$\langle m_1, \varepsilon_1, i_1, o_1 | m_2, \varepsilon_2, i_2, o_2 \rangle = \delta(m_1 - m_2)\delta_{\varepsilon_1,\varepsilon_2}\delta_{i_1,i_2}\delta_{o_1,o_2} \ . \tag{7.2}$$

After having defined the truncation of the Hilbert space we introduce the initial state representing a toy version of the in-vacuum in the context of Hawking radiation, namely

$$|\psi_0\rangle = \sum_{\substack{i=\pm\\ \varepsilon=\pm}} \int dm\ \psi_0(m, a_0+\epsilon_\varepsilon)|m,\varepsilon,i,i\rangle, \tag{7.3}$$

and the normalization condition $\langle\psi_0|\psi_0\rangle = 1$ implying

$$\int dm\ |\psi_0(m, a_0+\epsilon_\varepsilon)|^2 = \frac{1}{4}\ . \tag{7.4}$$

The key feature of the initial state is that it represents a state where the excitations in $\mathscr{H}_{in}$ and $\mathscr{H}_{out}$ are maximally correlated as in the standard in-vacuum. We can then apply the evolution law (5.60) to this state, a shift by $n\lambda$ is given by

$$|\psi\rangle = \sum_{\substack{i=\pm\\ \varepsilon=\pm}} \int dm\ e^{\frac{i}{2}\log\left(1+\frac{n\lambda}{a_0+\epsilon_\varepsilon}\right)\left(m+\frac{\mathrm{p}_i^2}{16\pi\ell_p^2 m}\right)}\psi_0(m, a_0+\epsilon_\varepsilon)|m,\epsilon_\varepsilon,i,i\rangle \tag{7.5}$$

$$= \sum_{\substack{i=\pm\\ \varepsilon=\pm}} \int dm\ C(m,\epsilon_\varepsilon,i,n)\ |m,\epsilon_\varepsilon,i,i\rangle\ , \tag{7.6}$$

where, in order to simplify the notation, we introduced

$$C(m,\epsilon_\varepsilon,i,n) = e^{\frac{i}{2}\log\left(1+\frac{n\lambda}{a_0+\epsilon_\varepsilon}\right)\left(m+\frac{\mathrm{p}_i^2}{16\pi\ell_p^2 m}\right)}\psi_0(m, a_0+\epsilon_\varepsilon)\ . \tag{7.7}$$

The previous is the quantum gravitational dynamics of the initial state (of maximally correlated Hawking partners). This dynamics encodes the back reaction of the Hawking particles with the quantum geometry exactly (in the sense of our simplified model). It only remains to study the dynamical evolution of the entanglement between the relevant d.o.f as the *inside* partner evolves toward the strong quantum gravity regime (the singularity) inside of the black hole.

7.2 The subsystems of interest and their reduced density matrices

We now have access to the density matrix of the system $\rho = |\psi\rangle\langle\psi|$ which is a pure state at any area a-time (by the unitarity of the quantum evolution 5.60). Its expression is given by

$$\rho = \sum_{\substack{i,j=\pm\\ \varepsilon,\varepsilon'=\pm}} \int dm dm'\ C(m,\epsilon_\varepsilon,i,n)\overline{C(m',\epsilon_{\varepsilon'},j,n)}|m,\epsilon_\varepsilon,i,i\rangle\langle m',\epsilon_{\varepsilon'},j,j|. \tag{7.8}$$

We determine now the reduced density matrices of the relevant subsystems. We will start by writing the density matrix of the subsystem $\mathscr{H}_\epsilon \otimes \mathscr{H}_{in}$ obtained from tracing out the $\mathscr{H}_m$ and $\mathscr{H}_{out}$. One can show that

$$\rho^{\epsilon,\text{in}} = \begin{pmatrix} 1/4 & 0 & D(\epsilon_1,\epsilon_2,+,+,n) & 0 \\ 0 & 1/4 & 0 & D(\epsilon_1,\epsilon_2,-,-,n) \\ \overline{D(\epsilon_1,\epsilon_2,+,+,n)} & 0 & 1/4 & 0 \\ 0 & \overline{D(\epsilon_1,\epsilon_2,-,-,n)} & 0 & 1/4 \end{pmatrix}\ , \tag{7.9}$$

where

$$D(\epsilon_\varepsilon, \epsilon_{\varepsilon'}, i, j; n) \equiv \int dm\ C(m, \epsilon_\varepsilon, i, n)\overline{C(m, \epsilon_{\varepsilon'}, j, n)}, \tag{7.10}$$

Tracing further over $\mathscr{H}_{in}$ we get the reduced density matrix of the subsystem $\mathscr{H}_\epsilon$

$$\rho^\epsilon = \begin{pmatrix} \dfrac{1/2}{D(\epsilon_1, \epsilon_2, +, +, n) + \overline{D(\epsilon_1, \epsilon_2, -, -, n)}} & D(\epsilon_1, \epsilon_2, +, +, n) + D(\epsilon_1, \epsilon_2, -, -, n) \\ & 1/2 \end{pmatrix}, \tag{7.11}$$

while tracing over $\mathscr{H}_\epsilon$ we obtain the reduced density matrix of the subsystem $\mathscr{H}_{in}$

$$\rho^{\text{in}} = \begin{pmatrix} 1/2 & 0 \\ 0 & 1/2 \end{pmatrix}. \tag{7.12}$$

One can notice that this last density matrix does not depend on time, which means that the entanglement entropy of this subsystem is constant. More generally, the results (7.9), (7.11) and (7.12) will be used in the next section to study the correlations between the two subsystems $\mathscr{H}_\epsilon$ and $\mathscr{H}_{in}$. But we are also interested by the evolution of the correlations between the subsystems $\mathscr{H}_{in}$ and $\mathscr{H}_{out}$. Consequently, we need the reduced density matrix associated to the subsystem $\mathscr{H}_{in} \otimes \mathscr{H}_{out}$. It follows that

$$\rho^{\text{in,out}} = \begin{pmatrix} 1/2 & 0 & 0 & D(\epsilon_1, \epsilon_1, -, +, n) + D(\epsilon_2, \epsilon_2, -, +, n) \\ 0 & 0 & 0 & 0 \\ 0 & 0 & 0 & 0 \\ \overline{D(\epsilon_1, \epsilon_1, -, +, n) + D(\epsilon_2, \epsilon_2, -, +, n)} & 0 & 0 & 1/2 \end{pmatrix}. \tag{7.13}$$

Finally, the last ingredient that one will need is the matrix density of the subsystem $\mathscr{H}_{out}$ given by

$$\rho^{\text{out}} = \begin{pmatrix} 1/2 & 0 \\ 0 & 1/2 \end{pmatrix}. \tag{7.14}$$

7.2.1 Computation of the interference terms

From the previous section, we have a complete knowledge for any a of the total system, cf (7.8), and also of the relevant subsystems $\mathscr{H}_{in}$ (matter inside), $\mathscr{H}_{out}$ (matter outside), $\mathscr{H}_\epsilon$ (quantum hair), $\mathscr{H}_{in} \otimes \mathscr{H}_\epsilon$, and $\mathscr{H}_{in} \otimes \mathscr{H}_{out}$ respectively given by (7.12), (7.14), (7.11), (7.9) and (7.13). We now want to study the entanglement of these subsystems with their environment which is encoded in the non diagonal terms of the different density matrices characterized by the complex function $D(\epsilon, \epsilon', i, j; n)$ appearing in (7.9), (7.11) and (7.13). In order to evaluate $D(\epsilon, \epsilon', i, j; n)$, we need to choose the form of initial wave function $\psi_0(m, a_0, \mathrm{p}_i)$ of the quantum geometry in (7.3). We take the following semiclassical state

$$\psi_0(m, a_0 + \epsilon_\varepsilon) = \frac{1}{2\sqrt{\sigma\sqrt{\pi}}} e^{-\frac{(m-m_0)^2}{2\sigma^2}}, \tag{7.15}$$

normalized according to (7.4), and centered at $m = m_0$ (with a spread 2σ) and $\mathrm{p}_m = 0$. Moreover, we assume that $m_0 \gg \sigma$. According to (5.81)—giving initial conditions at $a = 100\lambda\ell_p^2$ (an arbitrary

choice of initial time)—such state corresponds to a semiclassical state of the spacetime geometry corresponding to a Schwarzschild black hole of mass

$$M = \frac{\sqrt{4\pi}\ell_p^3 m_0^2}{5\ell_0^2\sqrt{\lambda}}. \tag{7.16}$$

The relevant amplitude $D(\epsilon, \epsilon', i, j)$ becomes

$$D(\epsilon_\varepsilon, \epsilon_{\varepsilon'}, i, j; n) = \frac{1}{4\sigma\sqrt{\pi}} \int_{-\infty}^{+\infty} dm\ e^{-\frac{(m-m_0)^2}{\sigma^2} + \frac{i}{2}\log\left(1+\frac{n\lambda}{a_0+\epsilon_\varepsilon}\right)\left(m+\frac{\mathrm{p}_i^2}{16\pi\ell_p^2 m}\right) - \frac{i}{2}\log\left(1+\frac{n\lambda}{a_0+\epsilon_{\varepsilon'}}\right)\left(m+\frac{\mathrm{p}_j^2}{16\pi\ell_p^2 m}\right)}. \tag{7.17}$$

In order to compute the previous integral we first change variables to $k = m - m_0$, with $k \in [-\infty, +\infty]$ and approximate the integral using the stationary phase method (Gaussian integrals). The result is

$$\begin{aligned} D(\epsilon_\varepsilon, \epsilon_{\varepsilon'}, i, j; n) \approx & \frac{e^{\frac{1}{2}i\left(\frac{\mathrm{p}_i^2}{16\pi\ell_p^2 m_0}+m_0\right)\log\left(\frac{a_0+\lambda n+\epsilon_\varepsilon}{a_0+\epsilon_\varepsilon}\right) - \frac{1}{2}i\left(\frac{\mathrm{p}_j^2}{16\pi\ell_p^2 m_0}+m_0\right)\log\left(1+\frac{n\lambda}{a_0+\epsilon_{\varepsilon'}}\right)}}{4\sigma\sqrt{\pi}} \\ & \times \int_{-\infty}^{+\infty} e^{k^2\left(\frac{i\mathrm{p}_i^2\log\left(1+\frac{n\lambda}{a_0+\epsilon_\varepsilon}\right)}{32\pi\ell_p^2 m_0^3} - \frac{i\mathrm{p}_j^2\log\left(1+\frac{n\lambda}{a_0+\epsilon_{\varepsilon'}}\right)}{32\pi\ell_p^2 m_0^3} - \frac{1}{\sigma^2}\right)} \\ & \times e^{k\left(\frac{1}{2}i\left(1-\frac{\mathrm{p}_i^2}{16\pi\ell_p^2 m_0^2}\right)\log\left(1+\frac{n\lambda}{a_0+\epsilon_\varepsilon}\right) - \frac{1}{2}i\left(1-\frac{\mathrm{p}_j^2}{16\pi\ell_p^2 m_0^2}\right)\log\left(\frac{a_0+\lambda n+\epsilon_{\varepsilon'}}{a_0+\epsilon_{\varepsilon'}}\right)\right)} dk. \end{aligned} \tag{7.18}$$

This integral is analytically computable and is equal to

$$\begin{aligned} D(\epsilon_\varepsilon, \epsilon_{\varepsilon'}, i, j; n) \approx & \frac{1}{\sigma\sqrt{-\frac{i\mathrm{p}_i^2\log\left(1+\frac{n\lambda}{a_0+\epsilon_\varepsilon}\right)}{\ell_p^2 m_0^3} + \frac{i\mathrm{p}_j^2\log\left(1+\frac{n\lambda}{a_0+\epsilon_{\varepsilon'}}\right)}{\ell_p^2 m_0^3} + \frac{32\pi}{\sigma^2}}} \\ & \times \exp\left(-\frac{\sigma^2\left(\left(\mathrm{p}_i^2 - 16\pi\ell_p^2 m_0^2\right)\log\left(1+\frac{n\lambda}{a_0+\epsilon_\varepsilon}\right) - \left(\mathrm{p}_j^2 - 16\pi\ell_p^2 m_0^2\right)\log\left(1+\frac{n\lambda}{a_0+\epsilon_{\varepsilon'}}\right)\right)^2}{128\pi\ell_p^2 m_0\left(-i\mathrm{p}_i^2\sigma^2\log\left(1+\frac{n\lambda}{a_0+\epsilon_\varepsilon}\right) + i\mathrm{p}_j^2\sigma^2\log\left(1+\frac{n\lambda}{a_0+\epsilon_{\varepsilon'}}\right) + 32\pi\ell_p^2 m_0^3\right)}\right) \\ & \times \sqrt{2\pi}\left(1+\frac{\lambda n}{a_0+\epsilon_\varepsilon}\right)^{\frac{1}{2}i\left(\frac{\mathrm{p}_i^2}{16\pi\ell_p^2 m_0}+m_0\right)}\left(1+\frac{\lambda n}{a_0+\epsilon_{\varepsilon'}}\right)^{-\frac{1}{2}i\left(\frac{\mathrm{p}_j^2}{16\pi\ell_p^2 m_0}+m_0\right)}. \end{aligned} \tag{7.19}$$

7.3 Evolution of the entanglement and correlations between the different subsystems

We have all we need to analyze the evolution of entanglement between the relevant d.o.f as the system evolves toward the singularity at $a = 0$. The question that remains is what measure of entanglement we use for interpretation. Here there are several alternatives which all encode the same physics in different terms. The simplest (yet to some extend basis dependent method) is the use of the so-called decoherence function. Mutual information is basis independent and provides a more clear ground for interpretation and will be defined in Section 7.3.2.

7.3.1 Decoherence function

It is often said that the entanglement of a system with its environment tend to kill the off diagonal terms of its density matrix. The consequence is that a system initially pure becomes mixed due to this interaction. It is possible to make a more precise statement thanks to the decoherence functions. Let us consider a general subsystem $\rho(t)$ written in a basis that we will note $\{|n\rangle\}_{n\in\mathbb{N}}$. This subsystem is initially pure and interacts with its environment. The decoherence functions will be noted $\Gamma_{nm}(t)$ and are define in the following way

$$|\langle n|\rho(t)|m\rangle| = \exp(\Gamma_{nm}(t)). \tag{7.20}$$

These functions describe the time evolution of the off diagonal terms of the density matrix and therefore encode the evolution of a subsystem from a pure state to a mixed one. For a system of dimension N there are $N(N-1)/2$ independent off diagonal terms in the density matrix, and as many decoherence functions. One can notice that these functions depend on the basis we chose to write the density matrix. There is however a natural basis, the 'energy basis', in which the diagonal terms are time independent . We will work in this basis here. We are interested first in the evolution of the purity of the ϵ subsystem (i.e. the Planckian geometrical d.o.f). One can see that it is easy to obtain the decoherence function for this subsystem, which is unique, from the expression (7.11)

$$\Gamma(n\lambda) = |D(\epsilon_1, \epsilon_1, -, +, n) + D(\epsilon_2, \epsilon_2, -, +, n)|. \tag{7.21}$$

One can now plot the evolution of this function in terms of the time variable $n\lambda$ in order to illustrate how the purity of the subsystem ϵ evolves, and how this evolution depends of the different parameter of the system m_0, p_+, σ (cf Fig 15).

7.3.2 Mutual information as an entanglement measure

The previous was a quick illustration about how the planckian d.o.f ϵ get entangles during the dynamical evolution and hence cannot be neglected in discussions of unitarity. However, the method used is not adapted for a clear interpretation due to its intrinsic basis dependent nature. Here we interpret the dynamical evolution of entanglement using a basis independent measure of entanglement: the mutual information. We first briefly remind the reader of a few definitions and then apply them to our system. The first ingredient we need is the notion of relative entropy. Relative entropy is a entanglement measure defined between two states described by the density matrix ρ and σ in the following way

$$S(\rho|\sigma) := \mathrm{Tr}(\rho\log\rho - \rho\log\sigma). \tag{7.22}$$

One can show that $S(\rho|\sigma) \geq 0$ and it is equal to zero when $\rho = \sigma$. It quantifies the distinguishability of ρ from σ. An important property of the relative entropy is that for any bounded operator $\hat{O}$, the relative entropy satisfies

$$\frac{\Big(\mathrm{Tr}(\hat{O}\rho) - \mathrm{Tr}(\hat{O}\sigma)\Big)^2}{||\hat{O}||} \leq S(\rho|\sigma), \tag{7.23}$$

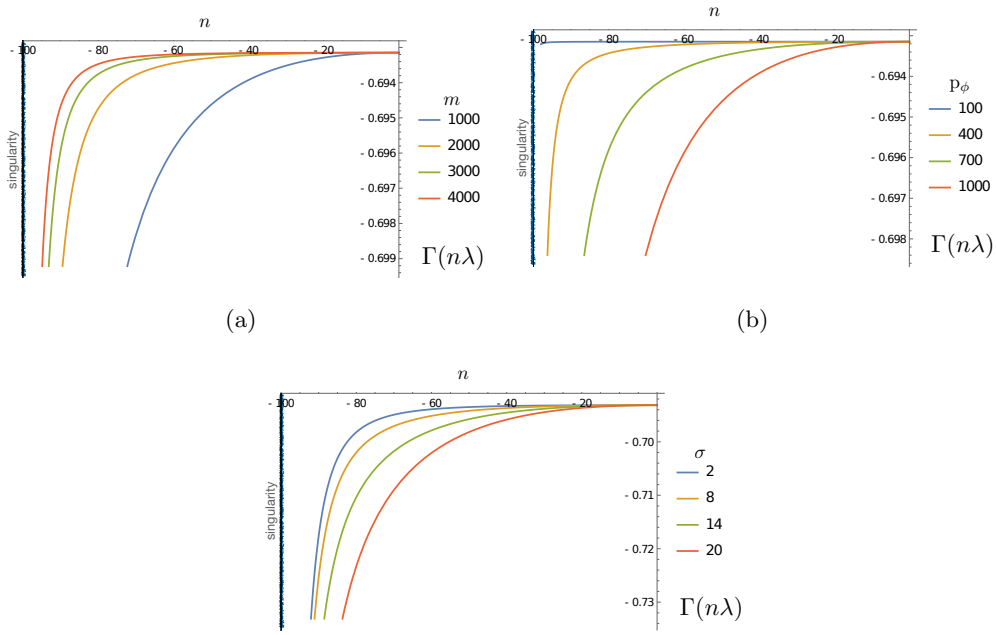


Figure 15: (a) Plot of Γ in terms of n evolution steps for $\sigma = 10$, $p_+ = 1000$ and for different values of m_0. (b) Plot of Γ in terms of n evolution steps for $m_0 = 1000$, $\sigma = 10$ and for different values of p_+. (c) Plot of Γ for $m_0 = 1000$, $p_+ = 1000$ and for different values of σ. The singularity correspond to the value $n\lambda = -100$ and is indicated by a black vertical line.

with $||\hat{O}|| = \sup\sqrt{\langle\psi|\,\hat{O}\,|\psi\rangle/\langle\psi|\,|\psi\rangle}$. The mutual information is a specific case of the relative entropy. Let us consider a system which can be decomposed into three subsystem A, B and C. We assume that the total system is in a pure state $|\psi\rangle$, the subsystem $A+B$ is described by the density matrix ρ_{AB} and the two subsystem A and B are respectively described by the density matrix ρ_A and ρ_B. The mutual information (between A and B when C is traced out) is given by

$$I_{AB|C} := S(\rho_{AB}|\rho_A \otimes \rho_B). \tag{7.24}$$

The mutual information is therefore also an entanglement measure and quantifies how much a mixed states is distinguishable from the uncorrelated state that we can get by treating the different subsystems as independent. By using (7.22), one can show that

$$I_{AB|C} = S_A + S_B - S_{AB}, \tag{7.25}$$

where S is the usual Von Neumann entropy. An important property of the mutual information comes from (7.23), which, in the case $\rho = \rho_{AB}$ and $\sigma = \rho_A \otimes \rho_B$ gives, for all $\hat{O} = \hat{O}_A \otimes \hat{O}_B$ such that $\hat{O}_A$ and $\hat{O}_B$ are bounded, the following relation

$$\frac{\left(\langle\psi|\,\hat{O}_A\hat{O}_B\,|\psi\rangle - \langle\psi|\,\hat{O}_A\,|\psi\rangle\,\langle\psi|\,\hat{O}_B\,|\psi\rangle\right)^2}{2||\hat{O}_A||||\hat{O}_B||} \leq I_{AB|C}(|\psi\rangle). \tag{7.26}$$

This relation means that the mutual information is an upper bound of the correlations between the subsystems A and B. Thus, we will use this entanglement measure to track the correlations

between the different subsystems in our model because it has a clear physical meaning in terms of entanglement and correlations.

Evolution of the correlations between the Hawking partners:

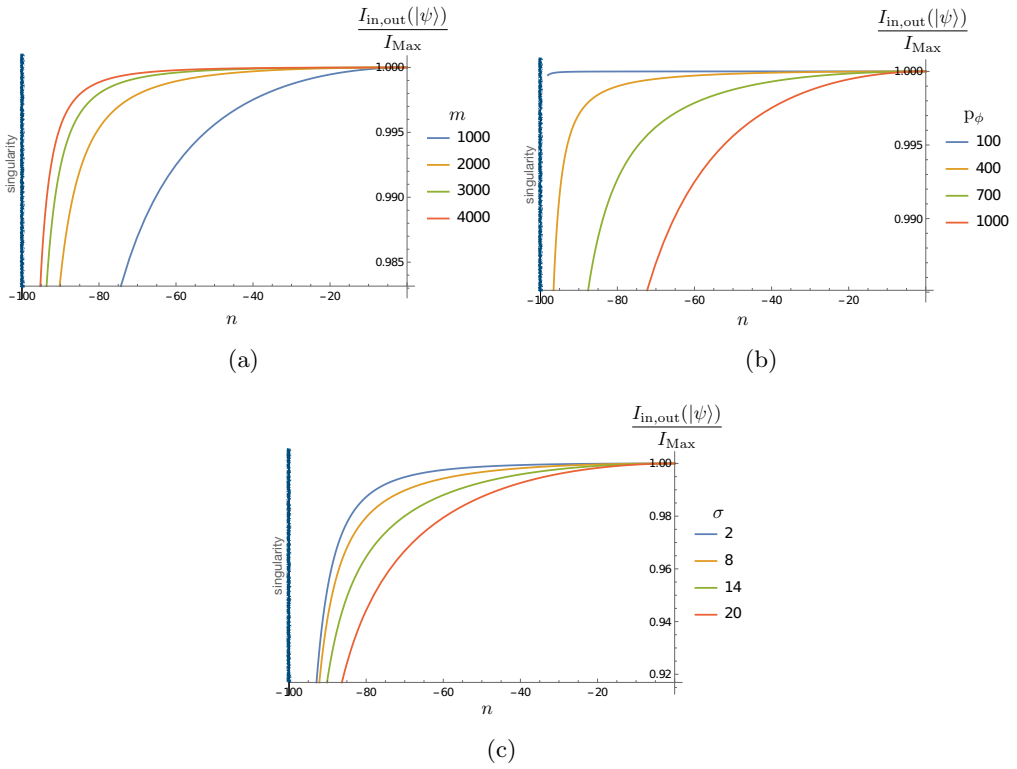


Figure 16: (a) Plot of $I_{\text{in,out}}(|\psi\rangle)/I_{\text{Max}}$ in term of n evolution steps for $\sigma = 10$, $p_+ = 1000$ and for different values of m_0. (b) Plot of $I_{\text{in,out}}(|\psi\rangle)/I_{\text{Max}}$ in terms of n evolution steps for $m_0 = 1000$, $\sigma = 10$ and for different values of p_+. (c) Plot of $I_{\text{in,out}}(|\psi\rangle)/I_{\text{Max}}$ in terms of n evolution steps for $m_0 = 1000$, $p_+ = 1000$ and for different values of σ. The singularity correspond to the value $n\lambda = -100$ and is indicated by a black vertical line.

We can compute the mutual information between the inside and the outside Hawking excitations in the matter sector

$$I_{\text{in,out}}(|\psi\rangle) = S(\rho^{\text{in}}) + S(\rho^{\text{out}}) - S(\rho^{\text{in,out}}) \tag{7.27}$$

From (7.12),(7.14) and (7.13) it follows that

$$\begin{aligned} I_{\text{in,out}}(|\psi\rangle) = {} & \frac{1}{2}\left(1 - 2|D(\epsilon_1,\epsilon_1,j,0,n) + D(\epsilon_2,\epsilon_2,j,0,n)|\right)\log\left(\frac{1}{2}\left(1 - 2|D(\epsilon_1,\epsilon_1,j,0,n) + D(\epsilon_2,\epsilon_2,j,0,n)|\right)\right) \\ & + \frac{1}{2}\left(1 + 2|D(\epsilon_1,\epsilon_1,j,0,n) + D(\epsilon_2,\epsilon_2,j,0,n)|\right)\log\left(\frac{1}{2}\left(1 + 2|D(\epsilon_1,\epsilon_1,j,0,n) + D(\epsilon_2,\epsilon_2,j,0,n)|\right)\right) \\ & + \log(4), \end{aligned} \tag{7.28}$$

which is the final explicit result if we use (7.19). We can now look at the evolution of the mutual information between the inside and outside Hawking pairs as a function of $a = n\lambda\ell_p^2$, for $n\lambda\ell_p^2 \in [0, a_0 - 2\lambda\ell_p^2]$. In other words, we can visualize the evolution of the entanglement/correlations between these two subsystems when the area decreases. As we can anticipate, this quantity will

depend on the choice of m_0 (recall that the mass $M \propto m_0^2$ from (7.16)), on the spread of the wave packet σ, and on the square of the 'characteristic energy' of the Hawking particle j.

The results are shown in Figure 16, where we observe the decrease of the mutual information between the Hawking partners (initially maximally correlated as in Hawking radiation) as the inside partner evolves toward the singularity. This is an expected feature: due to the back reaction of the inside particle on the quantum geometry correlations are transferred to d.o.f other than those encoded in $\mathscr{H}_{in}$. This tell us that an appropriate account of unitarity needs the inclusion of all the d.o.f. From such general perspective the result is expected; a trivial implication of the monogamy of entanglement in quantum mechanics. The non trivial feature here, that will become clear in Section 7.3.2, is that essential correlations are established with the planckian d.o.f (modeled here by the ϵ sectors).

Figure 16 shows that the decoherence effect (the decrease of the mutual information as the inside partner approaches the singularity) is 'faster' when the black hole is smaller (when m_0 decreases). The effect is less important initially for macroscopic black holes even when it always becomes relevant when the singularity approaches. Larger p_ϕ increases the effect as expected from the fact that this increases the back reaction on the geometry and planckian sectors. The dependence on the spread σ is consistent with the present analysis.

Evolution of the correlations between the in falling matter and the ϵ d.o.f:

We can then compute the mutual information between the ingoing and the ϵ d.o.f

$$I_{\mathrm{in},\epsilon}(|\psi\rangle) = S(\rho^{\mathrm{in}}) + S(\rho^{\epsilon}) - S(\rho^{\mathrm{in},\epsilon}) \tag{7.29}$$

As in the previous subsection, it follows

$$\begin{aligned}
I_{\mathrm{in},\epsilon}(|\psi\rangle) = {} & \frac{1}{4}(1-4|D(\epsilon_1,\epsilon_2,0,0,n)|)\log\left(\frac{1}{4}-|D(\epsilon_1,\epsilon_2,0,0,n)|\right) \\
& + \frac{1}{4}(1+4|D(\epsilon_1,\epsilon_2,0,0,n)|)\log\left(\frac{1}{4}+|D(\epsilon_1,\epsilon_2,0,0,n)|\right) \\
& + \frac{1}{4}(1-4|D(\epsilon_1,\epsilon_2,j,j,n)|)\log\left(\frac{1}{4}-|D(\epsilon_1,\epsilon_2,j,j,n)|\right) \\
& + \frac{1}{4}(1+4|D(\epsilon_1,\epsilon_2,j,j,n)|)\log\left(\frac{1}{4}+|D(\epsilon_1,\epsilon_2,j,j,n)|\right) \\
& + \frac{1}{2}(2|D(\epsilon_1,\epsilon_2,0,0,n)+D(\epsilon_1,\epsilon_2,j,j,n)|-1)\log\left(\frac{1}{2}-|D(\epsilon_1,\epsilon_2,0,0,n)+D(\epsilon_1,\epsilon_2,j,j,n)|\right) \\
& - \frac{1}{2}(2|D(\epsilon_1,\epsilon_2,0,0,n)+D(\epsilon_1,\epsilon_2,j,j,n)|+1)\log\left(\frac{1}{2}+|D(\epsilon_1,\epsilon_2,0,0,n)+D(\epsilon_1,\epsilon_2,j,j,n)|\right) \\
& + \log(2)\ ,
\end{aligned} \tag{7.30}$$

which can be evaluated using (7.19). Results are reported in Figure 17. We see that, as the correlations between the outside and inside Hawking excitations decrease (Figure 16), the correlations of the inside partner and the planckian d.o.f increase as evolution brings it toward the strong quantum gravity regime close to the singularity. As in the previous subsection, the dependence on the various parameters is the expected one.

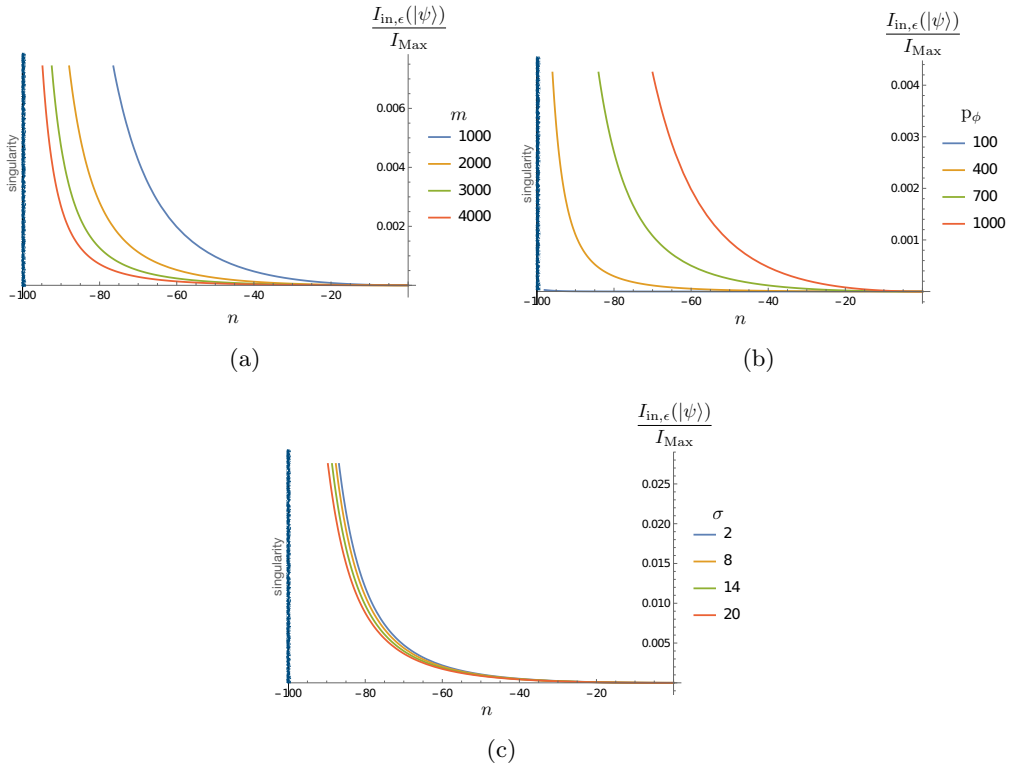


Figure 17: (a) Plot of $I_{\text{in},\epsilon}(|\psi\rangle)/I_{\text{Max}}$ in terms of n evolution steps for $\sigma = 10$, $p_+ = 1000$ and for different values of m_0. (b) Plot of $I_{\text{in},\epsilon}(|\psi\rangle)/I_{\text{Max}}$ in terms of n evolution steps for $m_0 = 1000$, $\sigma = 10$ and for different values of p_+. (c) Plot of $I_{\text{in},\epsilon}(|\psi\rangle)/I_{\text{Max}}$ in terms of n evolution steps for $m_0 = 1000$, $p_+ = 1000$ and for different values of σ. The singularity correspond to the value $n\lambda = -100$ and is indicated by a black vertical line.

Evolution of the correlations between the out going and the ϵ d.o.f:

In the previous subsection, we studied the correlations between inside Hawking partner and the planckian ϵ sector (the one representing Planckian granularity in our toy model). Correlations grow as the partner falls into the singularity as its back reaction on the planckian structure of the quantum geometry becomes more and more important as the singularity approaches. A quantum counterpart of this is the fact that the outside partner escaping at infinity will correlate with the quantum d.o.f of the geometry as well even if it never comes into direct interaction with them (this is a consequence of the monogamy of entanglement). Indeed it is very easy to relate (in our system) the mutual information $I_{\text{in},\epsilon}(|\psi\rangle)$ with $I_{\text{out},\epsilon}(|\psi\rangle)$. To see this one can first start from the definition of the mutual information between the subsystem corresponding to the outside partner and ϵ, namely

$$I_{\text{out},\epsilon}(|\psi\rangle) = S(\rho^{\text{out}}) + S(\rho^{\epsilon}) - S(\rho^{\text{out},\epsilon}). \tag{7.31}$$

By comparing the density matrices (7.12) and (7.14) one obtains that

$$I_{\text{in},\epsilon}(|\psi\rangle) = I_{\text{out},\epsilon}(|\psi\rangle). \tag{7.32}$$

Therefore, correlations between outside partner and the ϵ sector appear at the same rate as those between the inside partner and the ϵ sector.

Interpretation:

The results in this section show consistently how the information coded in the initial correlations between the Hawking partners in $\mathscr{H}_{in} \otimes \mathscr{H}_{out}$ are transferred to the other d.o.f involved. This is expected to be the case due to the gravitational interaction between the matter sector and the spacetime geometry. What is particularly interesting, and novel in our case, is the generic transfer of entanglement to the 'quantum hair' represented in our simple model by $\mathscr{H}_{\epsilon}$. The computations show clearly, in the results reported in Figures 15, 16, and 17, that correlations are established with these d.o.f during the evolution of the inside excitation toward the singularity. This indicates that, in a process where the mass of the black hole would completely disappear via Hawking evaporation (a process that our simple model cannot account for), unitarity could be maintained via the purification of Hawking radiation granted by d.o.f like the ϵ sector of this toy model. Despite the simplistic nature of the model, we notice that it complies with the expected behaviour of the back reaction: the lower the mass (the smaller m_0), or equivalently the smaller the black hole, the stronger the development of entanglement between the matter and the defects in the quantum geometry (stronger interaction with the Planckian granularity). The effect also grows with the particle momentum p_{ϕ} and dispersion σ, as expected.

7.4 Conclusion

In the approach we defend for solving the problem of loss of information, it is first necessary to identify the fundamental d.o.f. of geometry in regions of planckian curvature. Once this is done, one needs to understand the dynamical process by which unitarity is preserved when these are tracked during the black hole formation and evaporation. In particular, while the black hole is macroscopic and emits Hawking radiation, one needs to understand the mechanism by which the (initially) maximally correlated Hawking pairs evolve into a particle escaping to infinity as Hawking radiation correlated to the Planckian d.o.f inside that will emerge (after complete evaporation) as the purifying defects of the previous paragraph.

Both ingredients are shown to be present in the simple model of quantum black hole analyzed in this work. The model is expected to capture the dynamics of an ingoing scalar excitation when it is spherically symmetric in the near singularity approximation. It can be used to model the near singularity dynamics of a Hawking pair of scalar particles including the back reaction of the inside partner as it approaches the near singularity regime. On the one hand this model mimics the quantization of gravity in the framework of loop quantum gravity and thus contain the type of planckian 'weightless' d.o.f. More precisely, the spectrum of the mass operator is infinitely degenerate, due to the existence of quantum hair associated to (what we call) the ϵ sectors, Section 5.4.3. On the other hand, we showed explicitly how correlations are transferred dynamically to the 'hidden' quantum hair as the inside excitation approaches the near singularity regime. This was done first by using decoherence function (suitable intuitive method for the simplified setup of the toy model because there is a single such function), and later using the basis independent mutual information entanglement measure. Although this model does not allow to trace the complete evaporation of a black hole, it suggests that at the end of the process, the Hawking radiation, which is in a mixed state, is in fact entangled with planckian geometric d.o.f. Taking these d.o.f into account could therefore restore the purity of the total system.

This model is, however, too simple in several aspects to provide a complete resolution of the

information loss paradox. One problem is the assumption of spherical symmetry, which reduces the number of geometric d.o.f to a finite amount. The other problem, already mentioned, is that this model fails to describe the complete evaporation process. In particular, it does not explicitly show how the planckian degrees of freedom of the geometry can restore the purity of the system without storing energy. Indeed, all the energy is supposed to be in the form of Hawking radiation, with the possible exception of a Planck mass remnant. It will be the aim of the next chapter to discuss these issues.

8 Decoherence without dissipation in a QFT toy model

We concluded the previous chapter by pointing out that the symmetry reduced model used earlier does not fully describe the evaporation process of a black hole. However, it does suggest that the information purifying Hawking radiation resides in the Planckian d.o.f. of the geometry, which persist after evaporation is complete. To understand explicitly the nature of these d.o.f. and their interaction with matter, a theory of quantum gravitation is needed. From our point of view, the process of formation and evaporation of a black hole can be summarized as follows: the initial state consists of a pure state of matter and a geometry flat enough to be considered classical. The matter field collapses to form a black hole. When the ingoing modes of the field reach the region of planckian curvature, they trigger the planckian d.o.f. of the geometry, which plays a significant role at this scale, and transmit to them some of the information purifying Hawking radiation. The end of the black hole's evaporation corresponds to the moment when all the energy (with the exception of one Planck mass, which would correspond to a possible remnant) is reinjected into the matter field. The Planckian d.o.f. of the geometry may nevertheless persist, containing the information needed to purify the overall system but no energy.

The existence of such an evolution, inducing the decoherence of a subsystem (here the matter field) without energy dissipation was strongly questioned several decades ago [153]. Since then, it has been argued that this is actually possible [194–196]. A finite dimensional example illustrating such an evolution has been proposed in [197]. We begin this chapter by proposing a finite dimensional model which, like the Unruh model, provides a counterexample to the statement made in [153] and has the advantage of being realizable in practice.

Moreover, it is well known in condensed matter physics that a spin bath can generally induce decoherence of a finite dimensional system without causing energy dissipation, unlike a bath made up of harmonic oscillators [198]. The aim here is to take a further step towards modeling the evaporation of black holes by proposing a QFT model reproducing such an evolution. This chapter presents a toy model of QFT in (1+1)D, whose evolution is analogous to that described above. The aim is to show that it is possible for a system devoid of energy to still store information. In our toy model, such a system will be represented by a spin bath, analogous to the Planckian d.o.f. of geometry. Equivalently, we will see that a quantum field can decohere while retaining all its energy. This system will be represented by a collection of phonons, analogous to the field of quantum matter forming the black hole and generating Hawking radiation.

8.1 An example in quantum mechanics

As mentioned above, Unruh has already proposed a model for which it is possible for a finite dimensional system to evolve from a pure state to a mixed state [197]. His model may seem artificial, as it does not represent a physical system found in nature. We present here a unidmensional model that also illustrates an evolution with decoherence and without dissipation, but with the advantage of corresponding to a familiar physical system.

8.1.1 The Landau system

We consider a charged particle confined in the $z = 0$ plane in $\mathbb{R}^3$ moving under the influence of a uniform magnetic field $\vec{B} = B\hat{z}$. In a gauge where $\vec{A} = -By\hat{x}$ the Hamiltonian becomes

$$H = \frac{1}{2m}\left[\left(p_x + \frac{eB}{c}y\right)^2 + p_y^2\right]. \tag{8.1}$$

As p_x is conserved (a constant of motion) we can write the previous Hamiltonian in the Landau form

$$H = \frac{p_y^2}{2m} + \frac{1}{2}m\omega^2(y - y_0)^2, \tag{8.2}$$

where we introduced $\omega = \frac{|e|B}{mc}$ and $y_0 = -\frac{cp_x}{eB}$. The dynamics of this system is therefore identical to the one of an harmonic oscillator. The Schroedinger equation is therefore

$$\left[\frac{p_y^2}{2m} + \frac{1}{2}m\omega(y - y_0)^2 - E_n\right]|\psi\rangle = 0, \tag{8.3}$$

which is solved by

$$\langle x, y|n, p_x\rangle = \left(\frac{m\omega}{\pi(2^n n!)^2}\right)^{1/4} e^{ixp_x} e^{-\frac{m\omega(y-y_0)^2}{2}} H_n(\sqrt{m\omega}(y - y_0)), \tag{8.4}$$

where H_n denote the Hermite polynomials of order n, and

$$E_n = \omega\left(n + \frac{1}{2}\right), \tag{8.5}$$

called the Landau levels. Each energy level is infinitely degenerate. One can understand this from the fact that the charged particle classically moves around a circle whose center has coordinates (x_0, y_0) given by constants of motion (the second of which is given explicitly above, the first is $x_0 = p_y eB + x$ which can be explicitly shown to commute with H). The degeneracy corresponds then to placing the orbit at different locations which does not change the energy. One can easily show that the degeneracy is proportional to the area of the plane if the plane is finite (see [199] for details).

Not only the energy levels are degenerate but they are separated by an energy gap. It is therefore easy to imagine an interaction with another degree of freedom in a scattering process that would produce a non trivial entanglement between the intervening dynamical quantities without changing the energy of the scattering degree of freedom if the interaction is soft enough not to produce a transition between Landau levels of the charged particle.

An explicit solvable situation consists of a free particle moving in the z direction (idealizing a plane wave-packet in $\mathbb{R}^3$ transversal to the plane where the Landau system is) with a contact interaction

$$H_{\text{int}} = \delta(Z)F(p_x), \tag{8.6}$$

where $F(p_x)$ is some given function of p_x and Z is the coordinate of the free outside particle. The total Hamiltonian is

$$H_{\text{tot}} = H + \frac{P_Z^2}{2M} + \delta(Z)F(p_x). \tag{8.7}$$

The dynamics of the plane-wave packet along the z-axis can be reduced to a 1-dimensional problem with a delta function potential. The interaction term does not commute with the operator defining one of the coordinates of the center of the Landau orbits x_0 (previously a constant of motion). The passing of the plane-wave particle will change the value of x_0 and thus produce entanglement with the charged particle but this will not change the energy of the Landau particle and therefore also conserve the initial and final kinetic energies of the outside particle.

Explicitly, solutions of the Schroedinger equation can be written as

$$|n, P_Z, p_x; t\rangle = e^{-iE(n,P_Z)t} \, |n, p_x\rangle \, |P_Z\rangle \,, \tag{8.8}$$

where $E(n, P_Z) = \hbar\omega(n + 1/2) + P_Z^2/(2M)$, $|n, p_x\rangle$ is given by (8.4) and the $|P_Z\rangle$ satisfying the eigenvalue equation (for the incident particle degrees of freedom)

$$\left[-\frac{1}{2M}\frac{\partial^2}{\partial Z^2} + \delta(Z)F(p_x)\right] \langle Z|\phi\rangle = \left(\frac{P_Z^2}{2M}\right) \langle Z|\phi\rangle \,, \tag{8.9}$$

which reduces the dynamics to that of the outside particle scattering in a one-dimensional Dirac delta potential. Elementary methods lead to the solution

$$\langle Z|P_Z\rangle = \begin{cases} e^{i(P_Z Z - E(n,P_Z)t)} + \frac{1}{\frac{iP_Z}{MF(p_x)} - 1} e^{-i(P_Z Z + E(n,P_Z)t)} & \text{for} \quad z < 0 \\ \frac{1}{1 - \frac{MF(p_x)}{iP_Z}} e^{i(P_Z Z - E(n,P_Z)t)} & \text{for} \quad z > 0, \end{cases} \tag{8.10}$$

where there is a discontinuity in the Z-derivative of the wave function due to the presence of the delta function potential in the interaction.

One can superimpose stationary states (8.8) to form wave packets which are suitable for interpreting some of the important features of the physics involved. For instance, consider a superposition of states with $n = 0$ (the ground states in the charged particle degree of freedom) as

$$|\psi(t)\rangle = \int a_{x_0,y_0}(p_x) A_{Z_0,P_Z^0}(P_Z) \, |0, P_Z, p_x; t\rangle \, dp_x dP_Z, \tag{8.11}$$

with amplitudes $a_{x_0,y_0}(p_x)$ and $A_{Z_0,P_Z^0}(P_Z)$ such that the wave function of the full system $\langle x, y, Z|\psi(0)\rangle$ is initially peaked at some (x_0, y_0) in the 2-dimensional plate (as far as the degrees of freedom of the charged particle are concerned) while the outside particle wave function is peaked at $Z_0 \gg \Delta Z$ far to the right incident toward the plate with $P_Z^0 < 0$.

Under such conditions the incident particle will move toward the plate in a way that would be in practice indistinguishable from a regular free particle (as long as $\langle Z(t)\rangle$ remains much larger than the with of the packet ΔZ). Bob, who is unaware of the presence of the plate (very far to he left in his lab) could describe this particle as a free particle and conclude (after performing suitable experiments with that particle) that unitarity is respected during this phase of the dynamics on the far remote right of the plate.

Notice that the non-locality of quantum mechanics implies that no matter how far we are to the right, the exact solutions of the Schroedinger equation 'know' about the presence of the plate as solutions depend explicitly on the quantum numbers of the charged particle. There are involved experiments that Bob could perform to extract such dependence but, in practice, he will not think about doing them as they would not seem necessary nor natural from his perspective.

8.1.2 Generalization of the interaction Hamiltonian

We chose a very special type of interaction to make the problem explicitly solvable. However, the qualitative features of the previous model are generic as it can be seen from the perturbative treatment of a general interaction Hamiltonian of the form

$$\alpha H_{\text{int}} = \alpha H_{\text{int}}(x, y; \vec{X}), \tag{8.12}$$

where x, y are the coordinates of the charged particle in the plate, $\vec{X}$ the coordinates of an exterior particle, and $\alpha \ll 1$ a dimensionless coupling. One makes the ansatz

$$|\Psi(t)\rangle = \int \sum_n c_n(p_x, \vec{P}, t) e^{-i\left(\omega(n+\frac{1}{2})+\frac{\vec{P}^2}{2M}\right)} |n, p_x\rangle \, |\vec{P}\rangle \, dp_x d^3\vec{P}, \tag{8.13}$$

where $|n, p_x\rangle$ is given by (8.4), and $\langle \vec{X}|\vec{P}\rangle = e^{i\vec{P}.\vec{X}}$. The Schroedinger equation can be written in integral form (suitable for perturbation theory)

$$\begin{aligned} c_n(p_x, \vec{P}, t) =& i c_n(p_x, \vec{P}, t_0) - i \int \sum_{n'} \langle n, p_x, \vec{P}| \, \alpha H_{\text{int}} \, |n', p'_x, \vec{P}'\rangle \\ & \times \int_{t_0}^{t} c_{n'}(p'_x, \vec{P}', t') e^{-it'\left(\omega_H(n'-n)+\frac{\vec{P}'^2-\vec{P}^2}{2M}\right)} |n', p'_x, \vec{P}'\rangle \, dp'_x d^3\vec{P}' dt'. \end{aligned} \tag{8.14}$$

Taking the following initial conditions at $t_0 \to -\infty$

$$c_n(p_x, \vec{P}, -\infty) = \delta_{n,0}\delta(p_x - p_x^{\text{in}})\delta(\vec{P} - \vec{P}_{\text{in}}). \tag{8.15}$$

The transition amplitude (to first order in α) from $t = -\infty$ to $t = \infty$ is given by

$$\mathcal{M}_{|0,p_x^{\text{in}},\vec{P}_{\text{in}}\rangle \to |n,p_x^{\text{out}},\vec{P}_{\text{out}}\rangle} = -i \, \langle n, p_x^{\text{out}}, \vec{P}_{\text{out}}| \, H_{\text{int}} \, |0, p_x^{\text{in}}, \vec{P}_{\text{in}}\rangle \int_{-\infty}^{+\infty} e^{-it\left(-\omega n + \frac{\vec{P}_{\text{in}}^2 - \vec{P}_{\text{out}}^2}{2M}\right)} dt. \tag{8.16}$$

The transition amplitude vanishes if $\omega_H n - \frac{\vec{P}_0^{\,2}-\vec{P}^2}{2M} \neq 0$ as implied by energy conservation. This implies in particular that if $\frac{\vec{P}_0^{\,2}}{2M} < \omega$ (lower than the energy gap) the charged particle in the plate must remain in the ground state and thus the interaction takes place elastically without dissipation. While a non trivial entanglement with the (constants of motion at zero order) (x_0, y_0) will generically take place.

8.2 Presentation of the $1+1$ field theory model

This section contains the main result of the chapter. We introduce a discrete model of phonons in a one dimensional lattice of atoms with internal d.o.f represented by a $1/2$ spin. By appropriately engineering a simple but suitable interaction between the lattice excitations and the internal d.o.f at lattice sites we obtain a systems such that:

- The ground state is infinitely degenerate. The system contains a residual entropy in the sense of statistical thermodynamics (In a thermal bath at temperature T it violates the third law in the sense that $\lim S(T) \neq 0$ when $T \to 0$.)
- An effective (unitary) field theory description exists and is given by the naive continuum limit of the model. It corresponds to a $1+1$ QFT of phonons which approximates well low energy phonons (those with wave length $\lambda \ll a$ where a is the lattice spacing). Internal d.o.f can be ignored in this regime.
- Unitary effective descriptions of phonons with arbitrary wave length do not exist. Short wavelength phonons are dynamically entangled with the defects. Information is lost when the internal d.o.f of atoms is ignored.
- If we assume to have asymptotic regions where atoms have no internal d.o.f then the scattering of phonons through the region with internal d.o.f. happens without dissipation: the asymptotic energy in the phonon sector is preserved.

8.2.1 Classical dynamics of a 1D chain of oscillators

We first review the classical model of a chain of N identical oscillator of mass M connected by springs of constant K. The distance at rest between the oscillator is noted a, so the total length of the chain is $L = Na$. The displacement of the j^{th} oscillator with respect to its equilibrium position at time t is noted $u_j(t)$. One can apply Newton's second law to the j^{th} oscillator

$$\begin{aligned} M\frac{d^2u_j(t)}{dt^2} &= K(u_{j+1}(t) - u_j(t)) - K(u_j(t) - u_{j-1}(t)) \\ &= K(u_{j+1}(t) + u_j(t) - 2u_j(t)). \end{aligned} \tag{8.17}$$

In order to simplify the treatment we impose the periodic boundary condition $u_1 = u_{N+1}$. It is well known that in the limit $N \to +\infty$, this choice of boundary condition has no influence on the global dynamics. The system is solved by decomposing it into normal modes which concretely correspond to looking for plane wave solution of the form

$$u_j(t) = Ae^{i(qja - \omega_q t)}, \tag{8.18}$$

where q is the wave vector that can take the discrete values

$$q = \frac{2\pi n}{Na} \quad \text{with} \quad n \in \mathbb{Z}. \tag{8.19}$$

Inserting the plane wave ansatz (8.18) in (8.17) leads to the dispersion relation

$$\omega_q^2 = 2\frac{K}{M}(1 - \cos(qa)) = 4\frac{K}{M}\sin^2\left(\frac{qa}{2}\right). \tag{8.20}$$

This dispersion relation shows us that we can restrict the study to $q \in \left[-\frac{\pi}{a}, \frac{\pi}{a}\right]$ or equivalently to $n \in [\![-N/2, N/2]\!]$, which is known as the one Brillouin zone (OBZ).

The continuum limit can be easily obtain by writing equation (8.17) as

$$-\frac{M}{Ka^2}\frac{d^2u_j(t)}{dt^2} + \frac{(u_{j+1}(t) + u_j(t) - 2u_j(t))}{a^2} = 0, \tag{8.21}$$

and taking the limit $a \to 0$ while holding fixed $c^2 \equiv Ka^2/M$. One obtains the one dimensional scalar field equation

$$\left[-\frac{1}{c^2}\frac{\partial^2}{\partial t^2} + \frac{\partial^2}{\partial x^2}\right] u(t,x) = 0 \tag{8.22}$$

for phonons with propagation velocity c. At the discrete level, when the lattice constant a is fixed, the phase velocity v_φ instead depend on the wave number, namely

$$\begin{aligned} v_\varphi &= \frac{\omega_q}{q} = c\frac{|\sin\left(\frac{qa}{2}\right)|}{\frac{qa}{2}} \\ &= c\left(1 - \frac{q^2a^2}{24}\right) + \mathcal{O}\left((qa)^4\right), \end{aligned} \tag{8.23}$$

where in the second line we explicitly write the leading discreteness corrections in the low momentum limit. Similar considerations are applicable to the (more physical) group velocity

$$\begin{aligned} v_g &\equiv \frac{d\omega_q}{dq} = c\cos\left(\frac{qa}{2}\right) \\ &= c\left(1 - \frac{q^2a^2}{8}\right) + \mathcal{O}((qa)^4). \end{aligned} \tag{8.24}$$

Such deviations from linear dispersion relations induced by the lattice have been postulated phenomenologically as possible Lorentz invariance violating effects induced quantum gravity in the literature. In the present case its origin is clear and associated to the background lattice which selects a preferred notion of rest. Such naive violations seem impossible in the more realistic context of interacting quantum fields theory [200]. In this sense our simplistic model should not be take too literally when extrapolating the discussion to the realm of quantum gravity.

8.2.2 Quantization of the 1D chain

We now would like to determine the quantum dynamics of such a system. To do so, we will proceed to the usual canonical quantization procedure. We start from the classical Hamiltonian

$$H^{(0)} = \sum_{j=1}^{N}\left[\frac{p_j^2}{2M} + \frac{K}{2}(u_j - u_{j+1})^2\right], \tag{8.25}$$

where the Hamiltonian is denoted $H^{(0)}$ as we will later add an interaction term which will be denoted $H^{(1)}$ and treated in perturbation theory. The quantization is made by replacing the dynamical variables u_j and p_j by operators (we omit the hats to lighten the notation) satisfying the usual commutation relations

$$[u_i, u_j] = 0 \qquad [p_i, p_j] = 0 \qquad [u_i, p_j] = i\delta_{i,j}. \tag{8.26}$$

Let us review how the quantum dynamics of this system is equivalent to the one of N independent quantum harmonic oscillator. To do so, we will work in the Fourier space. We consider the discrete

Fourier transform of the position and momentum operators

$$u_q = \sum_{j=1}^{N} \frac{a}{2\pi} e^{-iqja} u_j \Leftrightarrow u_j = \sum_{q\in \mathrm{OBZ}} \frac{2\pi}{L} e^{iqja} u_q, \tag{8.27}$$

$$p_q = \sum_{j=1}^{N} \frac{a}{2\pi} e^{-iqja} p_j \Leftrightarrow p_j = \sum_{q\in \mathrm{OBZ}} \frac{2\pi}{L} e^{iqja} p_q. \tag{8.28}$$

With this convention for the Fourier series, one can check that the commutation relations (8.26) lead to

$$[u_q, u_{q'}] = 0 \quad [p_q, p_{q'}] = 0 \quad [u_q, p_{q'}] = \frac{La}{4\pi^2} i\delta_{q,-q'}. \tag{8.29}$$

In order to show the equivalence relation, one needs to use the two following completeness relations

$$\sum_{j=1}^{N} e^{i(q-q')ja} = N\delta_{q,q'} \qquad \text{and} \qquad \sum_{q\in \mathrm{OBZ}} e^{iq(j-j')a} = N\delta_{j,j'}. \tag{8.30}$$

A proof of relations (8.30) and of the equivalence relations can be found in the appendix D. Notice that $u_q^\dagger = u_{-q}$ and $p_q^\dagger = p_{-q}$. In term of this Fourier operators, the (normal ordered) Hamiltonian becomes

$$H^{(0)} =: \frac{4\pi^2}{L^2} \sum_{j,q,q'} e^{i(q+q')ja} \left[\frac{p_q p_{q'}}{2MN} + \frac{K u_q u_{q'}}{2N} (1 - e^{iqa})(1 - e^{iq'a}) \right] : \tag{8.31}$$

$$=: \frac{4\pi^2}{La} \sum_{q} \left[\frac{p_q p_{-q}}{2M} + K u_q u_{-q} (1 - \cos(qa)) \right] : \tag{8.32}$$

$$=: \frac{4\pi^2}{La} \sum_{q} \left[\frac{p_q p_{-q}}{2M} + \frac{M}{2} u_q u_{-q} w_q^2 \right] : . \tag{8.33}$$

The use of the normal ordered form of the Hamiltonian operator, denoted by "::", is not essential here. We make this choice here only in order to simplify the presentation. On the other hand, one can define creation and annihilation operators by

$$a_q := \frac{2\pi}{\sqrt{2M\omega_q La}} (M\omega_q u_q + i p_q) \qquad \text{and} \qquad a_q^\dagger := \frac{2\pi}{\sqrt{2M\omega_q La}} (M\omega_q u_{-q} - i p_{-q}), \tag{8.34}$$

which satisfies the usual commutation relations

$$\left[a_{q'}, a_q^\dagger \right] = \delta_{q,q'}. \tag{8.35}$$

On the other hand, one can invert the relations (8.34), leading to

$$u_q = \frac{1}{2\pi} \sqrt{\frac{La}{2M\omega_q}} (a_q + a_{-q}^\dagger) \qquad \text{and} \qquad p_q = \frac{1}{2\pi i} \sqrt{\frac{M\omega_q La}{2}} (a_q - a_{-q}^\dagger). \tag{8.36}$$

Using (8.36) and (8.27) it is easy to verify that the previous relations imply the variables u_j and p_j are self adjoint operators in the phonon Hilbert space. Finally, by inserting (8.36) in (8.31),

the Hamiltonian of the system becomes analogous to the one of N independent quantum harmonic oscillator labeled by q

$$H^{(0)} = \sum_q \omega_q \, a_q^\dagger a_q. \tag{8.37}$$

Usually, the Hilbert space describing this system is denoted $\mathcal{H}_{\text{phonons}} = \bigotimes_q \mathcal{H}_q$ where $\mathcal{H}_q$ is the Hilbert space describing the q harmonic oscillator, and the number states form a basis. Therefore, a basis of the total Hilbert space $\mathcal{H}_{\text{Phonon}}$ will be noted $\mathcal{B} = \{|\{n_q\}\rangle\}_{\{n_q\}}$ where $|\{n_q\}\rangle$ correspond to the state with n_q excitations in each modes q such that

$$H^{(0)} \, |\{n_q\}\rangle = E_{\{n_q\}} \, |\{n_q\}\rangle \quad \text{with} \quad E_{\{n_q\}} = \sum_q \omega_q n_q. \tag{8.38}$$

8.2.3 Adding a local defect

We now add a defect on one of the oscillators. More precisely, we add a spin operator S_z acting on a $\mathbb{C}^2$ Hilbert space and having as eigenvalues $+1$ and -1. This spin will eventually interact with the phonons propagating on the chain and we want it to be localized on the j^{th} oscillator. The interaction will be designed to become active when the phonons are close to the j^{th} oscillator (and hence be local). We will also require the interaction to preserve the degeneracy of the ground state. Thus we add to the free Hamiltonian $H^{(0)}$ an interaction Hamiltonian $H^{(1)}$, namely

$$\begin{aligned} H &= H^{(0)} + \alpha H^{(1)} \\ &= \sum_q \omega_q a_q^\dagger a_q + \alpha f(\{u_j\}, \{p_j\}) S_z, \end{aligned} \tag{8.39}$$

where f is *a priori* a function of the u_j and p_j operators such that the interaction is local and preservers the degeneracy of the ground state and $\alpha \ll 1$ is a small coupling constant. The Hilbert space of the total system is

$$\mathcal{H} = \mathcal{H}_{\text{phonons}} \otimes \mathcal{H}_{\text{spin}}, \tag{8.40}$$

where $\mathcal{H}_{\text{phonons}}$ has been defined in section 8.2.2, and $\mathcal{H}_{\text{spin}}$ is the Hilbert space describing the spin. A basis for this Hilbert space is the eigenbasis of the operator $\hat{S}_z$ that we will note $\{|s\rangle\}_{s=\pm 1}$ such that $\hat{S}_z \, |s\rangle = s \, |s\rangle$. In the new Hilbert space (8.40), extended to include the spin defect, the vacuum is obviously degenerate when $\alpha = 0$ as the Hamiltonian does not depend on the spin d.o.f. We have $H|_{\alpha=0} \, |0, s\rangle = H_0 \, |0, s\rangle = 0$ where $|0, s\rangle \equiv |0\rangle \, |s\rangle$.

8.3 Perturbative treatment of the dynamics

We will begin this section by reviewing the perturbative method of solving Schroedinger's equation by considering a fully general interaction Hamiltonian $H^{(1)}$ as a perturbation of the total Hamiltonian. We will then apply this method to a specific choice of $H^{(1)}$, allowing us to analyze the evolution of the energy and entropy of different subsystems.

8.3.1 Perturbative resolution

Let us quickly review how to study perturbatively the dynamics of a quantum system given by an Hamiltonian H we do not know how to diagonalize. This Hamiltonian is composed of a "free" Hamiltonian $H^{(0)}$ we know how to diagonalize and a small perturbation $\alpha H^{(1)}$. One can express the wave function of the system in the eigenbasis of $H^{(0)}$ as

$$|\psi(t)\rangle = \sum_{\{n_q\},s} h(\{n_q\},s,t)e^{-itE_{\{n_q\}}} |\{n_q\},s\rangle , \tag{8.41}$$

where $|\{n_q\},s\rangle = |\{n_q\}\rangle |s\rangle \in \mathcal{H}_{\text{phonons}} \otimes \mathcal{H}_{\text{spin}}$ with $|\{n_q\}\rangle$ are given in 8.38. The Schroedinger equation leads to

$$\begin{aligned}\sum_{\{n_q\},s} \left[i\frac{dh(\{n_q\},s,t)}{dt} + E_{\{n_q\}}h(\{n_q\},s,t)\right] e^{-itE_{\{n_q\}}} |\{n_q\},s\rangle \\ = \sum_{\{n_q\},s} \left[E_{\{n_q\}} + \alpha H^{(1)}\right] h(\{n_q\},s,t)e^{-itE_{\{n_q\}}} |\{n_q\},s\rangle\end{aligned} \tag{8.42}$$

which implies

$$i\frac{dh(\{n_q\},s,t)}{dt} = \sum_{\{n'_q\}} \alpha \langle\{n_q\},s| H^{(1)} |\{n'_q\},s\rangle h(\{n'_q\},s,t)e^{-it(E_{\{n'_q\}}-E_{\{n_q\}})} \tag{8.43}$$

or in integral form

$$h(\{n_q\},s,t) = h(\{n_q\},s,0) - i\alpha \sum_{\{n'_q\}} \langle\{n_q\},s| H^{(1)} |\{n'_q\},s\rangle \int_0^t h(\{n'_q\},s,t')e^{-it'(E_{\{n'_q\}}-E_{\{n_q\}})}dt'. \tag{8.44}$$

One can solve the previous integral equation perturbatively via the ansatz

$$h(\{n_q\},s,t) = h^{(0)}(\{n_q\},s,t) + \alpha h^{(1)}(\{n_q\},s,t) + \alpha^2 h^{(2)}(\{n_q\},s,t) + ... \tag{8.45}$$

As we will show in section 8.3.3, it is necessary to solve the dynamics to order α^2 to be able to calculate the leading order contributions to entanglement between the phonons and the spin defects. By inserting the expansion (8.45) in equation (8.44), one gets

$$h^{(0)}(\{n_q\},s) = h(\{n_q\},s,0) \tag{8.46}$$

$$h^{(1)}(\{n_q\},s,t) = -i \sum_{\{n'_q\}} \langle\{n_q\},s| H^{(1)} |\{n'_q\},s\rangle \int_0^t h^{(0)}(\{n'_q\},s)e^{-it'(E_{\{n'_q\}}-E_{\{n_q\}})}dt' \tag{8.47}$$

$$h^{(2)}(\{n_q\},s,t) = -i \sum_{\{n'_q\}} \langle\{n_q\},s| H^{(1)} |\{n'_q\},s\rangle \int_0^t h^{(1)}(\{n'_q\},s,t')e^{-it'(E_{\{n'_q\}}-E_{\{n_q\}})}dt'. \tag{8.48}$$

The validity of the perturbative solution is limited in time, indeed there is a time $t_\star$ for which $|\alpha h^{(1)}| \sim h^{(0)}$. This is due to the terms for which $E_{\{n'_q\}} = E_{\{n_q\}}$ in the sum defining $h^{(1)}$. When the norm of these contributions are of the same order than $h^{(0)}$, the perturbative solution is no longer

valid. We can bing a lower bound for the validity time $t_\star$ when this happen using that

$$\begin{aligned}
&\left|\sum_{\{n'_q\}} \alpha \langle\{n_q\}| H^{(1)} |\{n'_q\}\rangle h^{(0)}(\{n'_q\}, s) t_\star\right| \\
&\leq \mathrm{Max}_{\{n_q\}} \left|h^{(0)}(\{n_q\}, s)\right| \left|\sum_{\{n'_q\}} |\alpha \langle\{n_q\}| H^{(1)} |\{n'_q\}\rangle t_\star|\right| \\
&\leq \mathscr{N} \mathrm{Max}_{\{n_q\}} \left|h^{(0)}(\{n_q\}, s)\right| \mathrm{Max}_{\{n_q\},\{n'_q\}} \left|\alpha \langle\{n_q\}| H^{(1)} |\{n'_q\}\rangle t_\star\right| \qquad (8.49)
\end{aligned}$$

where the sums are over n'_q such that $E_{\{n'_q\}} = E_{\{n_q\}}$ and $\mathscr{N}$ is the dimension of the degenerate subspace. Therefore, we assume the perturbation theory fails when

$$\mathscr{N} \mathrm{Max}_{\{n_q\}} \left|h^{(0)}(\{n_q\}, s)\right| \mathrm{Max}_{\{n_q\},\{n'_q\}} \left|\alpha \langle\{n_q\}| H^{(1)} |\{n'_q\}\rangle t_\star\right| = \mathrm{Max}_{\{n_q\}} \left[|h^{(0)}(\{n_q\}, s)|\right]. \quad (8.50)$$

Thus we obtain

$$t_\star = \frac{1}{\mathscr{N} \alpha \mathrm{Max}_{\{n_q\},\{n'_q\}} \left[|\langle\{n_q\}| H^{(1)} |\{n'_q\}\rangle|\right]}, \qquad (8.51)$$

where the matrix elements are maximized in the degenerate sectors. We will soon see that, in the cases of interest, $t_\star$ is much bigger than the relevant dynamical characteristic times of the problem.

8.3.2 Choice of the interaction Hamiltonian

We will now make an explicit choice for the expression of the interaction Hamiltonian, i.e. for the f function. We will first choose an Hamiltonian which is simple enough to analytically perform the perturbative analysis, will then comment on the physical interpretation of this Hamiltonian in a second time

$$\begin{aligned}
H^{(1)} \equiv S_z : \left[\frac{p_j^2}{2M} + \frac{4\pi^2}{Na^2}\frac{M}{2N}\left(\sum_q \omega_q u_q e^{iqja}\right)^2\right] : \\
= \frac{S_z}{N} \sum_{q,q'} e^{-i(q-q')ja} \sqrt{\omega_q \omega_{q'}} a^\dagger_{q'} a_q \qquad (8.52)
\end{aligned}$$

where we chose the spin to be located on the j^{th} oscillator, the first expression is normal ordered, and to get to the second line one has to use the discrete Fourier transform (8.27) and (8.34).

Let us analyze each of the two terms in (8.52) separately. The first term is the kinetic energy of the corresponding oscillator where the spin defect is placed. This term is explicitly local. The second term has a simpler interpretation in the continuum limit $a \to 0$ with $Na = L$, in this limit we have

$$\begin{aligned}
\frac{4\pi^2}{Na^2}\frac{M}{2N}\left(\sum_q \omega_q u_q e^{-iqx}\right)^2 &= \frac{M}{2}\left(\sum_q \omega_q u_q e^{-iqx}\frac{2\pi}{L}\right)^2 \approx \frac{Mc^2}{2}\left(\sum_q |q| u_q e^{-iqx}\frac{2\pi}{L}\right)^2 \qquad (8.53) \\
&= \frac{K\pi^2 a^2}{L^2}\left(\sum_k \frac{\left(-1+(-1)^{j-k}\right)}{L\sin^2\left(\frac{(j-k)\pi}{N}\right)} u_k a\right)^2 \approx K\pi^2 a^2 \left(\int_0^L \frac{u(y)}{L^2 \sin^2\left(\frac{(x-y)\pi}{L}\right)} dy\right)^2.
\end{aligned}$$

with $x = ja$, $c \equiv a\sqrt{K/M}$. As the last expression shows, this term in the interaction Hamiltonian is non-local and depends on all of the $u's$ in the chain: it is proportional to the absolute value of the spacial derivative operator $|\nabla|$. However, oscillators close to the defect contribute the most. This property and the simplicity of the interaction—when expressed in terms of creation and annihilation operator (see second line in (8.52))—justifies the choice that will allow for certain explicit calculations below.

Notice for instance that the interaction Hamiltonian annihilates the phonon-vacuum $|0, s\rangle$ states which implies that the vacuum remains degenerate when including the perturbation. Moreover the interaction commutes with the total number operator $n_{total} \equiv \sum_q a_q^\dagger a_q$, namely

$$[H, n_{total}] = \alpha[H^{(1)}, n_{total}] = 0. \tag{8.54}$$

as

$$\sum_\ell [a_\ell^\dagger a_\ell, a_{q'}^\dagger a_q] = \sum_\ell a_\ell^\dagger [a_\ell, a_{q'}^\dagger] a_q + a_{q'}^\dagger [a_\ell^\dagger, a_q] a_\ell = a_{q'}^\dagger a_q - a_{q'}^\dagger a_q = 0. \tag{8.55}$$

Thus the interaction preserves the total number of excitations while it actually reshuffles quanta in the phonon state between different normal modes. The previous property implies that, while the interaction induces a non trivial dynamics for the spin d.o.f, the interaction does not remove vacuum degeneracy already present in the non interactive system. Note that the energy in the photon sector is not conserved as

$$\begin{aligned} [H, H^{(1)}] = [H^{(0)}, H^{(1)}] &= \frac{S_z}{N} \sum_{q,q'} e^{-i(q-q')ja} \sqrt{\omega_q \omega_{q'}} \sum_\ell \omega_\ell [a_\ell^\dagger a_\ell, a_{q'}^\dagger a_q] \\ &= \frac{S_z}{N} \sum_{q,q'} e^{-i(q-q')ja} \sqrt{\omega_q \omega_{q'}} (\omega_{q'} - \omega_q) a_{q'}^\dagger a_q, \end{aligned} \tag{8.56}$$

which implies that energy can flow from the phonons into the defect d.o.f. However, as the spin system does not have a contribution to the free Hamiltonian, once a localized phonon passes by, the energy will return to the phonon d.o.f. As we will see, the long term effect of the interaction in a scattering process will be encoded in memory effects including the modification of the spin at the defect and its entanglement with the phonon d.o.f. This follows from the obvious fact that the spin d.o.f is dynamical as

$$\begin{aligned} [H, S_x] &= i \frac{S_y}{N} \sum_{q,q'} e^{-i(q-q')ja} \sqrt{\omega_q \omega_{q'}} a_{q'}^\dagger a_q, \\ [H, S_y] &= -i \frac{S_x}{N} \sum_{q,q'} e^{-i(q-q')ja} \sqrt{\omega_q \omega_{q'}} a_{q'}^\dagger a_q. \end{aligned} \tag{8.57}$$

Already from the previous equations we can anticipate the key features of the model that we will confirm in what follows analyzing the dynamics in perturbation theory.

It is useful to compute the expectation value of (8.52) in a plane wave states $|n_q\rangle$ (defined at the end of section 8.2.2). One can show from (8.52) that

$$\langle n_q, s | H^{(1)} | n_q, s' \rangle = s \frac{\delta_{s,s'}}{N} n_q \omega_q \tag{8.58}$$

This result tells us that the expectation value of the energy of interaction when the vibration is a plane wave depend linearly on the frequency and on the number of particles in this mode. The bigger the frequency and the number of excitation is, the bigger the energy of interaction is. One can generalize this result by noticing that

$$\langle \{n_q\}, s| \, H^{(1)} \, |\{n_q\}, s'\rangle = s\frac{\delta_{s,s'}}{N}\sum_q n_q\omega_q = s\frac{\delta_{s,s'}}{N}\,\langle \{n_q\}, s| \, H^{(0)} \, |\{n_q\}, s'\rangle \,. \tag{8.59}$$

showing clearly that the modes contributing the more to the energy of interaction are the high frequency modes and those with a large number of occupation: high energy and/or high intensity of the phonons will make the effect of the defect more important[21]. Note that in spite of the proportionality between $\langle H^0\rangle$ and $\langle H^1\rangle$ the two operators are completely different since $H^{(0)}$ is diagonal in the basis $|\{n_q\}, s'\rangle$ while $H^{(1)}$ has all of its off-diagonal elements where the total number of quanta in the two states differ by one in arbitrarily different momenta is constant generically non vanishing, namely

$$\begin{aligned}\langle n_1, n_2, \cdots, n_\ell, \cdots, n_k+1, \cdots, n_N; s| \, H^{(1)} \, |n_1, n_2, \cdots, n_\ell+1, \cdots, n_k, \cdots n_N; s'\rangle = \\ = -is\frac{\delta_{s,s'}}{N}e^{-i(\ell-k)ja}\sqrt{\omega_\ell\omega_k(n_\ell+1)(n_k+1)}.\end{aligned} \tag{8.61}$$

as the contemplation of equation (8.52) shows.

One can now use the expression of the interacting Hamiltonian (8.52) in order to determine explicitly the perturbative solutions. We will consider in what follows two kind of initial states. The first one will be a plane wave, i.e.

$$|\psi_{\rm pw}(0)\rangle = \frac{1}{\sqrt{A}}\sum_{s=\pm1}|1_{q_0}, s\rangle \,, \tag{8.62}$$

while the second will be a Gaussian wave packet

$$|\psi_{\rm g}(0)\rangle = \frac{1}{\sqrt{A}}\sum_{q,s=\pm1} e^{-\frac{q-q_0}{2\sigma^2}}\,|1_q, s\rangle \,. \tag{8.63}$$

Since those states are linear combination of one particle states and since the interacting Hamiltonian preserves the number of particles, the final state will also be a linear combination of one particle states. The state at time t is obtained from (8.46) using that the suitable matrix element of the interaction Hamiltonian is

$$\langle 1_{q'}, s'| \, H^{(1)} \, |1_q, s\rangle = \frac{s\delta_{s,s'}}{N}e^{-ia(q-q')ja}\sqrt{\omega_q\omega_{q'}}. \tag{8.64}$$

[21] Incidentally, notice that we are finding the natural yet worth mentioning result that energy is (in expectation value) equally distributed on local oscillators, namely

$$\langle H_j\rangle \approx \langle : \left[\frac{p_j^2}{2M} + \frac{M}{2N}\left(\sum_q \omega_q u_q e^{-iqja}\right)^2\right] : \rangle = \frac{1}{N}\,\langle H^{(0)}\rangle \,. \tag{8.60}$$

.

The perturbative time evolution for the (initial) plane wave state (8.62) is given by

$$
\begin{aligned}
h^{(0)}_{\mathrm{pw}}(q,s,t) =& \delta_{q,q_0} \\
h^{(1)}_{\mathrm{pw}}(q,s,t) =& -\frac{is}{N} e^{-i(q_0-q)ja}\sqrt{\omega_q\omega_{q_0}}\int_0^t e^{-it'(\omega_{q_0}-\omega_q)}dt' \\
=& \frac{s}{N} e^{-i(q_0-q)ja}\sqrt{\omega_q\omega_{q_0}}\frac{1-e^{it(\omega_q-\omega_{q_0})}}{\omega_q-\omega_{q_0}} \\
h^{(2)}_{\mathrm{pw}}(q,s,t) =& -\left(\frac{s}{N}\right)^2 e^{-i(q_0-q)ja}\sum_{q'}\omega_{q'}\sqrt{\omega_q\omega_{q_0}}\int_0^t e^{-it'(\omega_{q'}-\omega_q)}\int_0^{t'} e^{-it''(\omega_{q_0}-\omega_{q'})}dt''dt' \\
=& \left(\frac{s}{N}\right)^2 e^{-i(q_0-q)ja}\sum_{q'}\omega_{q'}\sqrt{\omega_q\omega_{q_0}}\left(\frac{1-e^{it(\omega_q-\omega_{q_0})}}{(\omega_q-\omega_{q_0})(\omega_{q_0}-\omega_{q'})}+\frac{1-e^{it(\omega_q-\omega_{q'})}}{(\omega_q-\omega_{q'})(\omega_{q'}-\omega_{q_0})}\right)
\end{aligned}
\tag{8.65}
$$

One can then estimate the limiting time $t_\star$ for the validity of the perturbation theory is this specific case, namely

$$
t_\star = \frac{1}{\alpha|\langle 1_{q_0}|H^{(1)}|1_{q_0}\rangle|} = \frac{N}{\alpha}\frac{1}{\omega_{q_0}}. \tag{8.66}
$$

On the other hand, the perturbative solution for the initially Gaussian state (8.63) is

$$
\begin{aligned}
h^{(0)}_{\mathrm{g}}(q,s,t) =& e^{-\frac{(q-q_0)^2}{2\sigma^2}} \\
h^{(1)}_{\mathrm{g}}(q,s,t) =& -\frac{is}{N}\sum_{q'} e^{-i(q'-q)ja}\sqrt{\omega_q\omega_{q'}}e^{-\frac{(q'-q_0)^2}{2\sigma^2}}\int_0^t e^{-it'(\omega_{q'}-\omega_q)}dt' \\
=& \frac{s}{N}\sum_{q'} e^{-i(q'-q)ja}\sqrt{\omega_q\omega_{q'}}e^{-\frac{(q'-q_0)^2}{2\sigma^2}}\frac{1-e^{it(\omega_q-\omega_{q'})}}{\omega_q-\omega_{q'}} \\
h^{(2)}_{\mathrm{g}}(q,s,t) =& -\left(\frac{s}{N}\right)^2\sum_{q',q''} e^{-i(q''-q)ja}\omega_{q'}\sqrt{\omega_q\omega_{q''}}e^{-\frac{(q''-q_0)^2}{2\sigma^2}}\int_0^t e^{-it'(\omega_{q'}-\omega_q)}\int_0^{t'} e^{-it''(\omega_{q''}-\omega_{q'})}dt''dt' \\
=& \left(\frac{s}{N}\right)^2\sum_{q',q''} e^{-i(q''-q)ja}\omega_{q'}\sqrt{\omega_q\omega_{q''}}e^{-\frac{(q''-q_0)^2}{2\sigma^2}}\left(\frac{1-e^{it(\omega_q-\omega_{q''})}}{(\omega_q-\omega_{q''})(\omega_{q''}-\omega_{q'})}+\frac{1-e^{it(\omega_q-\omega_{q'})}}{(\omega_q-\omega_{q'})(\omega_{q'}-\omega_{q''})}\right)
\end{aligned}
\tag{8.67}
$$

Here again, we can estimate the limiting time $t_\star$ from (8.51)

$$
\begin{aligned}
t_\star &= \mathrm{Inf}_{q\in OBZ}\left[\frac{1}{\alpha|\langle 1_q|H^{(1)}|1_q\rangle|}\right] \\
&= \frac{N}{\alpha}\mathrm{Inf}_{q\in OBZ}\left[\frac{1}{\omega_q}\right] \\
&= \frac{N}{2\alpha}\sqrt{\frac{M}{K}} \\
&= \frac{L}{2\alpha c}.
\end{aligned}
\tag{8.68}
$$

And since $\alpha \ll 1$, we have $t_\star \gg \frac{L}{c}$ where L/c can be interpreted as the phonon transversing time. This means that perturbation theory is accurate for the purposes we are interested in.

8.3.3 Time evolution of the entanglement between the subsystems

We would like to describe the dynamics of the subsystems phonons-spin separately. To do so, it is convenient to work with their reduced density matrix. We consider only one-particle states of the general form

$$|\psi(t)\rangle = \frac{1}{\sqrt{A}} \sum_{q,s=\pm 1} h(q,s,t) e^{-it\omega_q} |1_q, s\rangle \,, \tag{8.69}$$

whose full density matrix is

$$\rho(t) = \frac{1}{|A|} \sum_{q,q',s,s'} h(q,s,t)\overline{h(q',s',t))} e^{-it(\omega_q - \omega_{q'})} |1_q, s\rangle \langle 1'_q, s'| \,. \tag{8.70}$$

One can then determine the reduced density matrices of the two subsystems by tracing over the complementary subsystem. One has

$$\langle 1_q| \rho_{\text{Phonon}} |1_{q'}\rangle = \frac{1}{|A|} \sum_{s} h(q,s,t)\overline{h(q',s,t))} e^{-it(\omega_q - \omega_{q'})} \tag{8.71}$$

$$\langle s| \rho_{\text{Spin}}(t) |s'\rangle = \frac{1}{|A|} \sum_{q} h(q,s,t)\overline{h(q,s',t)}. \tag{8.72}$$

As $q \in OBZ$, the dimension of the reduced density matrix ρ_{Phonon} is $(N+1)^2$ and is therefore complicated to study for large N. However, since we are interested here mainly in the entanglement between the phonons and the defects is more convenient to focus on the properties of the two-dimensional ρ_{Spin} using the fact that the full state is pure. For instance, if we were interested in the Von Neumann then we can use that $S_{\text{Phonon}} = S_{\text{Spin}}$.

We can can calculate the density matrix ρ_{Spin} to second order in α using the perturbative expansion (8.45)

$$\begin{aligned}\langle s| \rho_{\text{Spin}}(t) |s'\rangle = \frac{1}{|A|} \sum_{q} h^{(0)}(q)^2 + \alpha[h^{(0)}(q)\overline{h^{(1)}(q,s',t)} + h^{(1)}(q,s,t)h^{(0)}(q)] \\ + \alpha^2[h^{(1)}(q,s,t)\overline{h^{(1)}(q,s',t)} + h^{(0)}(q)\overline{h^{(2)}(q,s',t)} + h^{(2)}(q,s,t)h^{(0)}(q)],\end{aligned} \tag{8.73}$$

where we assume $h^{(0)}$ to be real, which is the case for the plane wave and the Gaussian wave packet (cf (8.65) and (8.67)). Moreover, one can show from (8.65) and (8.67) the following relations

$$\begin{aligned} h^{(1)}(q,s,t) &= s h^{(1)}(q,t) \\ h^{(2)}(q,s,t) &= h^{(2)}(q,t) \\ \overline{\sum_q h^{(0)}(q)h^{(1)}(q,s,t)} &= -\sum_q h^{(0)}(q)h^{(1)}(q,s,t). \end{aligned} \tag{8.74}$$

With these definitions, the expression (8.73) reduces to

$$\begin{aligned}\langle s| \rho_{\text{Spin}}(t) |s'\rangle &= \frac{1}{|A|} \sum_{q} h^{(0)}(q)^2 + \alpha(s-s')h^{(0)}(q)h^{(1)}(q,t) + \alpha^2[ss'|h^{(1)}(q,t)|^2 + h^{(0)}(q)(\overline{h^{(2)}(q,t)} + h^{(2)}(q,t))] \\ &= \frac{1}{2} + \frac{1}{|A|} \sum_{q} \alpha(s-s')h^{(0)}(q)h^{(1)}(q,t) + \alpha^2[ss'|h^{(1)}(q,t)|^2 + h^{(0)}(q)(\overline{h^{(2)}(q,t)} + h^{(2)}(q,t))] + \mathscr{O}(\alpha^3).\end{aligned} \tag{8.75}$$

Or in matrix form (in the basis $\{|+\rangle, |-\rangle\}$)

$$\rho_s = \begin{pmatrix} \frac{1}{2} & \frac{1}{2} + \alpha\beta + \alpha^2\delta \\ \frac{1}{2} - \alpha\beta + \alpha^2\delta & \frac{1}{2} \end{pmatrix} + \mathscr{O}(\alpha^3) \tag{8.76}$$

with

$$\beta = \frac{2}{|A|} \sum_q h^{(0)}(q) h^{(1)}(q,t) \quad \text{and} \quad \delta = \frac{1}{|A|} \sum_q h^{(0)}(q) (\overline{h^{(2)}(q,t)} + h^{(2)}(q,t)) - |h^{(1)}(q,t)|^2. \tag{8.77}$$

The eigenvalues of this matrix are $\lambda_\pm = \frac{1}{2} \pm \frac{\sqrt{1+4(\delta+|\beta|^2)\alpha^2+4\delta^2\alpha^4}}{2}$, and the entropy

$$S = \alpha^2(\delta + |\beta|^2) \left[\log\left(-(\delta + |\beta|^2)\alpha^2\right) - 1\right] + \mathscr{O}(\alpha^3). \tag{8.78}$$

For short times one can show that $2\delta + |\beta|^2$ (initially equal to 0) decreases. Thus, the entropy S increases initially. For instance in the case where the initial state is a plane wave, one can use the results (8.65) to explicitly determine β and δ

$$|\beta|^2 = \left(\frac{t\omega_{q_0}}{N}\right)^2 \tag{8.79}$$

and

$$\delta = -\frac{1}{N^2} \sum_q \omega_q \omega_{q_0} \left| \int_0^t e^{-it'(\omega_{q_0} - \omega_q)} dt' \right|^2, \tag{8.80}$$

leading to

$$\begin{aligned} (\delta + |\beta|^2) &= \left(\frac{t\omega_{q_0}}{N}\right)^2 - \frac{1}{N^2} \sum_q \omega_q \omega_{q_0} \left| \int_0^t e^{-it'(\omega_{q_0} - \omega_q)} dt' \right|^2 \\ &= -\frac{1}{N^2} \sum_{q \neq q_0} \frac{\omega_q \omega_{q_0}}{(\omega_q - \omega_{q_0})^2} \sin^2\left[\frac{t}{2}(\omega_q - \omega_{q_0})\right] \end{aligned} \tag{8.81}$$

For short times one can show that

$$(\delta + |\beta|^2) = -\left(\frac{t}{2N}\right)^2 \sum_{q \neq q_0} \omega_q \omega_{q_0} \left(1 + \mathscr{O}(t\omega_{q_0})\right). \tag{8.82}$$

The previous expression shows that entanglement between the phonon and the spin subsystem increases linearly with the frequency ω_{q_0} of the plane wave for short times. The long time behaviour is illustrated in Figure 18, where one also observes that entanglement increases with the frequency (or equivalently momentum q_0) as expected.

A similar behaviour is found in the case of a Gaussian wave packet although the complexity of the situation makes precludes a simple analytic treatment. However, it is still possible to study this case numerically (cf Fig.19). The figure shows the entropy grows faster when the momentum q_0 of the phonon wave packet is increased. One can also notice that there is a steep step in the evolution of the entropy. This step occurs approximately at the time (here $T \approx 5$) when the wave packet reaches the defect (here at the position $j = 5$) consistent with the speed of propagation $c = 1$ used

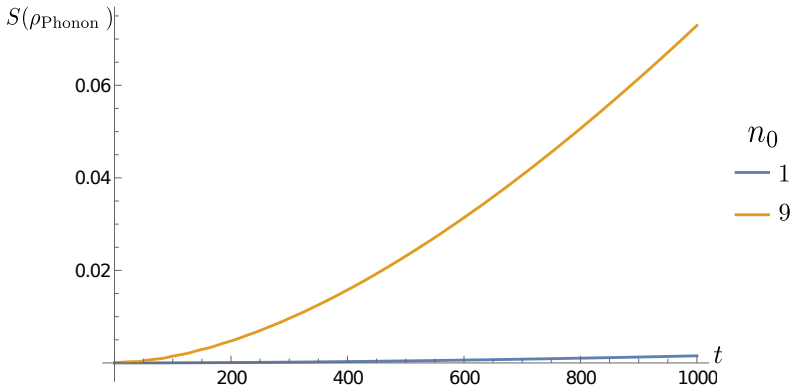


Figure 18: Plot representing the time evolution of the Von Neumann entropy of the spin subsystem (or the Von Neumann entropy of the phonon subsystem since the two are equal). There is here only one spin, and the phonon subsystem is initially described by a plane wave. The moment of the initial plane wave is parametrized by the integer n_0 and given by $q_0 = \frac{2\pi n_0}{Na}$. The blue curve corresponds to the case where $n_0 = 1$, and $n_0 = 9$ for the orange one. The spin is at the position $j = 5$, the chain is composed of $N = 20$ and periodic boundary conditions are imposed.

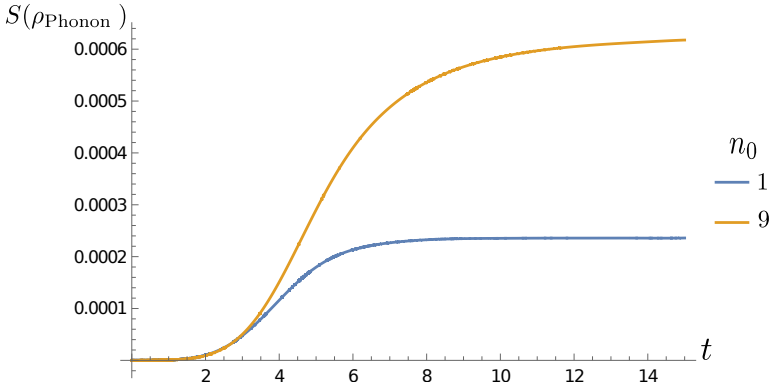


Figure 19: Plot representing the time evolution of the Von Neumann entropy of the phonon subsystem (or the Von Neumann entropy of the spin subsystem since the two are equal). There is here only one spin, and the phonons initially form a Gaussian wave packet. Its initial average moment is parametrized by the integer n_0 and given by $q_0 = \frac{2\pi n_0}{Na}$. The blue curve correspond to the case where $n_0 = 1$, and $n_0 = 9$ for the orange one. The spin is at the position $j = 5$, the chain is composed of $N = 20$ and periodic boundary conditions are imposed.

.

in the plot. This is an evidence that the entanglement between the two subsystem occurs in a local way. This conclusion is confirmed by changing the parameters in the numerical experiment. On can see on Fig.20 that the entropy evolve mainly when the wave packet reaches the defect. On the other hand, one can numerically study the evolution of the energy of the phonons. One can see on Fig.21 that there is an energy transfer from the phonons to the spin when the wave is close to the spin. However one can also see that the spin does not store energy and the initial energy of the phonons is recover when the wave packet moves away.

8.4 Generalization to N spins

We want to examine how the results obtained in the previous section are modified as the number of spins increases, by adding one to each oscillator. In particular, we want to verify that entropy

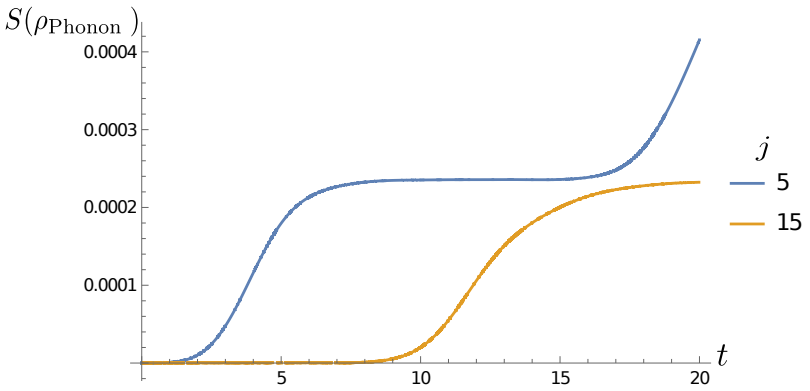


Figure 20: Plot representing the time evolution of the Von Neumann entropy of the phonon subsystem (or the Von Neumann entropy of the spin subsystem since the two are equal). There is only one spin, and the phonons initially form a Gaussian wave packet centered around a moment $q_0 = 1$. The blue curve correspond to the case where the spin is at the position $j = 5$, and $j = 15$ for the orange one. The chain is composed of $N = 20$ and periodic boundary conditions are imposed.

.

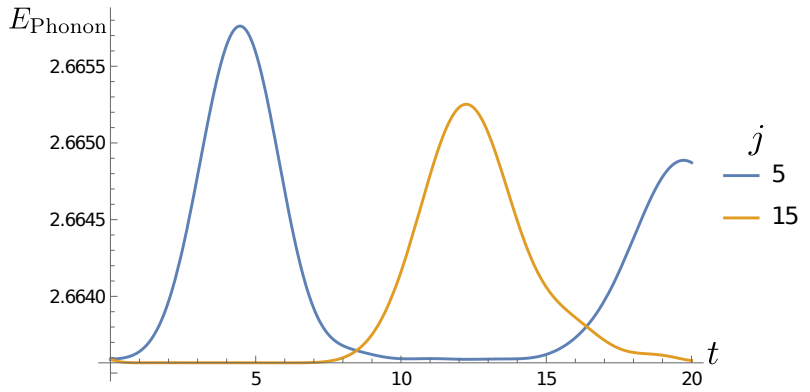


Figure 21: Plot representing the time evolution of the energy phonon subsystem. There is only one spin, and the phonons initially form a Gaussian wave packet centered around a moment $q_0 = 1$. The blue curve correspond to the case where the spin is at the position $j = 5$, and $j = 15$ for the orange one. The chain is composed of $N = 20$ and periodic boundary conditions are imposed.

.

does not diverge when $N \to +\infty$, and that phonon evolution does indeed become unitary again in the continuous limit.

8.4.1 Generalization of the model

In this case the Hilbert space associated to the phonon subsystem is unchanged and one associated to the spins is simply

$$\mathcal{H}_{\text{Spins}} = \bigotimes_{j=1}^{N} \mathcal{H}_{\text{Spin,j}}, \tag{8.83}$$

where $\mathcal{H}_{\text{Spin,j}}$ is the Hilbert space associated to the j^{th} spin, and has been defined in section 8.2.3. A basis of $\mathcal{H}_{\text{Spins}}$ will be noted $|\{s\}\rangle$ and is defined by $|\{s\}\rangle = \otimes_{j=1}^{N} |s_j\rangle$ with $s_j = \pm 1$. It represents the state for which the j^{th} spins are in the respective states $|s_j\rangle$. On the other hand the Hamiltonian

(8.39) is replaced by

$$H = \underbrace{\sum_{j=1}^{N} : \left[\frac{p_j^2}{2M} + \frac{K}{2}(u_j - u_{j+1})^2\right] :}_{H^{(0)}} + \underbrace{\alpha \sum_{j=1}^{N} S_{z_j} : \left[\frac{p_j^2}{2M} + \frac{4\pi^2}{Na^2}\frac{M}{2N}\left(\sum_q \omega_q u_q e^{-iqja}\right)^2\right] :}_{\alpha H^{(1)}} \tag{8.84}$$

$$= \sum_q \omega_q a_q^\dagger a_q + \frac{\alpha}{N}\sum_{j,q,q'} S_{z_j} e^{-i(q+q')ja}\sqrt{\omega_q \omega_{q'}}\, a_{-q'}^\dagger a_q \tag{8.85}$$

The perturbative analysis made in part 8.3 can directly be extended to this case. We just need to compute the relevant coefficients of this new interaction Hamiltonian defined in (8.84) and then use the result (8.46). So first, we need the relation

$$\langle 1_{q'}, \{s'\}| H^{(1)} |1_q, \{s\}\rangle = \frac{\delta_{\{s\},\{s'\}}}{N}\sum_j s_j e^{-ia(q-q')ja}\sqrt{\omega_q \omega_{q'}}. \tag{8.86}$$

As was done in the section 8.3.2, one can estimate the limiting time $t_\star$ of validity of the perturbative solution. We will limit ourself to estimate a lower bound of $t_\star$ and limit the study of the dynamics to this duration. To do so, one need to insert the result (8.86) in (8.51). One can see that

$$|\langle 1_q, \{s\}| H^{(1)} |1_q, \{s\}\rangle| \leq \omega_q, \tag{8.87}$$

therefore

$$t_\star = \frac{1}{\alpha\omega_q}. \tag{8.88}$$

Since $\alpha \ll 1$, one can say that the time of validity of the perturbative approximation is much bigger than the characteristic time of oscillation of a mode having a frequency ω_q.

8.4.2 Dynamics of the subsystems

In what follow, we will focus on the dynamics of a plane wave with all the spins in the eigenstate $|+_x\rangle$ of the operator S_x. More formally, the initial state will be

$$|\psi(0)\rangle = \frac{1}{\sqrt{2^N}}\sum_{\{s\}} |1_{q_0}, \{s\}\rangle \tag{8.89}$$

Therefore, since the initial state is a linear combination of one particle state and the interacting Hamiltonian preserves the number of particles, one can write the wave function at time t as follow

$$|\psi(t)\rangle = \frac{1}{\sqrt{2^N A}}\sum_{q,\{s\}} h(q, \{s\}, t) e^{-it\omega_q} |1_q, \{s\}\rangle . \tag{8.90}$$

One can then insert (8.86) and (8.89) in (8.46) to obtain the perturbative dynamics of this new system. One can show that

$$h^{(0)}(q,\{s\},t) = \delta_{q,q_0} \tag{8.91}$$

$$h^{(1)}(q,\{s\},t) = -\frac{i}{N}\sum_{j=1}^{N} s_j e^{-i(q_0-q)ja}\sqrt{\omega_q\omega_{q_0}}\int_0^t e^{-it'(\omega_{q_0}-\omega_q)}dt' \tag{8.92}$$

$$\begin{aligned} h^{(2)}(q,\{s\},t) = &-\frac{1}{N^2}\sum_{q',j,j'} s_j s_{j'} e^{-ia(q'-q)j} e^{-i(q_0-q')j'a}\omega_{q'}\sqrt{\omega_{q_0}\omega_q} \\ &\times \int_0^t e^{-it'(\omega_{q'}-\omega_q)}\int_0^{t'} e^{-it''(\omega_{q_0}-\omega_{q'})}dt''dt'. \end{aligned} \tag{8.93}$$

One can now study the dynamics of the two different subsystems phonons and spins. As before, we start by writing down the density matrix of the total state (8.90)

$$\rho(t) = \frac{1}{2^N}\sum_{q,q',\{s_1\},\{s_2\}} h(q,\{s_1\},t)\overline{h(q',\{s_2\},t))}e^{-it(\omega_q-\omega_{q'})}\left|1_q,\{s_1\}\right\rangle\left\langle 1'_q,\{s_2\}\right|. \tag{8.94}$$

One can then deduce the expression of the density matrices of the two subsystems

$$\left\langle 1_q\right|\rho_{\text{Phonon}}\left|1_{q'}\right\rangle = \frac{1}{2^N}\sum_{\{s\}} h(q,\{s\},t)\overline{h(q',\{s\},t))}e^{-it(\omega_q-\omega_{q'})} \tag{8.95}$$

$$\left\langle\{s_1\}\right|\rho_{\text{Spins}}(t)\left|\{s_2\}\right\rangle = \frac{1}{2^N}\sum_{q} h(q,\{s_1\},t)\overline{h(q,\{s_2\},t)}. \tag{8.96}$$

The analysis is more involved due to the fact that the dimension of the spins density matrix is now $2^N \times 2^N$ which make the direct computation of the Von Neumann entropy via diagonalization impractical. However, it is possible to use the replica trick implying that

$$S(\rho) = -\frac{\partial \log(\text{Tr}\rho^k)}{\partial k}\bigg|_{k=1}. \tag{8.97}$$

A lengthy calculation (see Appendix E) leads to the following result[22]

$$S(\rho_{\text{Spins}}) = 2\frac{\alpha^2}{N}\left(\sum_q \omega_q\omega_{q_0}\left(\frac{\sin\left(\frac{t}{2}(\omega_q-\omega_{q_0})\right)}{\omega_q-\omega_{q_0}}\right)^2 - (\omega_{q_0}t)^2\right) + \mathscr{O}(\alpha^3) \tag{8.98}$$

One expects a bound of the form $S \leq N\log(2)$ which is the entropy of the maximally mixed state. The Von Neumann entropy can grow in time and the time dependence we observe here is the one controlled by the perturbative approximation to second order in α. It is easy to find a constant bound for the previous expression in the large N limit and evaluating it at the maximum allowed time (8.88), namely

$$S \leq \frac{1}{2}. \tag{8.99}$$

[22] In our situation (to second order in α) all of the Rényi entropies coincide up to an overall factor.

The continuum limit of the entropy formula:

We can now take the large N limit of the previous entropy formula, namely $N \to \infty$. The sum in (8.98) becomes and integral which (by appropriate change of variables can be written as)

$$S = \frac{4\alpha^2\omega}{\pi\omega_p} F\left(t,\omega\right), \tag{8.100}$$

with

$$F\left(t,\omega\right) \equiv \int_0^{\frac{\pi}{2}} d\phi\, \omega_p^2 \sin(\phi) \left(\frac{\sin\left(\frac{t}{2}(\omega_p \sin(\phi) - \omega)\right)}{\omega_p \sin(\phi) - \omega} \right)^2, \tag{8.101}$$

and with $\omega_p = \sqrt{\frac{2K}{M}}$ the Planck frequency. As shown in figure 22, the F function, and therefore

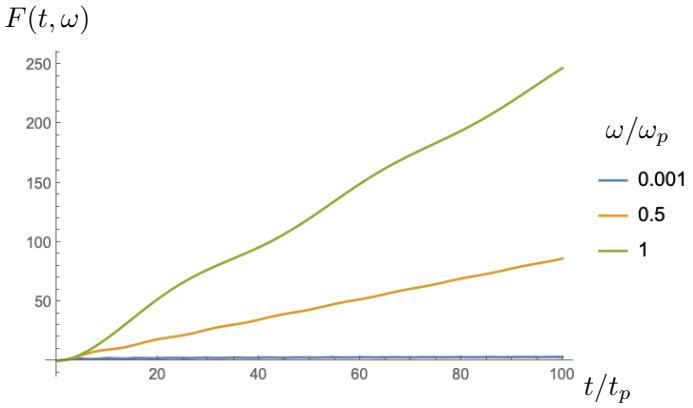


Figure 22: Plot of the form factor entering in the continuum limit of the entropy formula (8.100) for three characteristic values of the phonon frequency.

.

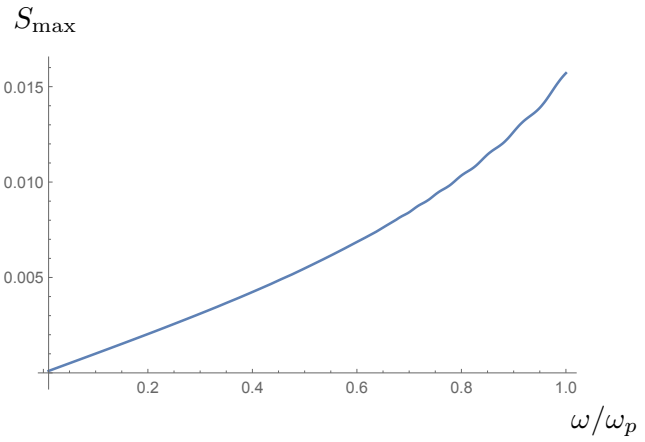


Figure 23: Value of the entropy at the maximum time $t_\star$ as a function of ω (for $\alpha = 10^{-2}$).

.

the entropy of the phonon subsystem S, increases faster with time as the frequency of the initial

mode increases. At the end, meaning for the longest time preserving the validity of the perturbative resolution, the entropy reached by this subsystem also increases significantly with frequency. As can be seen in figure 23, the maximum entropy reached by phonons when the initial mode has a frequency $\omega \ll \omega_p$ is completely negligible compared to its value when the mode has an initial frequency $\omega \sim \omega_p$. This brings us back to a result in line with those obtained in the previous subsections : the decoherence happens significantly only for high frequency modes.

Finally, let us consider the continuum limit corresponding to $a \to 0$. According to the definition of K and M given in subsection 8.2.1 this limit correspond to the case where $\omega_p \to +\infty$. It is possible to show after some algebraic manipulation on (8.101) that the entropy (8.100) verifies $S = \mathcal{O}\left(\frac{\omega}{\omega_p}\right)$ In other words, in this limit, corresponding to the usual framework of QFT where there is no fundamental UV cut off, the phonon subsystem decoherence phenomenon completely disappears and a unitary evolution is recovered. The effect of the spin defects is no longer felt.

The following paragraph is extremely speculative, since it extrapolates the results of this model to our world. The conclusions we draw about the physics of our world are merely analogies of the results of the model played out, but should not be taken as anything more than that. The result obtained in the limit $N \to +\infty$ therefore opens up the possibility that local defects like those considered here could be very present around us. We simply would not be sensitive to them for the simple reason that we have no experiments capable of producing energies (or frequencies) close to Planck energy (or Planck frequency). Moreover, the results obtained in the $a \to 0$ limit, which is the limit usually adopted in QFT, prevent us from having a theory capable of revealing the presence of these defects, as well as the possible decoherence of the highly energetic modes of matter with these defects, since in the continuum limit, the entropy of each of the subsystems vanishes.

8.4.3 Degeneracy of the eigenstates

One of the key features of the model is that the ground state as well as all energy levels have a degeneracy 2^N at zeroth order in α due to the absence of the spin variables in H_0 (8.37). Here we show that the degeneracy does not completely disappear when the spin dependent perturbation is taken into account. In particular, the ground state of the system remains degenerate, and that, for all orders in perturbation theory. In this sense, one can regard the underlying degeneracy of the ground state as one of the land marks of the model which sharply contrasts with what is generically assumed in the context of QFTs (indeed the uniqueness of the vacuum is one of the central axioms of the algebraic approach to QFT). Our model suggests that such an axiom can be abandoned without important consequences in the low energy regime.

Let us now prove the previous statement. At zeroth order in α we have that the energy eigen states are given by $|\psi^{(0)}_{\{n_q\},\{s\}}\rangle = |\{n_q\},\{s\}\rangle$ with energy eigenvalues

$$E^{(0)}_{\{n_q\},\{s\}} = \sum_q n_q \omega_q, \tag{8.102}$$

which are independent of the spins and therefore with and obvious degeneracy 2^N. This is particular true for the ground state $E^{(0)}_{\{0\},\{s\}} = 0$. Usually the perturbation theory raises such degeneracies; however, this is not the case in the present case. To see this we write the Schroedinger equation to

first order in α, namely

$$\left(H^{(0)} - E^{(0)}_{\{n_q\},\{s\}}\right) |\psi^{(1)}_{\{n_q\},\{s\}}\rangle + \left(H^{(1)} - E^{(1)}_{\{n_q\},\{s\}}\right) |\psi^{(0)}_{\{n_q\},\{s\}}\rangle = 0. \tag{8.103}$$

Contracting the previous equation with $\langle\psi^{(0)}_{\{n_q\},\{s\}}|$ one has

$$\begin{aligned} E^{(1)}_{\{n_q\},\{s\}} &= \langle\psi^{(0)}_{\{n_q\},\{s\}}|\, H^{(1)}\, |\psi^{(0)}_{\{n_q\},\{s\}}\rangle \\ &= \frac{\sum_j s_j}{N} \sum_q \omega_q n_q. \end{aligned} \tag{8.104}$$

One has (directly from (8.52) and (8.84)) that

$$\left(H^{(0)} + H^{(1)}\right) |\psi^{(0)}_{\{0\},\{s\}}\rangle = 0, \tag{8.105}$$

the zeroth order ground state is the ground state of the full Hamiltonian. There are no corrections to the ground state to arbitrary orders in α and the 2^N degeneracy of the phonon vacuum remains.

8.5 Conclusion

Let us now summarize the main features of the QFT model we have presented, with particular emphasis on their analogy with the process of black hole formation and evaporation, as described in subsection 6.2.4. We first observed in subsection 8.3.3 that spins do not store energy. This property is already expected, as suggested by the expressions of the free Hamiltonian (8.25) and the interaction Hamiltonian (8.52) or (8.84), which do not contain terms involving only spin operators. We have also seen that a wave packet evolving between two asymptotic spin free regions has the same energy at the beginning as at the end of its evolution. This is analogous to the evolution of an initially pure quantum field, which collapses to form a black hole. This field has an energy corresponding to the mass of the black hole and is initially located in a region of low curvature, where the planckian d.o.f of the geometry can be ignored. At the end of the black hole's life, the matter field, corresponding to Hawking radiation, is in a mixed state. It contains all the energy initially present (with the exception of a possible remnant of Planck mass) and is once again located in a region of low curvature. Moreover, in our model, the increase in phonon entropy is due to their entanglement with spins, which occures in a local way, i.e. when the phonon wave packetis close to these spin. They represent the planckian d.o.f. of the geometry which, in the case of black holes, induce decoherence of the matter field when it reaches regions of high curvature. Our model thus illustrates a decoherence process without energy dissipation, analogous to the black hole formation and evaporation scenario presented in subsection 6.2.4.

This evolution from a pure state to a mixed state is made possible in our model thanks to the degeneracy of the energy levels of the total system, and in particular of the fundamental level. This degeneracy allows the spins to be in a superposition of states, all of zero energy. This is again analogous to the scenario expected in the case of black hole evaporation: the final geometry, after complete evaporation of the black hole, should be in a superposition of states entangled with Hawking radiation, without containing any residual energy since all the energy is found in Hawking radiation. In our model, this decoherence process occurs only for high energy modes, while it

disappears for low energy ones. This distinction is essential to maintain the analogy with black hole physics and, more generally, with QFT in curved spacetime. Indeed, our scenario predicts that the unitarity of quantum field evolution is broken in high energy regimes close to the Planck scale, as is the case near the singularity of a black hole. On the other hand, it must be preserved in low energy regimes, where the quantum effects of geometry are negligible compared to the Planck energy.

In summary, our model demonstrates how, thanks to the degeneracy of the ground state and the possibility for spins to be in a superposition of zero energy states, it is possible to reproduce a decoherence process analogous to that expected for the formation and evaporation of black holes. This provides a picture of how Hawking radiation can maintain correlations with the remaining geometry after the black hole has completely evaporated, while respecting the conservation of energy.

Conclusion and outlooks

In this thesis, we explored perturbative as well as non perturbative approaches in order to formulate a quantum description of gravity. In particular, e focused on the physics of black holes, which necessitates extending the framework of general relativity currently used to describe them in several key aspects. Our work has focused on three of these aspects: studying the first quantum corrections appearing for physical quantities such as the energy of interaction of an object around a black hole, the singularity at its center, and the black hole evaporation phenomenon inducing information loss. We will now summarize the results obtained in this work and discuss several avenues for future research that could enrich the results presented here.

The starting point of this work was to adopt the EFT treatment of general relativity. In Chapter 1, we emphasized that, despite the non renormalizability of the theory, treating it as an EFT allows for finite and reliable predictions at low energy scales, where the curvature remains small compared to the Planck curvature. Importantly, the predictions obtained from this approach are independent of the underlying, yet unknown, complete theory of quantum gravity. Therefore, any future theory of quantum gravity must reproduce these low energy results, just as general relativity converges to Newtonian gravity in the appropriate limit.

From this EFT perspective, we explored in chapter 2 how perturbative quantum predictions can be compared to non perturbative quantum black hole models formulated as modified Schwarzschild metrics free of singularities. A central theme of this chapter was the use of the energy of interaction between two static sources to make this comparison explicit. This energy of interaction has been computed years ago within the perturbative framework, and it can also be estimated for non perturbative black hole models. It is expected that the latter has to reproduce the former in the low curvature regime since non perturbative approaches should match perturbative predictions in this regime. Special attention was given to handling gauge freedom consistently, ensuring a meaningful comparison. A point that has been a source of errors in previous studies. This careful approach allowed us to assess the validity of various modified Schwarzschild metrics against the perturbative predictions. Specifically, we found that the Hayward metric does not accurately reproduce the expected quantum corrections, which raises questions about its reliability. We concluded the chapter by outlining the most general form of a modified Schwarzschild metric that aligns with the perturbative computations.

In the future, it would be interesting to reproduce a similar analysis for other physical quantities. Specifically, it has been shown in [201] that the perturbative approach can estimate quantum corrections to the deviation angle of light rays near a black hole. It would therefore also be relevant to determine the most general modified black hole metric capable of reproducing this result. This would provide additional constraints on the most general metric compatible with perturbative predictions. However, it could be that the metric obtained by this comparison is incompatible with the one we have established in chapter 2. Such a result would be particularly interesting, as it would illustrate one of the main lessons of the EFT treatment of general relativity: a metric description of geometry becomes unsuitable at the Planck scale.

The interest in treating general relativity as an EFT is therefore obvious, but this approach does

not answer a number of questions concerning Planckian curvature regimes. This is why we then turned to a non perturbative approach to quantum gravity, namely LQG. The aim of chapter 3 was to recall the LQG formalism, while introducing models of quantum black holes inspired by this approach, known as polymer black holes. The main feature of these models is that they replace the classical singularity with a black to white hole transition (or a bounce by analogy with cosmology). However, they have certain shortcomings, which we mentioned at the end of this chapter. One of these is that these models rely on a regularization of classical dynamics that is not unique. In particular, this regularization is constructed from an arbitrary choice of the so called polymerization function.

In chapter 4, we investigate the effects of modifying these polymerization functions on the dynamics. We found that the following properties of these models are independent of this choice: the presence of at least one black to white hole transition, the existence of a minimal value for the area radius, the absence of curvature singularities, geodesic completeness, the possibility of a remnant left at the end of evaporation. On the other hand, other properties strongly depend on the choice of these functions: the asymptotic structure, the exact value for the minimal value of the area radius, the number of horizons and the number of bounces. We ended this chapter by showing that the results obtained in chapter 2 could impose certain constraints on this ambiguity. In particular, we found that the choice of sine functions, which is usually made, fails to recover the quantum correction of the energy of interaction derived from the perturbative approach. It is reasonable to expect that obtaining quantum corrections at higher orders would bring more constraints on the polymerization functions. But since higher order corrections requires to know the irrelevant coupling constants of gravity, this clearly illustrates that the non-renormalizability of general relativity is linked to the problem of ambiguity in the choice of regularization functions for polymer black hole models.

These polymer black holes also have the drawback of providing only an effective description of geometry at the Planck scale, and most of them do not account for the presence of matter. The goal of chapter 5 was to address these limitations while avoiding the ambiguity issues highlighted in the previous chapter. Our focus was on the dynamics within the deep interior of black holes, using a symmetry reduced model based on the Klein-Gordon equation for scalar fields. We showed that solutions to this equation, in a regime where $r \ll M$, behave similarly to those of the KS symmetry reduced model. This resemblance enables the study of backreaction effects for scalar matter fields falling into black holes, with the KS model providing a useful framework for understanding the near singularity dynamics. Our analysis suggested that the deep interior of a black hole can be treated as a simplified quantum system, where the complexities of full quantum gravity are reduced, allowing for more manageable calculations. By employing these symmetry reduced models, we proposed a quantization scheme similar to LQG, in which the area of constant radius spheres acquires a discrete spectrum. This quantization scheme naturally leads to a Hilbert space larger than the one obtained by the usual Schroedinger quantization. This enlargement is parametrized by a parameter called ϵ, which characterizes the geometry of our model at the Planck scale and to which a macroscopic observer is not sensitive. Remarkably, the model provided exact solutions, even at the quantum level, which could be interpreted through effective evolution equations that align with Einstein's equations in low energy regimes. This established a solid foundation for exploring how semiclassical states might behave near black hole singularities, suggesting that quantum corrections could either resolve or significantly mitigate the classical divergences typically found in such regions. One key

aspect of this model that we want to insist on is that in the vacuum case, we treated the mass operator as a Dirac observable, quantized it and explicitly determined its spectrum. We have established that the spectrum of this operator is degenerate, with this degeneracy characterized by the Planckian parameter ϵ, which we have interpreted as a quantum hair. A single value of the macroscopic observable M corresponds to an infinite number of Planckian states, parameterized by ϵ. This resembles the behavior of a typical thermodynamic system, where one set of state variables corresponds to a multitude of planckian configurations.

Before we address what this model might reveal about the information loss paradox, it is important to discuss a key assumption made throughout this part, which is critical to the framework. The model relies on certain simplifying symmetry considerations, hence the term symmetry reduced model. But can we relax some of these symmetry constraints? In the model presented in chapter 5, we considered only spherically symmetric field modes. An interesting extension would be to introduce modes that break this symmetry and examine their backreaction on the geometry. However, a general model without these symmetry consideration would be significantly more complex and challenging to analyze analytically. Primarily because spherical symmetry allows for a finite dimensional system, removing this symmetry would result in an infinite dimensional model. Despite the complications, it could still be valuable to gain a deeper understanding of how fluctuations of the energy momentum tensor behave in regions of planckian curvature. Strong fluctuations in this tensor are expected to have significant effects on the geometry, suggesting that quantum fluctuations in the geometry might not be negligible. If this is true, it would imply that an effective, smooth description of the geometry is no longer viable. This effect could play a particularly crucial role in understanding the process of black hole evaporation.

The final part of this thesis focused on the so called information loss puzzle. We began in chapter 6 with a reminder of the historical results of Hawking, Wald and Parker leading to a loss of information, or more formally to a breakdown of unitarity. We motivated the idea that this problem in black hole formation and evaporation necessitates a deep understanding of the strong quantum gravity regime near the singularity beyond the black hole horizon. This presents a challenge for both the holographic and non-holographic perspectives. In the holographic view, macroscopic black holes are believed to possess a finite number of internal d.o.f bounded by their horizon area. Consequently, they are expected to follow a standard Page curve, wherein the exterior entropy starts decreasing at the macroscopic stage known as the Page time. Conversely, in the non-holographic perspective, which is the framework of this work, the number of internal d.o.f inside black holes is unrelated to their horizon area. In the scenario we are defending, the exterior entropy continues to grow while the black hole is macroscopic, and the purification occurs after the semiclassical regime. Information is recovered after the complete evaporation of a black hole, and it is essential to identify the appropriate purifying d.o.f. Subsequently, understanding how the correlations between the Hawking partners are dynamically transferred to these d.o.f becomes crucial. Suitable d.o.f are those that can persist after complete evaporation without significantly affecting the energy budget, considering that there is at most a Planck mass energy available for the multitude of d.o.f needed to purify the total emitted Hawking radiation. These d.o.f. appear in planckian regimes and are the ones from which, according to the EFT treatment of general relativity, emerge the notion of smooth geometry and metrics in which the classical theory is formulated. However there is so far no non perturbative theory that can clearly identify them and fully describe their dynamics.

In chapter 7 we show how to use the model presented in chapter 5 to illustrate the scenario we are defending. Indeed this model was designed to capture the near-singularity dynamics of a scalar excitation, aiming at represent the ingoing Hawking modes, and to include its backreaction. The model incorporates planckian "weightless" d.o.f. Specifically, the mass operator's spectrum shows infinite degeneracy due to quantum hair parametrized by the quantity ϵ. By initially considering a scalar excitation correlated to a free excitation representing the outgoing Hawking radiation, we showed how correlations dynamically transfer to the quantum hair ϵ as the inner excitation nears the singularity. While this model does not track the complete evaporation of a black hole, it suggests that at the end of the process, the Hawking radiation remains entangled with planckian geometric d.o.f restoring the purity of the total system.

This model is however too simple to fully resolve the information loss paradox. In addition to not fully describing the evaporation of a black hole, this model relies on the assumption of spherical symmetry, which limits the number of d.o.f to a finite number. It is difficult to go any further without a complete theory of quantum gravitation. However, in chapter 8 we presented a quantum field theory model including a hidden sector (i.e. additional local d.o.f) able to induce matter field decoherence without storing any energy. The aim was to propose an analogy with the process of formation and evaporation of a black hole as we have imagined it up to now. This model shows that a matter field can develop correlations with a hidden sector, represented here by a collection of spins, analogous to the Planckian degrees of freedom of geometry. And this only in high energy regimes, similar to the Planckian curvature regime for a black hole. Furthermore, this decoherence occurs without the spins storing energy. This is made possible by the degeneracy of energy levels, parameterized by the different spin states. This is analogous to the mass operator degeneracy parameterized by ϵ in the symmetry reduced model of chapter 5.

In future, we would like to explore the role of quantum fluctuations in the energy of the matter field. We have already mentioned in the previous paragraph the interest of better understanding the role of quantum fluctuations of the energy momentum tensor in strong curvature regimes. This is in order to determine whether they induce significant fluctuations in the geometry, which would prevent an effective description of the latter. It seems more accessible, at least initially, to carry out this study within the framework of our simplified model. We expect a field mode to see its quantum energy fluctuations increase significantly as it interacts with the spins, but only for sufficiently high frequency modes. This should lead to large fluctuations in the spin state, making it impossible to provide an effective description of the spins.

Taken together, the results of this thesis provide a multi-faceted exploration of the quantum properties of black holes. By connecting perturbative and non-perturbative approaches, and by imagining simplified models, we have been able to bring some insight regarding the problem of singularity and the loss of information. Yet, even when one is still far from the full understanding of these issues, we hope that the indications provided by models presented here stimulate possibilities and new ideas that could show useful for researchers investigating these central problems.

A Background field formalism and the Heat Kernel method

We will review the Heat Kernel method which is a powerful technic to determine the counter terms to add to the action in order to remove the 1 loop divergences. In order to do so, it will be useful to introduce the Background Field formalism allowing to express the 1 loop effective action. The idea is to decompose the field of interest $\phi(x)$ as a quantum perturbation $\eta(x)$ around a classical background $\phi_o(x)$, i.e.

$$\phi(x) = \phi_o(x) + \eta(x). \tag{A.1}$$

The classical background is by definition a solution of the classical equation of motion and therefore satisfy

$$\frac{\delta S[\phi]}{\delta \phi}[\phi = \phi_0] = 0, \tag{A.2}$$

with $S[\phi] = \int d^4x \mathcal{L}[\phi(x)]$ is the action of the system. When we are interested by the quantum dynamics, it is useful to introduce the partition function which can be expressed as follow

$$Z[J] = \int D\phi e^{i\int d^4x(\mathcal{L}[\phi(x)]+J(x)\phi(x))}, \tag{A.3}$$

where $J(x)$ is a source term. One of the reason why this quantity is so important in quantum field theory is that it is the generating functional for n point correlation functions (which are perturbatively computed as the sum of all connected and disconnected Feynman diagrams). An other useful quantity is the generating functional of n points connected correlation functions (perturbatively computed as the sum of all connected Feynman diagrams), namely

$$W[J] = -i \log \frac{Z[J]}{Z[0]}. \tag{A.4}$$

From this relation, one can see that

$$\frac{\delta W}{\delta J} = \frac{\int D\phi\phi(x) e^{i\int d^4x(\mathcal{L}[\phi(x)]+J(x)\phi(x))}}{\int D\phi e^{i\int d^4x(\mathcal{L}[\phi(x)]+J(x)\phi(x))}} = \langle 0|\, \phi(x)\, |0\rangle =: \phi_c(x). \tag{A.5}$$

The quantity ϕ_c hence introduced correspond to the classical background field plus the expectation of the quantum with regards to the vacuum state. It is then possible to define the effective action $\Gamma[\phi_c]$ by a Legendre transformation of $W[J]$ as follow

$$\Gamma[\phi_c] = W[J] - \int d^4x J(x)\phi_c(x). \tag{A.6}$$

It is also possible to show that this quantity is the generating functional of one particle irreducible n point correlation functions (perturbatively computed as the sum of all connected Feynman diagrams which cannot lead to two piece by cutting a single internal line). Moreover, one can see from (A.6) that the effective action satisfies

$$\frac{\delta\Gamma[\phi]}{\delta\phi}[\phi=\phi_c]=-J(x) \tag{A.7}$$

In the case where there is no source, (A.7) becomes very similar to (A.2). This tells us that the classical background field corrected by the vacuum expectation of the perturbation does note extremize the action anymore but Γ. This is why this quantity is called the effective action. Let us see how the effective action is related to the original action. To do so, we can start by expanding the partition function (A.3) with respect to η (define by (A.1))

$$Z[J]\approx e^{\frac{i}{\hbar}\left(S[\phi_o]+\int d^4xJ(x)\phi_o(x)\right)}\int D\eta e^{\frac{i}{2\hbar}\frac{\partial^2 S}{\partial\phi(x)\partial\phi(y)}[\phi_o]\eta(x)\eta(y)+....} \tag{A.8}$$

$$\approx e^{\frac{i}{\hbar}\left(S[\phi_o]+\int d^4xJ(x)\phi_o(x)\right)}\det\left(\frac{\partial^2 S}{\partial\phi(x)\partial\phi(y)}[\phi_o]\right)^{-1/2}+\mathcal{O}(\hbar^2). \tag{A.9}$$

Then by using the relations (A.4) and (A.6) one can conclude that

$$\Gamma[\phi_c]=S[\phi_o]+\underbrace{\frac{i\hbar}{2}\log\left(\det\frac{\partial^2 S[\phi]}{\delta\phi(x)\delta\phi(y)}[\phi=\phi_o]\right)+\mathcal{O}(\hbar^2)}_{=\hbar\Gamma_{\text{1-loop}}} \tag{A.10}$$

One can also note than since $\phi_c(x)=\phi_o(x)+(\hbar)$ one can write the previous formula in the following way

$$\Gamma[\phi_o]=S[\phi_o]+\frac{i\hbar}{2}\log\left(\det\frac{\partial^2 S[\phi]}{\delta\phi(x)\delta\phi(y)}[\phi=\phi_o]\right)+\mathcal{O}(\hbar^2) \tag{A.11}$$

We can now come to the main point of this appendix which is to show how one can compute the effective action at 1 loop order (i.e. the second term of the left hand side of (A.11)) without going through perturbative computations but via the Heat Kernel method. This part is be based on [3, 202]. We will limit ourselves to giving a formal presentation of this method, a more rigorous presentation can be found in [202] and references therein. Let us start by introducing the following notations

$$D=\frac{\partial^2 S[\phi]}{\delta\phi(x)\delta\phi(y)}[\phi=\phi_o]\quad\text{and}\quad K(x,y,t,D)=e^{-tD}\delta(x,y), \tag{A.12}$$

implying for K to satisfy the heat equation (hence the name of the method)

$$\left(\frac{\partial}{\partial t}+D\right)K(x,y,t,D)=0\quad\text{with}\quad K(x,y,0,D)=\delta(x,y). \tag{A.13}$$

In the case where the system is described by a free Lagrangian, i.e. $D=D_0:=-\nabla_\mu\nabla^\mu+m^2$, the solution to (A.13) is given by

$$K(x,y,t,D_0)=\frac{1}{(4\pi t)^2}\exp\left(-\frac{(x-y)^2}{4t}-tm^2\right). \tag{A.14}$$

it turns out that this result remains the dominant contribution for a more general D (containing self-coupling terms or coupling with other fields) in the limit $\tau \to +\infty$. Corrections to this result can be written as follows

$$K(x,y,t,D) = K(x,y,t,D_0)(a_0 + ta_1(x,y) + t^2 a_2(x,y) + ...), \tag{A.15}$$

where the a_k are called the heat kernel (or DeWitt–Seeley– Gilkey) coefficients. Their exact form will depend on the exact expression of D. We now have everything we need to compute the one loop correction to the effective action (A.11). First let us write this quantity in the following way

$$\Gamma_{\text{1-loop}} = \frac{i\hbar}{2}\log(\det D) = \frac{i\hbar}{2}\text{Tr}(\log D), \tag{A.16}$$

where $\text{Tr}(D) = \int_{-\infty}^{+\infty} d^4x\sqrt{-g}D(x,x)$ (we consider that there are no internal indices in order to lighten the notations. In the case where there would be, the trace must also be taken over these indices). By applying the formula

$$\log\lambda = -\int_0^{+\infty}\frac{dt}{t}e^{-t\lambda} \tag{A.17}$$

(which is true up to a infinite constant which can be ignored) to any eigenvalue of the operator D, we end up with

$$\Gamma_{\text{1-loop}} = -\frac{i\hbar}{2}\int_0^{+\infty}\frac{dt}{t}\text{Tr}e^{-tD} \tag{A.18}$$

$$= -\frac{i\hbar}{2}\int_0^{+\infty}\frac{dt}{t}\int_{-\infty}^{+\infty} d^4x\sqrt{-g}K(x,x,t,D). \tag{A.19}$$

However the integral in (A.18) can diverge at both limits. On the one hand the null and negative eigenvalues of D are responsible of the divergence of the integral at $t = +\infty$. These divergences correspond to infrared divergences and will note be considered here. On the other hand, by inserting (A.15) in (A.18), one could see that the three first terms of the expansion (A.15) will lead to divergences at $t = 0$. They correspond to UV divergences, in order to regularize them we will introduce a UV cut off at $t = \Lambda^{-1}$. The diverging part of $\Gamma_{\text{1-loop}}$ in the limit $\Lambda \to +\infty$ is given by

$$\Gamma^{\text{div}}_{\text{1-loop}} = -\frac{1}{16\pi^2}\int d^4x\sqrt{-g}\left[\sum_{j+l<2}\Lambda^{2-2j-2l)}a_j(x,x)\frac{(-m^2)^l l!}{2-2j-2l} + \sum_{j+l=n}\log(\Lambda)(-m^2)^l l! a_j(x,x)\right] \tag{A.20}$$

We have therefore finally computed the divergent part of the effective action at one loop. These divergences correspond precisely to the counter terms to be added to the initial action to obtain finite physical predictions at this order. Interestingly, for $x = y$ heat kernel coefficients $a_k(x,y)$ are local polynomials of background fields and their derivatives [202]. This implies that the counter terms to be added in the action are, at least at one loop order, local polynomials of background fields and their derivatives. We finish this appendix by mentioning that the finite part of the effective action can also be computed and is given by

$$\Gamma^{\text{finite}}_{\text{1-loop}} = -\frac{1}{16\pi^2} m^4 \int d^4x \sqrt{-g} \sum_{j>2} \frac{\Gamma(2j-n)}{m^{2j}} a_j(x,x). \tag{A.21}$$

B Boundary term

In this Appendix we recall the derivation of the minisuperspace Lagrangian (4.6). We consider a single boundary given by a r=constant hypersurfaces outside the horizon. The total action including the Gibbons-Hawking-York boundary term is

$$S[C] = \frac{1}{16\pi}\int dr \int_C d^3x\sqrt{-g}R - \frac{1}{8\pi}\int_C d^3x\sqrt{|h|}K. \tag{B.1}$$

With the ansatz (4.1), we have

$$\sqrt{-g}R = \sin(\theta)\left(2\sqrt{\bar{n}} - \frac{4\bar{b}\dot{\bar{a}}\dot{\bar{b}}}{\sqrt{\bar{n}}} - \frac{2\bar{a}\dot{\bar{b}}^2}{\sqrt{\bar{n}}} + \frac{\bar{b}^2\dot{\bar{a}}\dot{\bar{n}}}{2\bar{n}^{3/2}} + \frac{2\bar{a}\bar{b}\dot{\bar{b}}\dot{\bar{n}}}{\bar{n}^{3/2}} - \frac{\bar{b}^2\ddot{\bar{a}}}{\sqrt{\bar{n}}} - \frac{4\bar{a}\bar{b}\ddot{\bar{b}}}{\sqrt{\bar{n}}}\right), \tag{B.2}$$

hence the Einstein-Hilbert term gives

$$\frac{1}{16\pi}\int_C d^3x\sqrt{-g}R = \frac{\ell_0\sqrt{\bar{n}}}{2}\left(\frac{\dot{\bar{a}}\dot{\bar{b}}\bar{b}}{\bar{n}} + \frac{\bar{a}\dot{\bar{b}}^2}{\bar{n}} + 1\right) - \ell_0\frac{\mathrm{d}}{\mathrm{d}r}\left(\frac{\dot{\bar{a}}\bar{b}^2}{4\sqrt{\bar{n}}} + \frac{\bar{a}\bar{b}\dot{\bar{b}}}{\sqrt{\bar{n}}}\right). \tag{B.3}$$

Coming to the boundary term, the unit-normal to the r foliation is, outside the horizon,

$$n = \sqrt{\frac{\bar{n}(r)}{\bar{a}(r)}}dr, \qquad n^2 = 1. \tag{B.4}$$

To this we associate the induced metric and extrinsic curvature

$$q_{\mu\nu} = g_{\mu\nu} - n_a n_b, \qquad K_{\mu\nu} = q^\rho_\mu\nabla_\rho n_\nu = \frac{1}{2}\pounds_n q_{\mu\nu}. \tag{B.5}$$

With the ansatz (4.1), we find

$$q = -\bar{a}\bar{b}^4\sin(\theta)^2, \qquad K = \frac{\dot{\bar{a}}}{2\sqrt{\bar{n}\bar{a}}} + \frac{2\sqrt{\bar{a}}\dot{\bar{b}}}{\sqrt{\bar{n}}\bar{b}}. \tag{B.6}$$

Hence the boundary term gives

$$\frac{1}{8\pi}\int d^3x\sqrt{h}K = \ell_0\left(\frac{\dot{\bar{a}}\bar{b}^2}{4\sqrt{\bar{n}}} + \frac{\bar{a}\bar{b}\dot{\bar{b}}}{\sqrt{\bar{n}}}\right). \tag{B.7}$$

Adding up, we recover (4.6).

C Asymptotic expansion of the metric components

In this Appendix, we provide details on the asymptotic expansion of the metric components (4.73) leading to (4.74). First, one can note that the only functions whose expansions are needed are $f_2(y(x))$ and $f_1'(z(x)) = \frac{\mathrm{d}f_1}{\mathrm{d}z}(z(x))$, while all dependencies of $f_1(z(x))$ have been replaced by the use of the Dirac observable K_1 and Eq. (4.53). This also fixed the function

$$z(x) = f_1^{-1}\left(3\lambda_1 K_1 x^3/2\right) . \tag{C.1}$$

With these notations, the formal Taylor expansions are given by

$$f_2(y(x)) = f_2'(0^\pm)y'(0^\pm)\,x + \frac{1}{2}\left(f_2''(0^\pm)y'(0^\pm)^2 + f_2'(0^\pm)y''(0^\pm)\right)\,x^2 + O\left(x^3\right), \tag{C.2a}$$

$$f_1'(z(x)) = f_1'(0^\pm) + f_1''(0^\pm)z'(0^\pm)\,x + \frac{1}{2}\left(f_1^{(3)}(0^\pm)z'(0^\pm)^2 + f_1''(0^\pm)z''(0^\pm)\right)\,x^2 + O\left(x^3\right) \tag{C.2b}$$

$$\overset{(C.1)}{=} f_1'(0^\pm) + O\left(x^3\right), \tag{C.2c}$$

with $f_i^{(n)}$ denoting the n-th derivative w.r.t. y or z, respectively, while $y' = \mathrm{d}y/\,\mathrm{d}x$ and respectively, y'', z' and z''. It was assumed and will be in the following that $f_i'(0^\pm) \neq 0$, which would also violate the classical limit. These expressions are formal however, as the derivatives $y'(0^\pm)$, $y''(0^\pm)$ are not specified. The derivatives z' and z'' follow from (C.1) and we see that linear and quadratic order vanish exactly. From the equations of motion (4.49) follow the expressions

$$y'(x) = \frac{f_2(y(x))}{x f_1'(z(x))} , \tag{C.3a}$$

$$y''(x) = \frac{f_2'(y(x))f_2(y(x))}{x^2 f_1'(z(x))^2} - \frac{f_2(y(x))}{x^2 f_1'(z(x))} - \frac{9K_1\lambda_1 f_1''(z(x))f_2(y(x))x}{2f_1'(z(x))^3} , \tag{C.3b}$$

Extracting $y'(0^\pm)$ requires then

$$y'(0^\pm) = \lim_{x\to 0} y'(x) = \frac{f_2'(0^\pm)}{f_1'(0^\pm)}y'(0^\pm). \tag{C.4}$$

This implies

$$f_1'(0^\pm) = f_2'(0^\pm), \tag{C.5}$$

with $y'(0^\pm)$ unconstrained.[23] Similarly, for the second derivative, we get

$$y''(0^\pm) = \lim_{x\to 0} y''(x) = \frac{y'(0^\pm)^2 f_2''(0^\pm) + f_2'(0^\pm)y''(0^\pm)}{2f_1'(0^\pm)} , \tag{C.6}$$

which can be solved to obtain

$$y''(0^\pm) = \frac{y'(0^\pm)^2 f_2''(0^\pm)}{f_2'(0^\pm)} . \tag{C.7}$$

[23] Recall that the fixed points are not part of the phase space but only reached asymptotically. This eliminates the possibility of solving (C.4) taking $y'(0^\pm) \equiv 0$.

Here we again used the constraint $f_1'(0^\pm) = f_2'(0^\pm)$. This makes the expansions (C.2) explicit and allows to compute the metric functions, leading to

$$g_{\tau\tau} = -\frac{\lambda_2^2}{16 f_2'(0^\pm)^2 y'(0^\pm)^2}\left(1 - \frac{2y'(0^\pm)\left(12K_1 f_2'(0^\pm)^2 + \lambda_2 f_2''(0^\pm)\right)}{\lambda_2 f_2'(0^\pm)}x\right) + O(x^2)\,, \tag{C.8a}$$

$$1/g_{bb} = f_1'(0^\pm)^2\left(1 - \frac{24K_1 f_2'(0^\pm)y'(0^\pm)}{\lambda_2}x\right) + O(x^2)\,. \tag{C.8b}$$

D Completeness relations

We review the proof of equations (8.30), one the one hand we have

$$\sum_{j=1}^{N} e^{i(q-q')ja} = \begin{cases} \frac{e^{i(q-q')a} - e^{i(q-q')(N+1)a}}{1-e^{i(q-q')}} & \text{if } q \neq q' \\ N & \text{otherwise.} \end{cases} \tag{D.1}$$

And since $q = \frac{2\pi n}{Na}$, we have $e^{i(q-q')(N+1)a} = e^{i(q-q')a}$, which leads to the result we wanted

$$\sum_{j=1}^{N} e^{i(q-q')ja} = N\delta_{q,q'}. \tag{D.2}$$

One the other hand we have

$$\sum_{q\in \mathrm{OBZ}} e^{iq(j-j')a} \tag{D.3}$$

$$= \sum_{n=-N/2+1}^{N/2} e^{2i\pi(j-j')n/N} \tag{D.4}$$

$$= e^{-i\pi(j-j')} \sum_{n=1}^{N} e^{2i\pi(j-j')n/N} \tag{D.5}$$

$$= \begin{cases} e^{-i\pi(j-j')} \frac{e^{2i\pi(j-j')/N} - e^{2i\pi(j-j')(N+1)/N}}{1-e^{2i\pi(j-j')/N}} & \text{if } j \neq j' \\ N & \text{otherwise.} \end{cases} \tag{D.6}$$

And since $q = \frac{2\pi n}{Na}$, we have $e^{iq(j-j')(N+1)a} = e^{iq(j-j')a}$, which leads to the result we wanted

$$\sum_{q\in \mathrm{OBZ}} e^{iq(j-j')a} = N\delta_{j,j'}. \tag{D.7}$$

With these completeness relations, one can now prove the equivalence relation (8.27)

$$u_j = \frac{1}{\sqrt{N}} \sum_{q\in \mathrm{OBZ}} e^{-iqja} u_q \tag{D.8}$$

$$\Rightarrow e^{iq'ja} u_j = \frac{1}{\sqrt{N}} \sum_{q\in \mathrm{OBZ}} e^{-i(q-q')ja} u_q \tag{D.9}$$

$$\Rightarrow \sum_{j=1}^{N} e^{iq'ja} u_j = \frac{1}{\sqrt{N}} \sum_{q\in \mathrm{OBZ}} \sum_{j=1}^{N} e^{-i(q-q')ja} u_q \tag{D.10}$$

$$\Rightarrow \sum_{j=1}^{N} e^{iq'ja} u_j = \sqrt{N} \sum_{q\in \mathrm{OBZ}} \delta_{q,q'} u_q \tag{D.11}$$

$$\Rightarrow \frac{1}{\sqrt{N}} \sum_{j=1}^{N} e^{iqja} u_j = u_q. \tag{D.12}$$

We also have to prove the relation in the other sense

$$u_q = \frac{1}{\sqrt{N}} \sum_{j=1}^{N} e^{iqja} u_j \tag{D.13}$$

$$\Rightarrow e^{-iqj'a} u_q = \frac{1}{\sqrt{N}} \sum_{j=1}^{N} e^{iq(j-j')a} u_j \tag{D.14}$$

$$\Rightarrow \sum_{q \in \mathrm{OBZ}} e^{-iqj'a} u_q = \frac{1}{\sqrt{N}} \sum_{j=1}^{N} \sum_{q \in \mathrm{OBZ}} e^{iq(j-j')a} u_j \tag{D.15}$$

$$\Rightarrow \sum_{q \in \mathrm{OBZ}} e^{-iqj'a} u_q = \sqrt{N} \sum_{j=1}^{N} \delta_{j,j'} u_j \tag{D.16}$$

$$\Rightarrow \frac{1}{\sqrt{N}} \sum_{j=1}^{N} e^{-iqja} u_q = u_j. \tag{D.17}$$

E Calculation of the Entropy using the replica trick

In this appendix, we give some details on the use of the replica trick to obtain the expression of the entropy mentioned in subsection 8.4.2. To do so, we start from the expression (8.95) which, at second order in α is given by

$$\begin{aligned}\langle\{s_1\}|\,\rho_{\text{Spins}}(t)\,|\{s_2\}\rangle =&\frac{1}{2^N}\Big[1+\alpha[h^{(1)}(q_0,\{s_1\},t)+\overline{h^{(1)}(q_0,\{s_2\},t)}] \\ &+\alpha^2[h^{(2)}(q_0,\{s_1\},t)+\overline{h^{(2)}(q_0,\{s_2\},t)}+\sum_q h^{(1)}(q,\{s_1\},t)\overline{h^{(1)}(q,\{s_2\},t)}]\Big].\end{aligned} \tag{E.1}$$

In order to simplify the notations, we will not write explicitly the t and q_0 dependence of each terms and we introduce

$$B(\{s_1\},\{s_2\})=h^{(2)}(\{s_1\})+\overline{h^{(2)}(\{s_2\})}+\sum_q h^{(1)}(q,\{s_1\})\overline{h^{(1)}(q,\{s_2\})}. \tag{E.2}$$

Therefore, one has

$$\langle\{s_1\}|\,\rho_{\text{Spins}}(t)\,|\{s_2\}\rangle=\frac{1}{2^N}\Big[1+\alpha(h^{(1)}(\{s_1\})+\overline{h^{(1)}(\{s_2\})})+\alpha^2 B(\{s_1\},\{s_2\})\Big]. \tag{E.3}$$

On the other hand, one has

$$\text{Tr}(\rho^k_{\text{Spins}})=\sum_{\{s_1\},\{s_2\}\dots\{s_k\}}\prod_{i=1}^k\langle\{s_i\}|\,\rho_{\text{Spins}}(t)\,|\{s_{i+1}\}\rangle \tag{E.4}$$

with $\{s_{k+1}\}=\{s_1\}$. By considering (E.3), one can show that

$$\begin{aligned}\prod_{i=1}^k\langle\{s_i\}|\,\rho_{\text{Spins}}(t)\,|\{s_{i+1}\}\rangle=&\frac{1}{2^{Nk}}\Big[1+\alpha\sum_{i=1}^k(h^{(1)}(\{s_i\})+\overline{h^{(1)}(\{s_{i+1}\})}) \\ &+\alpha^2\Big(\sum_{i=1}^k B(\{s_i\},\{s_{i+1}\})+\sum_{j>i}(h^{(1)}(\{s_i\})+\overline{h^{(1)}(\{s_{i+1}\})})(h^{(1)}(\{s_j\}) \\ &+\overline{h^{(1)}(\{s_{j+1}\})})\Big)\Big]\end{aligned} \tag{E.5}$$

Since $h^{(1)}(\{s\})$ is purely imaginary (as we can see from (8.91)), the term in order α vanishes. Summing over the spin configurations leads to

$$\begin{aligned}\text{Tr}(\rho^k_{\text{Spins}})=&1+\frac{2^{N(k-2)}}{2^{Nk}}\alpha^2\sum_{\{s_1\},\{s_2\}}(kB(\{s_1\},\{s_2\}) \\ &+\frac{k(k-1)}{2}(h^{(1)}(\{s_1\})+\overline{h^{(1)}(\{s_2\})})(h^{(1)}(\{s_2\})+\overline{h^{(1)}(\{s_1\})})\Big)\end{aligned} \tag{E.6}$$

$$\begin{aligned}=&1+\frac{\alpha^2}{2^{2N}}\sum_{\{s_1\},\{s_2\}}(kB(\{s_1\},\{s_2\}) \\ &+\frac{k(k-1)}{2}(h^{(1)}(\{s_1\})+\overline{h^{(1)}(\{s_2\})})(h^{(1)}(\{s_2\})+\overline{h^{(1)}(\{s_1\})})\Big).\end{aligned} \tag{E.7}$$

Finally, still at second order in α, one has

$$\log(\mathrm{Tr}\rho^k_{\mathrm{Spins}}) = -\frac{\alpha^2}{2^{2N}} \sum_{\{s_1\},\{s_2\}} \Big(kB(\{s_1\},\{s_2\}) + \frac{k(k-1)}{2}(h^{(1)}(\{s_1\}) + \overline{h^{(1)}(\{s_2\})})(h^{(1)}(\{s_2\}) + \overline{h^{(1)}(\{s_1\})}) \Big) . \tag{E.8}$$

In order to perform this computation, it will be useful to use the following simplification relations directly coming from the perturbative solution (8.91)

$$h^{(1)}(q_0,\{s_1\},t) + \overline{h^{(1)}(q_0,\{s_2\},t)} = -\frac{i}{N}\omega_{q_0} t \sum_{j=1}^{N}(s_{1j} - s_{2j}) \tag{E.9}$$

$$h^{(2)}(q_0,\{s\},t) = -\frac{1}{N^2}\sum_q \omega_{q_0}\omega_q \left| \sum_{j=1}^{N} s_j e^{-i(q-q_0)ja} \right|^2 \int_0^t \int_0^{t'} e^{-i(t'-t'')(\omega_q - \omega_{q_0})} dt' dt'' \tag{E.10}$$

$$= -\frac{1}{N^2}\sum_q \omega_{q_0}\omega_q \left| \sum_{j=1}^{N} s_j e^{-ia(q-q_0)j} \right|^2 \left(\frac{1 - e^{-it(\omega_q - \omega_{q_0})}}{(\omega_q - \omega_{q_0})^2} - \frac{it}{(\omega_q - \omega_{q_0})} \right)$$

$$\sum_q h^{(1)}(q,\{s_1\},t)\overline{h^{(1)}(q,\{s_2\},t)} = \frac{1}{N^2}\sum_q \omega_{q_0}\omega_q \sum_{j,j'=1}^{N} s_{1j}s_{2j'} e^{-ia(q_0-q)(j-j')} \left| \int_0^t e^{-it'(\omega_q - \omega_{q_0})} dt' \right|^2 \tag{E.11}$$

$$= \frac{1}{N^2}\sum_q \omega_{q_0}\omega_q \sum_{j,j'=1}^{N} s_{1j}s_{2j'} e^{-ia(q_0-q)(j-j')} \left(\frac{2\sin\left(\frac{t}{2}(\omega_q - \omega_{q_0})\right)}{\omega_q - \omega_{q_0}} \right)^2$$

$$h^{(2)}(q_0,\{s\},t) + \overline{h^{(2)}(q_0,\{s\},t)} = -\frac{1}{N^2}\sum_q \omega_{q_0}\omega_q \left| \sum_{j=1}^{N} s_j e^{-ia(q-q_0)j} \right|^2 \left(\frac{2\sin\left(\frac{t}{2}(\omega_q - \omega_{q_0})\right)}{\omega_q - \omega_{q_0}} \right)^2 . \tag{E.12}$$

By using the expression (E.2) of B and the simplification relations (E.9) one can show that

$$\log(\mathrm{Tr}\rho^k_{\mathrm{Spins}}) = -\frac{\alpha^2}{2^{2N}} \sum_{\{s_1\},\{s_2\}} \left(k(h^{(2)}(\{s_1\}) + \overline{h^{(2)}(\{s_2\})} + \sum_q h^{(1)}(q,\{s_1\})\overline{h^{(1)}(\{s_2\})}) \right. \tag{E.13}$$
$$\left. + \frac{k(k-1)}{2}(h^{(1)}(\{s_1\}) + \overline{h^{(1)}(\{s_2\})})(h^{(1)}(\{s_2\}) + \overline{h^{(1)}(\{s_1\})}) \right)$$
$$= -\frac{\alpha^2}{2^{2N}} \sum_{\{s_1\},\{s_2\}} \left(\frac{k}{2}(h^{(2)}(\{s_2\}) + \overline{h^{(2)}(\{s_1\})} + \sum_q h^{(1)}(q,\{s_1\})\overline{h^{(1)}(\{s_2\})} + \text{h.c.}) \right. \tag{E.14}$$
$$\left. + \frac{k(k-1)}{2}\left(\frac{\omega_{q_0} t}{N}\right)^2 \left| \sum_{j=1}^N (s_{1j} - s_{2j}) \right|^2 \right)$$
$$= \frac{\alpha^2}{2^{2N}N^2} \sum_{\{s_1\},\{s_2\}} \left(\frac{k}{2} \sum_q \omega_{q_0}\omega_q \left(\left| \sum_{j=1}^N s_{1j} e^{-ia(q-q_0)j} \right|^2 + \left| \sum_{j=1}^N s_{2j} e^{-ia(q-q_0)j} \right|^2 \right. \right. \tag{E.15}$$
$$\left. \left. -2 \sum_{j,j'=1}^N s_{1j} s_{2j'} \cos(a(q-q_0)(j-j')) \right) \left(\frac{2\sin\left(\frac{t}{2}(\omega_q - \omega_{q_0})\right)}{\omega_q - \omega_{q_0}} \right)^2 \right.$$
$$\left. - \frac{k(k-1)}{2}(\omega_{q_0} t)^2 \left| \sum_{j=1}^N (s_{1j} - s_{2j}) \right|^2 \right)$$
$$= \frac{\alpha^2}{2^{2N}N^2} \sum_{\{s_1\},\{s_2\}} \left(\frac{k}{2} \sum_q \omega_{q_0}\omega_q \left| \sum_{j=1}^N (s_{1j} - s_{2j}) e^{ia(q-q_0)j} \right|^2 \left(\frac{2\sin\left(\frac{t}{2}(\omega_q - \omega_{q_0})\right)}{\omega_q - \omega_{q_0}} \right)^2 \right. \tag{E.16}$$
$$\left. - \frac{k(k-1)}{2}(\omega_{q_0} t)^2 \left| \sum_{j=1}^N (s_{1j} - s_{2j}) \right|^2 \right)$$
$$= \frac{2\alpha^2}{N} \left(\frac{k}{2} \sum_q \omega_q \omega_{q_0} \left(\frac{\sin\left(\frac{t}{2}(\omega_q - \omega_{q_0})\right)}{\omega_q - \omega_{q_0}} \right)^2 - \frac{k(k-1)}{2}(\omega_{q_0} t)^2 \right). \tag{E.17}$$

We used the following equality for the sum over the spin configurations

$$\sum_{\{s_1\},\{s_2\}} (s_{1j} - s_{2j})(s_{1j'} - s_{2j'}) = \begin{cases} 0 & \text{if} \quad j \neq j' \\ 2^{2N+1} & \text{if} \quad j = j' \end{cases} \tag{E.18}$$

One can now use the formula (8.97) to obtain the following expression for the Von Neumann entropy

$$S(\rho_{\mathrm{Spins}}) = \frac{\alpha^2}{N} \left(\sum_q \omega_q \omega_{q_0} \left(\frac{\sin\left(\frac{t}{2}(\omega_q - \omega_{q_0})\right)}{\omega_q - \omega_{q_0}} \right)^2 - (\omega_{q_0} t)^2 \right) \tag{E.19}$$

References

[1] Gerard 't Hooft and M. J. G. Veltman. One loop divergencies in the theory of gravitation. *Ann. Inst. H. Poincare Phys. Theor. A*, 20:69–94, 1974.

[2] Marc H Goroff and Augusto Sagnotti. Quantum gravity at two loops. *Physics Letters B*, 160(1-3):81–86, 1985.

[3] John F. Donoghue, Mikhail M. Ivanov, and Andrey Shkerin. EPFL Lectures on General Relativity as a Quantum Field Theory. 2 2017.

[4] Cliff P Burgess. Quantum gravity in everyday life: General relativity as an effective field theory. *Living Reviews in Relativity*, 7:1–56, 2004.

[5] GG Kirilin and IB Khriplovich. Quantum power correction to the newton law. *Journal of Experimental and Theoretical Physics*, 95:981–986, 2002.

[6] A Akhundov, S Bellucci, and A Shiekh. Gravitational interaction to one loop in effective quantum gravity. *Physics Letters B*, 395(1-2):16–23, 1997.

[7] John F Donoghue. Leading quantum correction to the newtonian potential. *Physical Review Letters*, 72(19):2996, 1994.

[8] John F Donoghue. General relativity as an effective field theory: The leading quantum corrections. *Physical Review D*, 50(6):3874, 1994.

[9] N Emil J Bjerrum-Bohr, John F Donoghue, and Barry R Holstein. Quantum gravitational corrections to the nonrelativistic scattering potential of two masses. *Physical Review D*, 67(8):084033, 2003.

[10] Ivan J Muzinich and Stamatis Vokos. Long range forces in quantum gravity. *Physical Review D*, 52(6):3472, 1995.

[11] Sean A Hayward. Formation and evaporation of nonsingular black holes. *Physical review letters*, 96(3):031103, 2006.

[12] A. Ashtekar. New Variables for Classical and Quantum Gravity. *Phys. Rev. Lett.*, 57:2244–2247, 1986.

[13] A. Ashtekar. New Hamiltonian Formulation of General Relativity. *Phys. Rev. D*, 36:1587–1602, 1987.

[14] A. Perez. Introduction to loop quantum gravity and spin foams. *gr-qc/0409061*. Published in 2nd International Conference on Fundamental Interactions (ICFI 2004) 6-12 Jun 2004. Domingos Martins, Espirito Santo, Brazil.

[15] A. Ashtekar and J. Lewandowski. Background independent quantum gravity: A Status report. *Class. Quant. Grav.*, 21:R53, 2004.

[16] C. Rovelli. *Quantum Gravity*. Cambridge University Press, 2004.

[17] T. Thiemann. *Modern Canonical Quantum General Relativity*. Cambridge University Press, 2007.

[18] I. Agullo and P. Singh. Loop Quantum Cosmology. In *WSP*, pages 183–240. 2017.

[19] M. Bojowald. Absence of singularity in loop quantum cosmology. *Phys.Rev.Lett.*, 86:5227–5230, 2001.

[20] M. Bojowald. Loop quantum cosmology. *Living Rev. Rel.*, 8:11, 2005.

[21] A. Ashtekar, M. Bojowald, and J. Lewandowski. Mathematical structure of loop quantum cosmology. *Adv. Theor. Math. Phys.*, 7(2):233–268, 2003.

[22] A. Ashtekar and P. Singh. Loop Quantum Cosmology: A Status Report. *Class. Quant. Grav.*, 28:213001, 2011. http://arXiv.org/abs/1108.0893.

[23] V. Taveras. Corrections to the Friedmann Equations from LQG for a Universe with a Free Scalar Field. *Phys. Rev. D*, 78:064072, 2008.

[24] L. Modesto. Disappearance of black hole singularity in quantum gravity. *Phys. Rev.*, D70:124009, 2004.

[25] A. Ashtekar and M. Bojowald. Quantum geometry and the Schwarzschild singularity. *Class. Quant. Grav.*, 23:391–411, 2006. [gr-qc/0509075].

[26] L. Modesto. Loop quantum black hole. *Class. Quant. Grav.*, 23:5587–5602, 2006. [gr-qc/0509078].

[27] R. Gambini and J. Pullin. Loop quantization of the Schwarzschild black hole. *Phys. Rev. Lett.*, 110(21):211301, 2013.

[28] R. Gambini and J. Pullin. Black holes in loop quantum gravity: The Complete space-time. *Phys. Rev. Lett.*, 101:161301, 2008.

[29] R. Gambini, J. Olmedo, and J. Pullin. Quantum black holes in Loop Quantum Gravity. *Class. Quant. Grav.*, 31:095009, 2014.

[30] R. Gambini and J. Pullin. Quantum shells in a quantum space-time. *Class. Quant. Grav.*, 32(3):035003, 2015.

[31] A. Ashtekar, J. Olmedo, and P. Singh. Quantum Transfiguration of Kruskal Black Holes. *Phys. Rev. Lett.*, 121(24):241301, 2018.

[32] J. Olmedo. Brief review on black hole loop quantization. *Universe*, 2(2):12, 2016.

[33] R. Gambini, J. Olmedo, and J. Pullin. Quantum geometry and black holes.

[34] Abhay Ashtekar, Javier Olmedo, and Parampreet Singh. Regular black holes from Loop Quantum Gravity. 1 2023.

[35] P. Nicolini, E. Spallucci, and M. F. Wondrak. Quantum Corrected Black Holes from String T-Duality. *Phys. Lett. B*, 797:134888, 2019.

[36] B. Koch and F. Saueressig. Black holes within Asymptotic Safety. *Int. J. Mod. Phys. A*, 29(8):1430011, 2014.

[37] F. Saueressig, N. Alkofer, G. D'Odorico, and F. Vidotto. Black holes in Asymptotically Safe Gravity. *PoS*, FFP14:174, 2016.

[38] J. M. Bardeen. Non-singular general-relativistic gravitational collapse. In *Proc. Int. Conf. GR5, Tbilisi*, page 174, 1968.

[39] S. A. Hayward. Formation and evaporation of regular black holes. *Phys. Rev. Lett.*, 96:031103, 2006. [gr-qc/0506126].

[40] T. De Lorenzo, C. Pacilio, C. Rovelli, and S. Speziale. On the Effective Metric of a Planck Star. *Gen. Rel. Grav.*, 47(4):41, 2015. [1412.6015].

[41] V. P. Frolov. Notes on nonsingular models of black holes. *Phys. Rev. D*, 94(10):104056, 2016.

[42] Alejandro Perez. Regularization ambiguities in loop quantum gravity. *Physical Review D ,ÄîParticles, Fields, Gravitation, and Cosmology*, 73(4):044007, 2006.

[43] Norbert Bodendorfer, Fabio M Mele, and Johannes Münch. Effective quantum extended spacetime of polymer schwarzschild black hole. *Classical and Quantum Gravity*, 36(19):195015, 2019.

[44] Johannes Münch, Alejandro Perez, Simone Speziale, and Sami Viollet. Generic features of a polymer quantum black hole. *Classical and Quantum Gravity*, 40(13):135003, 2023.

[45] A. Perez, S. Ribisi, and S. Viollet. Modeling Quantum Particles Falling into a Black Hole: The Deep Interior Limit. *Universe*, 9(2):75, 2023. http://arXiv.org/abs/2301.03951.

[46] Stephen W Hawking. Particle creation by black holes. *Communications in mathematical physics*, 43(3):199–220, 1975.

[47] Robert M Wald. On particle creation by black holes. *Communications in Mathematical Physics*, 45(1):9–34, 1975.

[48] Leonard Parker. Probability distribution of particles created by a black hole. *Physical Review D*, 12(6):1519, 1975.

[49] Alejandro Perez and Sami Viollet. Discreteness unravels the black hole information puzzle: Insights from a quantum gravity toy model. *Entropy*, 25(11):1479, 2023.

[50] A. Perez and D. Sudarsky. A dialog on the fate of information in black hole evaporation. http://arXiv.org/abs/2205.08469.

[51] Stefano Ansoldi. Spherical black holes with regular center: a review of existing models including a recent realization with gaussian sources. *arXiv preprint arXiv:0802.0330*, 2008.

[52] Alessia Platania. Black holes in asymptotically safe gravity. *arXiv preprint arXiv:2302.04272*, 2023.

[53] Fabio Scardigli and Gaetano Lambiase. A metric for planck stars derived from gravity in asymptotic safety. In *Journal of Physics: Conference Series*, volume 2533, page 012035. IOP Publishing, 2023.

[54] Yi Ling and Meng-He Wu. Modified regular black holes with time delay and 1-loop quantum correction. *Chinese Physics C*, 46(2):025102, 2022.

[55] Tommaso De Lorenzo, Costantino Pacilio, Carlo Rovelli, and Simone Speziale. On the effective metric of a planck star. *General Relativity and Gravitation*, 47:1–16, 2015.

[56] M. B. Fröb, C. Rein, and R. Verch. Graviton corrections to the Newtonian potential using invariant observables. *JHEP*, 01:180, 2022.

[57] Markus B Fröb. Quantum gravitational corrections for spinning particles. *Journal of High Energy Physics*, 2016(10):1–46, 2016.

[58] Markus B Fröb and Enric Verdaguer. Quantum corrections for spinning particles in de sitter. *Journal of Cosmology and Astroparticle Physics*, 2017(04):022, 2017.

[59] Sami Viollet. Employing the effective field theory treatment of general relativity to constraint quantum black hole models. *To appear*, 2024.

[60] Seong-Youl Choi, JS Shim, and Hyunmi S Song. Factorization and polarization in linearized gravity. *Physical Review D*, 51(6):2751, 1995.

[61] Vladimir Fock. *The theory of space, time and gravitation*. Elsevier, 2015.

[62] Michael E Peskin. *An introduction to quantum field theory*. CRC press, 2018.

[63] Martin JG Veltman. Course 5 quantum theory of gravitation. *Methods in Field Theory: Les Houches Session XXVIII*, 28:265, 1981.

[64] Stanley Deser and Peter van Nieuwenhuizen. One-loop divergences of quantized einstein-maxwell fields. *Physical Review D*, 10(2):401, 1974.

[65] Cliff P Burgess. An introduction to effective field theory. *Annu. Rev. Nucl. Part. Sci.*, 57:329–362, 2007.

[66] John F Donoghue, Eugene Golowich, and Barry R Holstein. *Dynamics of the standard model*. Cambridge university press, 2014.

[67] C. P. Burgess. *Introduction to Effective Field Theory*. Cambridge University Press, 12 2020.

[68] Burt Ovrut and Howard J Schnitzer. New approach to effective field theories. *Physical Review D*, 21(12):3369, 1980.

[69] Burt A Ovrut and Howard J Schnitzer. Decoupling theorems for effective field theories. *Physical Review D*, 22(10):2518, 1980.

[70] S. W. Hawking and W. Israel. *General Relativity: An Einstein Centenary Survey*. Univ. Pr., Cambridge, UK, 1979.

[71] John F Donoghue. Introduction to the effective field theory description of gravity. *Advanced school on effective theories: Almunecar, Granada, Spain*, 26:217–240, 1995.

[72] Sidney Coleman. *Lectures of Sidney Coleman on Quantum Field Theory*. WSP, Hackensack, 12 2018.

[73] Myron Bander. Theories of quark confinement. *Physics Reports*, 75(4):205–286, 1981.

[74] Claude Cohen-Tannoudji, Bernard Diu, and Frank Laloe. Quantum mechanics, volume 2. *Quantum Mechanics*, 2:626, 1986.

[75] A. Zee. *Quantum field theory in a nutshell*. 2003.

[76] Giovanni Modanese. Potential energy in quantum gravity. *Nuclear Physics B*, 434(3):697–708, 1995.

[77] F. J. Belinfante and J. C. Garrison. On the Uniqueness of Fock's Harmonic Coordinate Systems in the Presence of Static, Spherically Symmetric Sources. *Phys. Rev.*, 125:1124–1130, 1962.

[78] Steven Weinberg. Gravitation and cosmology: principles and applications of the general theory of relativity. 1972.

[79] Jr. Callan, C. G., S. B. Giddings, J. A. Harvey, and A. Strominger. Evanescent black holes. *Phys. Rev. D*, 45(4):R1005, 1992. [hep-th/9111056].

[80] A. Ashtekar, F. Pretorius, and F. M. Ramazanoglu. Surprises in the Evaporation of 2-Dimensional Black Holes. *Phys. Rev. Lett.*, 106:161303, 2011. [1011.6442].

[81] A. Ashtekar, T. Pawlowski, and P. Singh. Quantum Nature of the Big Bang: Improved dynamics. *Phys. Rev. D*, 74:084003, 2006. [gr-qc/0607039].

[82] A. Ashtekar and P. Singh. Loop quantum cosmology: a status report. *Classical and Quantum Gravity*, 28:213001, 2011. [arXiv:1108.0893 [gr-qc]].

[83] J. G. Kelly, R. Santacruz, and E. Wilson-Ewing. Effective loop quantum gravity framework for vacuum spherically symmetric spacetimes. *Phys. Rev. D*, 102(10):106024, 2020. [2006.09302].

[84] J. B. Achour, F. Lamy, H. Liu, and K. Noui. Non-singular black holes and the Limiting Curvature Mechanism: A Hamiltonian perspective. *J. Cosmol. Astropart. Phys.*, 2018(05):72, 2017. [1712.03876].

[85] A. Ashtekar, J. Olmedo, and P. Singh. Quantum Transfiguration of Kruskal Black Holes. *Physical Review Letters*, 121:241301, 2018. [arXiv:1806.00648 [gr-qc]].

[86] N. Bodendorfer, F. M. Mele, and J. Münch. Effective quantum extended spacetime of polymer Schwarzschild black hole. *Classical and Quantum Gravity*, 36:195015, 2019. [arXiv:1902.04542 [gr-qc]].

[87] E. Alesci, S. Bahrami, and D. Pranzetti. Asymptotically de Sitter universe inside a Schwarzschild black hole. *Physical Review D*, 102:066010, 2020. [arXiv:2007.06664 [gr-qc]].

[88] V. Taveras. Corrections to the Friedmann equations from loop quantum gravity for a universe with a free scalar field. *Physical Review D*, 78:064072, 2008. [arXiv:0807.3325 [gr-qc]].

[89] L. Amadei, A. Perez, and S. Ribisi. The landscape of polymer quantum cosmology. [2203.07044].

[90] A. Perez. On the regularization ambiguities in loop quantum gravity. *Phys. Rev. D*, 73:044007, 2006. [gr-qc/0509118].

[91] Madhavan Varadarajan. Euclidean LQG Dynamics: An Electric Shift in Perspective. *Class. Quant. Grav.*, 38(13):135020, 2021. [2101.03115].

[92] Madhavan Varadarajan and Alejandro Perez. public and private discussion during LOOPs 22 conference, July 2022.

[93] E. Alesci, S. Bahrami, and D. Pranzetti. Quantum gravity predictionspolymerBHv2 for black hole interior geometry. *Phys. Lett. B*, 797:134908, 2019. [1904.12412].

[94] Carlo Rovelli and Lee Smolin. Discreteness of area and volume in quantum gravity. *Nuclear Physics B*, 442(3):593–619, 1995.

[95] Pietro Dona and Simone Speziale. Introductory lectures to loop quantum gravity. *arXiv preprint arXiv:1007.0402*, 2010.

[96] Alejandro Perez. Introduction to loop quantum gravity and spin foams. *arXiv preprint gr-qc/0409061*, 2004.

[97] Robert M Wald. *General relativity*. University of Chicago press, 2010.

[98] Nuno Barros E Sá. Hamiltonian analysis of general relativity with the immirzi parameter. *International Journal of Modern Physics D*, 10(03):261–272, 2001.

[99] István Montvay and Gernot Münster. *Quantum fields on a lattice*. Cambridge University Press, 1994.

[100] Alberto S Cattaneo and Alejandro Perez. A note on the poisson bracket of 2d smeared fluxes in loop quantum gravity. *Classical and Quantum Gravity*, 34(10):107001, 2017.

[101] Lautaro Amadei, Alejandro Perez, and Salvatore Ribisi. Landscape of polymer quantum cosmology. *Physical Review D*, 107(8):086007, 2023.

[102] Abhay Ashtekar, Alejandro Corichi, and Parampreet Singh. Robustness of key features of loop quantum cosmology. *Physical Review D ,ÄîParticles, Fields, Gravitation, and Cosmology*, 77(2):024046, 2008.

[103] Alejandro Corichi and Parampreet Singh. Is loop quantization in cosmology unique? *Physical Review D ,ÄîParticles, Fields, Gravitation, and Cosmology*, 78(2):024034, 2008.

[104] Wojciech Kaminski and Tomasz Pawlowski. Cosmic recall and the scattering picture of loop quantum cosmology. *Physical Review D ,ÄîParticles, Fields, Gravitation, and Cosmology*, 81(8):084027, 2010.

[105] Carlo Rovelli and Edward Wilson-Ewing. Why are the effective equations of loop quantum cosmology so accurate? *Physical Review D*, 90(2):023538, 2014.

[106] Eric G Brown, Robert Mann, and Leonardo Modesto. Mass inflation in the loop black hole. *Physical Review D ,ÄîParticles, Fields, Gravitation, and Cosmology*, 84(10):104041, 2011.

[107] M. Bojowald. Comment on "Towards a quantum notion of covariance in spherically symmetric loop quantum gravity". *Phys. Rev. D*, 105(10):108901, 2022. [2203.06049].

[108] M. Bojowald. Noncovariance of "covariant polymerization" in models of loop quantum gravity. *Phys. Rev. D*, 103(12):126025, 2021. [2102.11130].

[109] M. Bojowald. No-go result for covariance in models of loop quantum gravity. *Phys. Rev. D*, 102(4):046006, 2020. [2007.16066].

[110] M. Bojowald. Comment (2) on "Quantum Transfiguration of Kruskal Black Holes". [1906.04650].

[111] Babak Vakili. Classical Polymerization of the Schwarzschild Metric. *Advances in High Energy Physics*, 2018:1–10, 2018. [arXiv:1806.01837 [hep-th]].

[112] Alejandro Corichi and Parampreet Singh. Loop quantization of the Schwarzschild interior revisited. *Classical and Quantum Gravity*, 33:055006, 2016. [arXiv:1506.08015 [gr-qc]].

[113] Leonardo Modesto. Semiclassical Loop Quantum Black Hole. *International Journal of Theoretical Physics*, 49:1649–1683, 2010. [arXiv:0811.2196 [gr-qc]].

[114] C. G. Böhmer and K. Vandersloot. Loop quantum dynamics of the Schwarzschild interior. *Physical Review D*, 76:104030, 2007. [arXiv:0709.2129 [gr-qc]].

[115] J. Ben Achour, F. Lamy, H. Liu, and K. Noui. Polymer Schwarzschild black hole: An effective metric. *EPL (Europhysics Letters)*, 123:20006, aug 2018. [arXiv:1803.01152 [gr-qc]].

[116] A. Ashtekar, J. Olmedo, and P. Singh. Quantum extension of the Kruskal spacetime. *Physical Review D*, 98:126003, dec 2018. [arXiv:1806.02406 [gr-qc]].

[117] N. Bodendorfer, F. M. Mele, and J. Münch. A note on the Hamiltonian as a polymerisation parameter. *Classical and Quantum Gravity*, 36:187001, sep 2019. [arXiv:1902.04032 [gr-qc]].

[118] N. Bodendorfer, F. M. Mele, and J. Münch. Mass and horizon Dirac observables in effective models of quantum black-to-white hole transition. *Classical and Quantum Gravity*, 38:095002, may 2021. [arXiv:1912.00774 [gr-qc]].

[119] N. Bodendorfer, F. M. Mele, and J. Münch. (b,v)-type variables for black to white hole transitions in effective loop quantum gravity. *Physics Letters B*, 819:136390, aug 2021. [arXiv:1911.12646 [gr-qc]].

[120] M. Assanioussi, A. Dapor, and K. Liegener. Perspectives on the dynamics in a loop quantum gravity effective description of black hole interiors. *Physical Review D*, 101:026002, jan 2020. [arXiv:1908.05756 [gr-qc]].

[121] J. G. Kelly, R. Santacruz, and E. Wilson-Ewing. Effective loop quantum gravity framework for vacuum spherically symmetric spacetimes. *Physical Review D*, 102:106024, nov 2020. [arXiv:2006.09302 [gr-qc]].

[122] J. G. Kelly, R. Santacruz, and E. Wilson-Ewing. Black hole collapse and bounce in effective loop quantum gravity. *Classical and Quantum Gravity*, 38:04LT01, feb 2021. [arXiv:2006.09325 [gr-qc]].

[123] R. Gambini, J. Olmedo, and J. Pullin. Spherically symmetric loop quantum gravity: analysis of improved dynamics. *Classical and Quantum Gravity*, 37:205012, oct 2020. [arXiv:2006.01513 [gr-qc]].

[124] M. Geiller, E. R. Livine, and F. Sartini. Symmetries of the black hole interior and singularity regularization. *SciPost Physics*, 10:022, jan 2021. [arXiv:2010.07059 [gr-qc]].

[125] F. Sartini and M. Geiller. Quantum dynamics of the black hole interior in loop quantum cosmology. *Physical Review D*, 103:066014, mar 2021. [arXiv:2010.07056 [gr-qc]].

[126] M. Bouhmadi-López, S. Brahma, C.-Y. Chen, P. Chen, and D.-h. Yeom. Asymptotic non-flatness of an effective black hole model based on loop quantum gravity. *Physics of the Dark Universe*, 30:100701, dec 2020. [arXiv:1902.07874 [gr-qc]].

[127] W.-C. Gan, N. O. Santos, F.-W. Shu, and A. Wang. Properties of the spherically symmetric polymer black holes. *Physical Review D*, 102:124030, dec 2020. [arXiv:2008.09664 [gr-qc]].

[128] A. García-Quismondo and G. A. Mena Marugán. Exploring Alternatives to the Hamiltonian Calculation of the Ashtekar-Olmedo-Singh Black Hole Solution. *Frontiers in Astronomy and Space Sciences*, 8:115, jul 2021. [arXiv:2107.00947 [gr-qc]].

[129] R. Gambini, J. Olmedo, and J. Pullin. Loop Quantum Black Hole Extensions Within the Improved Dynamics. *Frontiers in Astronomy and Space Sciences*, 8:74, jun 2021. [arXiv:2012.14212 [gr-qc]].

[130] B. Elizaga Navascués, A. García-Quismondo, and G. A. Mena Marugán. Hamiltonian formulation and loop quantization of a recent extension of the Kruskal spacetime. *Phys. Rev. D*, 106(4):043531, 2022. [2208.00425].

[131] M. Geiller, E. R. Livine, and F. Sartini. Dynamical symmetries of homogeneous minisuperspace models. *Phys. Rev. D*, 106(6):064013, 2022. [2205.02615].

[132] C. Rovelli and E. Wilson-Ewing. Why are the effective equations of loop quantum cosmology so accurate? *Phys. Rev. D*, 90(2):023538, 2014. [1310.8654].

[133] C. Rovelli and F. Vidotto. Planck stars. *Int. J. Mod. Phys. D*, 23(12):1442026, 2014. [1401.6562].

[134] M. Bojowald. No-go result for covariance in models of loop quantum gravity. *Physical Review D*, 102:046006, aug 2020. [arXiv:2007.16066 [gr-qc]].

[135] H. M. Haggard and C. Rovelli. Quantum-gravity effects outside the horizon spark black to white hole tunneling. *Phys. Rev. D*, 92(10):104020, 2015. [1407.0989].

[136] A. Rignon-Bret and C. Rovelli. Black to white transition of a charged black hole. *Phys. Rev. D*, 105(8):086003, 2022. [2108.12823].

[137] M. Bojowald, S. Brahma, U. Buyukcam, and F. D'Ambrosio. Hypersurface-deformation algebroids and effective spacetime models. *Phys. Rev. D*, 94(10):104032, 2016. [1610.08355].

[138] C. Blohmann, M. Schiavina, and A. Weinstein. A Lie-Rinehart algebra in general relativity. [2201.02883].

[139] A. Alonso-Bardaji and D. Brizuela. Anomaly-free deformations of spherical general relativity coupled to matter. *Physical Review D*, 104:084064, oct 2021. [arXiv:2106.07595 [gr-qc]].

[140] R. Kantowski and R. K. Sachs. Some spatially homogeneous anisotropic relativistic cosmological mod-

els. *Journal of Mathematical Physics*, 7(3):443–446, 1966.

[141] A. Ashtekar and A. del Río. Probing cosmological singularities with quantum fields: Open and closed FLRW universes.

[142] A. Ashtekar, A. del Río, and M. Schneider. Space-like Singularities of General Relativity: A Phantom menace? *Gen. Rel. Grav.*, 54:45, 2022.

[143] B. C. Xanthopoulos and T. Zannias. Kantowski,ÄöSachs metrics with source: A massless scalar field. *Journal of Mathematical Physics*, 33(4):1415–1419, 1992.

[144] D. N. Page. Particle Emission Rates from a Black Hole: Massless Particles from an Uncharged, Non-rotating Hole. *Phys. Rev. D*, 13:198–206, 1976.

[145] E. Poisson and W. Israel. Internal structure of black holes. *Phys. Rev. D*, 41:1796–1809, 1990.

[146] A. Ashtekar and M. Varadarajan. Gravitational Dynamics—A Novel Shift in the Hamiltonian Paradigm. *Universe*, 7(1):13, 2021. http://arXiv.org/abs/2012.12094.

[147] M. Varadarajan. Anomaly free quantum dynamics for Euclidean LQG. http://arXiv.org/abs/2205.10779.

[148] A. Perez. No firewalls in quantum gravity: the role of discreteness of quantum geometry in resolving the information loss paradox. *Class. Quant. Grav.*, 32(8):084001, 2015. http://arXiv.org/abs/1410.7062.

[149] L. Amadei, H. Liu, and A. Perez. Unitarity and information in quantum gravity: a simple example. *Front. Astron. Space Sci.*, 8:46, 2021. http://arXiv.org/abs/1912.09750.

[150] J. F. Barbero G. and A. Perez. *Quantum Geometry and Black Holes*. WSP, 2017. http://arXiv.org/abs/1501.02963.

[151] A. Perez. Black Holes in Loop Quantum Gravity. *Rept. Prog. Phys.*, 80(12):126901, 2017. http://arXiv.org/abs/1703.09149.

[152] S. Hawking. Breakdown of Predictability in Gravitational Collapse. *Phys. Rev.*, D14:2460–2473, 1976.

[153] Thomas Banks, Leonard Susskind, and Michael E Peskin. Difficulties for the evolution of pure states into mixed states. *Nuclear Physics B*, 244(1):125–134, 1984.

[154] Alejandro Perez and Sami Viollet. Decoherence without dissipation in a quantum field theory model. *To appear*, 2024.

[155] Ted Jacobson. Introduction to quantum fields in curved spacetime and the hawking effect. In *Lectures on Quantum Gravity*, pages 39–89. Springer, 2005.

[156] Alessandro Fabbri and José Navarro-Salas. *Modeling black hole evaporation*. World Scientific, 2005.

[157] Samir D Mathur. The information paradox: a pedagogical introduction. *Classical and Quantum Gravity*, 26(22):224001, 2009.

[158] D. N. Page. IS BLACK HOLE EVAPORATION PREDICTABLE? *Phys. Rev. Lett.*, 44:301, 1980.

[159] Don N Page. Particle emission rates from a black hole. ii. massless particles from a rotating hole. *Physical Review D*, 14(12):3260, 1976.

[160] Don N Page. Particle emission rates from a black hole. iii. charged leptons from a nonrotating hole. *Physical Review D*, 16(8):2402, 1977.

[161] Jacob D Bekenstein. Black holes and the second law. In *JACOB BEKENSTEIN: The Conservative Revolutionary*, pages 303–306. World Scientific, 2020.

[162] D. N. Page. Information in black hole radiation. *Phys. Rev. Lett.*, 71:3743–3746, 1993. http://arXiv.org/abs/hep-th/9306083.

[163] Sabine Hossenfelder and Lee Smolin. Conservative solutions to the black hole information problem. *Physical Review D ,ÄîParticles, Fields, Gravitation, and Cosmology*, 81(6):064009, 2010.

[164] R. Bousso. The Holographic principle. *Rev. Mod. Phys.*, 74:825–874, 2002. http://arXiv.org/abs/hep-th/0203101.

[165] J. M. Maldacena. The Large N limit of superconformal field theories and supergravity. *Adv. Theor. Math. Phys.*, 2:231–252, 1998. http://arXiv.org/abs/hep-th/9711200.

[166] G. t'Hooft. The Scattering matrix approach for the quantum black hole: An Overview. *Int. J. Mod. Phys. A*, 11:4623–4688, 1996. http://arXiv.org/abs/gr-qc/9607022.

[167] L. Susskind, L. Thorlacius, and J. Uglum. The Stretched horizon and black hole complementarity. *Phys. Rev. D*, 48:3743–3761, 1993. http://arXiv.org/abs/hep-th/9306069.

[168] S. D. Mathur. The Fuzzball proposal for black holes: An Elementary review. *Fortsch. Phys.*, 53:793–827, 2005. http://arXiv.org/abs/hep-th/0502050.

[169] A. Almheiri, T. Hartman, J. Maldacena, E. Shaghoulian, and A. Tajdini. The entropy of Hawking radiation. *Rev. Mod. Phys.*, 93(3):035002, 2021. http://arXiv.org/abs/2006.06872.

[170] A. Almheiri, R. Mahajan, J. Maldacena, and Y. Zhao. The Page curve of Hawking radiation from semiclassical geometry. *JHEP*, 03:149, 2020. http://arXiv.org/abs/1908.10996.

[171] N. Engelhardt, S. Giddings, A. Perez, and S. Raju. Panel discussion during International Quantum Gravity Society meeting, 2021.

[172] S. B. Giddings. Constraints on black hole remnants. *Phys. Rev. D*, 49:947–957, 1994. http://arXiv.org/abs/hep-th/9304027.

[173] M. Christodoulou and T. De Lorenzo. Volume inside old black holes. *Phys. Rev.*, D94(10):104002, 2016. http://arXiv.org/abs/1604.07222.

[174] J. A. Wheeler. *Relativity, groups and topology.* 1964. Edited by C. De-Witt and B. DeWitt, Gordon and Breach, New York.

[175] A. Ashtekar. Black Hole evaporation: A Perspective from Loop Quantum Gravity. *Universe*, 6(2):21, 2020. http://arXiv.org/abs/2001.08833.

[176] Stephen DH Hsu. Spacetime topology change and black hole information. *Physics Letters B*, 644(1):67–71, 2007.

[177] D. N. Page. Black hole information. page 5, 1993. http://arXiv.org/abs/hep-th/9305040.

[178] X. Calmet, S. D. H. Hsu, and M. Sebastianutti. Quantum gravitational corrections to particle creation by black holes. *Phys. Lett. B*, 841:137820, 2023. http://arXiv.org/abs/2303.00310.

[179] X. Calmet and S. D. H. Hsu. Quantum Hair in Electrodynamics and Gravity. http://arXiv.org/abs/2209.12798.

[180] X. Calmet, R. Casadio, S. D. H. Hsu, and F. Kuipers. Quantum Hair During Gravitational Collapse. http://arXiv.org/abs/2305.09466.

[181] X. Calmet and S. D. H. Hsu. Quantum hair and black hole information. *Phys. Lett. B*, 827:136995, 2022. http://arXiv.org/abs/2112.05171.

[182] S. Raju. Lessons from the information paradox. *Phys. Rept.*, 943:1–80, 2022. http://arXiv.org/abs/2012.05770.

[183] S. Liberati, G. Tricella, and A. Trombettoni. The information loss problem: an analogue gravity perspective. *Entropy*, 21(10):940, 2019. http://arXiv.org/abs/1908.01036.

[184] A. Ashtekar and M. Bojowald. Black hole evaporation: A Paradigm. *Class.Quant.Grav.*, 22:3349–3362, 2005. http://arXiv.org/abs/gr-qc/0504029.

[185] M. Han, C. Rovelli, and F. Soltani. Geometry of the black-to-white hole transition within a single asymptotic region. *Phys. Rev. D*, 107(6):064011, 2023. http://arXiv.org/abs/2302.03872.

[186] K. V. Krasnov. Counting surface states in the loop quantum gravity. *Phys.Rev.*, D55:3505–3513, 1997.

http://arXiv.org/abs/gr-qc/9603025.

[187] C. Rovelli. Black hole entropy from loop quantum gravity. *Phys. Rev. Lett.*, 77:3288–3291, 1996. http://arXiv.org/abs/gr-qc/9603063.

[188] A. Ashtekar, J. Baez, A. Corichi, and K. Krasnov. Quantum geometry and black hole entropy. *Phys. Rev. Lett.*, 80:904–907, 1998. http://arXiv.org/abs/gr-qc/9710007.

[189] A. Ashtekar, J. C. Baez, and K. Krasnov. Quantum geometry of isolated horizons and black hole entropy. *Adv. Theor. Math. Phys.*, 4:1–94, 2000. http://arXiv.org/abs/gr-qc/0005126.

[190] J. Lewandowski, A. Okolow, H. Sahlmann, and T. Thiemann. Uniqueness of diffeomorphism invariant states on holonomy-flux algebras. *Commun.Math.Phys.*, 267:703–733, 2006. http://arXiv.org/abs/gr-qc/0504147.

[191] B. Dittrich. Modified Graviton Dynamics From Spin Foams: The Area Regge Action. http://arXiv.org/abs/2105.10808.

[192] B. Dittrich and A. Kogios. From spin foams to area metric dynamics to gravitons. *Class. Quant. Grav.*, 40(9):095011, 2023. http://arXiv.org/abs/2203.02409.

[193] J. N. Borissova and B. Dittrich. Towards effective actions for the continuum limit of spin foams. *Class. Quant. Grav.*, 40(10):105006, 2023. http://arXiv.org/abs/2207.03307.

[194] William G Unruh and Robert M Wald. Evolution laws taking pure states to mixed states in quantum field theory. *Physical Review D*, 52(4):2176, 1995.

[195] William G Unruh and Robert M Wald. Information loss. *Reports on Progress in Physics*, 80(9):092002, 2017.

[196] Hrvoje Nikolić. Violation of unitarity by hawking radiation does not violate energy-momentum conservation. *Journal of cosmology and astroparticle physics*, 2015(04):002, 2015.

[197] WG Unruh. Decoherence without dissipation. *Philosophical Transactions of the Royal Society A: Mathematical, Physical and Engineering Sciences*, 370(1975):4454–4459, 2012.

[198] NV Prokof'Ev and PCE Stamp. Theory of the spin bath. *Reports on Progress in Physics*, 63(4):669, 2000.

[199] Lev Davidovich Landau and Evgenii Mikhailovich Lifshitz. *Quantum mechanics: non-relativistic theory*, volume 3. Elsevier, 2013.

[200] John Collins, Alejandro Perez, and Daniel Sudarsky. Lorentz invariance violation and its role in quantum gravity phenomenology. *arXiv preprint hep-th/0603002*, 2006.

[201] Niels Emil J Bjerrum-Bohr, John F Donoghue, Barry R Holstein, Ludovic Planté, and Pierre Vanhove. Bending of light in quantum gravity. *Physical review letters*, 114(6):061301, 2015.

[202] Dmitri V Vassilevich. Heat kernel expansion: user's manual. *Physics reports*, 388(5-6):279–360, 2003.